Karlsruhe Institute of Technology

Tetrazole-containing Polymers: Synthesis and Characterization

Zur Erlangung des akademischen Grades eines

DOKTORS DER NATURWISSENSCHAFTEN

(Dr. rer. nat.)

von der KIT-Fakultät für Chemie und Biowissenschaften
des Karlsruher Instituts für Technologie (KIT)

genehmigte

DISSERTATION

von

M. Sc. Meryem S. Akdemir

aus

Gelibolu, Türkiye

KIT-Dekan: Prof. Dr. Hans-Achim Wagenknecht

1. Referent: Prof. Dr. Patrick Théato

2. Referent: Jun. Prof. Dr. Hatice Mutlu

Tag der mündlichen Prüfung: 23.10.2023

„Klein ist der Mensch, der Vergängliches sucht, groß aber, wer das Ewige im Sinn hat. “

—Antonius von Padua

Declaration

Die vorliegende Arbeit wurde im Zeitraum von September 2019 bis June 2023 am Institut für Technische Chemie und Polymerchemie (ITCP) und am Institut für Biologische Grenzflächen III (IBG-3) am Karlsruher Institut für Technologie (KIT) unter Anleitung von Prof. Dr. Patrick THÉATO angefertigt.

Hiermit versichere ich, dass ich die Arbeit selbstständig angefertigt, nur die angegebenen Quellen und Hilfsmittel benutzt und mich keiner unzulässigen Hilfe Dritter bedient habe. Insbesondere habe ich wörtlich oder sinngemäß aus anderen Werken übernommene Inhalte als solche kenntlich gemacht. Die Satzung des Karlsruher Institute für Technologie (KIT) zur Sicherung wissenschaftlicher Praxis habe ich beachtet. Des Weiteren erkläre ich, dass ich mich derzeit in keinem laufenden Promotionsverfahren befinde, und auch keine vorausgegangenen Promotionsversuche unternommen habe. Die elektronische Version der Arbeit stimmt mit der schriftlichen Version überein und die Primärdaten sind gemäß Abs. A (6) der Regeln zur Sicherung guter wissenschaftlicher Praxis des KIT beim Institut abgegeben und archiviert.

_____ _____

Ort, Datum Meryem S. Akdemir

For each one lost in the earthquake (*06.02.2023*) …

1 Abstract

The introduction of nitrogen-rich heterocyclic groups (i.e., quinoline, triazole, tetrazole) into polymer structures, either as side groups or integrated within the main structure, presents innovative avenues for generating novel polymer architectures. Of particular importance in the domain of organic chemistry is the tetrazole family (e.g., 1*H*-tetrazole, 5*H*-tetrazole 2,5 disubstituted tetrazoles). For many years, tetrazoles have been widely utilized across multiple disciplines of chemistry, such as materials science and medicinal chemistry. Particularly, 1,5 disubstituted tetrazoles (1,5 DSTs) offer a rich playground for scientific exploration, enabling the development of new compounds and materials with diverse applications. Especially, high thermal and chemical stability of 1,5 DST, fluoresce/phosphorescence property beside bioisosteric nature to amide bond are the most important properties to pave the way towards diverse applications (e.g., energy systems, nanomaterials, metal-organic frameworks and medicinal compounds). Nevertheless, the translation of the distinct molecular characteristics of 1,5 DSTs into new polymeric materials poses a formidable obstacle due to the limited synthetic methods, as evidenced by the scarcity of comprehensive literature on the subject matter. Therefore, the primary objective of this thesis is to contribute to the progress of the scientific discipline by creating and examining 1,5 DST-containing innovative polymers within various chemical architectures. Consequently, three separate projects have arisen within this framework and are outlined in the subsequent chapters.

In the first part of the thesis, the first-ever synthesis of main chain 1,5 DST-based compounds was investigated to showcase the possibility of polymer formation by using the Ugi-azide-four-multicomponent polymerization (UA-4MCP) strategy. Particularly, UA-4MC polymers were designed with various side groups (e.g., aliphatic or aromatic). In this regard, aliphatic substituted polymers demonstrated a moderate degree of thermal stability, with a slightly higher degradation temperature compared to their aromatic substituted counterparts. Furthermore, aliphatic substituted polymers displayed enhanced tendency for crystallization, concurrently accompanied by a decrease in the values of glass transition temperature (T_g) compared to the polymers with aromatic substituted counterparts. In addition, all polymers showed a unique emission characteristic (i.e., cluster-triggered emission, (CTE)), which is occurring through-space conjugation (TSC) obtained as a result of the clusterization of non-conventional chromophore-forming clusteroluminogens with extended electron delocalization and a rigid conformation between 1,5 DST units.

In the second project, the synthesis of pendant chain 1,5 DST-decorated polymers was targeted. For this purpose, the synthesis of 1,5 DST-decorated monomers with varying lengths of olefin handles has been accomplished through the Ugi-azide four-multicomponent reaction (UA-4MCR). Subsequently, the obtained monomers have been polymerized with dithiol derivatives of different lengths via the atom efficient thiol-ene chemistry. The investigation delved into two

aspects. Firstly, it was explored how the polymerization process is influenced by the length of α, ω-diene monomer olefin segments. Secondly, the impact of the thiol structure on the synthesis efficiency and final properties of the polymers was investigated. Accordingly, it has been observed that longer alkyl chain monomers (with a chain length of $(CH_2)_9$) showed more tendency to form polymers, compared to the short chain derivatives which presumably underwent cyclic oligomerization rather than polymerization. Additionally, it is found that all polymers had moderated thermal stability regardless of thiol derivatives. In addition, 1,5 DST-decorated polymers demonstrated T_g values below ambient temperature, providing enhanced processability, thereby broadening their potential applications. Last but not least, 1,5 DSTs-decorated polymers revealed CTE property as well.

In the third project, an advanced strategy for the synthesis of 1,5 DST-decorated polymers is described by utilizing post-polymerization modification method. A comprehensive view is provided with series of three different degrees of modification of poly (pentafluorophenyl acrylate), p(PFPA), parent polymer with 1,5 DST unit to understand the post-modification degree effect of 1,5 DST unit on the thermal properties of polymers. Subsequently, in-situ crosslinking formation was performed to construct a polymeric network, i.e., hydrogel, for the investigations of material properties. It was observed that the thermal stability has increased (from 192 °C value to 204 °C value) with the incensement of 1,5 DST content (from 20% to 60%, by weight). Moreover, the glassy-to-rubbery transition (i.e., T_g), which is an intrinsic property of any polymer, has been explored for the obtained hydrogels. An increased water uptake capacity was also demonstrated, with the incensement of 1,5 DST content within the network. In similar manner to the previously explored DSTs polymeric derivatives, the florescence properties in correlation with 1,5 DST content for hydrogels was represented.

Overall, in this thesis, the feasibility of various approaches, including direct polymerization, monomer synthesis followed by polymerization, and post-polymerization modification method, for the synthesis of novel containing 1,5 DSTs polymers is highlighted strategically. A comprehensive exploration was carried out to thoroughly understand the correlation between the positioning of 1,5 DST units -whether integrated into the main polymer chain or appended as pendant chains - and the subsequent properties. Beyond this, an advanced approach for the synthesis of 1,5 DST-containing polymeric network (i.e., hydrogels) with moderate thermal and optical properties was elaborated. Overall, all approaches to obtain 1,5 DST-containing polymers exemplify a milestone in polymer chemistry. The demonstrated versatility, structural robustness, and tunability of physical properties make 1,5 DST polymers promising candidates for various cutting-edge applications. Especially their fluorescent properties can play a crucial role in advancing scientific research, medical diagnostics, and technological applications.

Zusammenfassung

Die Einführung von stickstoffreichen heterocyclischen Gruppen (z.B. Chinolin, Triazol, Tetrazol) in Polymerstrukturen, entweder als Seitenketten oder integriert in die Hauptstruktur, eröffnet innovative Möglichkeiten zur Generierung neuer Polymerarchitekturen. Besondere Bedeutung in der Organischen Chemie kommt dabei der Tetrazolfamilie zu (z.B. 1*H*-Tetrazol, 5H-Tetrazol, 2,5-disubstituierte Tetrazole). Tetrazole werden seit vielen Jahren in verschiedenen Disziplinen der Chemie, wie Materialwissenschaften und Medizin, weitreichend eingesetzt. Insbesondere 1,5-disubstituierte Tetrazole (1,5 DSTs) bieten einen reichen Forschungsbereich für wissenschaftliche Erkundungen und ermöglichen die Entwicklung neuer Verbindungen und Materialien mit vielfältigen Anwendungen. Die hohe thermische und chemische Stabilität von 1,5 DSTs, ihre Fluoreszenz-/Phosphoreszenzeigenschaften sowie ihre bioisosterische Natur im Vergleich zur Amidbindung sind die wichtigsten Eigenschaften, die den Weg für vielfältigen Anwendungen (z.B. Energiesysteme, Nanomaterialien, Metall-organische Gerüste und medizinische Verbindungen) ebnen. Dennoch stellt die Übertragung der spezifischen molekularen Merkmale von 1,5 DSTs in neue polymere Materialien aufgrund begrenzter Synthesemethoden ein erhebliches Hindernis dar, wie durch die begrenzte Literatur zu diesem Thema belegt wird. Daher besteht das Hauptziel dieser Arbeit darin, zum Fortschritt der wissenschaftlichen Disziplin beizutragen, indem innovative Polymere mit 1,5 DSTs in verschiedenen chemischen Architekturen geschaffen und untersucht werden. Daraus ergeben sich innerhalb dieses Rahmens drei separate Projekte, die in den folgenden Kapiteln erläutert werden.

Im ersten Teil der Arbeit wurde die erstmalige Synthese von 1,5-DST in dem Polymerrückgrat untersucht, um die Möglichkeit der Polymerbildung mithilfe der Ugi-Azid-Vier-Mehrkomponenten-Polymerisation (UA-4MCP)-Strategie zu demonstrieren. Insbesondere wurden UA-4MC-Polymere mit verschiedenen Seitenketten entworfen (z.B. aliphatische und aromatische). In diesem Zusammenhang zeigten aliphatisch substituierte Polymere eine mäßige thermische Stabilität, mit einer leicht höheren Zersetzungstemperatur im Vergleich zu ihren aromatisch substituierten Gegenstücken. Des Weiteren wiesen aliphatisch substituierte Polymere eine erhöhte Neigung zur Kristallisation auf, begleitet von einer Abnahme der Glasübergangstemperatur (T_g) im Vergleich zu den Polymeren mit aromatisch substituierten Gegenstücken. Darüber hinaus zeigten alle Polymere eine einzigartige Emissionseigenschaft (d.h. clusterausgelöste Emission, cluster-triggered emission (CTE)), die durch Konjugation im Raum (through-space conjugation, TSC) aufgrund der Clusterbildung von nicht konventionellen Chromophor-bildenden Clusteroluminogenen mit erweiterter Elektronendelokalisierung und einer starren Konformation zwischen den 1,5-DST-Einheiten erfolgte.

Im zweiten Projekt wurde die Synthese von 1,5 DST-Seitenkettenpolymeren angestrebt. Zu diesem Zweck wurde die Synthese von 1,5 DST-verzierten Monomeren mit unterschiedlichen Längen von mittels der Ugi-Azid-Vier-Multikomponentenreaktion (Ugi-azide four-multicomponent reaction; UA-4MCR) durchgeführt. Anschließend wurden die erhaltenen Monomere mittels der atomökonomischen Thiol-En-Chemie mit Dithiol-Derivaten unterschiedlicher Längen polymerisiert. Die Untersuchung konzentrierte sich auf zwei Aspekte. Erstens wurde erforscht, wie der Polymerisationsprozess von der Länge der α, ω-Dienmonomer-Olefinsegmente beeinflusst wird. Zweitens wurde der Einfluss der Thiolstruktur auf die Syntheseeffizienz und die endgültigen Eigenschaften der Polymere untersucht. Es wurde beobachtet, dass Monomere mit längeren Alkylketten (mit einer Kettenlänge von $(CH_2)_9$) eher zur Bildung von Polymeren neigten im Vergleich zu den kurzkettigen Derivaten, die wahrscheinlich eine zyklische Oligomerisierung statt einer Polymerisierung durchliefen. Darüber hinaus wurde festgestellt, dass alle Polymere eine moderate thermische Stabilität aufwiesen, unabhängig von den Thiol-Derivaten. Außerdem zeigten 1,5 DST-verzierte Polymere T_g-Werte unterhalb der Raumtemperatur, was die Verarbeitbarkeit verbessert und somit ihr Anwendungspotenzial erweitert. Nicht zuletzt wiesen 1,5 DST- Seitenkettenpolymeren auch CTE-Eigenschaften auf.

Im dritten Projekt wird eine fortgeschrittene Strategie zur Synthese von 1,5-DST Seitenkettenpolymeren unter Verwendung einer Methode zur Post-Polymerisationsmodifikation beschrieben. Poly(pentafluorphenylacrylat), p(PFPA), wird mit verschiedenen Graden an 1,5-DST-Einheiten substituier, um den Einfluss der 1,5-DST-Einheiten auf die thermischen Eigenschaften zu untersuchen. Anschließend wurde eine in-situ-Vernetzung durchgeführt, um ein polymeres Netzwerk, d.h. ein Hydrogel, für die Untersuchung der Materialeigenschaften zu konstruieren. Es wurde beobachtet, dass die thermische Stabilität mit zunehmendem Gehalt an 1,5-DST (von 20% auf 60% nach Gewicht) gestiegen ist (von 192 °C auf 204 °C). Darüber hinaus wurde der Übergang von die glasübergangstemperatur (T_g), die eine intrinsische Eigenschaft jedes Polymers ist, für die erhaltenen Hydrogele untersucht. Eine erhöhte Wasserabsorptionsfähigkeit wurde ebenfalls gezeigt, mit zunehmendem Gehalt an 1,5-DST im Netzwerk. Auf ähnliche Weise wie bei den zuvor erforschten DST-Polymerderivaten wurden die Fluoreszenzeigenschaften in Bezug auf den 1,5-DST-Gehalt für die Hydrogele analysiet.

Übergreifend wird in dieser Arbeit die Durchführbarkeit verschiedener Ansätze, einschließlich der direkten Polymerisation, der Monomersynthese gefolgt von der Polymerisation und der Methode zur nachträglichen Polymermodifikation, für die Synthese neuartiger Polymere mit 1,5-DST-Einheiten strategisch hervorgehoben. Es wurde eine umfassende Untersuchung durchgeführt, um das Wechselspiel zwischen der Positionierung der 1,5-DST-Einheiten - ob sie in die Hauptpolymerkette integriert oder als Seitenketten angefügt wurden - und den darauffolgenden Eigenschaften gründlich zu verstehen. Darüber hinaus wurde ein

fortschrittlicher Ansatz zur Synthese von 1,5-DST-haltigen. Hydrogele mit moderaten thermischen und optischen Eigenschaften gezeigt. Insgesamt repräsentieren alle Ansätze zur Gewinnung von 1,5-DST-haltigen Polymeren einen Meilenstein in der Polymerchemie. Die gezeigte Vielseitigkeit, strukturelle Robustheit und Anpassbarkeit der physikalischen Eigenschaften machen 1,5-DST-Polymere zu vielversprechenden Kandidaten für verschiedene hochmoderne Anwendungen. Insbesondere ihre fluoreszierenden Eigenschaften können eine entscheidende Rolle bei der Förderung wissenschaftlicher Forschung, medizinischer Diagnostik und technologischer Anwendungen spielen.

2 Table of Contents

1 Introduction

Tetrazoles are specifically a five-membered aromatic ring containing four nitrogen atoms and one carbon atom.[1] Especially, 1,5-disubstituted tetrazoles (1,5 DSTs) and their respective analogues have garnered special attention. This is due to the presence of two nitrogen atoms in the 1,5 DST ring, which imparts stability by allowing nitrogen to delocalize electron density and distribute the charge.[2] Recently it has been shown that the nitrogen atoms of 1,5 DST act as electron-rich sites, forming strong bonds with metal centres, and is utilized in coordination chemistry as well as catalysis.[3-6] Furthermore, 1,5 DSTs possess desirable properties for energetic materials, such as high energy content, good thermal stability, low sensitivity to impact and friction, and controlled burn rates.[2, 7-8] Additionally, 1,5 DST unit in medical chemistry as small molecules drug derivatives have been extensity used due to their remarkable biological activities (e.g., antiviral, anti-inflammatory, antibacterial, and antifungal) beside ability to target specific diseases, and potential use as diagnostic tools.[9] Nonetheless, 1,5 DST have not been explored inclusively in the realm of polymer chemistry that constitute a new domain with largely unstudied potential. Several methods have been utilized to produce 1,5 DSTs containing polymers, including the synthesis of appropriate monomers followed by a polymerization (either radical [10] or anionic[11]) depending on the nature of the monomers. Furthermore, a post-polymerization modification approach has been employed to convert reactive groups (such as azide or alkyne) through the Huisgen 1,3-dipolar cycloaddition reaction.[12-13] Nevertheless, the knowledge transfer of 1,5 DST moieties from organic chemistry into polymer chemistry still poses challenges, thereby the restricting the application of 1,5 DST moieties in the field of polymer science to only a few instances.

Importantly, the existing literature is restricted because of certain disadvantages of synthesizing 1,5 DST-containing polymers concerning toxicity, side reactions, low selectivity, complex reaction conditions or synthetic challenges in multi-step sequences. Hence, it is necessary to employ novel approaches to achieve a more concise comprehension of the synthesis and characteristics of 1,5 DST containing polymeric structures, whether utilized as the main chain or as pendant groups, since they possess potential as an attractive alternative to traditional synthetic polymers due to their exceptional thermal stability, coordination capacity and biological activity.

Therefore, the research presented within this thesis is focused on the development of a framework to investigate the synthesis of 1,5 DST-containing polymeric structures. In this content, the design of the research scope has considered the following objectives:

Objective 1: *Exploring of the alternative synthesis pathway of main chain 1,5 DST-based polymeric structure*

Objective 2 *Investigating of innovative synthetic routines for the design of 1,5 DST-decorated polymers*

Objective 3 *Evaluating the feasibility of integrating a 1,5 DST unit into the pre-existing polymers to create polymeric networks adorned with 1,5 DST decorations.*

In accordance with the objectives, a broad analysis toolbox has been undertaken to establish a detailed understanding of the chemical, thermal, and optical properties of these novel polymers for possible applications.

Accordingly, to ensure a comprehensive understanding of the research, a detailed exposition of the theoretical background will be provided in the following chapter, encompassing the following key points: a) an overview of the general properties and synthesis methods of tetrazole and its derivatives; b) a literature survey of tetrazole-containing polymers; c) an examination of the current state of 1,5-disubstituted tetrazole derivatives and their applications beside a summary of 1,5 tetrazole-containing polymeric systems in literature. Moreover, a brief summary of the methods employed for the synthesis of 1,5 DST-containing polymeric structures will be provided. Additionally, driving motivation of the research and the key aspects of the present thesis pertaining to 1,5 DST-containing polymeric systems will be highlighted.

3 Theoretical Background

The current chapter provides the essential background information to understand better the concepts, methods, and reaction mechanisms used in this work. For this purpose, some general information on tetrazoles, followed by 1,5-disubstitute tetrazoles (1,5 DST) and, accordingly, their application in polymer chemistry is first given. In addition, some synthetic tools, e.g., Ugi-azide four- multicomponent reaction (UA-4MCR) or Ugi- azide four- multicomponent polymerization (UA-4MCP), besides post-polymerization modification reaction and thiol-ene chemistry are described for the developing tetrazole-containing polymeric materials.

3.1 Tetrazoles

3.1.1 Fundamental aspects and history

Tetrazoles are a class of doubly unsaturated heterocyclic compounds consisting of a five-membered ring containing four nitrogen atoms and one carbon atom.[14] They do not exist in nature. Tetrazole itself may exist in three different tautomeric forms i.e., 1*H*-tetrazole (a), 2*H*-tetrazolium (b) and 5*H*-tetrazole the position of the hydrogen atom attached to nitrogen being indeterminate as can been seen in **Figure 2.1**.[15] While 1*H*-tetrazole (a) tautomer is predominant, 2*H*-tetrazolium (b) tautomer is stable in the gas phase.[16] Nonetheless, 5*H*-tetrazole tautomer is not a stable member of this family, as it does not possess aromatic character.

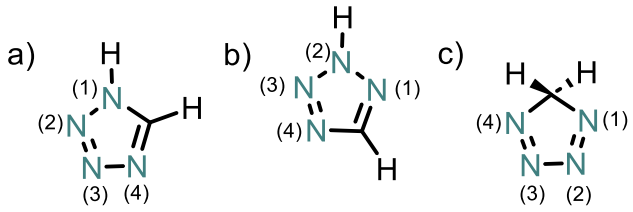

Figure 2. 1 Structure of regioisomeric tetrazole ring; a) 1*H*-tetrazole, b) 2*H*-tetrazolium, and c) 5H-tetrazole, respectively.

Tetrazoles can be classified into three main types; mono-(i.e., 1-substituted, 5 substituted), di-(i.e., 1,5-disubstituted), tri-(1,3,5 trisubstituted). In terms of composition, the 5-substituted tetrazole derivatives dominate the group with a majority representation of 58%, flowed by 1-monosubstituted and 1,5 DSTs behind at 18% and 14%, respectively as depicted **Figure 2.2**. The position number in each substitution class refers to the nitrogen atom that is substituted in the tetrazole ring as shown in **Figure 2.3**.

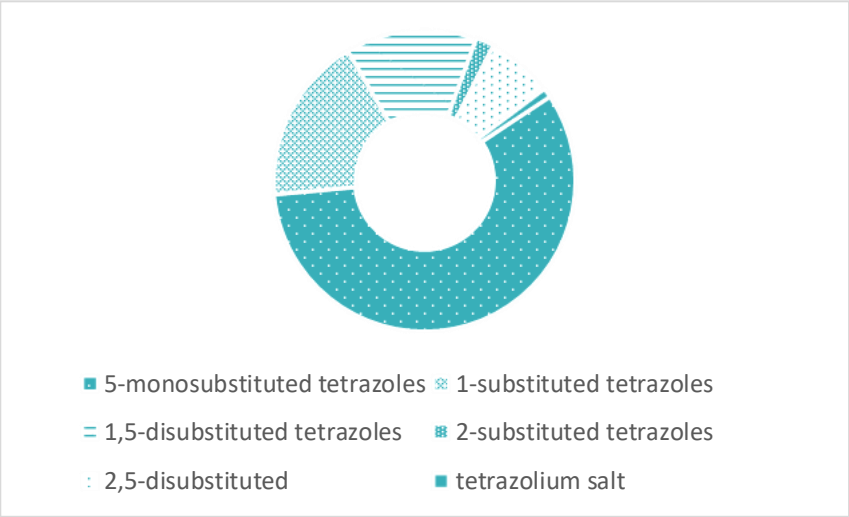

Figure 2. 2 Classification of the cocrystal structures of tetrazole derivatives from the Protein Data Bank (PDB).[14]

The substituent on the tetrazole ring can be any organic or inorganic group, and the properties of the tetrazole molecule can vary depending on the type and position of the substituent. It is known that 1-substituted compounds have higher melting points compared to 2-substituted compounds due to inductive effects. In similar manner, when substituents are present at positions 1 and 2, the resulting derivatives exhibit significantly higher melting points compared to 1,5 DST and 2,5-disubstituted (2,5 DST) compounds, primarily because of the formation of hydrogen bonds. Furthermore, at ambient temperature, most tetrazoles with substitutions at positions 1,5 and 2,5 are stable crystalline materials.[17] Indeed, tetrazoles are highly polar compounds and typically demonstrate outstanding solubility in polar solvents.[1] The solubility of tetrazole derivatives is highly dependent on the substituents at the ring moiety. Their enthalpies of formation are also relatively high, with 1*H*-tetrazole exhibiting a value of 28.1 eV (648 kcal mol^{-1}), which is consistent with the calculated value of 27.7 eV.[18] Thus, tetrazoles are considered energy-rich molecules. Furthermore, tetrazole and its 5-substituted derivatives display a spectrum of weak acidity, with pK_a values ranging from 1.1 to 6.3, and interestingly, this range is comparable to that of carbonic acids.[19] In addition, tetrazole ring exhibits lower basicity than aniline, with typical pK_b values ranging from 9.7 (1-methyl-1*H*-tetrazole) to 12.9 (5-amino-1-phenyl-1*H*-tetrazole). A protonation usually occurs at N(4) position [20] (see **Figure 2.1.**) and electrophiles tend to attack tetrazoles at one of the ring nitrogen atoms.[21] While acylation[22] of 5-monosubstituted tetrazoles selectively proceeds at N(2) in most cases, alkylation is non-selective and resulting in mixes of 1,5 and 2,5 DSTs.[23] Therefore, it is obvious that the position of the electrophile attack strongly depends on the substituent at C(5), the reaction conditions, and the reagent. In addition, the presence of sp^2 hybridization and a conjugated π system in tetrazole enables the electrons to be spread out across the ring, promoting intermolecular interactions between nitrogen atoms.

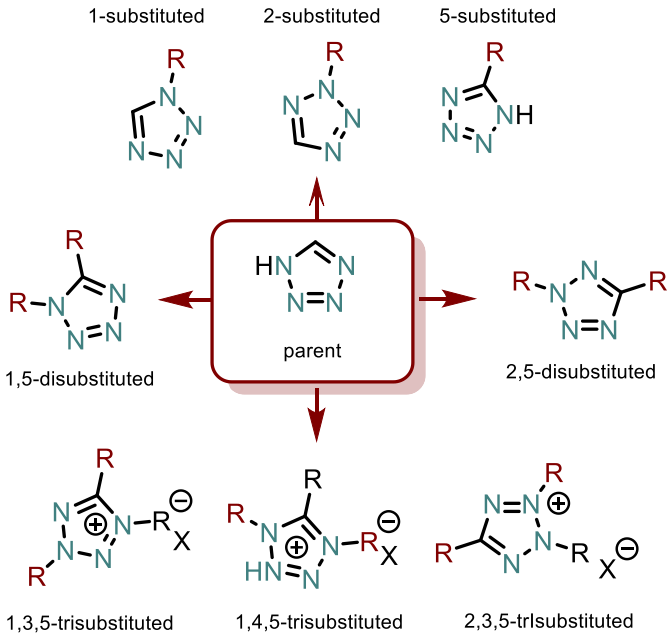

Figure 2. 3 Classification of tetrazoles based on the number of substituents and their position.

This interaction plays a crucial role in enhancing the thermal stability of tetrazoles. However, it should be noted that their stability is often limited, and they have a tendency to decompose around or near their melting point (i.e., 110-130 °C).[24] The type and position of substituents on the tetrazole ring greatly affect both the quantity and characteristics of the degradation products. The diverse stability levels of tetrazoles at different temperatures also lead to the expectation of various decomposition pathways. For instance, 1,5 DST undergo thermolysis by ring opening to form α-azido-imines and loss of N(2), which leads to the creation of an imino nitrene as depicted in **Scheme 2.1.a.** Yet, there are two pathways that can result from 5-substituted tetrazoles degradation; first pathway leads to the corresponding nitrile and HN_3, while the second pathway results in the formation of nitrilimine and nitrogen (N_2) (**Scheme 2.1.b**) In addition, photodegradation of tetrazoles is also possible.[25-26] The result of photolysis using UV light on tetrazoles is the creation of reactive intermediates, but molecular nitrogen formation is also observable. Afterward, these intermediates undergo stabilization through fragmentation and isomerization as also represented in **Scheme 2.1.c**. [27]

Actually, discovery of tetrazoles dates back to the late 19th and early 20th centuries. The first tetrazole derivative was reported by J. A. Bladin in 1885.[28] Like other azole compounds which are nitrogen-rich heterocyclic rings, tetrazoles received little interest; almost a century later only just 300 tetrazole derivatives were known.[9] During the mid-20th century, the potential of the azoles in explosives, photography and agriculture gained importance as key building blocks for the synthesis of a wide range of organic compounds.[15, 29] Particularly, around the sixties, the

discovery of their biochemical and pharmaceutical activities e.g. antiallergic[30], anti-inflammatory[31], antibiotic[32], anti-hypertensive[33] and anti-tubercular agents[34-35] drew the attention back to them. More importantly, tetrazoles have been reported to exhibit fluorescence properties in certain conditions due to capability of delocalizing charges within their unsaturated π-system.[36] The fluorescence emission of tetrazoles can be influenced by factors such as pH[37], solvent polarity[38], and the presence of certain metal ions[39] and exhibit a unique form of luminescence, known as cluster-triggered emission luminescence[40], which is associated with unconventional chromophores. Up to now over 25K tetrazole chemistry researches, such as publications, reviews, and book chapters, have been found in the Scifinder database, exploring advancements in synthesis methods. Accordingly, the next sections will provide a brief introduction to classical synthesis strategies and green routes for tetrazoles and its disubstituted derivatives.

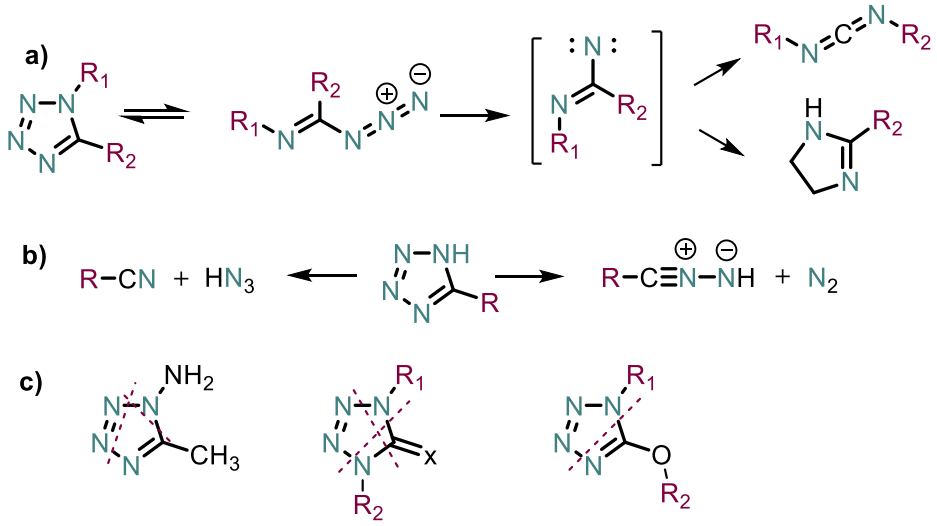

Scheme 2. 1 Schematic representation of the diverse decomposition pathways of a) 1,5-disubstituted tetrazoles, b) 5-substituted tetrazoles, and c) possible photolysis patterns for several tetrazole derivatives, respectively.

3.1.2 Synthesis of tetrazole and its derivatives

One of the well-established classical synthesis methods for the synthesis of monosubstituted-tetrazoles is reacting substituted amines with triethyl orthoformate and sodium azide in water[41] or dimethylsulfoxide (DMSO)[42] (**Scheme 2.2.a**). In the next breath, an effective pathway is developed by utilizing [3+2] cycloaddition reaction between hydrazoic acid (HN_3) and cyanide.[43] Likewise, other synthesis methods are shown in **Scheme 2.2.b**. In principle, isocyanides can be reacted with azidotrimethylsilane in methanol (MeOH) in the presence of a catalytic amount of hydrochloric acid (HCl) at 60 °C to obtain mono substituted tetrazoles.[44] Commonly used method for preparing 5-substituted tetrazoles involves reacting isocyanide,

sodium azide (NaN_3), ammonium chloride (NH_4Cl), and lithium chloride (LiCl) in dimethylformamide (DMF) at 110 °C.[9, 45-46]

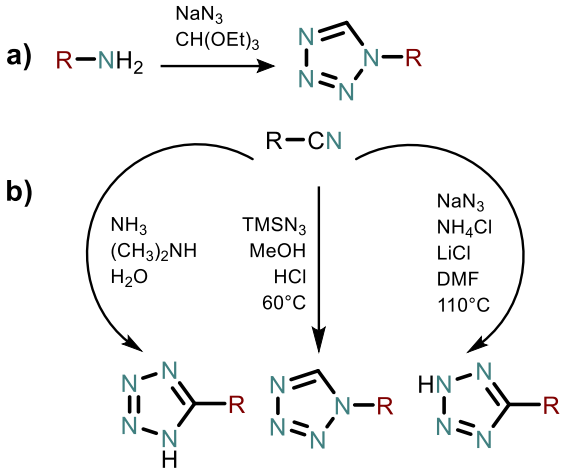

Scheme 2. 2 Some classical synthesis routes of monosubstituted tetrazoles in the presence of a) amine ($R\text{-}NH_2$) with triethyl orthoformate ($CH(Ot)_3$) and sodium azide (NaN_3) and b) isocyanide (R-CN) with dimethylamine ($(CH_3)_2NH$) and (NH_3); azidotrimethylsilane ($TMSN_3$); sodium azide (NaN_3) in the presence of ammonium chloride (NH_4Cl), and lithium chloride (LiCl).

On the other side, there are several classical methods to prepare disubstituted (e.g., 2,5 and 1,5 DST) tetrazoles as shown in **Scheme 2.3**. The synthesis of 2,5 DSTs is known to be considerably challenging.[47] One of the most effective routes for synthesizing 2,5 DST uses lithium trimethylsilyl diazomethane (generated from trimethylsilyl diazomethane ($TMSCHN_2$) and lithium diisopropylamide (LDA)) to react with methyl esters of carboxylic acids at 0 °C, resulting in good yields of the tetrazoles (**Scheme 2.3.a**).[48] Apart from that, an oxyphosphonium salt ($C_3H_9N_3Si$) can be prepared under mild, neutral conditions at 0 °C from amide, followed by reaction with trimethylsilyl azide, leading to the desired 1,5 DST (**Scheme 2.3.b**).[49] However, classical methods are often multistep reactions[50-52] and pose potential hazards due to their harmful and explosive nature, alternative and more environmentally friendly homogenous catalytic methods are currently being introduced to the literature.

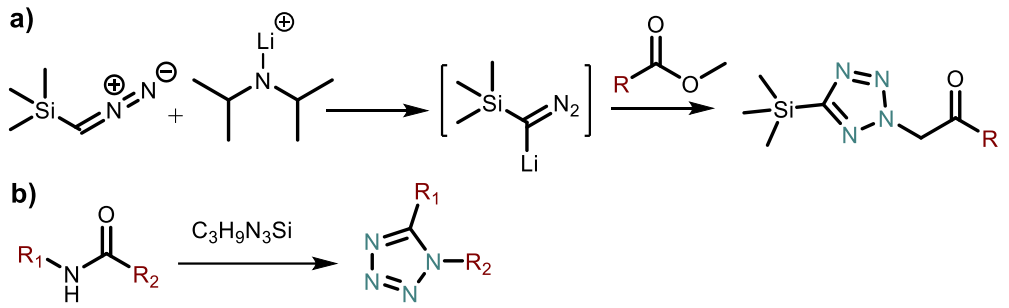

Scheme 2. 3 Some classical synthesis routes of a) 2,5 DST and b) 1,5 DST.

In this regard, recent researches mostly focus on the synthesis of mono substituted tetrazoles in the presence of heterogeneous and homogeneous catalysts (e.g. ZrP_2O_7/ZnS[53], $NiFe_2O_4$[54], Pd/Co[55], gold[56] nanoparticles, Pd[57], *L*-proline[58]) by using [3+2] cycloaddition or multicomponent reactions *via* microwave/ultrasound-assisted synthesis methods.[16] For instance, 2,5 DST can be synthesized by utilizing a Cu_2O-catalyzed aerobic oxidative protocol, which allows to directly cross-couple N-H free tetrazoles with low toxic boronic acids.[47] Also, 2,5 DSTs can be obtained by subjecting one-pot sequential reactions of aryldiazonium salts with amidines to treatment with I_2/KI under basic conditions.[59] This methods allows for the synthesis of 1,5 DST with high efficiency and structural diversity. Upon the exploration of advantages of using catalyst containing systems for the facile synthesis of 1,5 DST, some of catalyst such as $ZnCl_2$[60], $FeCl_3$-SiO_2[61],$CuCl_2$[62] and CuO-NiO-ZnO[63] have been also employed.

However, despite their application in the literature, the various approaches for synthesizing tetrazoles have their own limitations. One major drawback is the significant reaction time involved (that varies from hours to days), which renders the process impractical for numerous synthetic applications. Additionally, these methods heavily depend on the utilization of costly metals, thereby inflating the overall expenses associated with the process. Hence, alternative strategies have been explored to overcome these shortcomings and achieve the synthesis of tetrazoles. One example is a technique that utilizes microwaves to irradiate a reaction of primary alcohols and aldehydes in the presence of iodine and ammonia solution, all in a single vessel (**Scheme 2.4.a**).[64] This resulted in the production of intermediate nitriles, which then underwent [3+2] cycloaddition with dicyandiamide and sodium azide. In similar manner, a range of primary amines with different substitutions were used in a chemical reaction with sodium azide and ethyl orthoformate, which led to the production of 1-monosubstituted tetrazoles (**Scheme 2.4.b**).[65] Due to the diversity of tetrazoles derivatives, there is broad spectrum of method which have been applied. Besides the aforementioned synthesis approaches, one significant approach is the multi-component reaction (MCR), which will be discussed in the following section. Specifically, a comprehensive literature review on the synthesis of 1,5 DSTs *via* MCR, such as the Ugi-multicomponent reaction (Ugi-MCR), will be presented.

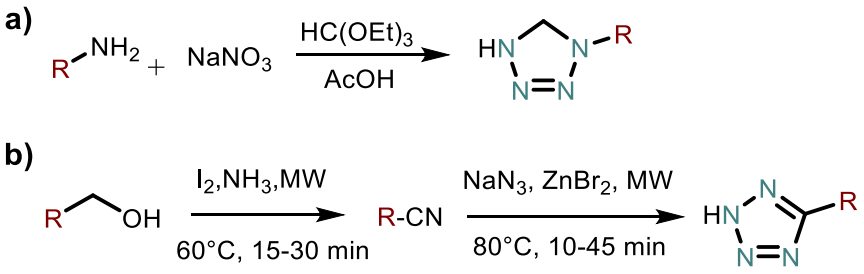

Scheme 2. 4 Some green approaches for the synthesis of tetrazoles.

3.1.3 Characteristics and applications

The increasing demand for environmentally friendly alternatives arises from the toxic nature of existing energetic materials upon decomposition. In this regard, tetrazoles offer a promising solution as they generate only molecular nitrogen and CO/CO_2 as by-products when are decomposed. Consequently, tetrazoles serve as a viable alternative due to their ability to produce decomposition products limited to molecular nitrogen and CO/CO_2. Moreover, tetrazole groups hold great importance in the pharmaceutical industry worldwide, particularly in medications that utilize them as active pharmaceutical ingredients. Furthermore, the field of medicinal chemistry related to tetrazoles is advancing rapidly as new compounds with diverse biological properties and potential therapeutic applications are being discovered. In relation to the topic of the thesis, this section aims to provide a concise overview of the distinctive features of tetrazole and its derivatives, such as their energetic capacity and ability to form metal-ion complexes. Additionally, it will examine their biological aspects, including bioisosterism and various biological activities.

Energetic capacity: Nitrogen-rich heterocyclic compounds with fused rings and conjugated structures are considerably stable and mechanically less sensitive. Therefore, they are ideal for creating new high-performance energetic materials.[66] Indeed the molecular structure of energetic materials determines their enthalpy properties. The incensement of the nitrogen content from imidazole (with a heat of formation of 14.0 kcal mol^{-1})[67], 1,2,4-triazole (with a heat of formation of 26.1 kcal mol^{-1}), to tetrazole (with a heat of formation of 56.7 kcal mol^{-1}) shows an obvious trend in heats of formation. Thereof, tetrazoles are popular choices among chemists as building blocks for high-performance energetic materials.[68] Their nitrogen-rich properties enhance explosive performance and gas production, while their low carbon-hydrogen content results in cleaner combustion products that reduce environmental harm. Additionally, the energy of tetrazole derivatives can be improved by increasing the number of N=N and N-N bonds.[69] For examples, 5-aminotetrazoles[70] been studied as a potential gas-generating compound for use in gas generators[70] and inflators[71] for airbags due to its high gas yield and low toxicity, Similarly, nitro functional groups containing bis/di tetrazole compounds have investigated to discover their potential replacement for the traditional energetic materials.[72]

Metal-ion complexes ability: It has been a long-established fact that the tetrazole ring possesses the capability to form stable chelate complexes with transition metal ions (i.e. Co[73], Pt[74-75], Ni[4]). They can bind to metal ions in different ways, including as monodentate, bidentate, or tridentate ligands.[76] Thus, they have been used in various applications, such as catalysis, sensing, and biological studies. Some example of the use of tetrazoles (e.g., 5-(azulen-1-yldiazenyl)-1*H*-tetrazole,[77] pyridyl-triazole-tetrazole[78]) with complexes of Pb, Co revealed their magnetic and catalytic properties which have been used in the design of highly selective

sensors for biological environmentally applications.[79] Also, Ni metal complexes of some tetrazole derivatives have been reported to possess potential antimicrobial activity against various bacterial and fungal strains.[80] Last but not least, one of the use of tetrazoles (i.e., 2,5 DSTs) complexes with cadmium (Cd),[81] zinc (Zn)[37] have shown fluorescence and phosphorescence which can be utilized in the design of luminescent metal complexes for various applications such as sensing, imaging, and lighting.[82]

***Bioisosterism*:** Bioisosterism refers to the chemical phenomenon of replacing one functional group or atom with another while retaining the biological activity of the original compound. The concept of bioisosterism is widely used in drug design to improve the pharmacokinetic and pharmacodynamic properties of drugs.[83-84] This concept initially defined by Friedman, provides support for the effective integration of tetrazoles as constituents of medicinal materials.[85]

On the one side, the carboxylic acid functional group plays a crucial role in the pharmacophores of various therapeutic agents. Drugs containing carboxylic acid (e.g., antibiotics, anticoagulants, and statins) have been widely marketed globally due to their acidity, strong electrostatic interactions, and ability to form hydrogen bonds.[86] However, carboxylic acids have certain disadvantages, including metabolic instability, toxicity, and limited ability to cross biological membranes, meaning they have low lipophilicity.[87] Thus, in the search for alternatives to carboxylic acids, chemists have turned to tetrazoles as effective bioisosteres.[88] Particularly 5-substituted tetrazole is the best known and the most frequently used bioisosteres of a carboxylic acid functionality.[89] Indeed, tetrazoles and carboxylic acids exhibit planar characteristics; however, tetrazoles possess both aliphatic and aromatic properties and share similar pK_a values (4.5-4.9) compared to carboxylic acids (4.2-4.4). At physiological pH (around 7.4), 5-substituted tetrazoles become ionized and demonstrate 10 times greater lipophilicity than carboxylates (**Figure 2.4**).[14] This increased lipophilicity aids in their binding affinities and enables easier passage through cell membranes. The nitrogen-rich nature of tetrazoles allows for the formation of more hydrogen bonds with receptor recognition sites, thereby enhancing their binding affinity.[90-91]

On the other side, amide functional group (-C(O)NH-) is a very important functional group in biochemistry because of its unique ability to form hydrogen bonding interactions.[92] Hence amide bonds (*cis* or *trans*) is present in many biomolecules, including amino acids, peptides, proteins, nucleotides, and many clinically approved drugs. Despite its valuable role, amides possess limited proteolytic stability. Consequently, researchers have explored the potential of the tetrazole ring as a bioisostere for amides. As a result, the tetrazole ring has gained recognition as a viable substitute for amide bonds.[93-95] Particularly, capability of 1,5 DSTs examined as an amide bioisostere, and subsequently, tetrazole gained attention due to its viability for amide bond replacement (**Figure 2.4**).[96] 1,5 DST ring has a dipole moment to the *cis*-amide bond. It also

has a similar ability to form hydrogen bonds and to participate in hydrophobic interactions with other molecules. These similarities make 1,5 DSTs attractive non-classical bioisosteres of the *cis*-amide bond.[97]

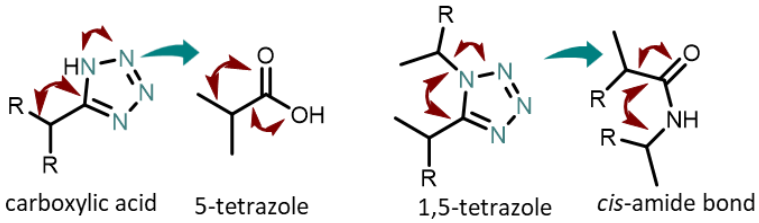

Figure 2. 4 Conformational representation of 5-tetrazole (left-side) and 1,5-tetrazole (right-side) bioisosteres for carboxylic acid and *cis*-amide bond, respectively.

Biological activities: Surprisingly, the rapid advancement of tetrazole chemistry is fuelled by the extensive research conducted in the field of developing new pharmaceuticals.[98] In recent decades, there has been a significant increase in published studies focusing on the biological activity of compounds containing the tetrazole ring. In particular, some derivatives of tetrazoles have been the subject of numerous studies, which reveals their antibacterial and antifungal properties, as well as their potential for anti-inflammatory, analgesic, anticancer, anticonvulsant, antihypertensive, hypoglycemic, antiparasitic, and antiviral activities.[88, 99] Additionally, significant progress has been made in medicinal chemistry with the development of tetrazole-based antifungal drugs.[100] For instance, 1-monosubstituted tetrazole containing drugs (e.g., Oteseconazole, Quilseconazole) have high selectivity and broad-spectrum antifungal capacity. They also possess high activity as anticoagulants due to low lipophilicity and affinity to thrombin's active centres.[101] In recent times, the most remarkable breakthrough in medicinal chemistry concerning 2-monosubstituted tetrazoles is the identification of Cenobamate as an antiepileptic medication which accelerates the inactivation of sodium channels and suppresses the constant component of sodium current and is also a positive allosteric modulator of gamma-aminobutyric acid (GABA) receptors.[102] Additionally, the widespread use of 2-monosubstituted tetrazole as a bioisostere of the carboxyl group is attributed to the success in developing antihypertensive drugs like Losartan and its analogues.[88] Besides, the successful substitution of a carboxyl group with a 5-substituted tetrazole fragment has led to the development of a drug that displays antiarrhythmic activity in both in vitro and in vivo experiments.[103] Aside all these properties, anti-inflammatory effect of 5-substituted tetrazole play an important role in medical biology.[9] Moreover, an increasing number of articles have documented the replacement of an ester group with a 2,5 DST moiety since they have significantly higher metabolic stability in comparison with the ester group.[104] Despite attempts to replace the carboxylic acid ester component with the 2,5 DST structure as a potential treatment for enhancing cognitive function in Alzheimer's disease, the desired efficacy has not been adequately demonstrated. Nevertheless,

the replacement of the 2,5 DST ring resulted in a 20-50 times improvement in effectiveness, greater metabolic stability, improved bioavailability after oral administration, and a significant increase in the duration of action.[105] On the flip side, 1,5 DST moiety exhibited significant biological activities as well (i.e., antibacterial antifungal etc.) which will be discussed in following section in detail.

3.1.4 Reactions of tetrazoles

Tetrazoles are reactive compounds. The reactivity of tetrazoles is a result of their electron-rich nature, aromaticity, resonance effects of multiple nitrogen atoms in the ring. These factors allow tetrazoles to engage in a variety of reactions. Some common reactions of tetrazoles include:

Nucleophilic Substitution Reactions: Tetrazoles can react with nucleophiles, such as amines or alkoxides, to undergo nucleophilic substitution reactions.[106] Additionally, in some cases, tetrazoles can undergo aromatic nucleophilic substitution reactions, where the nucleophile attacks the tetrazole ring and displaces a substituent. This can lead to the introduction of new substituents onto the tetrazole ring.[107]

Ring Opening Reactions: Ring-opening reactions of tetrazoles involve breaking one or more bonds within the tetrazole ring, resulting in the formation of acyclic compounds.[2, 108] These reactions can lead to the introduction of new functional groups and the creation of diverse chemical structures.[109] Furthermore, tetrazoles with electrophilic substituents can undergo nucleophilic ring opening reactions. Nucleophiles attack the electrophilic substituents, resulting in bond cleavage and the formation of new products.[110] This type of reaction is similar to nucleophilic substitution but involves the opening of the tetrazole ring.[27]

Reduction Reactions: Reduction reactions of tetrazoles involve the addition of electrons or hydrogen atoms to the tetrazole ring, leading to the formation of reduced products.[111] These reactions can result in the cleavage of nitrogen-nitrogen bonds or the reduction of other functional groups within the tetrazole molecule.[112] Mostly, tetrazoles can be reduced to corresponding amines using reducing agents like hydrazine or hydrogen gas in the presence of a catalyst. This reduction can occur at the tetrazole ring's nitrogen atoms, leading to the formation of substituted amines (**Scheme 2.5**).[113]

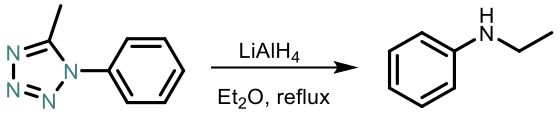

Scheme 2. 5 An example of reduction reaction of 1,5-disubstituted tetrazole.

Oxidation Reactions: Oxidation reactions of tetrazoles involve the addition of oxygen or removal of electrons from the tetrazole molecule, resulting in the formation of oxidized products (**Scheme**

2.6). These reactions can modify the chemical reactivity and properties of tetrazoles and are valuable for synthesizing compounds with different functional groups.

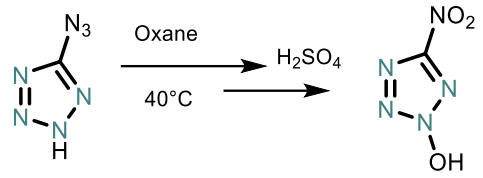

Scheme 2. 6 An example of oxidation reaction of 5-substituted tetrazole.[114]

1,3-Dipolar Cycloaddition (Click Reactions): Tetrazoles are known to participate in 1,3-dipolar cycloaddition reactions, especially with alkynes and nitrile compounds, to form 1,2,3-triazole derivatives. This reaction is commonly referred to as a "click reaction" and is widely used in the synthesis of various compounds and materials. For example, tetrazoles undergo 1,3-dipolar cycloaddition with alkenes which can lead to the formation of pyrazoles (**Scheme 2.7**).[115] This type of reaction often requires high temperatures or other activation methods due to the lower reactivity of alkenes compared to alkynes.[116] Also, when tetrazoles react with nitriles in a 1,3-dipolar cycloaddition it can yield pyrazolines.[117]

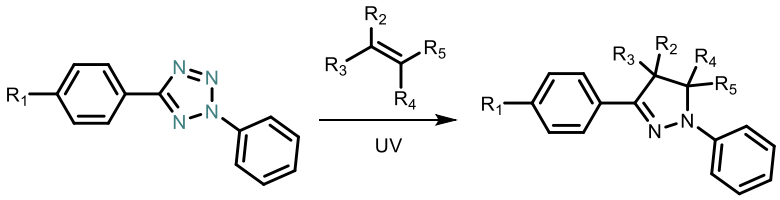

Scheme 2. 7 1,3 dipolar cycloaddition reaction of 2,5-disubstituted tetrazole for the formation of pyrazole.

Tetrazole-thiol reaction: The tetrazole-thiol click reaction, also known as tetrazole-thiol coupling, is a valuable tool in modern organic synthesis, enabling the efficient and regioselective formation of carbon-sulfur bonds under UV irradiation. The reaction occurs rapidly at ambient temperature, demonstrating excellent efficiency and without the presence of any catalyst. The mechanism of the tetrazole-thiol click reaction involves the nucleophilic attack of the sulfur atom of a thiol compound onto a carbon atom of the tetrazole ring with UV irradiation (**Scheme 2.8**).[118]

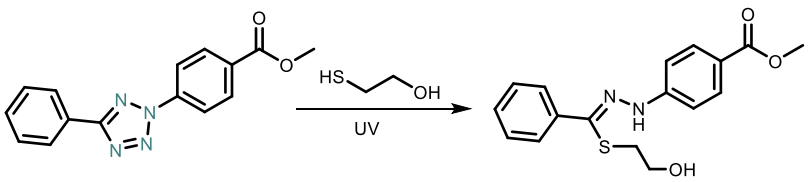

Scheme 2. 8 An example of UV-induced tetrazole-thiol reaction.[118]

3.2 1,5-disubstituted tetrazoles

Among tetrazole family, 1,5 DSTs have been extensively studied because of their bioisosteric nature to *cis*-amide bond that makes them one of the premium classes of heterocycles to be used in medicinal chemistry. as anti-inflammatory antiviral (i.e., human immunodeficiency virus (HIV), antibiotics, antiulcer, anxiety, anti-tubercular.[119-120] Thus, the significance of building up libraries of 1,5 DSTs for high-throughput screening and other low-throughput pharmaceutical research underscores the need for effective and time-saving synthetic methods. In this section, detailed discussions will be held on the properties and applications of 1,5 DSTs, alongside the evaluation of the currently available synthesis methods.

3.2.1 Characteristics and synthesis of 1,5-disubstituted tetrazoles

As expectedly, the high nitrogen content of 1,5 DSTs contributes to their substantial utility as ligands in coordination chemistry and as precursors for nitrogen-rich materials. Notably, their substituted characteristics contribute to their heightened thermal and chemical stability, thus minimizing the probability of decomposition or reactivity with other substances under typical storage and handling conditions. The latter property makes them safer to handle and store than some other energetic materials. In addition, one important optical property of 1,5 DSTs is their ability to fluoresce. When excited by a light source of the appropriate wavelength, they emit light of a different colour.[121] The wavelength of the emitted light can vary depending on the specific tetrazole compound and its environment.[122] Furthermore, 1,5 DSTs can exhibit phosphorescence, which is similar to fluorescence but occurs over a longer timescale. This property is useful in a variety of applications, including the development of organic light-emitting diodes (OLEDs) and other optoelectronic devices.[123] Due to their bioisosteric nature to *cis*-amide bonds, 1,5 DSTs are considered to be among the most valuable classes for use in medicinal chemistry. Because amides (*cis*- or *trans*-) remain a highly regarded and reliable functional group due to their unique characteristics, such as high polarity, stability, and conformational diversity. Furthermore, amide linkages have a dual significance in medicine. Firstly, they are crucial chemical bonds in proteins. Secondly, they serve as the foundational units for numerous synthetic polymers which has application in drug delivery. Their formation is one of the most frequently executed reactions in organic chemistry[124] and pharmaceutical industry.[125] Nonetheless, it is a misconception that there are no remaining challenges in synthesizing them. In reality, finding the ideal strategy for successful synthesis of *cis*-amide bond is challenging, as it heavily depends on the substrates used. One must consider several issues when evaluating and selecting the methodology, such as the problem of chemo selectivity for amidation in the presence of

unprotected hydroxy or amino groups, or the possibility of racemization when using chiral starting materials. Additionally, one must analysis the entire process, considering experimental factors, solvents, reaction temperature, work-up, and isolation procedures, which greatly affect the process mass intensification (PMI). Lastly, the toxicity and environmental impact of the synthetic approach are crucial aspects that need consideration. Hence even the simplest *cis*-amides can be challenging to create, often necessitating the use of more intricate and expensive reagents.[92, 126] As a result, there is a strong demand for new and improved methods of *cis*-amide synthesis since the current synthetic methods have not fulfilled their potential. However, 1,5 DST moiety would be considered as a bioisostere to replace the *cis*-amide bond. Actually, it is a well-established fact that when the amide group is replaced by the tetrazole ring, the biological activity profile of compounds remains intact and there is a significant improvement in their metabolic stability.[14, 127] Therefore the 1,5 DST is gaining attention to be utilized in medicinal chemistry and drug design as amide group bioisosteres. It has been proven that the presence of the 1,5 DST in the drug structure induced the interacting with the target protein and consequently impact of the cellular uptake and drug delivery capacity. This can be because of the interaction of the tetrazole ring with a receptor site enhanced due to ability of all its nitrogen atoms to act as hydrogen bond acceptors. In this regard, another hypothesis is that 1,5 DST is specified as weak bases; however; they have relatively high hydrogen bonding basicity constant compared to traditional proton donors. These facts partially explain why the 1,5 DST ring is capable of forming stable complexes that involve individual atoms and functional groups of targeted molecules such as the catalytic side of cyclooxygenase-2 (COX-2).[128] This characteristic feature gives them anti-inflammatory activity. Additionally, 1,5 DST are important in biology and medicine as nicotinamide adenine dinucleotide phosphate (NAD(P)H) oxidase inhibitors, glucokinase activators, hepatitis C virus (HCV) serine protease NS3 inhibitors, calcitonin gene-related peptide receptor antagonists, and antimigraine agents[129] Moreover, the addition of a 1,5 DST moiety to steroid hormones can have a significant effect on their biological function, which is also important to acknowledge.[130] Furthermore, numerous studies have been conducted to synthesize a variety of compounds containing 1,5 DST and evaluate their antibacterial properties. In fact, several semisynthetic antibiotics from different generations (i.e., Cefazaflur from the first generation[131] and Cefonicid and Cefamandole from the second generation,[132-133]) incorporate the 1-methyl-1*H*-tetrazol-5-ylthiomethyl group into the thiazine portion gives them their antibacterial properties.

Over the past few decades, a number of general approaches have been established for the synthesis of 1,5 DSTs. In the beginning, the Huisgen 1,3-dipolar cycloaddition reaction between nitriles and azides (either azide ion or hydrazoic acid) is a one of the commonly used method for synthesizing 1,5 DSTs.[134-135] However, the range of reactions between nitriles and organic azides is restricted due to the requirement of nitrile substrates possessing strong electron-

withdrawing groups to effectively participate as dipolarophilic partners with organic azides. These groups tend to decrease the energy of the lowest unoccupied molecular orbital (LUMO) in nitriles, thereby promoting their interaction with the highest occupied molecular orbital (HOMO) of the azide.[136] Therefore, in this process, nitriles and azides can react and form 1,5 DSTs without the need for a catalyst, provided that the nitrile has electron-withdrawing groups to activate it. Most of the time, his reaction is carried out at higher temperatures using various nitriles that have these electron-withdrawing groups, resulting in the production of 1,5 DST compounds (**Scheme 2.9.a**).[137] One of the another strategy employed in the synthesis of various 1,5 DSTs involved the combination of aromatic and aliphatic azides with ptoluenesulfonyl cyanide (TsCN) without the use of a solvent (**Scheme 2.9.b**).[134] Based on similar cycloaddition reaction, an efficient method have been developed for synthesizing 1-glycosylmethyl-5-tosyl tetrazoles including benzylated or acetylated glycosylmethyl azides (azidomethyl glycosides) at 100 °C (**Scheme 2.9.c)**.[138] In subsequent reports, the synthesis of 1,5 DSTs has been conducted using acyl cyanides in place of TsCN (**Scheme 2.9.d**). The latter method offers numerous advantages, such as high yields and a straightforward workup process.[139] Similarly, the process of combining organomercury(II) azides with organonitriles through a 1,3-dipolar cycloaddition reaction has been also used for 1,5 DSTs due to several benefits, such as being highly selective, not requiring a catalyst. However, the process also resulted in obtaining the 2,5 DST regioisomers (**Scheme 2.9.e**).[135] Since, the organic azides and nitriles can be combined through intramolecular [3+2] cycloaddition reaction to produce fused 1,5 DSTs products in high yields.[140] If the azide and nitrile functional groups are present in the same molecule, the cycloaddition rates can be significantly improved. Various research groups have illustrated the synthesis of fused polycyclic 1,5 DSTs *via* intramolecular [3+2] cycloaddition reaction where a series of azidoalkyl cyanides were subjected to acid-catalyzed cyclization to generate fused polycyclic 1,5 DST **(Scheme 2.9.f**).[141] Although the reaction pathways involving nitriles and azides resulted in the formation of 1,5 DST, the harsh reaction conditions such as high temperatures and multistep processes required, along with a low yield at the end, were significant drawbacks.

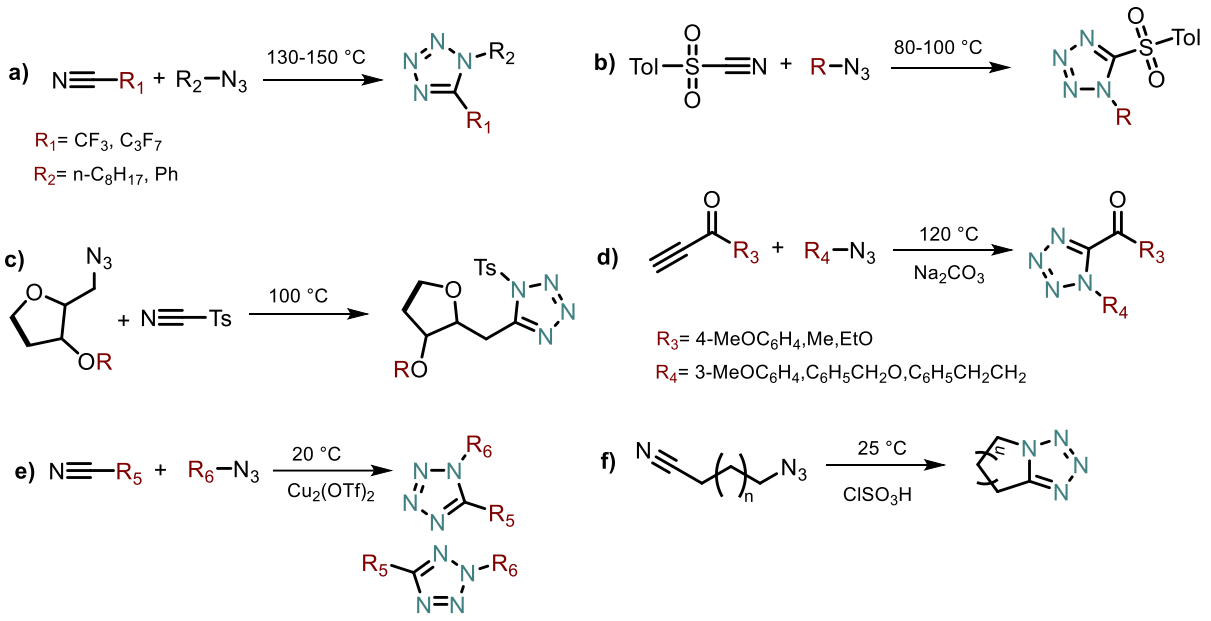

Scheme 2. 9 Some examples of traditional 1,5-disubstituted tetrazoles (1,5 DSTs) synthesis pathways by using azides and nitriles.

In addition, the process of converting an amide or thioamide bond into a 1,5 DSTs has been achieved in the presence of PCl_5[142], $POCl_3$[143], $SOCl_2$[144] *via* formation of imidoyl chloride and imidoyl azide intermediates. It was found that *N*-substituted imidoyl chlorides could be converted into 1,5 DSTs through nucleophilic replacement by an azide ion (from HN_3 or NaN_3), followed by cyclization (**Scheme 2.10.a**).[143] More recently, a variety of commercially available amine and hydrazine compounds have been utilized in conjunction with three parts of cyanogen azide dissolved in a mixture of acetonitrile (MeCN) and water (4:1) to generate a diverse range of imidoyl azide intermediates. These intermediates can undergo cyclization, leading to the production of 1,5 DSTs. Furthermore, this method has been employed to synthesize bis- and tris 1,5 DSTs derivatives.(**Scheme 2.10.b**).[145]

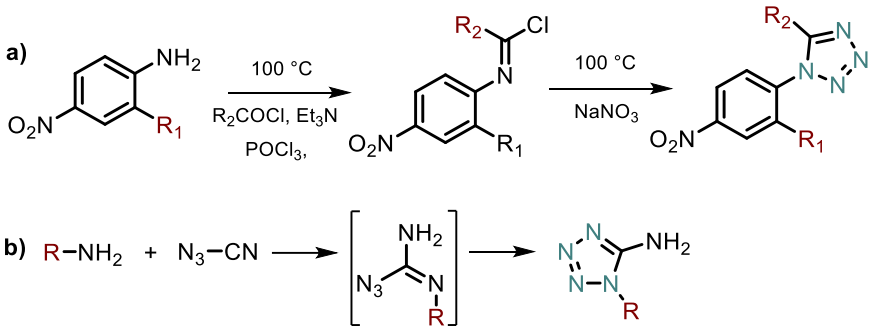

Scheme 2. 10 Some examples of 1,5-disubstituted tetrazoles (1,5 DSTs) synthesis pathways by using amides.

Moreover, several methods have been established for the efficient preparation of 1,5 DSTs utilizing ketones. On one hand, the reaction between $TMSN_3$ and ketones, catalysed by a Lewis acid, through Schmidt rearrangement, proves to be a highly effective process. For example, an efficient system involving the direct transformation of ketones or α,β-unsaturated ketones by using $SiCl_4/NaN_3$ (**Scheme 2.11.a**)[146] and $ZnBr_2/TMSN_3$ have been also used for the formation of to 1,5 DSTs (**Scheme 2.11.b**), [147] respectively. Furthermore, ketones can also be reacted with HN_3 or NaN_3 in the presence of a small amount of $TiCl_4$ to obtain 1,5 DSTs.[148-149]

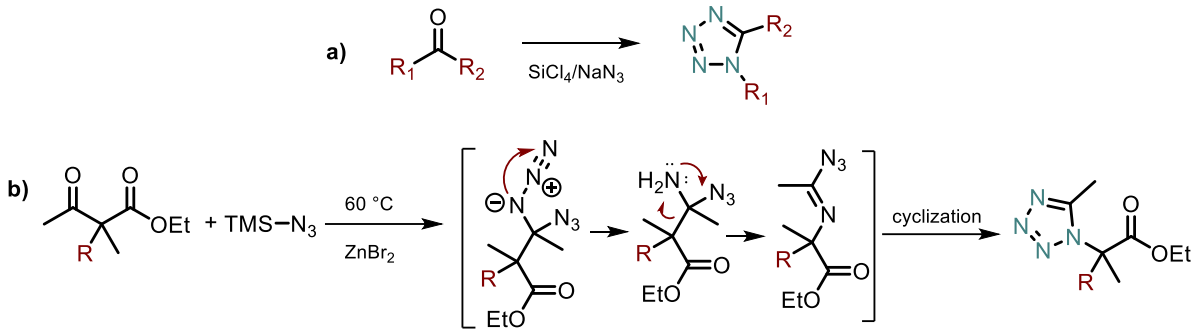

Scheme 2. 11 Some example of 1,5-disubstituted tetrazoles (1,5 DSTs) synthesis pathways by using ketones.

Also, another way for producing 1,5 DSTs involves the substitution of 5-substituted tetrazoles at the N(1) atom. However, this procedure can lead to a mixture of both 1,5- and 2,5 DSTs, and the proportion of each isomer can be influenced by the reaction temperature and the characteristics of the substituent at the 5-position. In recent years, various reactions have been reported that entail the treatment of 5-substituted tetrazoles with alkyl halides in the presence of a base, resulting in a mixture of 1,5- and 2,5 DST derivatives, with the 2,5 DST isomers being the primary products(**Scheme 2.12**).[150-151]

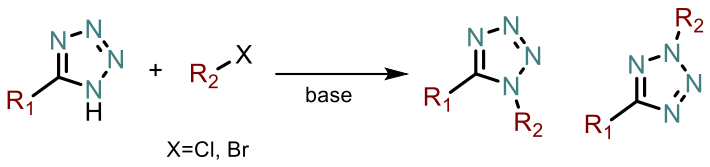

Scheme 2. 12 Example of 1,5-disubstituted tetrazoles (1,5 DSTs) synthesis pathways through 5-monosubstituted tetrazole.

In summary, numerous methods have been developed to enhance the synthesis of 1,5 DSTs. However, these methods often come with drawbacks such as the use of toxic and/or explosive reagents, complicated workup procedures, elevated reaction temperatures, inseparable regioisomers, and the requirement of complex and uncommon starting materials. As a result, researchers have been compelled to search for alternative strategies. Simplifying the process of synthesizing 1,5 DSTs derivatives would greatly increase the value of this compound class, as

ease of use is a critical factor in achieving successful reactions. Thus, a considerable number of studies have been reported in the literature with the aim of addressing the aforementioned drawbacks of 1,5 DST synthesis. For instance, 1,5 DSTs were prepared by using easily accessible starting materials such as amines, with aldehydes, isocyanides and the $TMSN_3$ in MeOH at ambient temperature or using mild microwave initiated conditions under catalyst-free conditions with excellent yields (88-95%), as depicted in **Scheme 2.13.a**.[152] In similar manner, recently, a recent report has detailed an effective technique for producing 1,5 DSTs within a water medium. This procedure makes use of a micellar catalyst named tetradecyltrimethylammonium bromide (TTAB), aligning with the principles of green chemistry. The goal is to decrease or even eliminate the requirement for hazardous substances (such as NaN_3, strong bases, flammable solvents) that could result in the creation of side products. Fundamentally, the synthesis of 1,5 DSTs involves the utilization of $TMSN_3$ as a source of azide, with the reaction taking place in water alongside aldehyde and amine constituents (**Scheme 2.13.b**).[119]

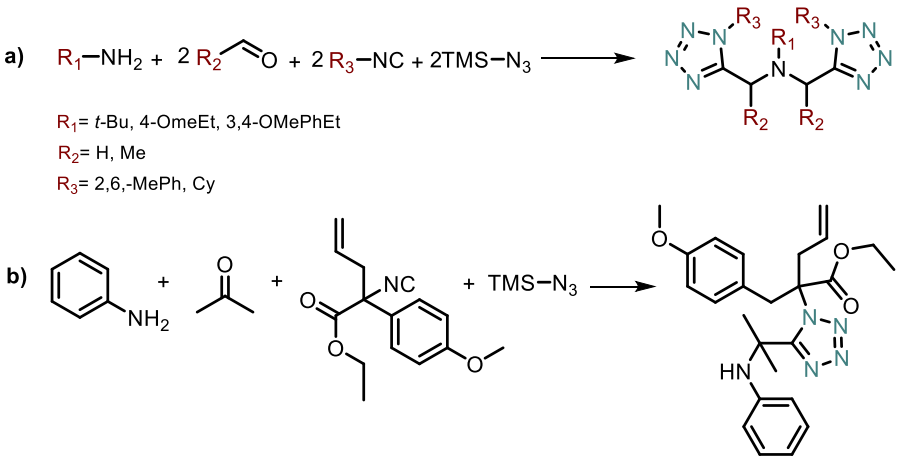

Scheme 2. 13 Some examples of 1,5-disubstituted tetrazoles (1,5 DSTs) synthesis pathways *via* multicomponent reactions in the presence of aldehydes, amides, isocyanides and $TMSN_3$.

Critically, all of these new methods share a common characteristic, which is the utilization of MCRs. MCRs are renowned as one of the most efficient synthetic tools employed in the field of organic chemistry.[153] Indeed, MRCs have several advantages over traditional stepwise synthesis of 1,5 DSTs: i) MCRs) offer the opportunity to synthesize intricate molecules in a solitary step, resulting in time and resource savings when compared to conventional stepwise synthesis techniques. This characteristic renders MCRs an exceedingly efficient and pragmatic approach for synthesizing 1,5 DSTs; ii) MCRs generate a wide range of structurally diverse derivatives of 1,5 DSTs, making them ideal for applications in drug discovery and materials science; iii) MCRs are frequently conducted using mild conditions and a reduced number of reagents, making them a synthesis method that is more ecologically sustainable. This is due to the decreased amount of reaction steps involved, resulting in less waste production and a reduced need for solvents.

Consequently, MCRs have a lesser impact on the environment; iv) MCRs can tolerate a wide range of functional groups, ensuring them highly versatile for the synthesis of diverse structures. Overall, multicomponent reactions offer a highly efficient, versatile, and environmentally friendly approach to synthesizing 1,5 DSTs with diversity.[154] Accordingly, the synthesis of 1,5 DSTs using MRCs will be discussed in detailed in the following section.

3.2.2 Multi component reactions (MRCs) for the synthesis of 1,5-disubstituted tetrazoles

The objective of simplifying the synthesis of 1,5 DSTs with improved ease, efficiency, and affordability has led to a shift in organic synthesis paradigms. In the past, efficiency was primarily measured by selectivity and atom economy. However, the efficiency of reaction processing is also considered significant nowadays. As a result, MCRs have gained popularity for their remarkable ability to synthesize tetrazole and its derivatives with great synthetic efficiency.[155-156]

Typically, MCRs are highly efficient processes in which three or more reactants are combined and effectively transformed into a single resulting product.[157] Bond forming efficiency (BFE) is a key determinant of MRC quality, as it reflects the number of bonds formed in a single operation. Different from traditional approaches, they facilitate the formation of multiple bonds simultaneously, without intermediate isolation, changes to reaction conditions, or the introduction of further reagents (**Figure 2. 5**). BFE significantly enhance molecular complexity and diversity in products due to their ability to incorporate all employed reactants.[158] This allows for the synthesis of compound libraries with a wide range of starting materials, making transferability a key feature for general application. Therefore, MCRs are ideal for 1,5 DSTs synthesis. At the outset of MRCs evolution, the majority relied on traditional reactions involving carbonyl compounds and a range of nucleophiles. Of particular note is the Strecker synthesis, which was the first known MCR and involved the conversion of aldehydes, potassium cyanide, and ammonium chloride into amino acids, as reported in 1850.[159] Subsequently, with more accessible methods for synthesizing isocyanides, a new class of MCRs emerged, known as isocyanide-based multi component reactions (IMCRs).[160-161]

These reactions utilize the distinctive characteristics of isocyanides, which possess both hydrophilic and hydrophobic properties, enabling them to act as nucleophiles and electrophiles simultaneously. In simple terms, an isocyanide, also known as isonitrile or carbylamine, is an organic compound that contains a different isomer of the nitrile group, represented by the functional group N≡C. For over a hundred years, researchers have been investigating its

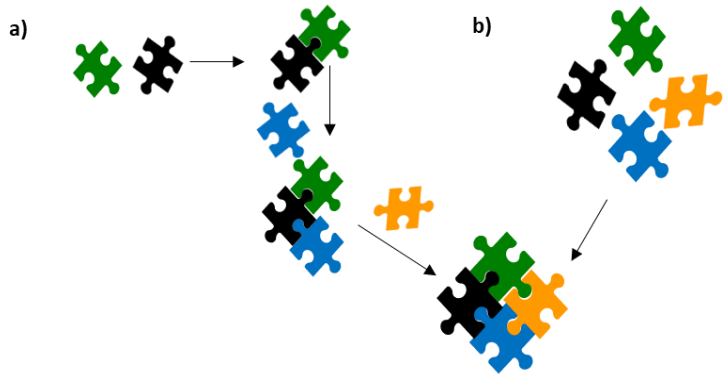

Figure 2. 5 Illustrative comparisons of a a) classical reaction *vs* b) multicomponent reaction.

exceptional structure and reactivity. The reactivity of the isocyanide group distinguishes it from other functional groups. In conventional IMCRs, the crucial intermediate known as the reactive nitrilium ion arises from the interaction between the imine and the isocyanide. Typically, this nitrilium ion is targeted by an external nucleophile. Nevertheless, in the case of bifunctional reactants possessing multiple nucleophilic groups, they can also participate in the MCR. This enables the nitrilium intermediate to be captured by an intramolecular nucleophilic attack, resulting in the formation of diverse heterocycles.[160, 162-164] The Passerini three-component reaction (P-3CR) and the Ugi four-component reaction (U-4CR) are considered the most successful instances of IMCR. These reactions, namely P-3CR and U-4CR, have greatly expanded the scope of possible transformations that can be accomplished for the synthesis of organic compounds.[165] The established procedure for the P-3CR and U-4CR can be seen in Scheme **2.14.a** and **b**, respectively. P-3CR involves the reaction of an aldehyde, an isocyanide, and a carboxylic acid to form a compound with an α-aminoacyl group. In this reaction, the isocyanide acts as a nucleophile and reacts with the carbonyl group of the aldehyde. The carboxylic acid then reacts with the resulting imine to form an α-aminoacyl intermediate, which undergoes cyclization to form the final product.[166] The U-4CR includes the reaction of an amine, an isocyanide, an aldehyde, and a carboxylic acid to form a peptidomimetic compound. The reaction proceeds through the formation of an imine intermediate, which undergoes a nucleophilic addition by the amine to form an intermediate α-aminoamide. The carboxylic acid then reacts with the isocyanide to form an isourea intermediate, which undergoes cyclization with the α-aminoamide to form the final product.[163, 167] In summary, while both P-3CR and U-4CR are multicomponent reactions that involve isocyanides, aldehydes, and carboxylic acids, the U-4CR involves an additional component, an amine, and proceeds through a different intermediate, an α-aminoamide, which then reacts with an isourea intermediate formed from the carboxylic acid and isocyanide.

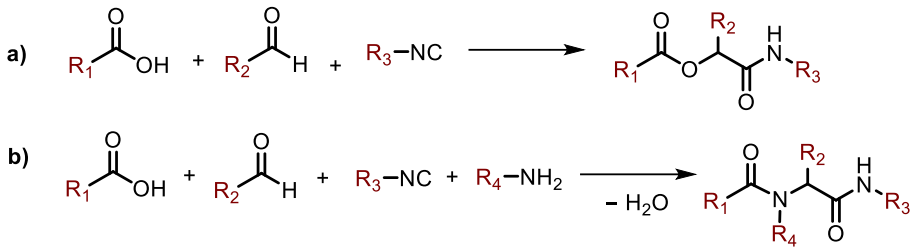

Scheme 2. 14 Schematic representation of a) the Passerini three-component reaction (P-3CR) and b) the Ugi four-component reaction (U-4CR).

P-3CR has been also used for the synthesis of 1,5 DSTS in the literature, particularly after the utilization of HN_3, $Al(N_3)_3$ and [(salen)Al^3Cl][168] as the primary acid isostere, as depicted in **Scheme 2.15**.[169] Since then, this particular reaction has become widely adopted as a typical approach for synthesizing 1,5 DSTs. In particular, a small modification has been made by substituting HN_3 with $TMSN_3$ as the azide source, which has expanded the options for synthesizing tetrazoles in an efficient and sustainable manner.[170-171] However, it is important to note that the reported P-3CRs are not well-suited for aromatic aldehydes.[172] In addition, when $TMSN_3$ was used as an azide provider in the P-3CR, the yield was notably low, and the primary product obtained was TMS-ether. Similarly, when protected amino aldehydes were used in dichloromethane (DCM), the yields were generally low as well, and the reaction times extended up to 96 hours.[171, 173] Moreover, the P-3CR method usually necessitates severe reaction conditions and has a restricted range of starting materials, whereas the U-4CR method can be carried out under milder conditions using various carboxylic acids, amines, aldehydes, and isocyanides. Furthermore, one key benefit of the U-4CR technique is its ability to accommodate a broader array of starting materials and reaction conditions, leading to the formation of more diverse and intricate products compared to the P-3CR method. Consequently, when synthesizing 1,5 DSTs, it is commonly preferred to focus on the U-4CR approach.

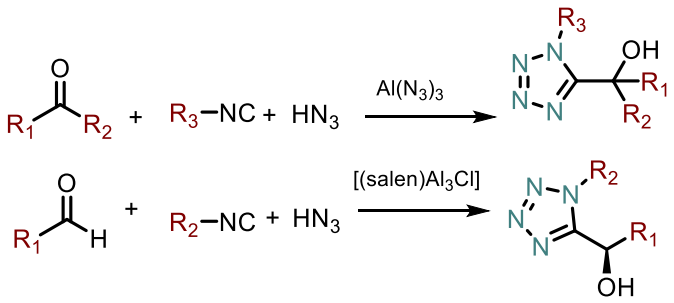

Scheme 2. 15 Some example of 1,5-disubstituted tetrazoles (1,5 DSTs) synthesis pathways *via* Passerini three-component reaction (P-3CR).

Indeed, the process of creating 1,5 DSTs through Ugi-4CR follows a distinct approach compared to conventional techniques. Instead of utilizing a carboxylic acid, which is commonly employed in the classical method, an azide source such as $TMSN_3$ or NaN_3 is used to capture the

intermediate iminium ion. This alternative method results in the formation 1,5 DST compounds. (**Scheme 2.16.)** Thus, it has been named as Ugi-azide Multicomponent reaction (UA-MCR) in which the azide reacts with the isocyanide-iminium ion intermediate to form an azide-iminium ion intermediate, which undergoes a nucleophilic attack by a primary amine to give the final 1,5 DST derivatives. In addition, the UA-MCR is more exothermic than the traditional U-MCR condensation method. Accordingly, the detail information about the synthesis of 1,5 DSTs *via* UA-MCR will be discussed in the following section.

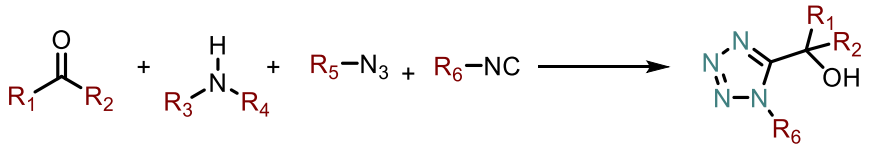

Scheme 2. 16 Representation of 1,5-disubstituted tetrazoles (1,5 DSTs) synthesis pathways *via* Ugi-azide multicomponent reaction (UA-MCR).

3.2.3 Ugi-azide multi component reaction (UA-MCR) for the synthesis of 1,5-disubstituted tetrazoles

As stated earlier, the UA-MCR follows a process where all the reactants, reagents, and catalysts are introduced together at the start of the reaction. They subsequently interact in a predetermined sequence, under identical reaction conditions. While the sequence of introducing components in the Ugi reaction does not significantly affect the yields, it is generally advised to start with the oxo component, then add the amine, followed by the isocyanide, and finally, the azide source.[14] Although methanol is frequently utilized as a solvent in UA-MCR, alternative research has investigated the utilization of 2,2,2-trifluoroethanol, biphasic mixtures of water and chloroform, and tetrahydrofuran, as documented in different literature sources.[174-176] The reaction typically proceeds rapidly at ambient temperature, although some particular combinations of starting materials may require heat activation. While the precise mechanism underlying the reaction remains incompletely understood, it is hypothesized to involve a succession of intermediate steps that ultimately culminate in the generation of the final product.[177]

The UA-MCR can have varying numbers of components, which depend on the particular reaction conditions and the desired compound. At a minimum, the reaction requires three components: an isocyanide, an aldehyde or ketone, and an amine. This combination is commonly referred to as the Ugi-Azide three-component reaction (UA-3MCR).[178-179] However, additional components can be added to the reaction to introduce new functionality or complexity to the final product. For example, the addition of an azide to the reaction mixture can lead to the formation of a tetrazole ring in the final product. In this case, the Ugi-azide MCR would involve four components: an isocyanide, an aldehyde or ketone, an amine, and an azide. In other words, it can

also call Ugi-Azide four component reaction (UA-4MCR). Similarly, the addition of other components such as carboxylic acids, alcohols, or thiols can also be incorporated into the reaction to produce more complex products. As a result, The UA-MCR can encompass different numbers of components, such as five, six, or seven, depending on the specific reaction conditions and the desired product. These variations are known as Ugi-azide five-component reaction (UA-5MCR), Ugi-azide six-component reaction (UA-6MCR), and Ugi-azide seven-component reaction (UA-7MCR), respectively. In this regard, the synthesis of 1,5 DSTs has also been conducted using UA-3MCR, UA-4MCR, UA-6MCR, and UA-7MCR methods. **Figure 2.6** provides an illustrative example showing the various components employed in these processes.[14]

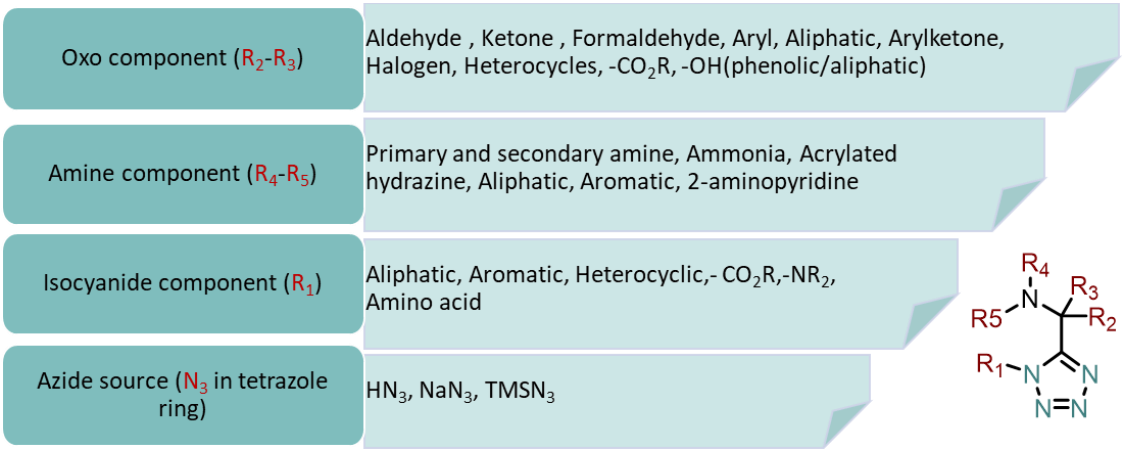

Figure 2. 6 Various components utilized in the production of 1,5-disubstituted tetrazoles (1,5 DSTs) through UA-4MCR.

Due to the toxic and explosive characteristics of HN_3, the use of $TMSN_3$ is preferred as a safe alternative in MCRs.[180] Alternatively, NaN_3 can be used as a hydrazoic acid source. Surprisingly, a convenient synthesis of 1,5 DSTs *via* UA-3CRs is very rare in the literature. For example, very recently, a method, employing a specific proline derivative ligand (*L*-RaPr2), was developed to synthesize asymmetric 1,5 DSTs, 1,2-dihydroisoquinoline, and hydrothiazole derivatives through catalysis. The researchers employed four different techniques to generate two types of enantioenriched derivatives of 1,5 DSTs by utilizing the zwitterionic intermediate formed by an isocyanide nucleophilic attack in alkylidene malonates. This process was facilitated by a proline derivative ligand chiral complex (MgII/*N, N*-dioxide) catalyst. However, the study noted that the yield obtained from UA-3CRs was relatively low in specific cases.[165] Likewise, a method was reported for the production of 1,5 DSTs by employing chiral cyclic imines in the AU-3CR process. The process began with the preparation of chiral imines through a two-step procedure. Firstly, the primary alcoholic group of a chiral lactam was protected, followed by the reduction of the lactam using Zirconium (Zr). Subsequently, the reaction was conducted between chiral cyclic imines $TMSN_3$ and isocyanides, utilizing gentle reaction conditions.[181]

Recently, synthesis of novel 1,5-DT moieties was also designed, synthesized, and evaluated as a copper(II) recognizing agent *via* UA-5MCR as depicted in **Scheme 2.17.a**.[121]. Additionally, Ugi-azide-multicomponent reaction UA-6MCR[182] **(Scheme 2.17.b)** and UA-7MCR (**Scheme 2.17.c**).[183] have been applied in order to obtain bis-1,5 DTs from easily available starting materials with high yield (~75-90%). Consequently, all aforementioned Ugi-azide five, six or seven multicomponent reactions can produce a wide range of molecules with diverse structures and functions in one pot under mild conditions and does not require the use of harsh reagents or high temperatures. Beside they enable the rapid and efficient generation of a large number of structurally diverse compounds, making it an attractive approach for drug discovery and other chemical applications.

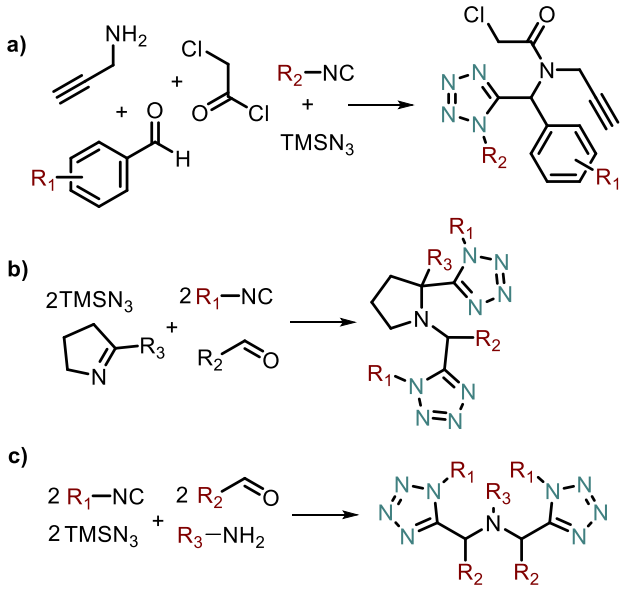

Scheme 2. 17 Some example of 1,5-disubstituted tetrazoles (1,5 DSTs) synthesis pathways *via* Ugi-azide five-component reaction (UA-5MCR), Ugi-azide six-component reaction (UA-6MCR), and Ugi-azide seven-component reaction (UA-7MCR).

However, the reactions UA-5MCR, UA-6MCR, and UA-7MCR mentioned above involve using more intricate initial substances and challenging reaction conditions. These factors can result in reduced yields and increased production of unwanted by-products. Additionally, these reactions necessitate more extensive purification procedures, which can decrease overall reaction efficiency. Consequently, after conducting deep research in the literature, it was found that 1,5 DSTs are typically synthesized through UA-4MCR when compared to alternative reaction partners, unless a highly complex molecular structure is specifically needed. Accordingly, the detail information about the synthesis of 1,5 DSTs *via* UA-4MCR will be discussed in the following section.

3.2.4 UA-4MCR for 1,5-disubstituted tetrazoles

As the demand for more efficient and sustainable methods of chemical synthesis continues to grow, the UA-4MCR holds significant promise in the field of organic chemistry. The versatility, efficiency, and ability of UA-4MCR to produce compound libraries make it a valuable tool in drug discovery, particularly for synthesizing a wide range of tetrazole derivatives. Despite lacking a complete understanding, the estimated mechanism of the AU-4MCR can be elucidated through the subsequent explanation. From the point of 1,5 DSTs synthesis, the general mechanism of the AU-4CR subdivided into four diverse steps in the literature. In the initially step, the iminium-ion is formed by a reaction between an aldehyde with a secondary amine.[183] Upon the formation of an iminium-ion, the isocyanide reacts as a nucleophilic reaction partner and undergoes an addition reaction on the charged side of the iminium ion. Thereby a farther charged intermediate is generated, which undergoes an addition with the formed hydrazoic acid.[183] The last step of the reaction is the ring forming step which delivers the 1,5 DST (**Scheme 2.18**). This reaction is performed at ambient temperature due to the high energetic substances which can easily explode at high temperatures.

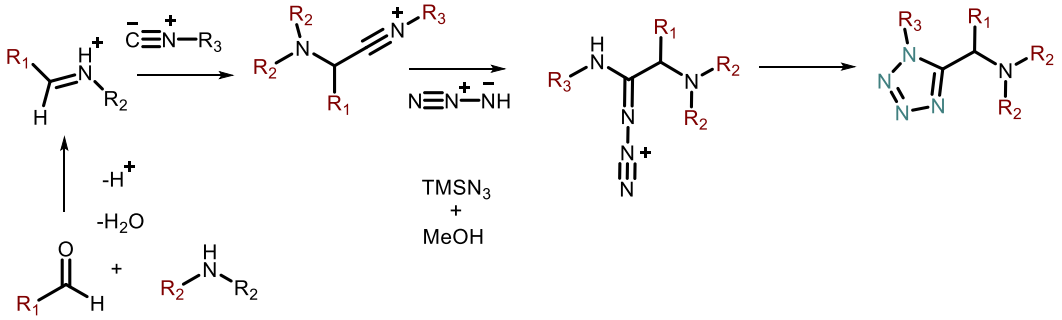

Scheme 2. 18 Estimated mechanism of the reaction of Ugi-azide four-multicomponent reaction (UA-4MCR) for the synthesis of 1,5-disubstituted tetrazoles (1,5 DSTs).

There are numerous publications about the synthesize of 1,5 DST and its derivatives *via* AU-4CR reaction in the literature.[45, 152, 184-188] In general, it has been observed that the oxo components, namely aldehydes, ketones, and their substituted variants, exhibit excellent performance. Additionally, both primary and secondary aliphatic or aromatic amines are highly compatible with the AU-4CR reaction mechanism. Furthermore, the AU-4CR process can accommodate both aromatic and aliphatic isocyanides, and functional groups present on the isocyanide side chain are generally well-tolerated.[189] Taken to the together, The AU-4CR is a remarkably simple process that can be effectively applied to a wide range of starting materials, resulting in the production of various complex functionalized structures. For instance, very recently, a notable achievement has been the synthesis of quarter 1,5 DSTs incorporating tetrazole derivatives (e.g., 1,4,7,10-tetrakis((1*H*-tetrazol-5-yl) methyl)-1,4,7,10-tetraazacyclo-dodecane (TEMDO) *via* UA-4MCR which have shown excellent yields (>99%) as chelating

agents for imaging, as shown in **Scheme 2.19.a**. Subsequently the four β-cyanoethyl groups were selectively cleaved using NaOH at ambient temperature, yielding highly pure TEMDO ligand (86%) in order to assess the chelating property of TEMDO towards the lanthanide element gadolinium.[190] Following the same line, same group have reported the synthesis of novel and complex molecules of tetrakis-tetrazole *via* UA-4MCR in one pot manner from easily accessible starting materials to use as chelating agents and organ catalysts (**Scheme 2.19.b**).[191]

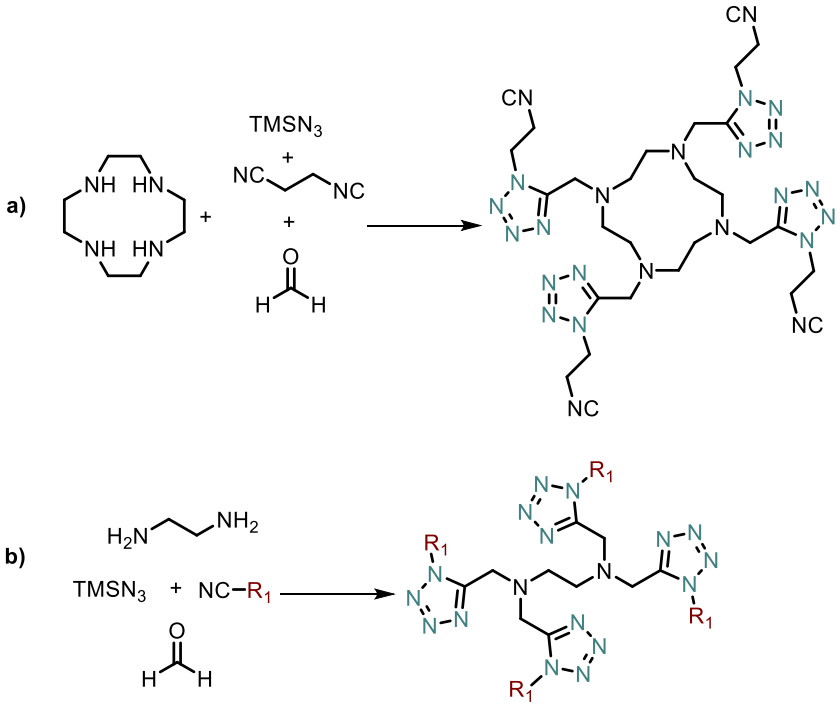

Scheme 2. 19 Example of synthesizing complex 1,5-disubstituted tetrazoles (1,5 DSTs) *via* Ugi-azide four-multicomponent reaction (UA-4MCR).

Overall, tetrazoles, especially 1,5 DSTs are a class of organic compounds with unique physical and chemical in addition to biological properties that make them highly useful in a variety of applications, including in polymer chemistry. Their ability to form strong hydrogen bonds and their high polarity make them ideal for use in the synthesis of polyelectrolytes, functional polymers, and materials for energy storage. As research continues into new materials and their applications, it is highly probable that tetrazoles will continue to play an important role in the development of such materials that possess unique and beneficial properties. Therefore, the subsequent section will provide an overview of tetrazole-containing polymers, highlighting their potential for utilization by leveraging the aforementioned properties.

3.3 Tetrazoles in polymer chemistry

Indeed, distinct characteristics of tetrazoles, including exceptional thermal stability, favourable solubility in diverse solvents, and versatile reactivity towards functional groups, render them valuable in a wide range of applications. Especially, tetrazoles play a significant role in polymer chemistry by serving as a nitrogen source for the synthesis of polymers containing nitrogen. These nitrogen-containing polymers hold immense potential across a diverse range of applications, such as gas separation, the development of electroactive materials, and the production of military or civil explosives. In this context, there is a good example of tetrazole-containing polymer which has been synthetized *via* chain-growth polymerization of vinyltetrazole monomers[192-193] by thermal initiated free-radical polymerization in the presence of initiator (i.e., azobisisobutyronitrile (AIBN), 2,2'-Azobis(2-methylpropionamidine) dihydrochloride (V50)), resulting in the production of side chain polyvinyl tetrazole (PVT) polymers [10, 194], as can be seen **Scheme 2.20.a**. Furthermore, the present literature has utilized the free radical polymerization based on tetrazole-containing (meth)acrylamide monomers to reveal superabsorbent polymer gels (**Scheme 2.20.b**).[195-196]

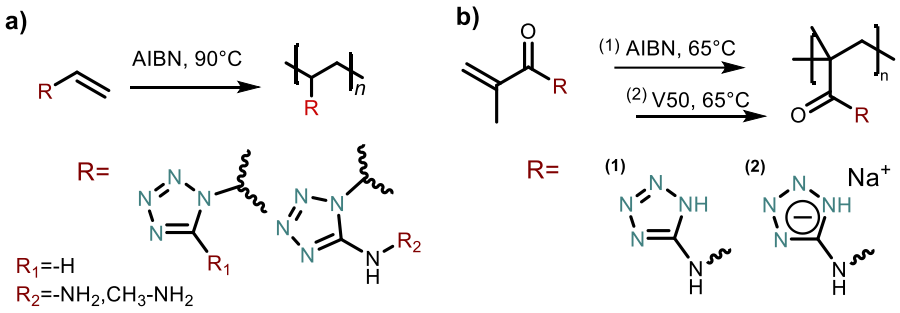

Scheme 2. 20 Some example of tetrazole-tethered polymer synthesis *via* chain-growth polymerization.

In addition to employing free radical polymerization, an alternative and widely employed method for delivering tetrazole-containing polymers involves post-polymerization modification reactions. This synthetic approach offers a *via*ble strategy for modifying polymers with tetrazole functionalities. In this approach nitrile group containing aliphatic-[197-198] (**Scheme 2.21.a**) and aromatic-[199-201] (**Scheme 2.21.b**) based polymers could reacted with sodium azide *via* [2+3] cycloaddition of nitrile groups with sodium azide for the applications of gas generating systems and electrolyte membrane fuel cells, respectively. This approach refers to a set of reactions that are highly efficient, selective, and proceed under mild conditions in the presence of metal catalyst (e.g., $ZnBr_2$, $ZnCl_3$) to create tetrazole-tethered polymeric structures. Furthermore, the incorporation of tetrazole moieties into the polymer backbone can be achieved through the utilization of polyvinylchloride (PVC) as a polymer precursor, whereby the reaction between

PVC and tetrazole anion initiates the expulsion of hydrogen chloride and the subsequent inclusion of tetrazole moieties within the polymer backbone.[202]

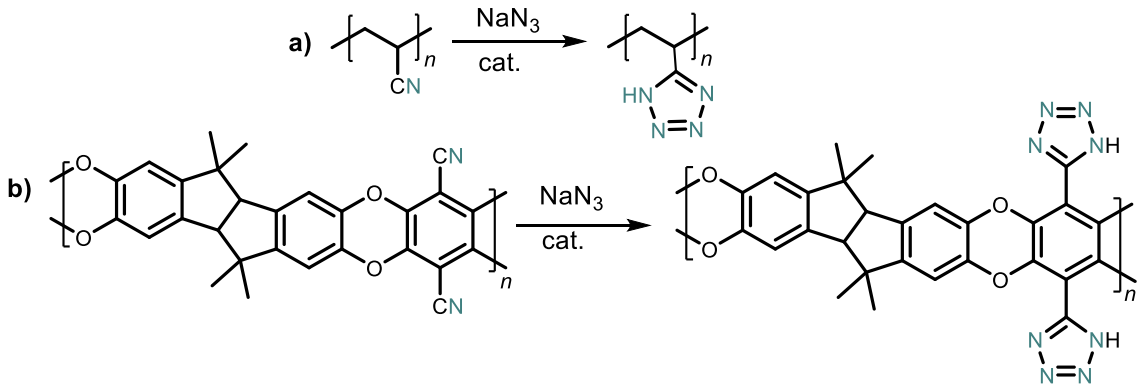

Scheme 2. 21 Some example of tetrazole-tethered polymer synthesis *via* post-polymerization reaction.

Furthermore, a few examples of synthesis of tetrazole-based polymers *via* polycondensation is also available in the literature as promising candidates for energetic applications. For instance, 5-chloromethyltetrazole has been utilized to polyvinyl tetrazole polymers due to its dual properties as both a nucleophile (tetrazole-NH) and a highly electrophilic compound (CH_2Cl). When triethylamine (TEA) is present as a base, the tetrazole ring can be deprotonated, resulting in the formation of polyalkylation, namely poly (methylene tetrazole) (M_n=2.0 kg mol^{-1}) (**Scheme 2.22**). It is important to note that the polymer possesses a high nitrogen content of up to 68%, which is almost 10% more than PVT which could be a suitable option for gas-generating systems.[203] Aside, the synthesis of tetrazole-containing polymers with various structures can be achieved through combination of polycondensation, followed by polyalkylation reaction.[204-205]

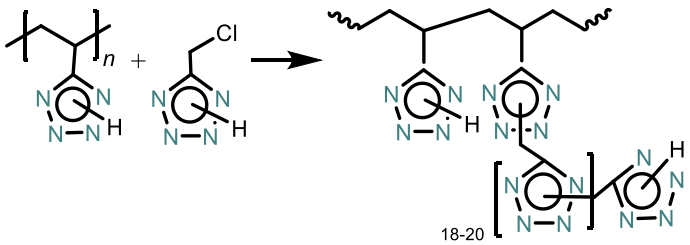

Scheme 2. 22 Tetrazole-containing polymer synthesis *via* polycondensation polymerization.[203]

Apart from above mentioned methods, the use of polymeric precursors containing hydroxy groups is a different method for synthesizing tetrazole-containing polymers. The process involves adding acrylonitrile to the hydroxy groups of the polymer, followed by converting the nitrile groups into tetrazole rings. In the literature, this protocol was utilized to synthesize tetrazolylethylated cellulose, and nearly complete conversion of the hydroxy and nitrile groups was achieved during the cyanoethylation and azidation steps, as depicted in **Scheme 2.23**.[206] In parallel with, the synthesis of tetrazole containing natural based polymers by using chitosan,

starch, and arabinogalactan have been also synthesized to generate hydrogel networks that are able to form polyelectrolyte in aqueous environments.[207]

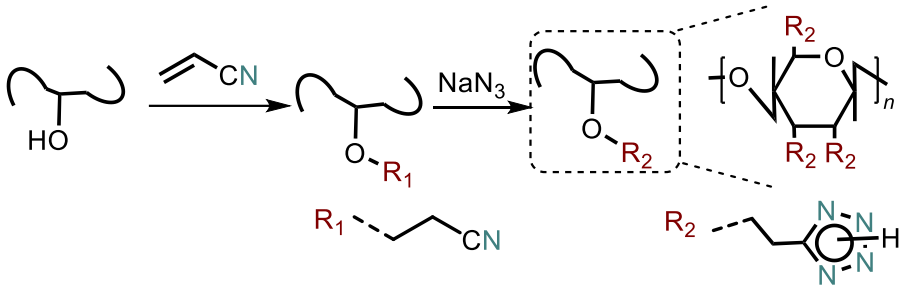

Scheme 2. 23 Tetrazole-containing polymer synthesis through hydroxy (-OH) group.

Additionally, the literature acknowledged the introduction of a methacrylate monomer containing both tetrazole and azobenzene for the synthesis of polymers through reversible addition fragmentation chain transfer (RAFT) polymerization. However, insufficient attention was given by the authors to the existence of tetrazole. Their main emphasis in examining the well-defined (co)polymers was centred on the behaviour of the attached azo- group during photoisomerization.[208] Later on, a significant contributions were made to the literature through the development of well-defined luminescent Re(I)-polymer hybrid materials by using tetrazole moiety. Briefly, this was achieved *via* the utilization of (RAFT) polymerization of pentafluorophenyl acrylate (p(PFPA)), followed by post-polymerization modification with 5-tetrazole unit. The tetrazole-containing polymers were utilized as macromolecular ligands for rhenium(I) tricarbonyl diimine luminescent complexes, with direct coordination to the tetrazolato species.[209] In addition, the synthesis of tetrazole-containing random copolymers was demonstrated by photopolymerization of p(PFPA), followed by post-polymerization modification of activated ester side-groups with primary amine-containing 5-tetrazole moieties. These copolymers are served as macromolecular chelating species for luminescent Ir(III) and Re(I) metal, investigating tissue imaging applications, with the potential to be tuned in both luminescent properties and biological specificity.[210] Consequently, the introduction of new functionalities to the resulting polymers by attaching tetrazole groups was deemed innovative, but the resulting linear polymers were found to have limitations in terms of mechanical strength, thermal stability, and chemical resistance due to their morphological properties. More importantly, despite the widespread use of poly(pentafluorophenyl acrylate) p(PFPA), polymers, there exists only one instance of utilizing p(PFPA) polymers to achieve insoluble networks.[211]

In conclusion, there has been a significant focus on the incorporation of tetrazole units in polymers due to their energetic and coordination properties. This has led to a valuable example of tetrazole-containing polymers in the literature. Explicitly, the researchers have mainly concentrated on the 5-monosubstituted tetrazole unit, disregarding the other members within the

tetrazole family. However, the primary issue with 5-monosubstituted tetrazole is its limited and challenging control over regioselectivity. Whether the tetrazolat anion is alkylated with or without a substituent at the 5-position, it typically results in a combination of 1- and 2-alkyltetrazole isomers in different proportions Similarly, other modifications like arylation and acylation follow a similar pattern.[212] Therefore, aforementioned synthetic strategies have not adequately addressed the integration of different tetrazole units into the polymeric structure. Hence, alternative synthesis strategies are required to facilitate the production of highly diverse and complex tetrazole-containing polymeric structures, using simple precursors and yielding high yields. Most importantly, 1,5 DSTs, one of the most significant members of tetrazoles, are even considered as isosteres for the *cis*-amide bond in peptides, they have not been integrated into polymer chemistry. Only a limited number of polymers incorporating 1,5 DSTs have been identified in the literature. Accordingly, the following chapter of thesis will give an overview about 1,5 DSTs and their existing application in polymer chemistry.

3.3.1 1,5-disubstituted tetrazoles in polymer chemistry

It is a widely acknowledged fact that the introduction of novel groups into polymer chemistry is indispensable for advancing the field. The ability to fine-tune polymer properties and create new types of polymers with unique characteristics is crucial for the development of innovative applications across various fields. Moreover, the exploration of novel groups as a basis for new synthetic strategies can lead to the formation of polymers with intricate and customized structures. Surprisingly, despite their significance as nitrogen-rich heterocycles, 1,5 DST have not received substantial attention in polymer chemistry. Specifically, there are only a few notable examples of 1,5 DST-containing polymers documented in the literature.

The first examples of 1,5 DST-containing polymers in the literature were introduced *via* in situ 1,5 DST formation through a [2+3] cycloaddition reaction with azide derivatives on polyacrylonitrile polymers **(Scheme 2.21.a**). This method is simple and convenient, and uses cheap and commercially available acrylonitrile monomer.[13] Apart from that ,1,5 DST moiety has been used for special application, in an alkaline anion exchange membrane to obtain 1,5 DST-decorated polymers with a quaternary ammonium (QA) linkage. It has been reported that the presence of tetrazole moiety contributes on the formation of long range hydrogen bond network which facilitates the alignment of QA groups, promoting the hydroxide ion transport at a low water content (**Scheme 2.24**).[11]

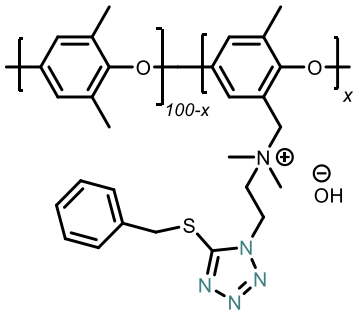

Scheme 2. 24 Example of 1,5-disubstituted tetrazoles (1,5 DST)-tethered polymers as an alkaline anion exchange membrane

For the first time, main chain 1,5 DST-based polymers were synthesized by polymerizing 1-(2-hydroxyethyl)-1*H*-tetrazolyl)methyl-hydrazine and hexamethylene diisocyanate *via* polycondensation in bulk. These polymers possess a nitrogen content of 33% and exhibit high thermal stability up to 260 °C, as well as no sensitivity towards friction or impact (**Scheme 2.25.a)**.[213] The same research group, later, investigated various synthesis pathways for main chain 1,5 DST-based nitrogen-rich energetic polymers, employing radical, anionic, and cationic polymerization methods in solution. However, it was found that only the radical polymerization approach yielded promising materials for the development of new gas-generating compositions (**Scheme 2.25.b**).[214] Additionally, the research group utilized both 1-(1-vinyl-1*H*-tetrazol-5-yl) hydrazine and 1-methyl-1-(1-vinyl-1*H*-tetrazol-5-yl) hydrazine, obtained through substitution reactions of hydrazine derivatives and 5-bromo-1-vinyl-1*H*-tetrazole, to synthesize 1,5 DST-tethered polymers *via* radical polymerization strategy. Subsequently, the poly-1-(1-vinyl-1*H*-tetrazol-5-yl) hydrazine was converted into the corresponding 5-azidotetrazolyl-containing polymer through a reaction with sodium nitrite to enrich the range of polymer types and investigate their energetic characteristics (**Scheme 2.25.c**).[10]

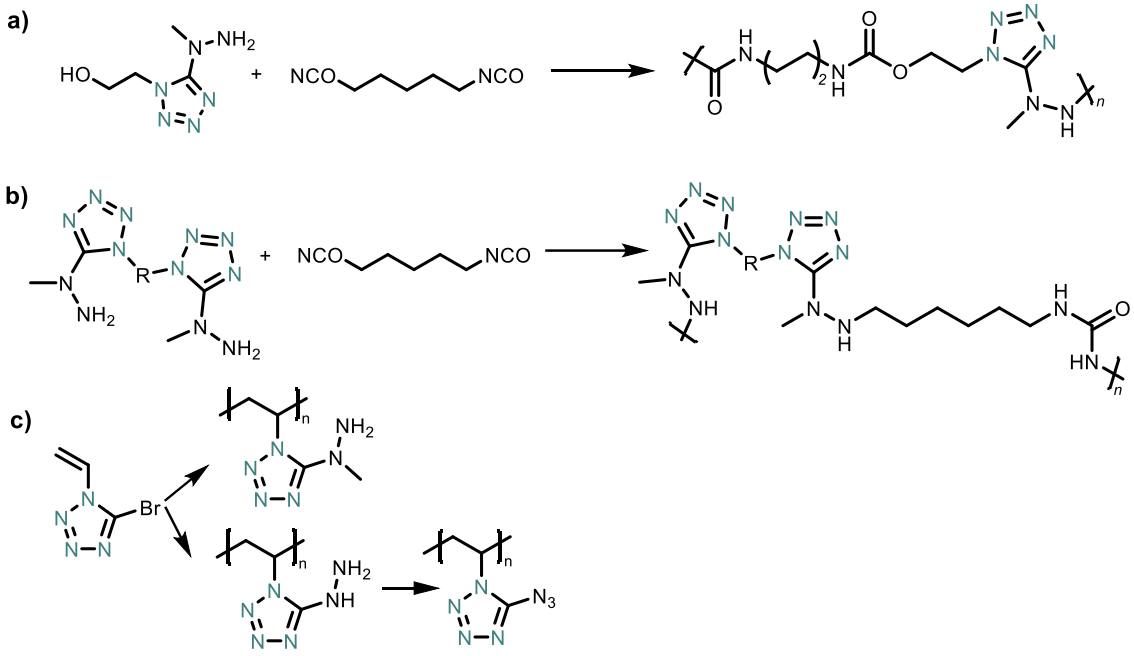

Scheme 2. 25. A few examples of synthesizing a, b) main chain 1,5-disubstituted tetrazoles (1,5 DST)-based; and c) 1,5 DST-decorated polymers.

In conclusion, it can be stated that tetrazoles are continuously attracting interest in the field of polymeric science. In the coming years, a variety of applications involving tetrazole-based electrolyte membranes[215] or as environmental friendly nitrogen-rich polymers[10], may be explored in the literature. However, to the best of my knowledge, there are currently no other 1,5 DST-containing polymers in the existing literature.

3.4 Synthetic toolboxes for the synthesis 1,5-disubstituted tetrazole-containing polymeric systems

Synthetic toolboxes for synthesizing 1,5 DST-containing polymeric systems refer to a collection of techniques and methodologies used to create and manipulate polymers with controlled structures and properties. Given the focus of this thesis, in-depth discussions will be given in the following sections about post-polymerization modification and thiol-ene chemistry to provide a thorough comprehension.

3.4.1 Post-polymerization modification

Modern polymer chemistry toolbox is captivating, offering infinite possibilities to produce original materials with exceptional attributes. It is possible to produce materials with varying characteristics like strength, flexibility, and transparency by selecting the appropriate building blocks and combining methods while maintaining precise control over the composition, molecular weight, and architecture of the polymers. Apart from that, polymer chemistry can also be used to modify existing materials to provide new features to the polymer. For this purpose, post-polymerization modification (PPM) is a technique that allows for the modification of polymer structures after their initial formation, facilitating the development of advanced polymeric materials.[216] (**Figure 2.8**) The fundamental idea behind this approach is to polymerize or copolymerize monomers that have chemo selective handles and are inert towards polymerization conditions. The procedure leads to the formation of reactive precursor polymers, which can subsequently be converted into different functional groups with great effectiveness. PPM is the preferred choice for generating organized polymer libraries due to its numerous advantages.[217] These benefits arise from its ability to systematically integrate multiple functional groups in a controlled manner, eliminating the need for complex synthesis methods. Moreover, it excels in incorporating functional groups that are not compatible with typical polymerization conditions.[218]

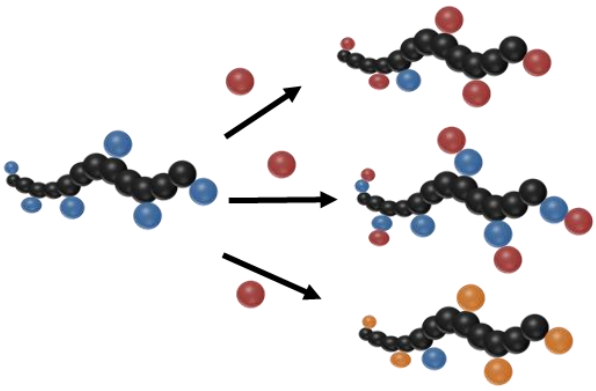

Figure 2. 7 Schematic representation showing the process of creating polymers through post-polymerization modification

In the literature, there are several commonly used precursor polymers, such as polymeric active esters, polymeric anhydrides, isocyanates, oxazolones, and epoxides.[216] Among them a detailed explanation will be provided on polymeric active esters; with a specific focus on pentafluorophenyl (PFP)-based polymers within the framework of the thesis in the following section.

3.4.1.1 Post-polymerization modification *via* Activated Esters

Polymeric active esters have shown great potential for creating reactive precursor polymers due to their lack of metal and the use of mild reaction conditions. This discovery was initially reported by Ferruti et al.[219] and Ringsdorf et al.[220] in the 1970s. Among the extensively studied polymeric active esters, *N*-hydroxysuccinimide (NHS) based active ester polymers and pentafluorophenyl (PFP)-based active ester polymers have gained significant popularity.

The active ester polymers within the NHS group such as poly(*N*-hydroxysuccinimide acrylate) p(NAS) and poly(*N*-hydroxysuccinimide methacrylate) p(NMAS) are considered the oldest. Impressively, they possess a dual benefit. Firstly, they exhibit a reasonable level of resistance to hydrolysis, although not completely impervious. Secondly, they can readily undergo nucleophilic aminolysis with primary and secondary amines, producing functionalized derivatives of polyacrylamide, all under mild reaction conditions. However, it is crucial to acknowledge that the disadvantages associated with NHS-based active ester polymers cannot be negligible. The limited solubility of p(NAS) and p(NMAS) in most organic solvents, except for DMF and DMSO, restricts their use as standard polymers. Hence, NAS and NMAS are commonly copolymerized with other monomers to enhance the solubility of the resulting polymer. As a result, it leads to the inclusion of additional work-up routine. Furthermore, side reactions can occur during the aminolysis step, such as the succinimide functionality undergoing ring-opening and the formation of *N*-substituted glutarimides when amides attack neighbouring activated esters.[221] Consequently, post-polymerization of NHS-based active ester polymers is considered more challenging compared to their counterparts, which are based on pentafluorophenyl (PFP) active esters.

In fact, PFP-based active ester polymers such as p(PFPA) or poly (pentafluorophenyl methyl acrylate) (p(PFPMA)) have emerged as valuable fluorinated polymers in recent years due to their unique properties, including high thermal stability, increased reactivity, chemical resistance, enhanced solubility, and low surface energy. Critically, p(PFPA) and p (PFPMA) have the ability to be dissolved in a wide range of organic solvents, including DCM, tetrahydrofuran (THF), 1,4 dioxane, and DMF. Moreover, they have slightly higher reactivity compared to NHS ester-based polymers. Furthermore, PFP ester-based polymers can be conveniently tracked using ^{19}F NMR spectroscopy due to the presence of fluorine on the PFP leaving group, enabling easy monitoring of their PPM. PFP-based active ester polymers can be obtained by homopolymerizing PFP ester monomers through either free radical polymerization[222] or RAFT[223] polymerization. Following the polymerization process, PFP ester-containing polymers can undergo different chemical reactions, including nucleophilic amine substitution and transesterification for PPM. On the one hand, the transesterification approach stands out as the predominant and extensively employed method in various fields of PPM.

A comprehensive investigation of p(PFPA) efficacy and adaptability was presented in 2015, which effectively showcased its potential for anchoring a wide range of functional alcohols, encompassing primary, secondary, and phenolic alcohols, that feature diverse functional groups such as alkene, alkyne, or acrylate, to the PFP sites through substitution. Moreover, this research also demonstrated the ability of the transesterification process to enable sequential functionalization of the resulting product through click reactions, thereby showcasing its versatility and potential for further applications.[224] Interestingly, the substitution of PFP esters with nucleophilic amines has been discovered as a straightforward method to achieve a wide range of functions by undergoing simple reactions with complete conversion.[225] For instance, post-polymerization modification of p(PFPA) films with amines has been used to obtain free-standing robust fluorescent films by layer-by-layer assembly based on covalent bonds between active ester polymers and poly(allyl amine).[226] As a conclusion, , it was observed that the ratio of substitution is influenced by the specific type of amine derivatives. Primary amines exhibit a stronger attraction to PFP esters compared to secondary amines, whereas aromatic amines display the least capability for substitution. However, to gain more insights into the PPM of p(PFPA) polymers by active ester-amine chemistry was required for practical applications.

Last but not least, it is important mentioned when the fluorine atom incorporated into polymers, it forms a robust C-F bond (485 kJ mol^{-1}). By replacing five hydrogen atoms on phenyl groups with five electron-withdrawing fluorine atoms, PFP aromatic groups are produced. These PFP groups feature a highly positive para-carbon atom, making them susceptible to attack by nucleophiles, resulting in the formation of 2,3,5,6-tetrafluorophenyl derivatives through a reaction known as para-fluoro substitution reaction (PFSR). The inclusion of this strategic substitution enhances the versatility of polymer materials that incorporate PFP groups. Consequently, it serves as a valuable tool for post-polymerization modifications of p(PFPA) polymers, except for the active ester changing method. Basically, the reactivity of the para-fluorine of the p(PFPA) is significantly influenced by the specific type of nucleophiles involved. In general, softer nucleophiles exhibit higher reactivity compared to harder nucleophiles, following the order of $HS\text{-}CH_2R > H_2N\text{-}CH_2R >> HO\text{-}CH_2R$. This has led to the adoption of nucleophiles for modifying PFP groups in PFSR, enabling the synthesis of various derivatives with distinct properties. Particularly, high nucleophilicity of thiols and sulfur-based nucleophiles has led to their widespread study in PFSR by many researchers making them the most commonly employed nucleophiles for this particular reaction namely para-fluoro-thiol reaction (PFTR). Unfortunately, the thesis does not incorporate a detailed discussion of the PFTR within its conceptual framework. Nevertheless, it should be noted that thiols, also known as sulfhydryl compounds, play a crucial role in polymer chemistry due to their unique chemical properties and diverse applications. Especially, the thiol-ene reaction which is a chemical reaction between a thiol (-SH) and an alkene (also known as an olefin, containing a carbon-carbon double bond)

resulting in the formation of a thioether linkage (-S-C-), are important in polymer chemistry, offering efficient and versatile ways to create polymers and functional materials. Therefore, in the following section, a detailed explanation will be provided on thiol-ene chemistry within the framework of the thesis.

3.4.2 Thiol-ene click chemistry

Thiol-ene chemistry denotes a radical-mediated process where a thiol is introduced across an unsaturated linkage (-ene bond). This chemical process remains independent from many frequently employed reactions and can be carried out using different solvents. Moreover, it is not affected by oxygen and has at times been regarded as a "click" type of reaction.[227-228] The thiol-ene click reaction presents a considerable opportunity for producing valuable substances *via* synthesis. It addresses issues frequently faced in conventional organic synthesis, such as the existence of undesired side products and the need for extensive purification procedures. Beyond its characteristic "click" nature, thiol-ene chemistry possesses numerous advantages that distinguish it from other click reactions. For example, a wide range of molecules containing enes and thiol groups are available, each having varying structures and reactivity. This adaptability allows the reaction to be highly versatile and adaptable to various needs. Additionally, the reaction forms strong bonds with substrates because of the durable stability of thioether linkages in different chemical environments. Unlike many other click reactions, thiol-ene employs sulfur chemistry that is sensitive to redox reactions, providing extra possibilities for modifying materials. Consequently, thiol-ene coupling is an outstanding tool for applications requiring high-performance materials, like those in optics, biomedicine, and sensing. This is especially significant when the sensitivity to by-products is a concern.[229]

The thiol-ene reaction's process initiates with the creation of a thiyl radical through the removal of a hydrogen atom from the thiol group. This can occur *via* a thermal or photo-initiator for radical thiol-ene reactions, or with the involvement of a nucleophile in thiol-Michael reactions. In the latter case, a thiol-centred anion is typically generated instead of a radical. Subsequently, the thiyl species directly adds to the -C=C- double bond, resulting in the formation of a carbon-centred intermediate. This intermediate then performs a hydrogen abstraction from another thiol molecule, following an anti-Markovnikov orientation[227] (as illustrated in **Figure 2.9**). As the mechanism relies on the creation of radical or ionic intermediates, the chemical structure of the species involved is crucial for their stabilization, thereby significantly influencing the progression of the reaction.[229]

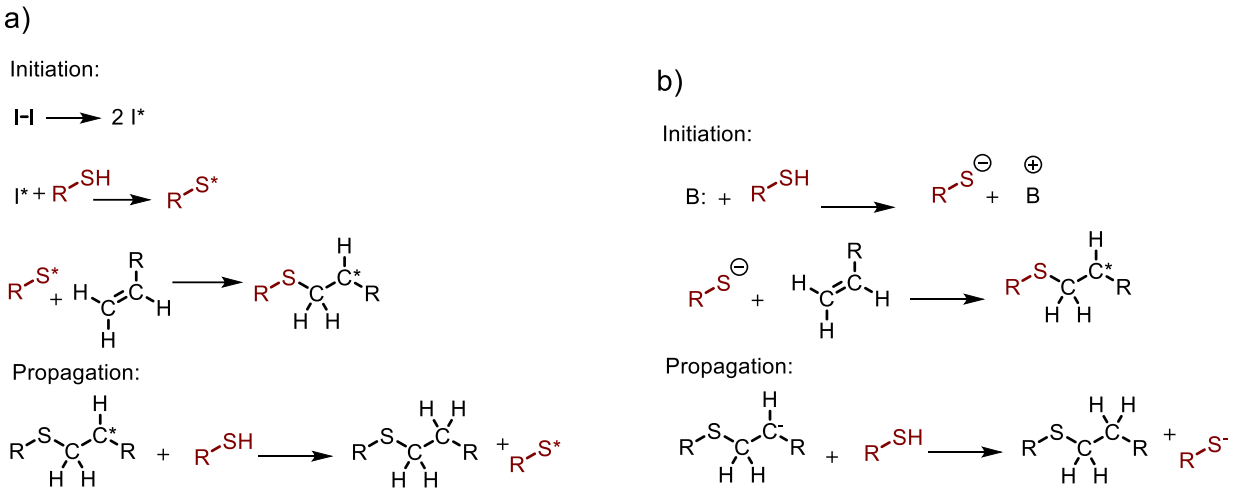

Figure 2. 8 General mechanism of a thiol-ene reaction: In the initiation process, a thiyl radical/ion forms by a) the aid of a thermal or photo initiator, or b) nucleophile-mediated hydrogen abstraction. Propagation involves a two-step process, where the thiyl species adds to a -C=C- double bond, forming a carbon-center radical. The carbon-centered radical reacts with another thiol molecule to form the thiol-ene product and create a second thiyl radical/ion to complete the cycle.

The reactivity of the thiol-ene reaction can vary based on the electron density and substitution level of the thiol and ene components. When it comes to thiols with fewer hydrogen atoms that can be easily abstracted, their chain-transfer to a carbon-centred radical is reduced. On the other hand, electron-deficient enes tend to restrict the addition of thiyl radicals.[230] A diverse range of ene-containing monomers has been assessed and categorized by their reactivity. This spectrum ranges from highly reactive compounds like norbornene and vinyl, allyl ethers, methacrylate, acrylate, styrene, to less reactive conjugated enes.[231] The decrease in thiol-ene reactivity follows the electron density of the -C=C- double bonds, except for norbornene, which is exceptionally reactive. Steric effects also play a role, with terminal double bonds reacting more swiftly than internal or substituted ones. The structure of thiol molecules can also impact reaction kinetics; for instance, groups that weaken the sulfur-hydrogen bond enhance the reaction rate. [232]

Thiol-ene reactions, much like various other click reactions, are progressively employed in the modification of surfaces[233-234], biomolecules,[235-237] and polymers[238-239]. When a combination of versatile ene and thiol compounds is utilized, the thiol-ene coupling results in thiol-ene polymerization.[239] Thiol-ene polymerization is a type of step-growth polyaddition, where a polythioether network is formed by the stepwise addition of thiol groups to carbon-carbon double bonds.[229] The growth of the molecular weight of the oligomers and polymers formed is highly dependent of the conversion rates. On one hand, delaying the formation of higher molecular weight structures offers advantages in terms of manufacturing by maintaining system viscosity and improving processability. Thiol-ene photopolymerization overcome significant drawbacks of chain-growth mechanisms, such as inhibition by oxygen and stress development, and the formation of highly heterogeneous polymer networks.[240] However, the step-growth mechanism

also presents a major challenge in thiol-ene polymerization. Achieving high conversion rates is challenging, typically resulting in the production of low molecular weight compounds with limited thermo-mechanical properties, such as stiffness and a low glass transition temperature for the polymers. Potential solutions to overcome this challenge include the use of highly branched and rigid monomer structures, blending with other materials, applying post-polymerization modifications like oxidizing sulfur centers in the main chains,[241-242] or using different reaction environments that encourage high conversions.[243]

The growth of chains and evolution of the average molecular weight in a step-growth mechanism are described by Carother's equation, where only at high degrees of conversion of the functions it is possible to achieve considerable values of molecular weights (Figure 2.3). n a system containing pairs of A-A and B-B, where A and B represent specific chemical groups originating from similar monomers, the step-growth process initiates by forming dimers of (A-A)-(B-B). These dimers retain available end components that facilitate subsequent connections. As a result, two dimers can bond together, leading to the creation of a structure denoted as (A-A-B-B)-(A-A-B-B). Subsequently, oligomers combine *via* their remaining unreacted end groups, gradually constructing the interconnected chains of the network until the available functional groups are used up.[244] (**Figure 2.10**)

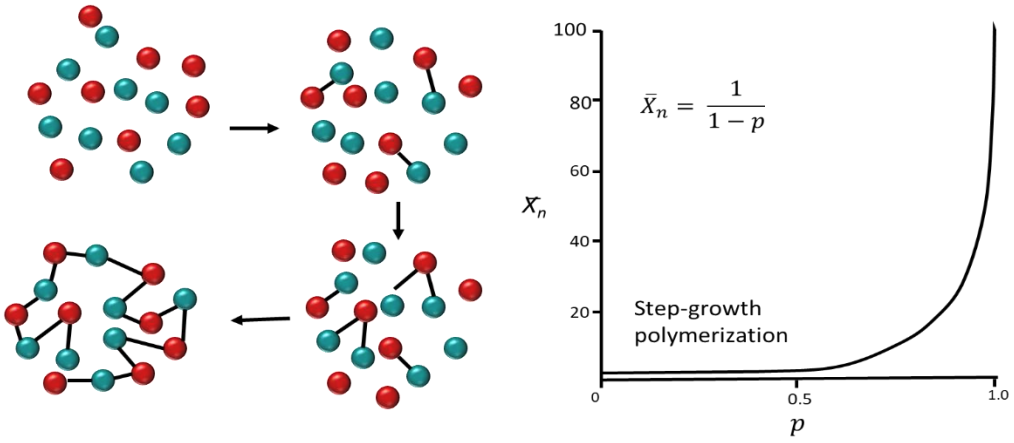

Figure 2. 9 Scheme of a step-growth mechanism polymerization. The medium contains red and green spheres representing two distinct functions (left-side). The process involves sequentially the formation of first dimers, then trimers, longer oligomers and eventually long chain polymers. On the right side, a graphical representation depicts the correlation between the growth in the average molecular weight of a polymer and the conversion of functionalities in step-growth polymerization methods.

The development of step-growth polymerization is dependent on the alteration of the terminal groups.[245] Each reaction step implies that the reactive end of a monomer or polymer encounters another species with which it can form a link. The functional group at the end of a monomer is usually assumed to have the same reactivity as that on a polymer chain of any size. Using the relationship described in **Equation 2.1**, the extent of conversion (p) is calculated by comparing

the number of moieties that have been converted (N_0-N) to the initial number of moieties present in the system (N_0).[245-246]

$$p = \frac{N_0 - \mathrm{N}}{N_0} \qquad \text{(Equation 2.1)}$$

This equation is valid when the opposite functionality is present in equal concentration and there are no side reactions. The number-average of the degree of polymerization ($\bar{X}_n$) of the mixture is defined as the average number of monomeric units in a polymer molecule (**Equation 2.2**). For an A-A-B-B polymerization, a repeating unit is made of two monomeric units. The theoretical average molecular weight $\bar{M}_n$ is then the number-average of repeating units $\bar{X}_n$ times the molecular weight of a repeating unit M_{rp} (**Equation 2.3**). As the polymerization process yields polymer chains of different sizes, a more realistic depiction of the distribution of molecular weight around the average is given by the dispersity index (*Đ*). In a purely step-growth linear polymerization, Đ can reach a maximum of 2 for p=1 (100%) (**Equation 2.4**). Impurities and side reactions can provoke de*via*tions in this value. This value is also defined as the ration between the weight-average molecular weight ($\bar{M}_w$) and the number-average molecular weight ($\bar{M}_n$) of a polymer. Here it is possible to observe how the average molecular weight evolves with the polymerization: at time t=0, the process has not yet started and therefore p = 0 and $\bar{X}_n$ is equal to 1, illustrating the presence only of the initiating monomers. Halfway the polymerization process, where 50% of the A-A (or B-B) have been converted, $\bar{X}_n$ yields only 2 monomeric units in the main chain. When the reaction reaches 98%, 50 monomeric units can in average be found. This number is still moderate to build a high molecular weight polymer. Steep increases are only reached at nearly complete conversions, as illustrated by a model conversion of 99% that yields chains with 100 monomeric units per polymer chain **(Figure 2.1.4)**.[245]

$$\bar{X}_n = \frac{1}{1-p} \qquad \text{(Equation 2.2)}$$

$$M_n = M_{rp}\, x\, \bar{X}_n \qquad \text{(Equation 2.3)}$$

$$Đ = \frac{\bar{M}_w}{\bar{M}_n} = 1 + p \qquad \text{(Equation 2.4)}$$

In an ideal thiol-ene system, the only mechanism controlling the polymerization process is the step-growth mechanism. In the case where the only reaction occurring is the one where the thiyl radicals reacts with the -C=C- double bonds, forming carbon-centred radicals to produce a thioether linkage and produce a new radical, the polymerization will follow a classical step-growth kinetics. The resulting stepwise addition of reactive species with free terminal

functionalities will form dimers, then small oligomers, and so on in a sequence of individual reactions until the full conversion of all free functionalities.[246]

4 Motivation

As it can be seen from the above-mentioned theoretical background, tetrazoles have diverse applications in various fields of chemistry, including organic synthesis, materials science and medicinal chemistry. Within the tetrazole family, 1,5 DSTs have garnered particular interest owing to their exceptional physicochemical properties, notably their energetic capacity and fluoresce behaviour, which holds great promise for potential applications in the pharmaceutical industry and energetic materials realm. Nevertheless, the practical implementation of 1,5 DST-containing polymeric architectures still needs to be more circumscribed in the present literature. Consequently, strategically incorporating 1,5 DST moieties into the polymeric structure is a novel avenue for developing polymer materials endowed with hitherto unexplored properties. Furthermore, it is essential to point out that the current shortage of practical techniques for producing 1,5 DST-containing polymers with good yields and efficiency still needs to be solved. Thus, discovering new approaches to create such materials requires thorough investigation to unlock the full potential of their unique properties.

Therefore, the primary motivation of this thesis is to investigate the synthesis of 1,5 DST containing polymeric structures. For this purpose, as it depicted in **Figure 3.1**, three distinct strategies are employed: i) main chain 1,5 DST-based polymer synthesis (**Chapter 5.1**) and ii) positioning 1,5 DST moiety as a pendant group in order to have 1,5 DST-decorated polymers (**Chapter 5.2**), and iii) incorporation of 1,5 DST moiety into the already existing polymeric structure ((e.g., poly (pentafluorophenyl acrylate) (p(PFPA)) for the *in-situ* formation of 1,5 DST-decorated polymeric networks (particularly, hydrogels) (**Chapter 5.3**).

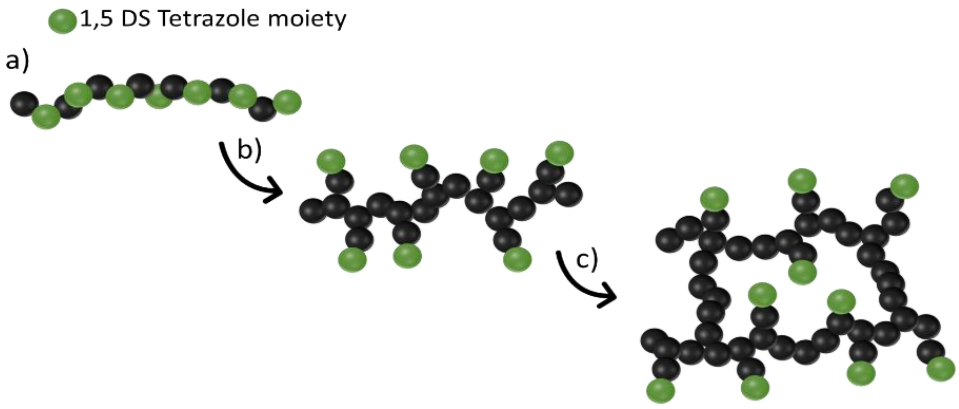

Figure 3. 1 Schematic depiction of the intended concept of the present thesis. Synthesis of a) main chain 1,5 DST-based polymers; b) 1,5 DST-decorated polymers; c) 1,5 DST-decorated polymeric networks.

By conducting above-mentioned projects, the ultimate goal is to introduce to the literature novel type of polymers by utilizing different synthesis approaches besides a comprehensive understanding of the relationship between the structure and properties of novel 1,5 DST-containing polymeric materials.

5 Results and Discussion

5.1 Main chain 1,5 DS Tetrazole-based polymers

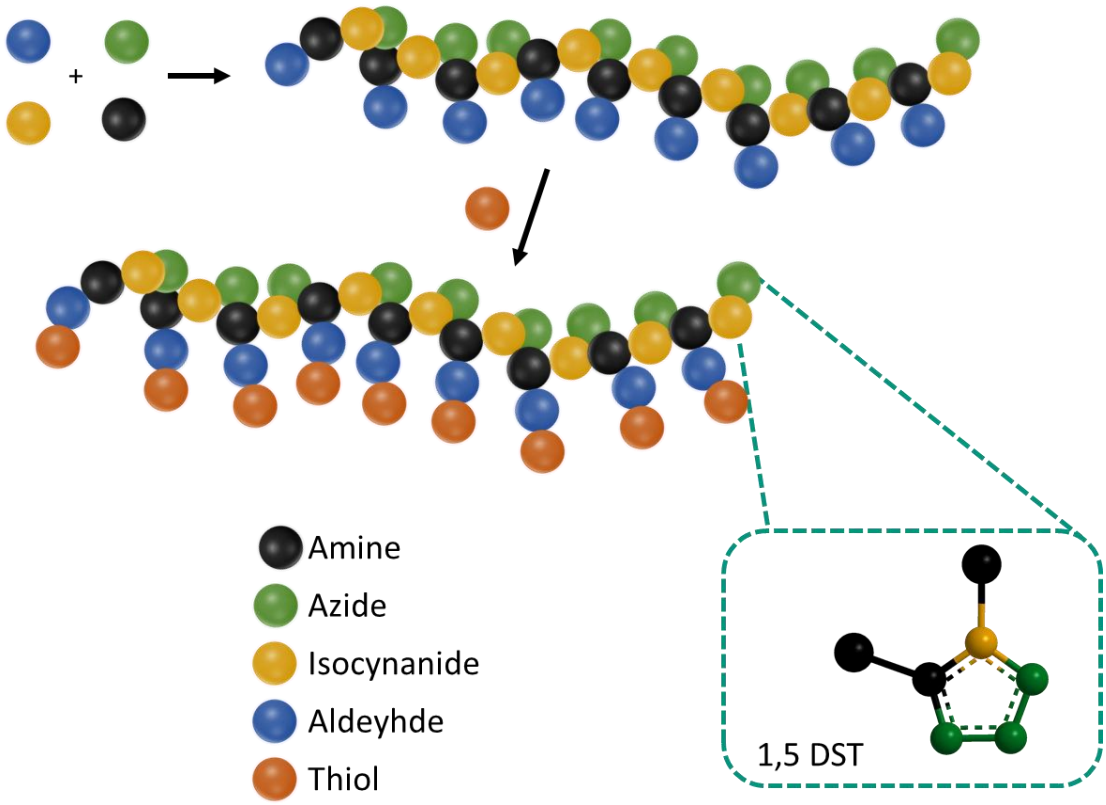

Parts of this chapter are published as "Akdemir, M. S., Huber, B., Simian, M., Theato, P., Mutlu, H., Main Chain 1,5-Disubstituted-1*H*-Tetrazole-Based Polymers *via* Ugi-Azide-Four-Multicomponent Polymerization (UA-4MCP). *ACS Appl. Polym. Mater*. **2023**, 5, 6643-6650. https://doi.org/10.1021/acsapm.3c01231"and adapted with permission from ACS, 2023.

5.1.1 Prologue

As stated in **Chapter 2.3**, the available literature on polymers incorporating 1,5 DST into the main chain is quite limited. Sproll et al. introduced the first notable instance of tetrazole-containing polymers in the main chain.[214] They achieved this through a bulk polycondensation process involving 1-(2-hydroxyethyl)-1*H*-tetrazolyl)methyl hydrazine and hexamethylene diisocyanate. As a result, 33% nitrogen content was detected with remarkable thermal stability, up to 260 °C.[213] Later on, the same group also illustrated the synthesis of tetrazole-based polymers by reacting the corresponding tetrazolyl hydrazine with hexamethylene diisocyanate and bis(5-methylhydrazinyl-1*H*-tetrazolyl)alkanes. These resulting polymers contained 40% nitrogen and were proven to possess moderate explosive properties, along with thermal stability up to 240 °C.[214] However, the methods used to create the mentioned polymers required harsh conditions, such as high temperatures and acidic substances. Moreover, the synthetic procedure applied involves a complex series of steps, resulting in solubility issue. Thus, it is important to underline the significance of developing practical and efficient ways to synthesize 1,5 DST-containing polymers under mild conditions. Furthermore, most of the polymers in the literature cannot be easily modified using subsequent polymerization methods to adjust their properties. As a result, there is a need for research that focuses on a more convenient and suitable approach to produce main chain tetrazole-containing polymers, allowing for further customization of their properties.

Therefore, a pioneering concept has been constructed in this study in order to overcome the mentioned challenges for the synthesis of main chain 1,5 DST-based polymer with an effective strategy in one pot under mild reaction conditions. Afterwards, by the rational design of the synthesis, the obtained polymer has been applied to further reactions in order to show the possibility of post-polymerization modification. Accordingly, the UA-4MC polymers were subjected to a detailed analysis using various techniques, including size exclusion chromatography (SEC), nuclear magnetic resonance (NMR), attenuated total reflectance infrared spectroscopy (ATR-IR), thermal gravimetric analysis (TGA), differential scanning calorimetry (DSC), as well as UV-Visible (UV-Vis) and fluorescence spectroscopy. Subsequently, the following section presents a comprehensive explanation of the experimental part, coupled with the presentation of characterization results and an in-depth discussion thereof.

5.1.2 Synthesis and Characterization

In this study, polymer synthesis is constructed on the base of UA-4MCP. The UA-4MCP strategy uses 1,6-diisocyanide as a reactive partner in a nucleophilic reaction to create main chain 1,5 DST-based polymers. Thus, the synthesis of 1,6-diisocyanide has been conducted based on the previously reported literature.[247] (see Experimental part, Section 7.3.1) Upon synthesizing the 1,6 diisocyanide derivative, the emphasis shifted to investigating the optimal reaction conditions (i.e., (i.e., solvent, concentration and reaction time) for UA-4MCP. Hence, preliminary polymerization attempts were performed by employing different concentrations (0.5M, 1M, and 4M) in a mixture of DMF: MeOH (1:1). Concisely, 1,6-diisocyanide, *N, N*-dimethyl-1,6-hexanediamine, $TMSN_3$, and hexanal in the presence of the catalyst 1,8-diazabicyclo(5.4.0)undec-7-ene (DBU) were reacted under an inert atmosphere at 50 °C for overnight, namely model polymerization reaction (**MPR**). Then, the substance was purified through precipitation in cold MeOH (**Scheme 5.1.1**).

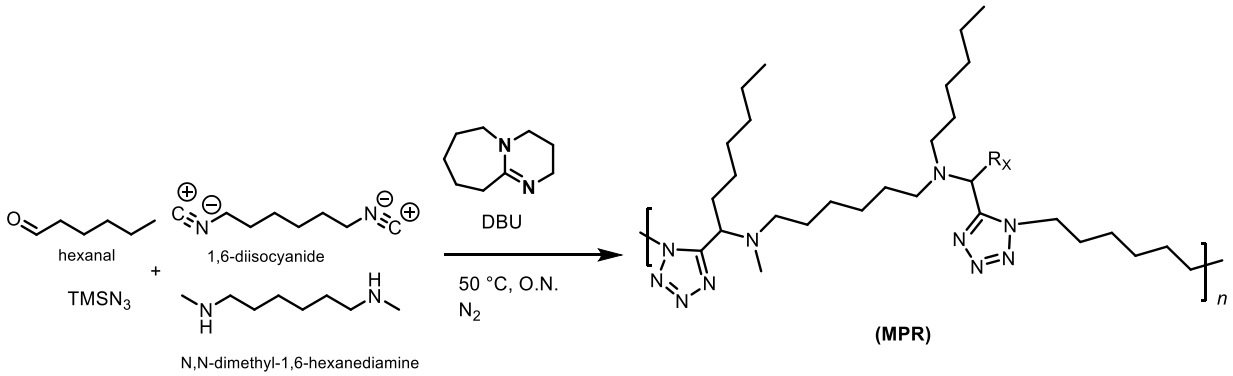

Scheme 5. 1. 1 Route for the synthesis of model polymers in order to detect optimum reaction conditions *via* Ugi-azide four-multicomponent polymerization (UA-4MCP).

SEC was utilized to analyze the **MPR** compound comprehensively. The results revealed that, in line with expectations under step-growth polymerization conditions, the formation of the **MPR** compound reached its highest M_n value at 1M (see **Figure 8.1** in the Appendix). While Ugi-4CRs are typically performed using methanol (MeOH) or a MeOH-tetrahydrofuran (THF) mixture, different solvents were also explored to optimize the **MPR** compound. This exploration encompassed combinations like THF: MeOH and DMF: MeOH, with varying ratios (1:1, 2:1, and 1:2) maintained at 1M concentration. Depending on the SEC results, using THF: MeOH mixture resulted in only oligomer formation (**Figure 8.2.** in the Appendix), whereas DMF: MeOH yielded polymer formation with a high M_n (**Figure 8.3.** in the Appendix). Thus, DMF: MeOH (1:1) was chosen as the optimum solvent mixture for UA-4MCP polymer synthesis for further steps.

Upon optimizing the conditions, the UA-4MCP reactions were performed by employing various aldehyde derivatives (aliphatic and aromatic) at 1M in DMF: MeOH (1:1) mixture. In particular, the primary purpose is to employ aliphatic and aromatic aldehyde groups for introducing various substitutions onto the main chain of 1,5 DSTs polymer. Consequently, this allows for exploring of how distinct side chains influence the thermal and optical properties. Furthermore, this method also simplifies the incorporation of functional groups to enable subsequent modifications. Briefly, 1,6-diisocyanide, *N, N*-dimethyl-1,6-hexanediamine, $TMSN_3$, and corresponding aldehyde derivatives were reacted in the presence of the catalyst DBU under an inert atmosphere at 50 °C. (see Experimental part, Section 7.3.1) **Scheme 5.1.2** illustrates the synthesis pathways for various polymers. Each polymer is distinguished by a unique colour code, corresponding to the aldehyde derivative used in its synthesis. For instance, aliphatic substituted main chain 1,5 DST polymers; MC-Tet_1 (synthesized using hexanal) is represented by a black line, MC-Tet_2 (synthesized from decanal) by a red line, MC-Tet_3 (derived from undecanal) by a blue line, MC-Tet_4 (obtained from citronellal) by a green line, aromatic substituted polymers; MC-Tet_5 (made with benzaldehyde) by a brown line, MC-Tet_6 (produced using 4-(trifluoromethyl) benzaldehyde) by an orange line, and finally, MC-Tet_7 (formed from 5-norbornene-2-carboxaldehyde) is depicted by a purple line.

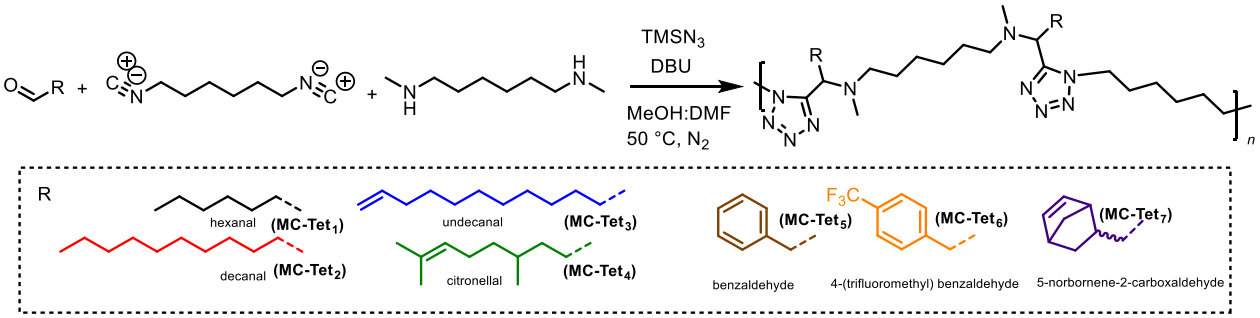

Scheme 5. 1. 2 Schematic representation of Ugi-azide four-multicomponent polymerization (UA-4MCP) to provide main chain 1,5 DST-based polymers with different side groups (R) from aliphatic (e.g., hexanal (black line), decanal (red line), undecanal (blue line), citronellal (green line)) to aromatic (e.g., benzaldehyde (brown line), 4-(trifluoromethyl) benzaldehyde (orange line) and 5-norbornene-2-carboxaldehyde (purple line)).

Accordingly, SEC was employed to monitor the synthesis of UA-4MC polymers. The traces for the main chain 1,5 DST-based polymers with aliphatic and aromatic substitutions are illustrated in **Figure 5.1.1.a** and **5.1.1.b**, respectively. Additionally, the *Đ* values of obtained polymers are listed in **Table 5.1.1**. It can be seen in **Figure 5.1.1** that SEC traces for all polymers showed a major peak at the high molecular weight and a number of minor peaks at the lower molecular weight. On the one side, the latter can be attributed to the oligomer formation during the step-growth polymerization. Notably, the obtained low *Đ* values in the range of 1.2-1.7 (**Table 5.1.1**) can also be assigned to oligomer formation and, correspondingly, underrepresented due to the precipitation process. On the other side, the formation of cyclic products might be the primary reason for the longer retention time observed at the higher retention time in the SEC traces. Unfortunately, all these lower fractions of the SEC curves could not be removed not only *via* precipitation in different solvents but also with dialysis.

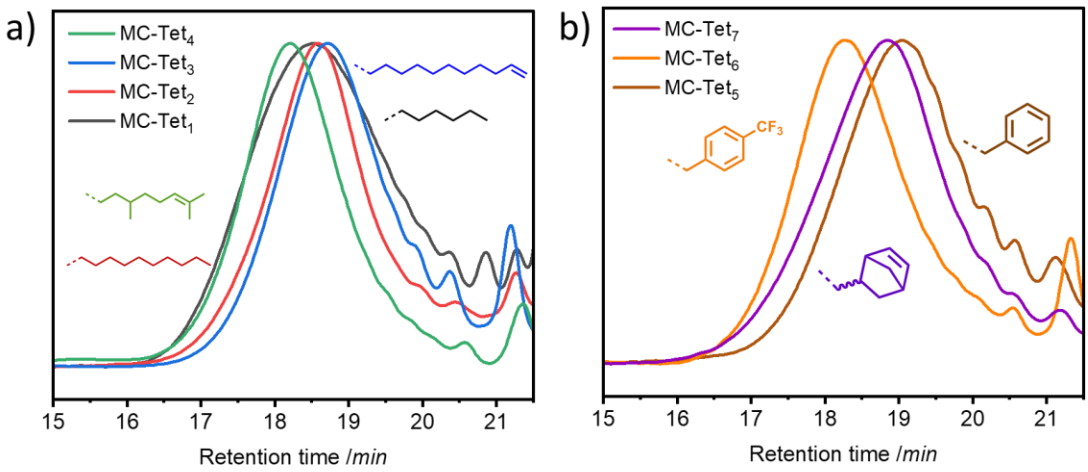

Figure 5. 1. 1 Comparative SEC traces of a) aliphatic side chain containing UA-4MC polymers MC-Tet$_1$ (black line), MC-Tet$_2$ (red line), MC-Tet$_3$ (blue line), MC-Tet$_4$ (green line)), b) aromatic side chain containing UA-4MC polymers MC-Tet$_5$ (brown line), MC-Tet$_6$ (orange line), MC-Tet$_7$ (purple line).

Indeed, optimization studies indicated that the reaction time significantly influenced the formation of UA-4MC polymers. Obviously, short reaction time resulted in the formation of only dimers, trimers, or oligomers. Therefore, polymerization reactions were conducted to yield polymers, thoroughly considering the potential reactivity effects stemming from aliphatic and aromatic aldehydes. Accordingly, **Table 5.1.1** lists the optimum reaction times. Interestingly, UA-4MCP showed a broad reaction time that varies depending on the aldehyde source (**Table 5.1.1**). While aromatic aldehydes with varied functionalities could undergo the reactions rapidly (overnight reaction) to provide expected UA-4MCP products (MC-Tet$_5$ - MC-Tet$_7$) with relatively higher M_n compared to aliphatic counterparts, aliphatic aldehyde-containing polymers (MC-Tet$_1$ - MC-Tet$_4$) were formed only upon extending the polymerization reaction time from

days to weeks. It is important to highlight that the longer reaction time did not influence the M_n of the resultant polymers.

Explicitly, the aromatic aldehyde derivatives have not showcased a noticeable effect on the reaction kinetics. In contrast, longer alkyl chain aliphatic aldehydes (e.g., decanal, MC-Tet$_2$) demonstrated a slower reaction rate than short-chain derivatives (e.g., hexanal, MC-Tet$_1$). Cao and Yu et al. have emphasized that the latter behaviour may arise from the remarkable selectivity of imine-ions, which displays in a given multicomponent reaction and the nature of the substituents of the corresponding aldehydes and amine.[248] Indeed, the UA-4MCP reaction begins with creating an iminium-ion by reacting an aldehyde with a secondary amine. The reaction is followed by nucleophilic addition of diisocyanide to the iminium-ion. As a result, a charged intermediate is produced, which then reacts with hydrazoic acid. Ultimately, this sequence of reactions leads to the formation of 1,5 DSTs through the ring-forming step. (**Figure 8.4.** in Appendix). Shortly, the behaviour of imine ions and the specific properties of corresponding aldehydes and amines significantly affect the reaction kinetics. Therefore, it can be postulated that since the bond localization energy of aldehyde is higher in the aromatic structure due to hyper-conjugation with the adjacent (C-H) orbitals compared to their aliphatic counterparts, the rapid imine ion formation facilitates accelerated polymerization for aromatic aldehyde-containing reactions. Accordingly, the shorter reaction time observed for aromatic aldehyde-containing polymers (MC-Tet$_5$ - MC-Tet$_7$) exhibiting higher reactivity, accordingly, faster polymerization than their aliphatic counterparts (MC-Tet$_1$ - MC-Tet$_4$).

Table 5. 1. 1 Molecular characterization of UA-4MC polymers (MC-Tet$_1$ - MC-Tet$_7$) obtained *via* UA-4MCP. Typical reaction conditions were as follows: 1,6-diisocyanide (1.00 eq.), *N*, *N*-dimethyl-1,6-hexanediamine (1.00 eq.), $TMSN_3$ (2.00 eq.) and aldehyde derivatives (2.00 eq.) were reacted in the presence of the catalyst 1,8-diazabicyclo (5.4.0) undec-7-ene (DBU) under inert atmosphere at 50 °C.

Polymer	Time (h)	Conversion (%)[a]	Yields	$M_{n,\,SEC}$ (kg mol^{-1}) [b]	$Đ$ [M_w/M_n]
MC-Tet$_1$	240	73	77	6.7	1.4
MC-Tet$_2$	240	67	85	6.7	1.3
MC-Tet$_3$	72	60	85	5.6	1.3
MC-Tet$_4$	48	93	92	8.5	1.7
MC-Tet$_5$	60	87	78	8.5	1.5
MC-Tet$_6$	72	85	84	8.0	1.5
MC-Tet$_7$	24	62	70	5.6	1.2

[a]Polymer conversions calculated from ^{1}H NMR; [b]Determined by SEC using THF as an eluent.

The synthesis of UA-4MC polymers was also examined through ^{1}H NMR spectroscopy to understand the polymerization process better. For aliphatic-substituted polymers (MC-Tet$_1$ - MC-Tet$_4$), the analysis can be found in **Figure 5.1.2.a**, when **Figure 5.1.2.b** presents the analysis for aromatic-substituted main chain 1,5 DST-based polymer (MC-Tet$_5$ - MC-Tet$_7$). Furthermore, the

COSY-NMR spectra of all polymers are also shown in the **Figure 8.5** in the Appendix. The magnetic resonance of the only proton associated with the tetrazole moiety was detected at ~3.8-4.2 ppm (a) for MC-Tet$_1$ - MC-Tet$_6$, except from a broad peak between 4.2-4.4 ppm for MC-Tet$_7$.

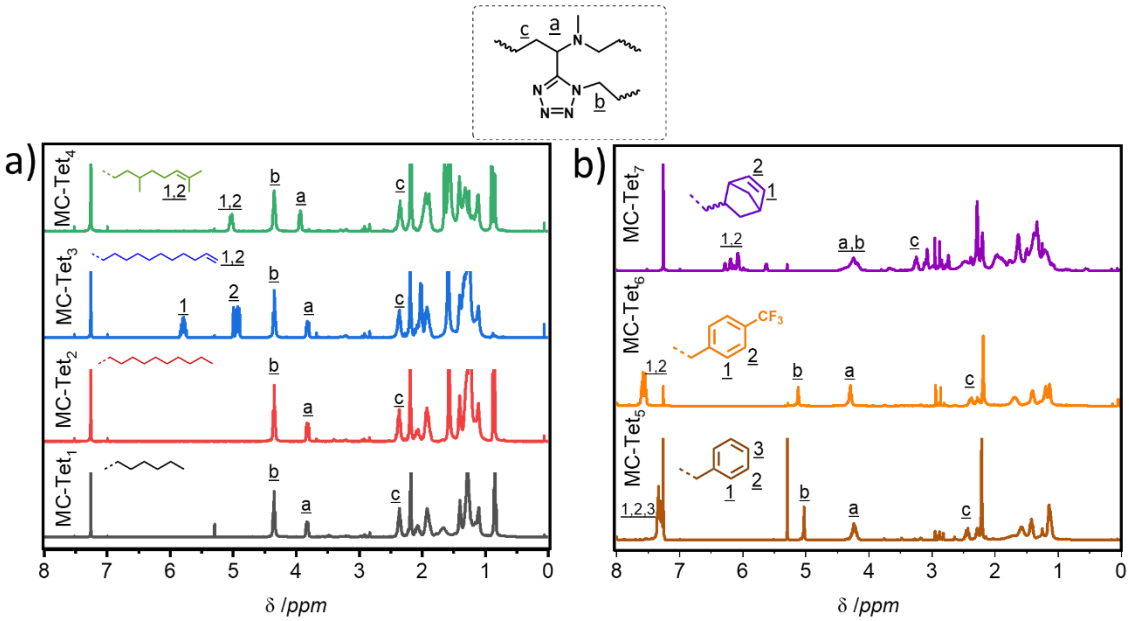

Figure 5. 1. 2 Comparative: ^{1}H-NMR ($CDCl_3$, 400 MHz) of a) aliphatic side chain containing UA-4MC polymers MC-Tet$_1$ (black line), MC-Tet$_2$ (red line), MC-Tet$_3$ (blue line), MC-Tet$_4$ (green line)), b) aromatic side chain containing UA-4MC polymers MC-Tet$_5$ (brown line), MC-Tet$_6$ (orange line), MC-Tet$_7$ (purple line).

Furthermore, the formation of the methylene group adherent to 1,5 DST moiety at ~4.3 ppm (b) originating from diisocyanide and at ~2.3 ppm (c) stemming from diamine for MC-Tet$_1$ - MC-Tet$_6$ was detected as a proof of polymer formation, whereas these peaks were located at 4.3 and 3.2 ppm (a, b) for MC-Tet$_7$, which would only be seen as proof of UA-4MC polymer construction. Crucially, the magnetic resonances arising from the olefin functional groups of MC-Tet$_3$ and MC-Tet$_7$ were also detected between 4.86-5.85 ppm (1, 2) and 5.23-5.55 ppm (1, 2), respectively. In general, conversion reached over 60% of polymers formation as well as, a relatively high yield of over 70% after purification, as listed in **Table 5.1.1**.

Moreover, the characterization of the UA-4MC polymer was carried out using ATR-IR analysis. (**Figure 5.1.3**) The band located at 1382 cm^{-1} was identified as the antisymmetric stretching of the -N=N- bond, whereas the band at 1108 cm^{-1} was associated with the vibration of the -C=N- bond. Moreover, the band at 1058 cm^{-1} was also attributed to the vibration of the -N-N- bond present in the 1,5 DST unit. Furthermore, the ATR-IR analysis of the polymers indicated the existence of two absorption bands at 3104 and 1640 cm^{-1} (stretching vibration of the -C-H- bond and -C=C- bond), which were assigned to the olefin handles for MC-Tet$_3$ and MC-Tet$_7$. (**Figure 5.1.3**)

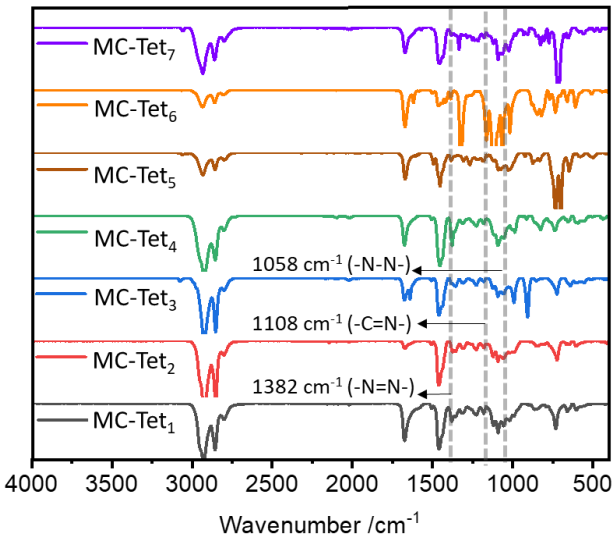

Figure 5. 1. 3 ATR-IR spectra of MC-Tet$_1$ (black line), MC-Tet$_2$ (red line), MC-Tet$_3$ (blue line), MC-Tet$_4$ (green line), MC-Tet$_5$ (brown line), MC-Tet$_6$ (orange line), MC-Tet$_7$ (purple line).

Additionally, TGA was conducted to examine the thermal characteristics of the UA-4MC polymers. The thermal degradation (T_d) profile of the aliphatic-substituted polymers (MC-Tet$_1$ - MC-Tet$_4$) are illustrated in **Figure 5.1.4.a**, whereas **Figure 5.1.4.b** displays similar date for the aromatic-substituted main chain 1,5 DST-based polymer (MC-Tet$_5$ - MC-Tet$_7$), along with **Table 5.1.2** for reference. As can be seen from **Figure 5.1.4**, a multistep degradation pattern was observed under inert conditions at 10 K min^{-1} for all polymers. The relative thermal stability of MC-Tet$_1$ - MC-Tet$_7$ have been evaluated by comparing the decomposition temperatures at different percentage weight loss. The results show that the mass losses of the first decomposition step are all within 55wt%, regardless of different side groups (**Figure 5.1.4**). This suggests that the weight loss at the first step is due to the degradation of the polymer main chain, while the second step can be attributed to the 1,5 DST unit degradation in combination with the aliphatic and aromatic side group (**Figure 5.1.4**). The first T_d was around 305 °C, followed by the second thermal degradation step ~450 °C for aliphatic substituted MC-Tet$_1$- MC-Tet$_4$ (see **Table 5.1.1**). Interestingly, the first degradation occurred ~300 °C, followed by the second step at ~430 °C for aromatic substituted MC-Tet$_5$ - MC-Tet$_7$ (see **Table 5.1.2**). The polymer degradation process exhibited a high degree of completion at a temperature of 520 °C, except for polymers MC-Tet$_5$, MC-Tet$_6$ and MC-Tet$_7$. These particular polymers displayed up to 20% char formation owing to their inherent aromatic structure.

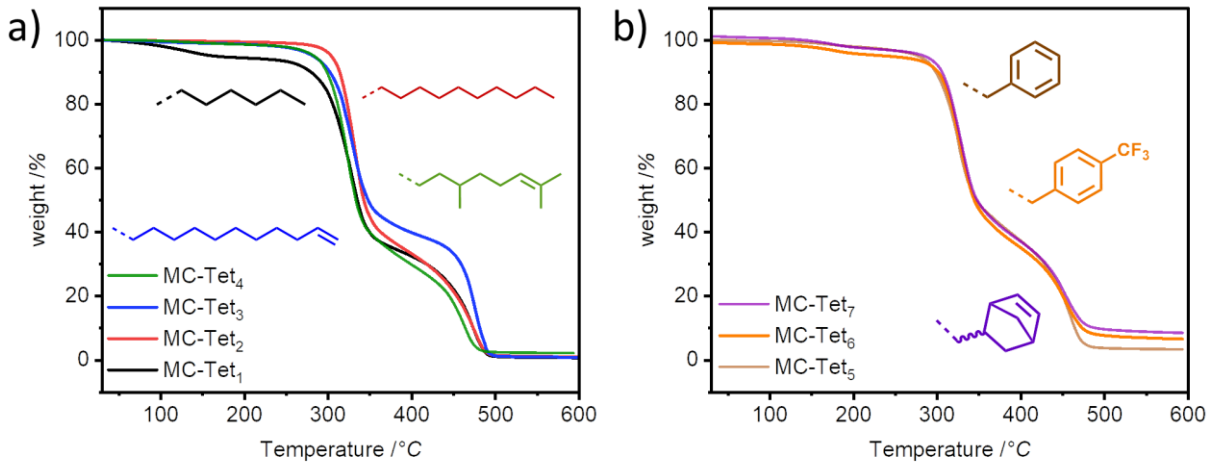

Figure 5. 1. 4 Comparative: TGA curves of a) aliphatic side chain containing UA-4MC polymers MC-Tet_1 (black line), MC-Tet_2 (red line), MC-Tet_3 (blue line), MC-Tet_4 (green), b) aromatic side chain containing UA-4MC polymers MC-Tet_5 (brown line), MC-Tet_6 (orange line), MC-Tet_7 (purple line).

Indeed, it is known that the thermal stability of a polymer depends very much on its chemical structure, degree of crystallinity, and molecular mass.[249] Even though the presence of the aromatic groups in the polymeric structure improves the thermal stability of polymers,[250] the TGA results displayed that the longer aliphatic chain substituted polymers MC-Tet_2 - MC-Tet_4 had similar $T_{d,5\%}$ compared to aromatic substituted counterparts MC-Tet_5 - MC-Tet_6. On the one hand, this behaviour can be explained by several factors that are in following; a) increased steric hindrance in the presence of bulky aliphatic groups for MC-Tet_2 - MC-Tet_6 can hinder the movement of the backbone and make it more difficult for the compound to undergo thermal degradation, b) the ability of the aliphatic side chain to form a more ordered and compact structure lead to stabilize the 1,5 DST resulting in enhanced the thermal stability, c) the effect of the packing structure can contribute to the overall conjugation of intermolecular interactions of the 1,5-DS-T units which can increase its thermal stability.[251-252] On the other hand, it can also be attributed to the electronic effects of aromaticity that may influence the thermal stability of the polymeric structure. In other words, an aromatic group's existence results in a decreased stability, accelerating the degradation processes due to weak intermolecular forces besides preventing 1,5 DSTs intramolecular interaction.[253] Remarkably, the first T_d values exhibit a positive correlation with the incensement of aliphatic chains lengths (e.g., MC-Tet_1 (6 carbon), T_d 280 °C, MC-Tet_2 (10 carbon), T_d 300 °C). Additionally, it has been observed that the inclusion of the vinyl group in the molecular structure resulted in an increase in the first T_d, as can be seen in **Figure 5.1.4.a** and **Table 5.1.2** (e.g., MC-Tet_2 (10 carbon), T_d 300 °C, MC-Tet_4 (10 carbon) T_d 310 °C). In addition, the inclusion of a fluorinated benzene compound as a side group within the polymeric structure (e.g., MC-Tet_6, T_d 303 °C), enhanced T_d in contrast to its analogous counterpart comprised solely of a benzene ring, (e.g., MC-Tet_5, T_d 300 °C) due to strong carbon-

fluorine bond. Furthermore, the highest first T_d have been observed for MC-Tet$_4$ (e.g., T_d 310 °C). On the one side, since the T_d properties of main chain tetrazole-containing polymers have never been investigated, the comparison of UA-4MC products was made by comparing the pendant chain tetrazole containing polymers in the literature. As a result, UA-4MC products revealed partially improved thermal stability compared to 5(2,6oxyphenyl) tetrazole ($T_{d,5\%}$ ~210-290)[201], 5-aminotetrazole ($T_{d,5\%}$ ~250 °C)[254] 5-azidotetrazole ($T_{d,5\%}$ ~280 °C)[10] containing polymers. On the other side, compared to main chain triazole polymers ($T_{d,5\%}$ ~200-250 °C)[255-256], which are also an important group of nitrogen-containing five-membered heterocyclic ring with three nitrogen, UA-4MC products showed a significantly enhanced thermal stability.

Table 5. 1. 2 Thermal analysis of UA-4MC polymers (MC-Tet$_1$ - MC-Tet$_7$)

Polymer	T_d [°C][a]		T_g [°C][b]
	1st T_d[c]	*2nd T_d*	
MC-Tet$_1$	280	450	0
MC-Tet$_2$	300	448	-25
MC-Tet$_3$	305	458	-30
MC-Tet$_4$	310	444	-12
MC-Tet$_5$	300	433	26
MC-Tet$_6$	303	435	38
MC-Tet$_7$	308	430	54

[a]The decomposition temperatures (T_d) were detected by TGA; [b] The glass transition temperature (T_g) observed during the second heating measurement by DSC analysis. [c]First degradation temperatures defined as the temperature at 5% weight loss.

Furthermore, the thermal transitions of the polymers were investigated *via* DSC. The DSC heat flow graphs for MC-Tet$_1$ - MC-Tet$_7$ are illustrated in **Figure 5.1.5.a**, displaying the results for the aliphatic substituted chain, and in **Figure 5.1.5.b**, displaying the results for the aromatic substituted chain, along with **Table 5.1.2** for reference. Clearly, DSC analysis showed that the main differences originate from the side group reflected in polymer chain packing.[257-258] The inclusion of aromatic groups in the polymer structure, as seen in MC-Tet$_5$ - MC-Tet$_7$, led to glass-T_g higher than ambient temperature, specifically 26, 38, and 54 °C for MC-Tet$_5$, MC-Tet$_6$, and MC-Tet$_7$, respectively. No melting points were observed for any of the polymers (MC-Tet$_1$ - MC-Tet$_7$) within the temperature range of -75 to 150 °C, using a heat rate of 10 K min^{-1}. On the other hand, the aliphatic substituted polymers, namely MC-Tet$_1$ - MC-Tet$_4$, exhibited significantly lower glass-transition temperatures, below ambient temperature, with values of 0, -25, -30, and -12 °C for MC-Tet$_1$, MC-Tet$_2$, MC-Tet$_3$, and MC-Tet$_4$, respectively. It is estimated that crystallization is facilitated by the large aromatic side groups of the polymer backbone, while chain regularity is disrupted by aliphatic groups, thereby favouring an amorphous phase. Furthermore, softening and plasticizing effects have been observed by altering the alkyl chain length from shorter (e.g., MC-Tet$_1$) to longer (e.g., MC-Tet$_3$). This is attributed to the higher flexibility of longer chains, which permits the molecular motion of polymer.

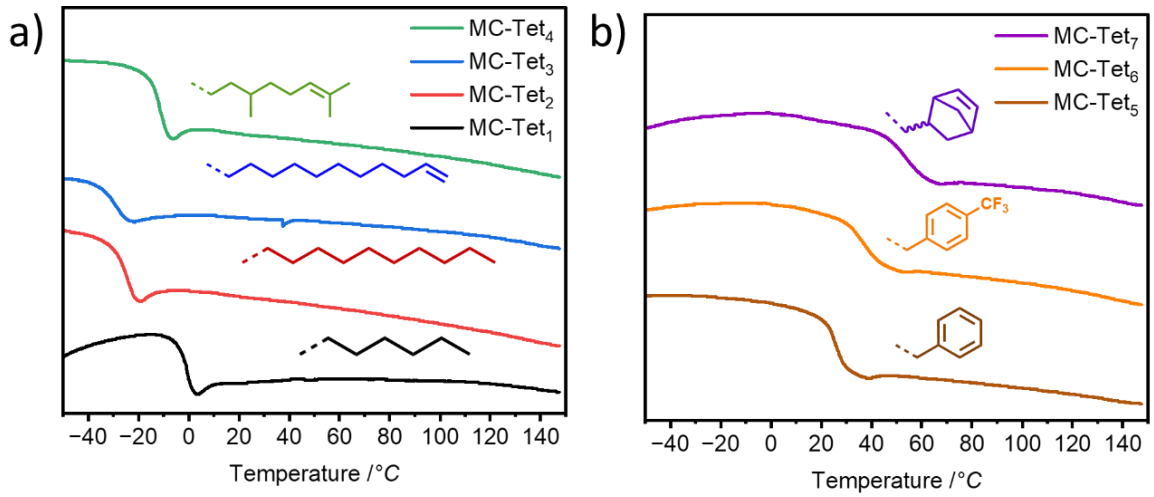

Figure 5. 1. 5 Comparative: DSC curves of a) aliphatic side chain containing UA-4MC polymers MC-Tet_1 (black line), MC-Tet_2 (red line), MC-Tet_3 (blue line), MC-Tet_4 (green), b) aromatic side chain containing UA-4MC polymers MC-Tet_5 (brown line), MC-Tet_6 (orange line), MC-Tet_7 (purple line).

The photophysical properties of main chain 1,5 DST-based polymers were also examined using UV-Vis and fluorescence spectroscopy. All data is given in **Table 8.1** in Appendix. The absorbance spectra of the Ugi-4CP products in DCM at 1.2 M are shown in **Figure 5.1.6**. In general, the intensity of absorption bands exhibited an increment from the aliphatic-substituted polymers to the aromatic-substituted polymers (e.g., MC-Tet_1: 0.78 a.u., MC-Tet_6: 2.97 a.u.) (**Figure 5.1.6**, **Table 8.1** in the Appendix). Furthermore, a bathochromic shift is observed from MC-Tet_1 - MC-Tet_4 to MC-Tet_5 - MC-Tet_7. Additionally, the intensities of MC-Tet_1 - MC-Tet_4 increased with increases in the alkyl unit content on the side chain (from MC-Tet_1 to MC-Tet_4, **Figure 5.1.6** and **Figure 8.6** in Appendix). More importantly, the increased length of the alkyl unit on the side group also caused a bathochromic effect. For instance, the UV–vis spectrum of MC-Tet_1 depicted the following absorbances at 235 and 276 nm, which in turn shifted to higher wavelengths (241 and 308 nm) with the increment of the side group alky chain of MC-Tet_3 (from -$(CH_2)_6$ to -$(CH_2)_{10}$). It is considered that this to be because the wavelengths tend to be shifted toward the long wavelength region as the 1,5 DST conjugation system gets larger with the participation of longer side chain containing polymers (e.g., MC-Tet_1 - MC-Tet_2) and aromatic groups containing polymers (e.g., MC-Tet_5 - MC-Tet_7). Moreover, as the concentration increased, an increment in the absorption intensity, as well as a redshift also occurred for MC-Tet_1 - MC-Tet_7 (**Figure 8.6** and **Table 8.1** in Appendix). The latter negligible impact is mainly attributed to the nonconventional luminescent materials.

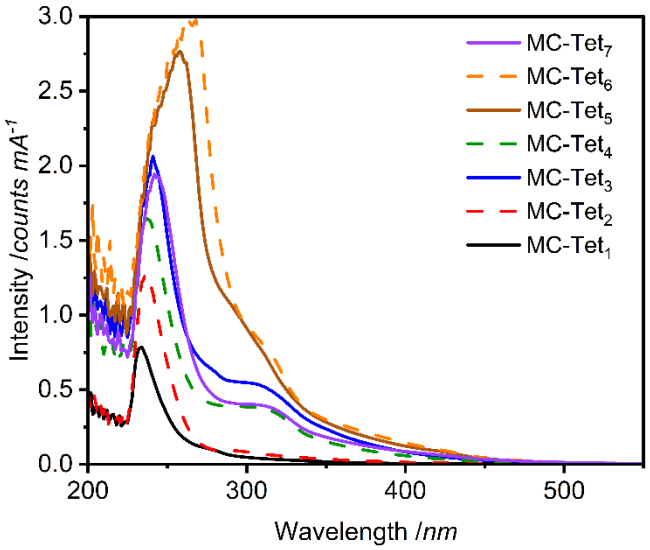

Figure 5. 1. 6 Comparative absorption traces of MC-Tet$_1$ (black line), MC-Tet$_2$ (red dot line), MC-Tet$_3$ (blue line), MC-Tet$_4$ (green dot line), MC-Tet$_5$ (brown line), MC-Tet$_6$ (orange dot line), MC-Tet$_7$ (purple line) at 1.2 M concentration in DCM.

To get more information about the photophysical properties of the polymers, their emissions by varying excitation wavelengths (λ_{ex}) have been determined. Different emission behaviour was observed under the excitation at different wavelengths (**Figure 8.7** in Appendix). For instance, no emission was detected under excitation at λ_{ex}=300 nm (**Figure 5.1.7**). A maximal emission was seen for MC-Tet$_1$- MC-Tet$_4$, and MC-Tet$_7$ (**Figure 5.1.7**) at λ_{ex} = 340 nm. The emission started to weaken with the increase in excitation wavelength λ_{ex}. Nevertheless, it is important to emphasize that MC-Tet$_5$ and MC-Tet$_6$ exhibited the strongest emission at λ=400 nm, illustrating that different side group molecular organizations can influence optical properties (**Figure 5.1.7**). Furthermore, in general, as the concentration increases, a significant increase in fluorescence emission intensity, and a slight redshift of the emission bands was observed (**Figure 5.1.7**, **Table 8.1** in Appendix). For instance, emission peak of MC-Tet$_1$ shifted from 391 nm to 398 nm with increased intensity from 423 to 1384 a.u. for aliphatic-substituted polymers. Likewise, emission peak of aromatic polymer MC-Tet$_6$ shifted from 477 nm to 483 nm with increased intensity from 591 a.u. to 1200 a.u (**Figure 5.1.7**, **Table 8.1** in Appendix). Hence, the results indicate that the polymers exhibit unusual emission properties that are triggered by clusters formed through various intra- and intermolecular interactions. These interactions involve electron-rich groups like -C=C-, -N=N-, and -N-N-, as well as conjugated aromatic 1,5 DST units, leading to n-π^* or π-π^* transitions. In conclusion, the polymers display a cluster-induced emission (CTE) characteristic based on these results.[259-262]

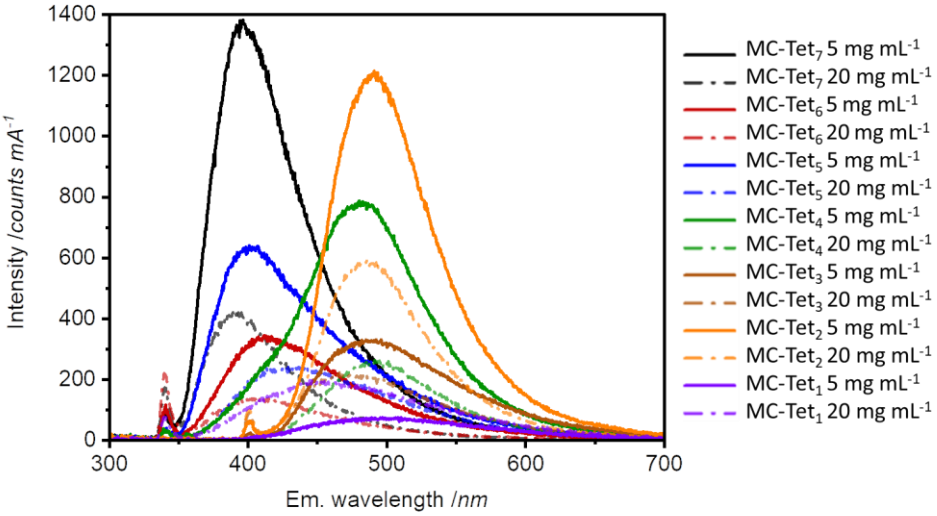

Figure 5. 1. 7 Comparative emission traces of MC-Tet_1 (black line), MC-Tet_2 (red line), MC-Tet_3 (blue line), MC-Tet_4 (green line), MC-Tet_5 (brown line), MC-Tet_6 (orange line), MC-Tet_7 (purple line) in DCM at two different concentrations (20 mg mL^{-1} (straight lines) and 5 mg mL^{-1} (dash dot lines), respectively).

5.1.3 Recapitulation

The present chapter of the thesis successfully demonstrated the development of a highly efficient one-pot synthetic strategy for the preparation of main chain 1,5 DST-based polymers. This innovative approach utilized the UA-4MCP technique for the first time in the literature for the synthesis of seven different types of different substituted (aromatic and aliphatic) main-chain 1,5 DST-based polymer synthesis. In general, all polymerization reactions were carried out under remarkably mild conditions. Moreover, the reactivity of aldehyde derivatives in the synthesis of main chain 1,5 DST-based polymers was explored. It was determined that aromatic aldehydes displayed swifter tendency to form polymers compared to their aliphatic counterparts. Furthermore, the impact of solvent polarity and reaction time was also examined, revealing that a mixture of protic and aprotic solvents, like DMF and MeOH, was effective regardless of polymer type. Also, completion of the polymerization reactions showed a wide range of time (from days to weeks) depending on aldehyde source. In addition, the polymers exhibited moderate degradation temperatures up to 300 °C. Furthermore, complete degradation was observed around 500 °C for all polymers. Other than that, the observed broad range of T_g values (from -25 to 54 °C) showcased intriguing prospects for enhancing processability, thereby broadening the potential application space of these polymers. Significantly, all the polymers exhibited fluorescence because of conjugated aromatic 1,5 DST units. Interestingly, diverse substitutions in side groups induced changes in the CTE properties of polymers.

5.2 Pendant chain 1,5 DS Tetrazole-decorated polymers

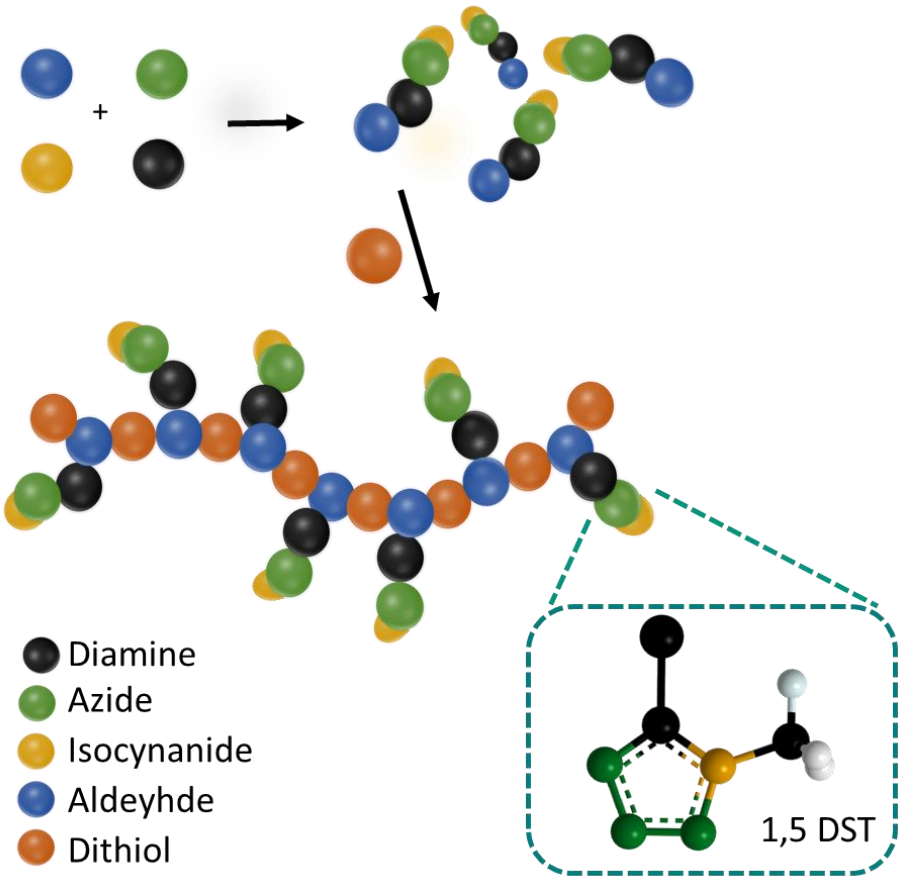

Parts of this chapter are published as "Akdemir, M. S., Simian, M., Theato, P., Mutlu, H., Synthesis of Novel (bis-) 1,5-Disubstituted-1*H*-tetrazole-Decorated Monomers and Their Respective Polymers *via* Thiol-ene Polymerization. *Macromol. Chem. Phys*. **2023**, 224, 2200371. https://doi.org/10.1002/macp.202200371"and adapted with permission from Wiley, 2023.

5.2.1 Prologue

At present, most of the existing examples of tetrazole-decorated polymers are based on 5-substituted tetrazoles (5-STs) as a pendant group, as described in **Chapter 2.3**.[263] [264] Those polymers are synthesized either *via* the polyaddition reactions of tetrazole-decorated dihydrazine monomers with diisocyanate or the radical polymerization of 1-(vinyl-1*H*-tetrazole).[196, 265] Alternatively, the functional group conversion of polyvinyl nitrile into the tetrazole moiety *via* a [2+3] cycloaddition reaction with azide derivatives acid has been reported.[13, 266] Despite existing literature, 1,5 DST units appear to be less investigated than their tetrazole counterparts due to synthetic challenges occurring either during the synthesis of the respective monomer or the respective polymerizations.[11, 194, 267] Therefore, there is still a need to incorporate 1,5 DSTs into the polymer chain as a pendant group to explore the 1,5 DST-containing polymers. Mostly, 1,5 DST synthesis as a small compound, relies on MCRs, such as Passerini or Ugi (especially UA-MCR), as stated in **Chapter 2.3**.[183] However, the UA-4MCR has never been utilized for monomer syntheses, despite the fact that UA-4MCR provides diversity and complexity and allows the preparation of highly attractive 1,5 DST derivatives. Moreover, implementing of the light-induced thiol-ene reaction as a polymerization approach to deliver tetrazole-containing polymers has yet to be fully explored in the literature. Remarkably, it has been shown that 2,5 DST can indeed undergo tetrazole-thiol reaction in the presence of a thiol group, resulting in a thioether linkage formation.[118] However, the 1,5 DST group has never been investigated in this regard. Therefore, there are still certain inquiries that necessitate clarification regarding the implications of the thiol-ene reaction when the 1,5 DST unit.

Therefore, this particular section of the thesis explores the potential thiol-ene reaction involving the presence of 1,5 DST unit, initially within the main chain structure as an expansion of the concepts discussed in **Chapter 5.1**. Additionally, the investigation includes strategy where the 1,5 DST unit is attached as a pendant chain. For pendant chain approach, the concept has been constructed as an efficient synthetic route for a novel type of bis-1,5 DST α,ω-diene monomers on rapid and effective UA-MCR. Subsequently, polymerization reactions of those monomers have been performed *via* thiol-ene click reaction with a series of different dithiol derivatives not only to broaden the toolbox of 1,5 DST-decorated polymers but also to reveal the potential of thiol-ene polymerization in the presence of 1,5 DST derivative. Accordingly, the polymers were subjected to a detailed analysis using various techniques, including SEC, NMR, ATR-IR, TGA, and DSC, as well as UV-Vis and fluorescence spectroscopy. Subsequently, the following section presents a comprehensive explanation of the experimental part, coupled with the presentation of characterization results and an in-depth discussion thereof.

5.2.1 Synthesis and Characterization

Before the polymer synthesis *via* thiol-ene reaction, it was essential to ensure that 1,5 DST units remains intact during the light-induced reaction with the thiol derivatives to understand the feasibility and potential outcomes of thiol-ene reactions. For this purpose, previously synthesized main chain 1,5 DST containing polymers have been evaluated. A thiol-ene photo-click reaction, initiated by light at a wavelength of 365 nm, was employed for the post-polymerization of alkene-functionalized MC-Tet$_3$ and MC-Tet$_7$ (see Chapter 5.1) (**Scheme 5.2.1**). Briefly, 1-dodecanthiol and MC-Tet$_3$/Tet$_7$ were reacted with a molar ratio of 1:5 thiol-to-ene, using DMAP as the photo initiator. The reaction took place in a solvent mixture of DCM/MeOH in a 1:1 ratio and was subjected to UV irradiation (λ= 365 nm) for 2 hours. Subsequently, the resulting polymers were purified through precipitation into cold MeOH (see Experimental part, Section 7.3.2.).

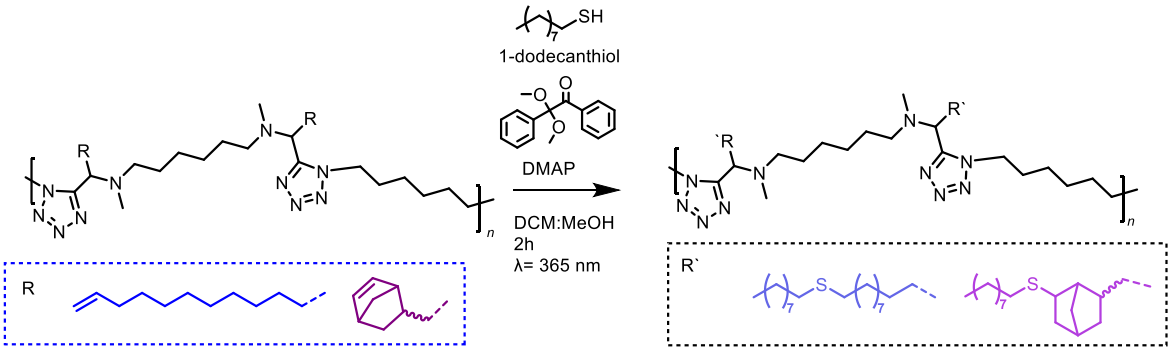

Scheme 5. 2. 1 Schematic representation of post-polymerization modification reaction of MC-Tet$_3$ (R= undecanal, blue line) and MC-Tet$_7$ (R= norbornene, purple line) with 1-dodecanthiol *via* light initiation (λ=365 nm).

The olefin handles were rapidly modified by using the post-polymerization approach, resulting in a successful conversion of over 90%. The effectiveness of the method was supported by ^{1}H NMR results, which demonstrated the disappearance of peaks in the 4.8-5.8 (1-2) ppm and 5.5-6.3 (1-2) ppm ranges for MC-Tet$_3$ (MC-Tet$_{3ppm}$, pale blue line, **Figure 5.2.1.a**) and MC-Tet$_7$ (MC-Tet$_{7ppm}$, pale purple line **Figure 5.2.1.b**), respectively, indicating successful modification of the terminal olefin handles. Importantly, with the aid of ^{1}H NMR characterization, it has also been observed that the 1,5 DST moiety remains intact during the post-polymerization modification process, even in the presence of the thiol group ((R (i.e., aliphatic, aromatic)-SH), which typically reacts with 2,5 disubstituted tetrazole derivatives (i.e., 2,5-diphenyltetrazole).[268]

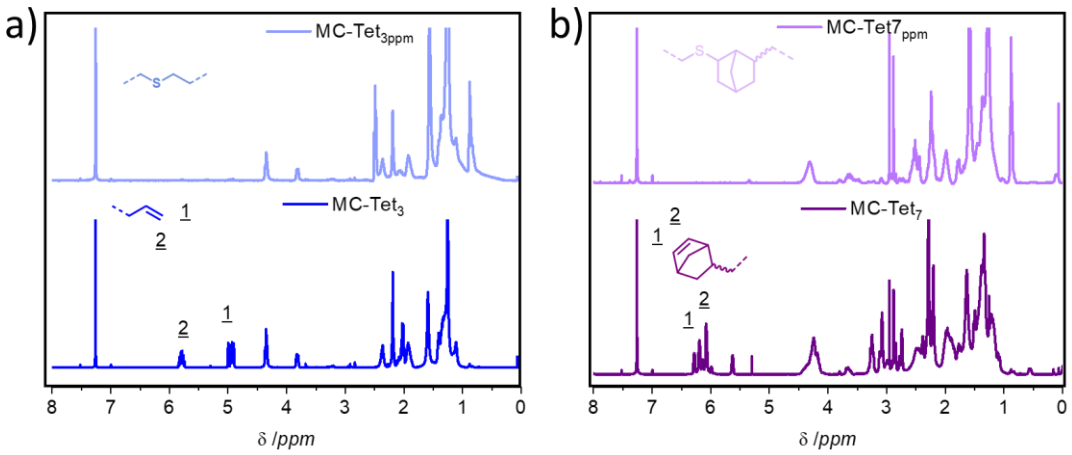

Figure 5. 2. 1 Comparative ^{1}H NMR ($CDCl_3$, 400 MHz) spectrum of before (MC-Tet_3, blue line; MC-Tet_7, purple line) and after (MC-Tet_{3ppm}, pale blue line; MC-Tet_{7ppm}, pale purple line) post-polymerization modification reaction.

Additionally, post-polymerization reaction of the UA-4MC polymers were approved by SEC data (**Figure 5.2.2**). Introducing of 1-dodecano aliphatic chains into the main chain 1,5 DST-based structure *via* post-polymerization reaction led to a noticeable increase in molecular weights. According to the SEC results, there was a rise in M_n from 5.6 kg mol^{-1} ($Đ$ = 1.3) for MC-Tet_3 to 7.7 kg mol^{-1} ($Đ$ = 1.3) (MC-Tet_{3ppm}), and an increase from 8.5 kg mol^{-1} (Đ = 1.3) for MC-Tet_7. to M_n 9.2 kg mol^{-1} ($Đ$= 1.3) (MC-Tet_{7ppm}). (**Figure 5.2.2.a**). Moreover, **Figure 5.2.2.b** displays the comparative ATR-IR spectra of MC-Tet_3 and MC-Tet_7, before and after the post-polymerization reaction. The results indicate that the modification led to the disappearance of absorption bands at 3104 cm^{-1}, which correspond to the olefin functionalized handles of MC-Tet_3 and MC-Tet_7, demonstrating the successful modification process. Nevertheless, the characteristic absorption bands of the 1,5 DST unit remained intact at 1056 cm^{-1}, 1114 cm^{-1}, 1234 cm^{-1}, and 1382 cm^{-1}, indicating that the 1,5 DST unit was preserved during the post-polymerization process. This preservation demonstrates the efficiency of the thiol-ene click reaction in modifying the 1,5 DSTs unit, which is consistent with the results obtained from NMR analysis.

Consequently, the incorporation of olefin groups into the polymer structure provided the possibility of post-polymerization modifications *via* thiol-ene photo-click reactions without and decomposition of 1,5 DST units in the main structure. This result can be clarified by the fact that when the main structure contains the 1,5 DST unit, it is likely to be in a more stable and controlled environment, which could potentially protect it from external factors. The surrounding molecular structure may contribute to stability and prevent the unit from undergoing any unwanted chemical reactions. However, when 1,5 DST unit becomes part of a pendant chain, there is possiblity of 1,5 DST moiety becomes more prone to interacting with reactive substance or external factors due to its location. This exposure could lead to the initiation of a reaction with thiol group, resulting in the observed reactivity. Hence, it was necessary to conduct an inquiry into utilizing

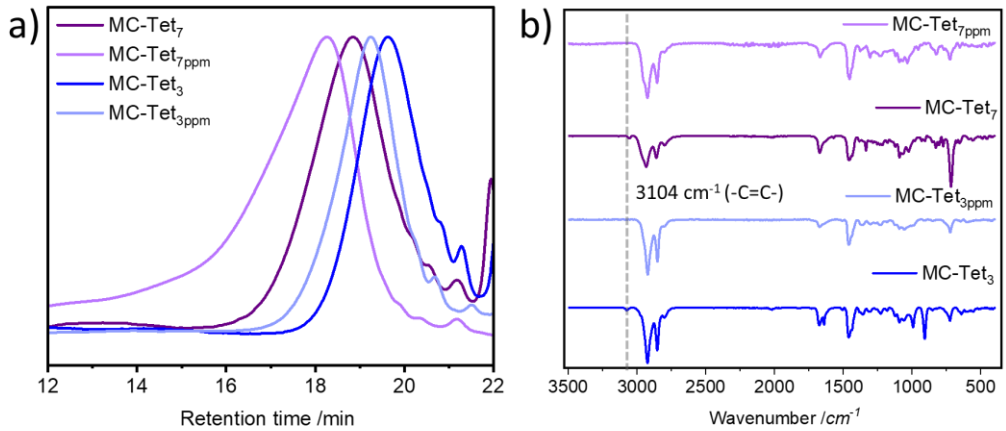

Figure 5. 2. 2 Comparative before and after post-polymerization modification reaction a) SEC traces, b) ATR-IR spectra of MC-Tet$_3$ (blue line), MC-Tet$_7$ (purple line) and MC-Tet$_{3ppm}$ (pale blue line), MC-Tet$_{7ppm}$, respectively.

the 1,5 DST unit as a pendant group to ascertain the viability of the thio-ene polymerization technique. Accordingly, 1,5 DST-containing model compound (MC) was synthesized *via* UA-4MCR by reacting undecanal, butyl isocyanide diethylamine, and $TMSN_3$ in the presence of DBU under an inert atmosphere (**Scheme 5.2.2**).[183] (see Experimental part. Section 7.3.2) Upon the synthesis of the MC, an initial investigation of a light-initiated (λ = 365 nm) thiol-ene reaction, whose product is depicted as model reaction (MR), was performed by using 1-dodecanthiol (1:1 thiol-to-ene molar ratio) and MC in the presence of DMAP as the photoinitiator (**Scheme 5.2.2**). The resulting MR was obtained with a total yield of 98% after purification by column chromatography. (see Experimental part, Section 7.3.2)

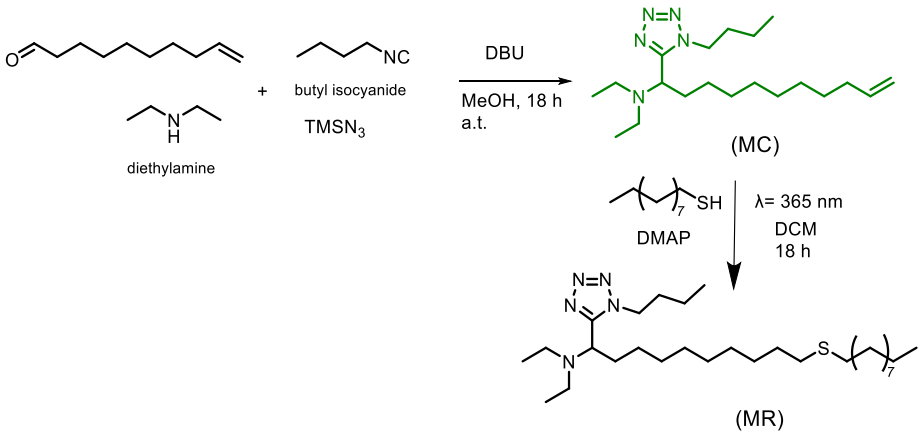

Scheme 5. 2. 2 Synthesis pathway of model compound *via* UA-4MCR and its thiol-ene reaction with 1-dodecanthiol under UV irradiation (λ = 365 nm).

The chemical structures of MC and MR were confirmed using ^{1}H NMR spectroscopy, as depicted in **Figure 5.2.3.a** (shown in green line for MC, black line for MR). Furthermore, **Figure 8.8** in Appendix showcases the COSY-NMR findings for MC. On the one side, the ^{1}H NMR of MC

analysis (in **Figure 5.2.3.a, green**) revealed the presence of magnetic resonance of the only proton associated with the tetrazole moiety at ~3.8 ppm (a) (**Figure 5.2.3.a**). Furthermore, it was of utmost importance to validate the retention of the olefin end groups while conducting the synthesis. This verification was substantiated by the identification of magnetic resonances originating from the olefin functional group, which were observed at approximately 5.0-4.8 (1) ppm and 5.7 (2) ppm in ^{1}H NMR as depicted in **Figure 5.2.3.a**. Additionally, the magnetic resonances at 115 ppm and 139 ppm in ^{13}C NMR for MC (**Figure 8.9** in Appendix) were attributed to the olefin functionality. Moreover, the magnetic resonance at 155 ppm corresponded to the only carbon atom in the 1,5 DST moiety. On the other side, after the thiol-ene reaction, ^{1}H NMR results for MR (depicted in **Figure 5.2.3.a** as a black line) provided clear evidence that no photolytic decomposition of 1,5 DST occurred during the reaction. Explicitly, it was observed that magnetic resonance at 3.8 ppm (a), associated with 1,5 DST moiety, remained intact. Furthermore, the presence of the 1,5 DST unit in the compound was verified by identifying the bands observed at 1382, 1234 and 1063 cm^{-1}, which correspond to the stretching vibrations of -N=N-, -C=N- and -C-N- bonds, respectively, in the ATR-IR spectrum (**Figure 5.2.3.b** as a green line). Additionally, -C=C- absorption bands (3104 and 1640 cm^{-1}), which correspond to olefin functionalized handles of MC, have disappeared, while the characteristic absorption bands of tetrazole unit detected at 1056, 1114, 1234, and 1382 cm^{-1} remained intact for MR (in **Figure 5.2.3.b**, black line). Aside, according to the SEC results represented in **Figure 8.10** in Appendix, there is an increase in M_n for MR, providing additional confirmation of the successful light-induced thiol-ene reaction.

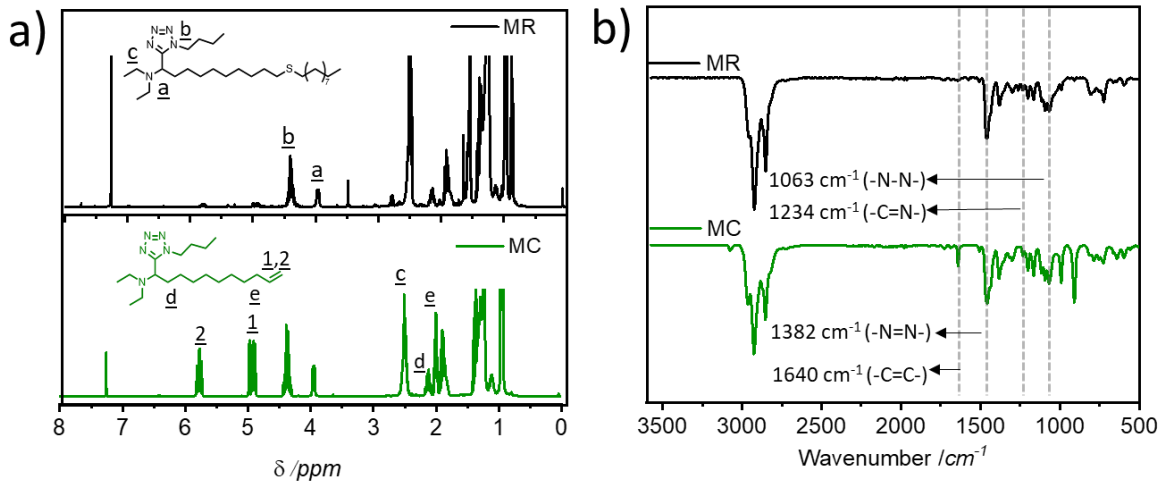

Figure 5. 2. 3 Comparative: a) ^{1}H-NMR ($CDCl_3$, 400 MHz) and b) ATR-IR spectra of MC (green line) and MR (black line), respectively**.**

Upon confirming that the 1,5 DST unit is unreactive during the photo-induced thiol-ene reaction, in the next step, bis-1,5 DST α,ω-diene monomers were synthesized by adopting procedure mentioned above (shown in **Scheme 5.2.3**). Briefly, targeted α, ω-diene monomers M1 and M2

were synthesized by using the appropriate aldehyde (i.e.,10-undecenal and 4-pentenal for M1 and M2, respectively), *N,N*-dimethyl-1,6-hexanediamine, butyl isocyanide, $TMSN_3$ and DBU (as a catalyst) in MeOH (1M) at ambient temperature for 18 h. Subsequently, the monomers were isolated in reasonably good yields (95% and 89% for M1 and M2, respectively) upon column chromatography (DCM: MeOH (19:1)). (see Experimental part, Section 7.3.2)

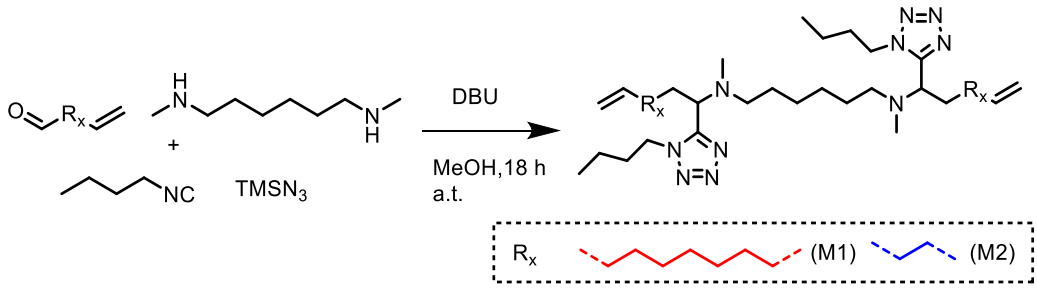

Scheme 5. 2. 3 Synthesis pathways of M1 and M2 *via* UA-4MCR.

The chemical structure of α, ω -diene monomers (M1 and M2) was confirmed by ^{1}H NMR in addition to ATR-IR spectroscopy. On the one hand, as can be seen in **Figure 5.2.4**, the magnetic resonances at ~5.0-5.7 (1,2) and 3.8 ppm (a) in ^{1}H NMR spectrum corresponding to the protons on the terminal olefin and bis-1,5 DST moieties, respectively, for both M1 and M2, were observed. On the other hand, as in the case of the ATR-IR analysis for MC, all analogous bands at 1382, 1234 and 1064 cm^{-1} confirming the presence of tetrazole moiety can be detected in the comparative spectra for M1 and M2 in **Figure 8.11** in Appendix.

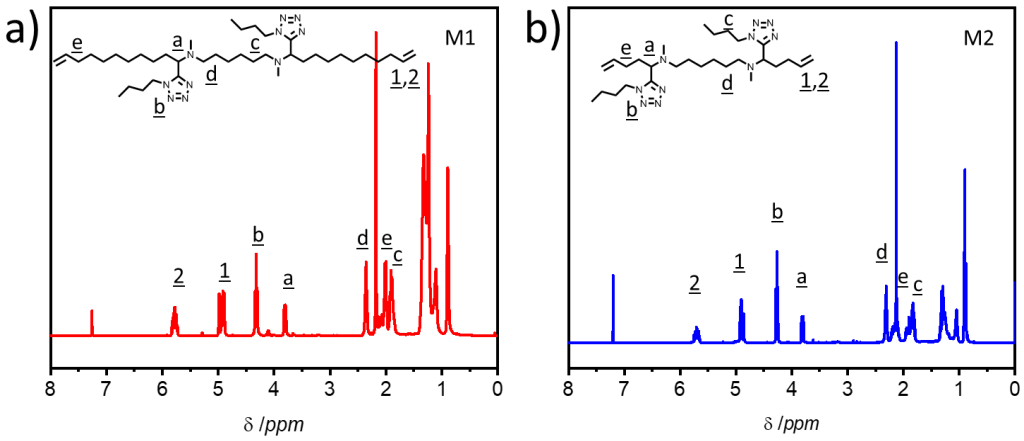

Figure 5. 2. 4 ^{1}H-NMR ($CDCl_3$, 400 MHz) spectrum of a) M1 (red line, left) and b) M2 (blue line, right).

Motivated by the successful results of the test reaction performed with MC, the light-induced thiol-ene polymerizations of M1 and M2 were conducted in the presence of stoichiometric amounts of various dithiol derivatives, which are represented in **Scheme 5.2.4** to deliver pendant chain 1,5 DST-decorated polymers (PC-Tet_1-PCTet_{12}) under UV initiation (λ=365 nm). In

general, light-initiated thiol-ene polymerizations for M1 and M2 were performed with different kinds of dithiol maintaining a 1:1 functional group stoichiometry (e.g., 1,4-butanedithiol (**DT1**, 1.04 g ml^{-1}), 1,6-hexanedithiol (**DT2**, 0.98 g mL^{-1}), 1,8-octanedithiol (**DT3**, 0.97 g mL^{-1}), 1,9-nonanedithiol (**DT4**), dithiothreitol (**DT5**, crystalline) and 3,6-dioxa-1,8-octanedithiol (**DT6**, 0.97 g mL^{-1}) by following the same procedure of the model thiol-ene reaction in the presence of DMPA for 18 h at ambient temperature in a photo reactor **(Scheme 5.2.4)**. (see Experimental part, Section 7.3.2)

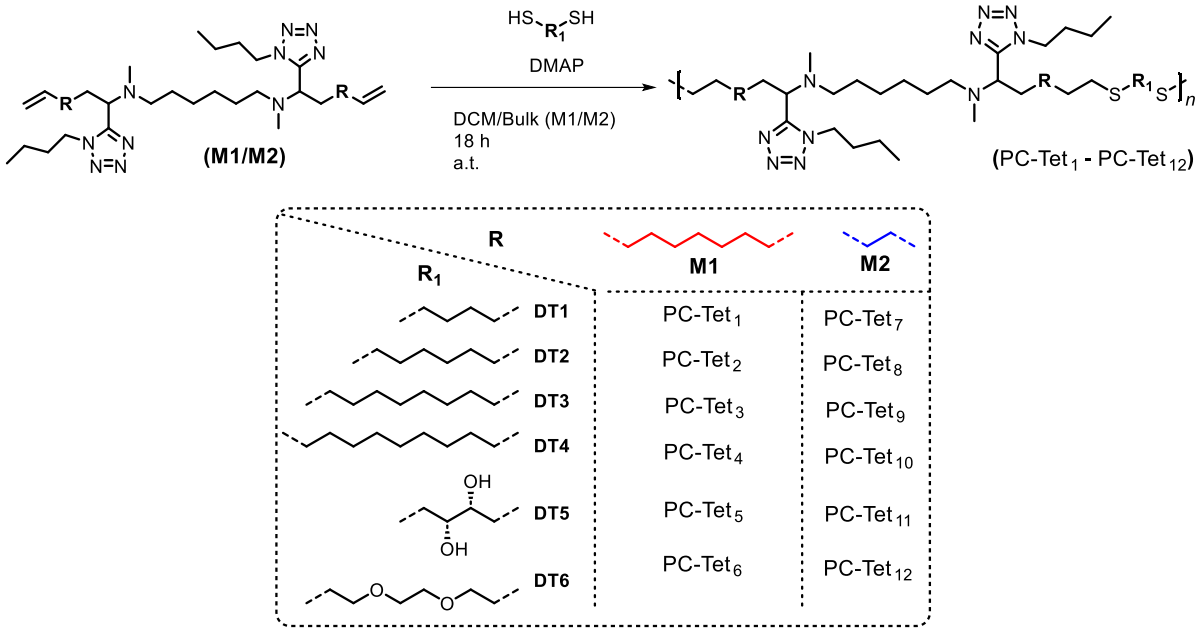

Scheme 5. 2. 4 Synthesis approaches for the preparation of bis-1,5 DST containing α,ω-diene monomers M1 and M2 to deliver bis-1,5 DST containing polymers *via* thiol-ene reaction with dithiols (e.g., 1,4-butanedithiol (DT1), 1,6-hexanedithiol (DT2), 1,8-octanedithiol (DT3), 1,9-nonanedithiol (DT4), dithiothreitol (DT5) and 3,6-dioxa-1,8-octanedithiol (DT6) which are represented in table from PC-Tet$_1$ – PC-Tet$_{12}$ under light initiation (λ = 365 nm). R and R1 donate different functional groups as they are depicted within the table.

However, it is crucial to note in advance that attempting a one-pot tandem multicomponent polymerization approach, where the respective dithiol derivative reacts with precursors to produce tetrazole-decorated monomers (such as aldehyde derivative, diamine *N,N*-dimethyl-1,6-hexanediamine, butyl isocyanide, $TMSN_3$, and DBU), is not a *via*ble option.[269-270] Certainly, a comprehensive review of the literature indicates that thiol derivatives, both aliphatic and aromatic, exhibit efficient reactions with isocyanides in both radical and nucleophilic[271] manner, As a result, this process will prevent the formation of any polymer with the desired chemical structure, namely (bis-1,5 DST). Nevertheless, in order to address the drawbacks of limited monomer mobility and reactivity, which lead to a reduction in the degree of polymerization (DP) and the average molecular weight (M_n), the polymerization process has initially utilized 1,9-nonanedithiol (DT4). Indeed, DT4, as the longest alkyl chain dithiol derivative, has the lowest density (i.e., 0.95 g mL^{-1}) and the most flexible aliphatic chain length compared to all dithiol

derivatives used to show the modularity of the approach. In fact, it has been previously reported that when step-growth polymerizations utilize monomers with lengthier alkyl chains, the resulting polymers can exhibit enhanced diffusibility, even during solid-state polymerization under ambient temperature and time conditions, as compared to polymers derived from shorter alkyl chain derivatives.[272] Moreover, shorter-chain monomers usually depict greater intramolecular cyclization during step-growth polymerization.[273]

Accordingly, M1 reacted efficiently with DT4 to yield polymer PC-Tet_4 (**Scheme 5.2.5**). ^{1}H-NMR spectroscopy of PC-Tet_4 confirmed the formation of the targeted poly(thioether) decorated with bis-1,5 DST unit in each repeating unit. It revealed a high monomer conversion as determined by the decreased signal intensity of olefinic protons at 5.7 and 4.9 ppm (**Figure 5.2.5.a,** red line). Similarly, the presence of the magnetic resonances at 2.5 (a) and 1.9 (b) ppm corresponding to the protons at the α- and β-positions adjacent to the thioether bond, in addition to the tetrazole proton appearing at 3.8 ppm (c), confirmed the expected chemical structure of the repeating units of the polymer (**Figure 5.2.5.a,** red line). Moreover, ATR-IR analysis of polymer PC-Tet_4 (**Figure 5.2.5.b,** red line) indicated that the -C=C- absorption bands (3104 and 1640 cm^{-1}), which correspond to alkene functionalized handles of M1, have disappeared, while the characteristic absorption bands of tetrazole unit detected at 1056, 1114, 1234, and 1382 cm^{-1} remained intact.

Upon the successful polymerization of M1, the same conditions have been adopted to polymerize M2. Nevertheless, M2 failed to polymerize under the mentioned conditions (i.e., 1M, in DCM, a.t.). As it has already been mentioned in the literature that explored cyclic oligomerization competing with the polymerization in step-growth processes for short alkyl chain length derivatives and described self-dilution as a common characteristic for conventional step-growth polymerization of such monomers.[270] Therefore, it is assumed that possible cyclic oligomerization could occur between the reactive groups of the short-chain α,ω-diene monomer M2 and prevent the polymer formation. Thus, a bulk polymerization of M2 with DT4 has been performed alternatively under λ=365 nm for 24 h, which resulted in polymer formation, i.e., PC-Tet_{10} (**Scheme 5.2.4**). The chemical structure of PC-Tet_{10} was also confirmed analogously to PC-Tet_4 by NMR and ATR-IR spectroscopy (**Figures 5.2.5.c** and **5.2.5.d,** blue line).

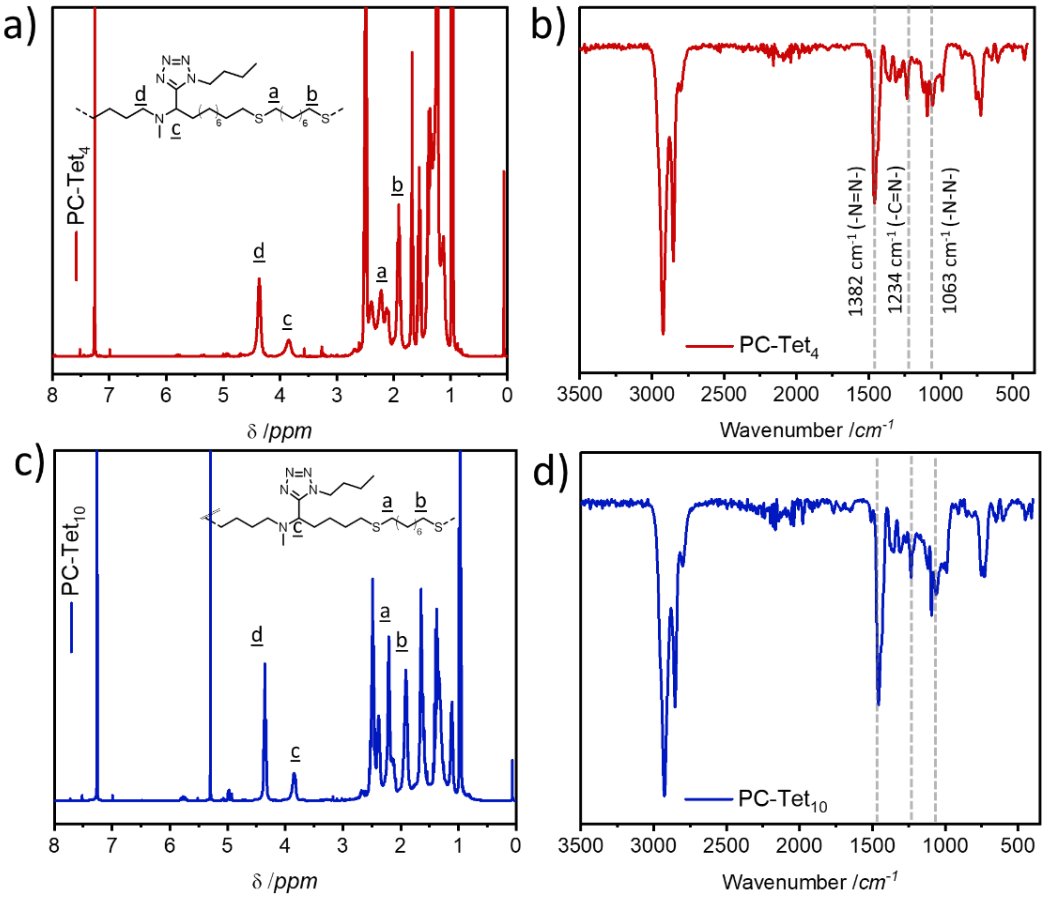

Figure 5. 2. 5 ^{1}H NMR ($CDCl_3$, 400 MHz) of PC-Tet_4 (a, red line) and PC-Tet_{10} (c, blue line); ATR-IR spectrum of PC-Tet_4 (a, red line) and PC-Tet_{10} (c, blue line).

Subsequently, the photo-initiated thiol-ene polymerization was employed to produce a family of polymers of the new tetrazole-decorated α, ω-diene monomers M1 and M2 in the presence of various dithiols (DT1-DT6) (**Scheme 5.2.4**). Accordingly, in Appendix, some exemplary NMR and IR results of the obtained polymers are presented in **Figures 8.12** and **8.13**, respectively. It is important to repeat that the polymerization of M1 was performed in DCM, whereas M2 was usually polymerized in bulk. Additionally, depending on the SEC results (**Figure 5.2.6**), all polymers have a moderate number average molecular mass ($20.5 < M_n < 62.8$ kg mol^{-1}) and expected step-growth dispersity values ($1.4 < Đ < 3.2$) were obtained for the aliphatic dithiol derivatives as shown in **Table 5.2.1,** as well.

Surprisingly, the polymerization of M1 with DT1 delivered a polymer with a considerably high dispersity value ($Đ$ of 5.0, compare **Table 5.2.1**). In fact, high dispersity values are rather typical for polymer chains with a relatively high cyclisation tendency. The latter particularly take place during the step-growth polymerization of any short alkyl chain length derivatives, such as DT1. Clearly, it has been emphasized in the literature that decreasing the alkene length in any reactive bifunctional monomer induces the cyclization tendency of the system (defined as the ratio of rate

constants of cyclization *vs.* chain extension).[274] Therefore, a typical step-growth polymer can contain predominantly linear species and varying cyclic species.[243] Actually, bimodal molecular weight distributions are usually detected in such polymerizations as cyclic products are mainly oligomers, whereas linear chains have high molecular weight. [275]

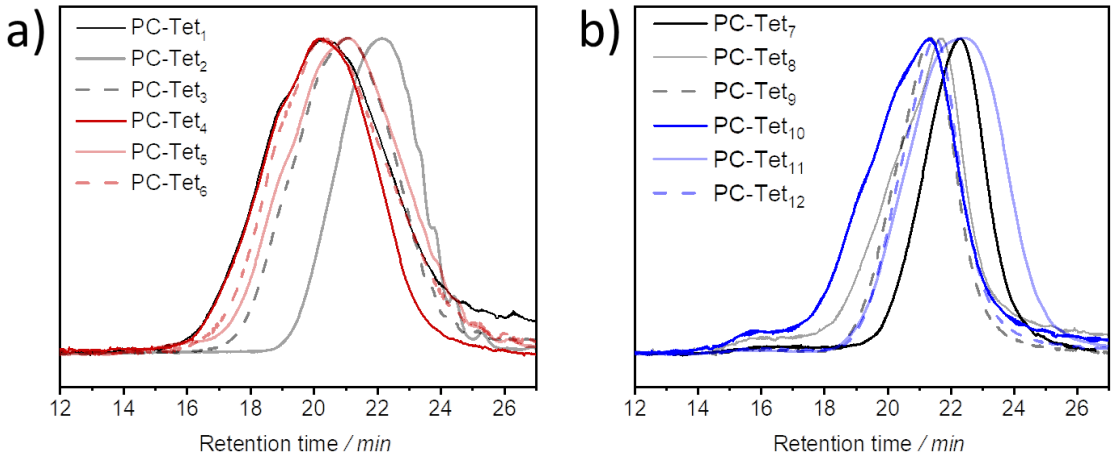

Figure 5. 2. 6 Comparative SEC traces of polymer a) PC-Tet$_1$ - PC-Tet$_6$ obtained from the reaction of M1 and dithiol derivatives. b) PC-Tet$_7$ - PC-Tet$_{12}$ synthesized from M2 and dithiol derivatives**.**

Table 5. 2. 1 Molecular characterization of tetrazole-decorated polymers (PC-Tet$_1$ - PCTet$_{12}$) obtained *via* thiol-ene polyaddition reaction.

Polymer	Dithiol	M_n (kg mol^{-1}) SEC[a]	$Đ$ (M_w/M_n)
PC-Tet$_1$*	DT1	34.2	5.0
PC-Tet$_2$*	DT2	23.8	1.6
PC-Tet$_3$*	DT3	62.8	3.2
PC-Tet$_4$*	DT4	40.2	2.3
PC-Tet$_5$*	DT5	49.1	2.9
PC-Tet$_6$*	DT6	42.5	2.5
PC-Tet$_7$**	DT1	24.8	1.3
PC-Tet$_8$**	DT2	35.6	1.4
PC-Tet$_9$**	DT3	38.5	1.4
PC-Tet$_{10}$**	DT4	50.1	1.9
PC-Tet$_{11}$**	DT5	20.5	1.9
PC-Tet$_{12}$**	DT6	37.3	1.4

*M1 has been used as the monomer, ** M2 has been used as monomer. [a]Dithiol derivatives:1,4-butanedithiol (DT1), 1,6-hexanedithiol (DT2), 1,8-octanedithiol (DT3), 1,9-nonanedithiol (DT4), dithiothreitol (DT5) and 3,6-dioxa-1,8-octanedithiol ((DT6). [a]Determined by SEC using THF as an eluent.

On the contrary, lower $Đ$ values were obtained for samples prepared in bulk as for PC-Tet$_7$ ($Đ$ of 1.3), which was synthesized from M2 and DT1, both monomers possessing the shortest methylene spacers and with only moderate conversion. Actually, the decrease of the dispersity by applying bulk conditions is predictable as the Ruggli-Ziegler-Dilution Principle, which in turn states that the lower concentration of reagents leads to a higher amount of cyclic molecules and a lower degree of polymerization.[259] Delightfully, polar dithiol monomers such as dithiothreitol

(DT5) and 3,6-dioxa-1,8-octanedithiol (DT6) also resulted in polymers (**Table 5.2.1**). Indeed, it has been observed that the pendant polar hydroxyl, in addition to the polar 1,5 DST groups, allow polymers (PC-Tet$_5$ and PC-Tet$_{11}$) to be good soluble not only in conventional organic solvents, such as THF, DCM, and DMF, but also in a polar solvent, such as methanol.

Moreover, TGA was applied in order to detect the thermal properties of the novel developed polymers. As shown in **Figure 5.2.7** and listed in **Table 5.2.2**, a multi-step degradation pattern was observed with $T_{d,5\%}$ ~300 and ~280 °C under inert conditions (i.e., nitrogen gas) for PC-Tet$_1$ - PC-Tet$_6$ (**Figure 5.2.7.a**) and PC-Tet$_7$ - PC-Tet$_{12}$ (**Figure 5.2.7.b**), respectively resulting from the polymerizations of M1 and M2 with a series of the dithiols shown in **Scheme 5.2.4**. The first degradation steps occurred between 280 and 395 °C followed by the second step around 400 to 470 °C. The first degradation can be attributed to the elimination of the 1,5 DST pendant groups, while the second step is relevant to the backbone degradation. Importantly, almost no char residue was observed for most of the polymers, aside from polymer PC-Tet$_8$. In addition, the different chain lengths of the dithiol derivatives had a relatively small influence on $T_{d,5\%}$, as can be seen in **Figure 5.2.7.b** (shorter length of PC-Tet$_1$ or PC-Tet$_7$, vs. longer length of PC-Tet$_4$ or PC-Tet$_{10}$). Whereas TGA curves of PC-Tet$_5$ and PC-Tet$_{11}$, which contain hydrogen-bond interaction originating from DT5, have shown a significant decrease in the composition temperature ($T_{d,5\%}$). As a result, it can be said that the synthesized polymers have shown enhanced degradation profile compared to pendant chain tetrazole decorated aliphatic counter partners in the literature, such as poly-l-vinyl-5-methyltetrazole ($T_{d,5\%}$ ~270 °C) and poly-l-vinyl-5-phenyltetrazole ($T_{d,5\%}$ ~230 °C).[276]

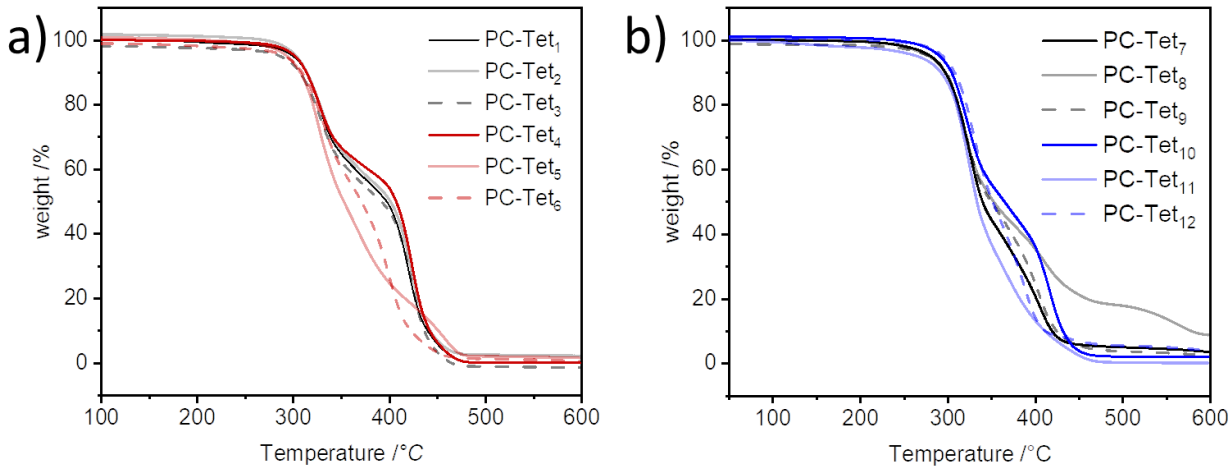

Figure 5. 2. 7 Comparative TGA traces of polymer a) PC-Tet$_1$ - PC-Tet$_6$ obtained from the reaction of M1 and dithiol derivatives. b) PC-Tet$_7$ - PC-Tet$_{12}$ synthesized from M2 and dithiol derivatives.

Table 5.2.2 Thermal analysis of tetrazole-decorated polymers (PC-Tet$_1$ - PCTet$_{12}$) obtained *via* thiol-ene polyaddition reaction.

Polymer	Dithiol[a]	$T_{d,5\%}$ (°C)[a]	T_g (°C)[b]
PC-Tet$_1$*	DT1	299	-31
PC-Tet$_2$*	DT2	298	-37
PC-Tet$_3$*	DT3	301	-32
PC-Tet$_4$*	DT4	301	-34
PC-Tet$_5$*	DT5	288	-13
PC-Tet$_6$*	DT6	301	-42
PC-Tet$_7$**	DT1	280	-20
PC-Tet$_8$**	DT2	280	-29
PC-Tet$_9$**	DT3	286	-23
PC-Tet$_{10}$**	DT4	286	-28
PC-Tet$_{11}$**	DT5	267	-21
PC-Tet$_{12}$**	DT6	292	-32

[a]The decomposition temperature ($T_{d,5\%}$) defined as the temperature at 5% weight loss was detected by TGA. [b]The glass transition temperature (T_g) observed during the second heating measurement *via* DSC analysis.

Next, the thermal transitions of the polymers were investigated *via* DSC (**Figure 5.2.8** and **Table 5.2.2**). In general, the DSC studies indicated that the polymers were in an amorphous state, characterized by low T_g values (T_g < -10 °C). Moreover, it was detected that PC-Tet$_1$ - PC-Tet$_6$ (polymers derived from M1) featured a lower glass transition temperature than PC-Tet$_7$ - PC-Tet$_{12}$ (polymers derived from M2). Indeed, it can be hypothesized that decreasing the spacing between the inflexible components, especially in the 1,5 DST-decorated components, may lead to the creation of polymers with elevated T_g values. Regarding the impact of dithiol derivatives, **DT6** further increased the distance and chain-flexibility between rigid backbone components leading to the lowest observed T_g of the dithiol linkers at -42 °C for PC-Tet$_6$ and -32 °C PC-Tet$_{12}$., respectively (see **Table 5.2.2**).

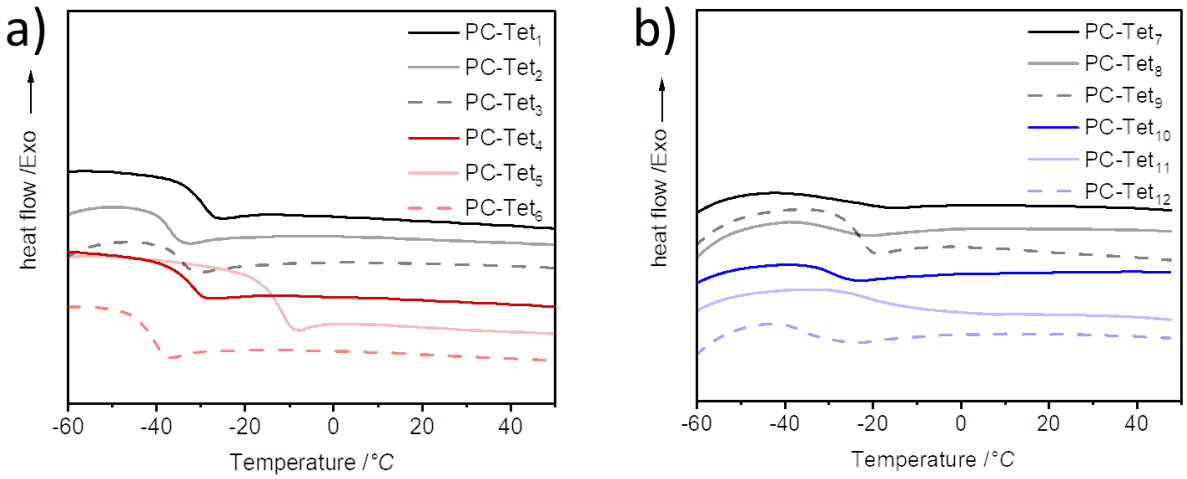

Figure 5. 2. 8 Comparative DSC traces of polymer a) PC-Tet$_1$ - PC-Tet$_6$ obtained from the reaction of M1 and dithiol derivatives. b) PC-Tet$_7$ - PC-Tet$_{12}$ synthesized from M2 and dithiol derivatives

Subsequently, the photophysical characteristics of the synthesized polymers (PC-Tet_1 - PC-Tet_{12}) were examined because they possess the potential to exhibit luminescent properties. For that, UV-visible and fluorescence spectroscopy have been employed. Preliminary investigations were performed by analysing the absorption spectra of MC and M1 (chemically similar to M2) in MeOH, owing to their simplicity. On the one hand, the UV-Vis spectrum of MC depicted the following absorbances and weak fluorescence at ~238 nm, 304 nm and ~364 nm, which in turn shifted to higher wavelengths (250 nm, 308 nm and ~374 nm, respectively) with the increment of concentration (from 2.5 mg mL^{-1} to 5 mg mL^{-1} in MeOH) as shown in **Figure 5.2.9.a**. Furthermore, as the concentration increased, an increment in the absorption intensity was also observed (**Figure 5.2.9.a**). The calculated quantum yield (QY) of MC was Φ-MC=1.92 % (**Figure 8.14** in Appendix), which can be related to low luminescence materials. On the other hand, monomer M1 showed slightly different behaviour (**Figure 5.2.9.b**)., i.e., the absorption spectrum (at a concentration of 2.5 mg mL^{-1} in MeOH) featured two maxima centred at 247 nm and 346 nm in addition to an absorption band at 389 nm as a shoulder. The absorption band, which was detected at 247 nm, was shifted to a higher wavelength at 270 nm with the increased concentration from 2.5 mg mL^{-1} to 20 mg mL^{-1}, while the absorption intensity at first has increased, and then, decreased at a concentration of 20 mg mL^{-1} (**Figure 5.2.9.b**). On the contrary, the absorption bands at 346 nm and 389 nm have remained practically in the same wavelength range, accompanied with an increment in the absorption intensity (**Figure 5.2.9.b**).

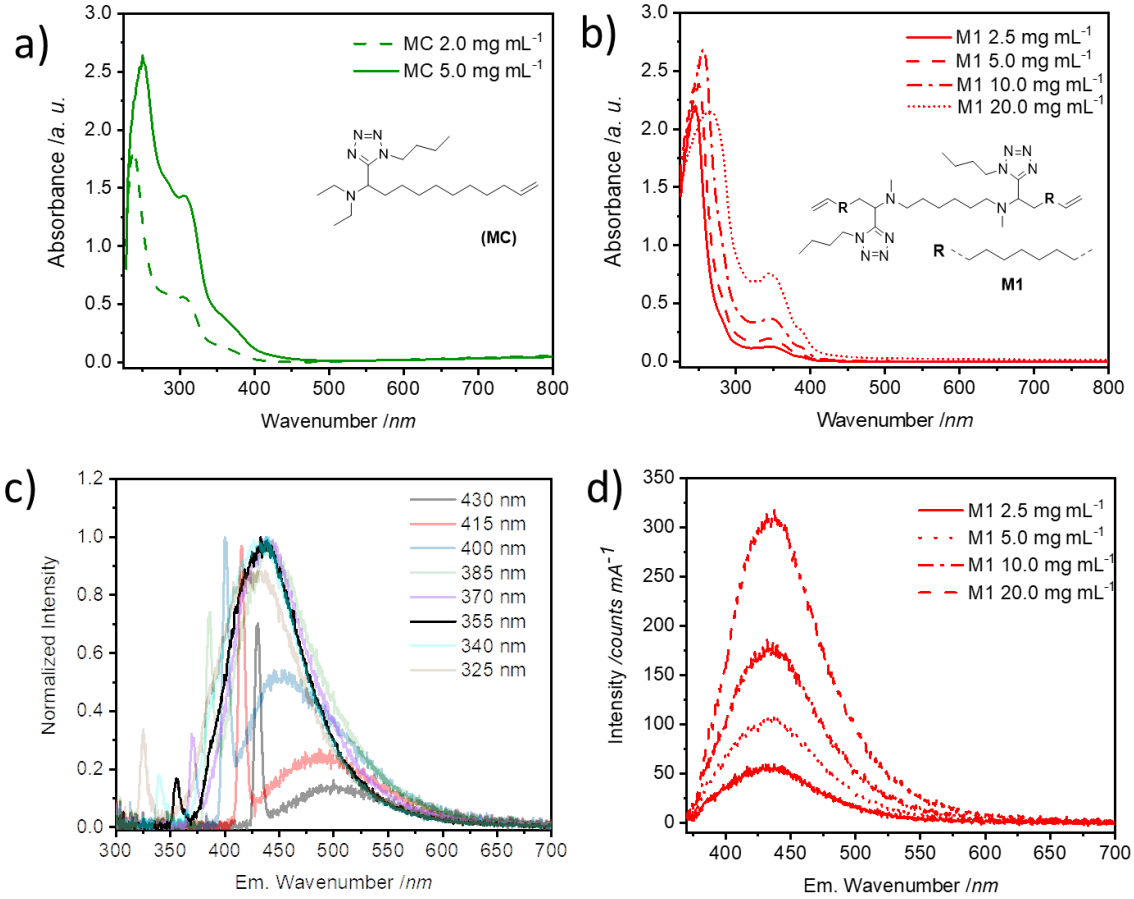

Figure 5. 2. 9 a, b) Absorption traces of MC and M1, respectively, at different concentrations in MeOH c) Emission spectra of M1 at various excitation wavelengths (from 325 to 430 nm) in MeOH (c = 20 mg mL^{-1}). d) Emission spectra of M1 at different concentrations in MeOH (298 K) at λ_{ex} = 355 nm.

To get more information about the photophysical properties of M1, its emissions by varying excitation wavelengths (λ_{ex}) have been determined. In fact, the fluorescence emission of the M1 (**Figure 5.2.9.c**) showed a significant change upon different excitation wavelengths from 325 to 420 nm. The photoluminescence peak shifts to longer wavelengths, and its intensity decreases rapidly with the strongest peak excited at the absorption band. This is a compelling photoluminescence phenomenon generally exhibited by nonconventional luminescent materials (either small molecules or polymers). This behaviour is mainly attributed to the materials containing different chromophores with degenerate energy levels. Furthermore, concentration is a crucial parameter to adjust the non-conventional intrinsic luminescence behaviour of small molecules and polymers, and to identify emission centres. Fluorescence emission spectra of M1 solutions with different concentrations were measured at λ_{ex}=355 nm (**Figure 5.2.9.d**). In fact, a significant increase in fluorescence emission intensity was observed in addition to a slight red shift of the emission band located at 427 nm to a higher wavelength of 440 nm when the M1

concentration was varied from 2.5 mg mL^{-1} to 20.0 mg ml^{-1}. Thus, we inferred that M1 possessed the cluster-induced emission characteristic.

Subsequently, the exemplary M1-derived polymers PC-Tet_1, PC-Tet_4, and PC-Tet_6 underwent examination and were compared to the M2-derived polymers PC-Tet_7, PC-Tet_{10}, and PC-Tet_{12} in terms of their optical properties. In fact, the UV-vis spectra of all polymers depicted a similar behaviour, which was comparative to monomer M1 (**Figures 8.15** in Appendix). In other words, an absorbance max at ~245 nm with a shoulder peak at 343 nm was observed for all polymers. The increase of the concentration (from 2.5 to 10.0 mg mL^{-1} in DCM) was accompanied by an increment of the absorption intensity and a redshift of the absorbance maxima (to ~254 nm) in addition to an extension of the tail extended to the visible region, as it is shown in **Figure 5.2.10**, along, **Figures 8.15** in Appendix. A negligible impact on absorption intensity was observed by varying the type of the dithiols (DT1, DT4 and DT6) polymerized with monomer M2 (see **Figure 8.15**, Appendix). Polymers (PC-Tet_1, PC-Tet_4, and PC-Tet_6) derived from M1 showed explicit dependency on the dithiol used, i.e., the incorporation of DT6 in polymer PC-Tet_6 resulted in the maximum absorption intensity (compare **Figure 5.2.10.a** and **Figure 8.15** in Appendix). Furthermore, with increasing concentration, visible blue emission was observed for all polymers when it gets to 10.0 mg mL^{-1}. As it is depicted in Figure **5.2.10.b** and **Figure 8.16** in Appendix, the photoluminescence intensity progressively has become higher and redshifted as the concentration increased from 2.5 mg mL^{-1} to 10.0 mg mL^{-1} with an Em (photoluminescent emission) at 438 nm (λ_{ex} = 355 nm), which can be ascribed to the clustering of tetrazole and thioether moieties along with the conformation rigidification. The photographs of all polymers in DCM under the illumination of a 365 nm UV lamp are shown in **Figure 5.2.10.a** in addition to **Figure 8.16** in Appendix. Moreover, the emission spectra of the solution of PC-Tet_6 (10.0 mg mL^{-1}) with varying λ_{ex} values also verified the presence of different emission centers (**Figure 5.2.10.c**). Actually, the Em values were conspicuously redshifted as λ_{ex} increased from 325 to 430 nm. Furthermore, when dissolved in different solvents, such as MeOH, the emission spectra of all polymers exhibit a slightly varied emission profile (**Figures 8.16**, Appendix), indicating the different emissive clusters in varying solvents.

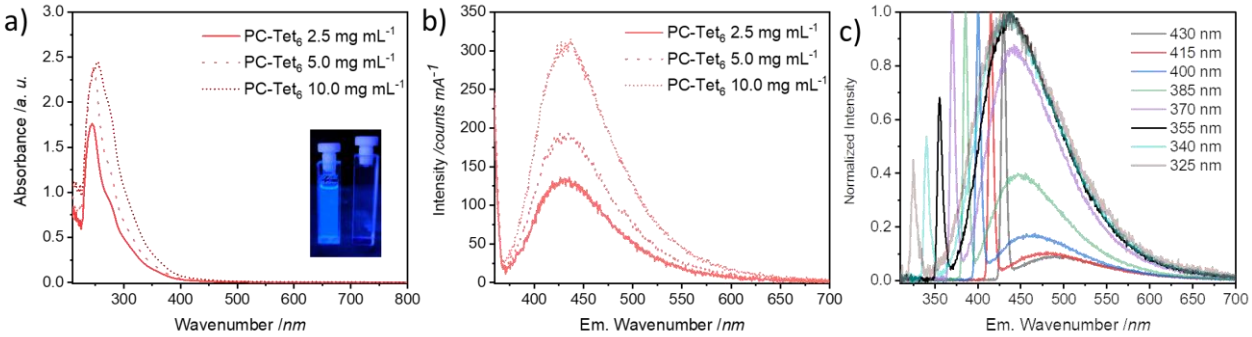

Figure 5. 2. 10 a, b) Absorption and emission (λ_{ex} = 355 nm) traces of PC-Tet$_6$, respectively, at different concentrations in DCM c) Emission spectra of PC-Tet$_6$ at various excitation wavelengths (from 325 to 430 nm) in DCM (c = 10.0 mg mL^{-1}). Photograph were taken under 365 nm UV light of PC-Tet$_6$ (10.0 mg mL^{-1}1 in DCM, left) and pure DCM (right).

Taking PC-Tet$_6$ as an example, multiple intra- and intermolecular interactions like arising from n–π* or π–π* transitions between electron-rich -C-C-, -N=N- and -N-N-, and the conjugated aromatic tetrazole units can be considered as the possible mainspring for cluster triggered emission.

5.2.2 Recapitulation

This chapter of the thesis successfully demonstrated the first attempt for the synthesis of tetrazole-decorated monomers *via* the Ugi-azide four-multicomponent reaction (UA-4MCR) and their subsequent polymerization through thiol-ene chemistry. The fundamental synthetic idea primarily revolved around exploring the feasibility of using thiol-ene reaction with 1,5 DST units, either incorporated into the main polymer chain or attached as pendant chains, in order to investigate the potential occurrence of a reaction between tetrazole and thiol groups. Upon illustrating the evidence that 1,5-tetrazole units within the main chain do not undergo reactions with thiol derivatives, a continuation from the preceding section, the same concept was extended to pendant chain tetrazole units. A model compound equipped with bis-1,5 DST was employed to ensure the reliability and effectiveness of the reaction. This step aimed to confirm that the thiol derivatives involved in the process would not undergo any undesired side reactions with the corresponding tetrazole units during the light-induced thiol-ene addition reaction, particularly when the 1,5 tetrazole group is part of the pendant chain. Following the successful establishment of the synthetic approach, synthesizing two distinct α, ω-diene monomers decorated with bis-1,5 DST units was carried out with remarkable efficiency. Strategically, two different lengths of the alkyl chain (e.g., -$(CH_2)_4$ and -$(CH_2)_9$) were targeted for the monomer synthesis to explore the effect on the polymerization process. Upon the synthesis of monomers, the light-induced thiol-ene polyaddition reaction was employed, utilizing various dithiol derivatives, which enabled the construction of a diverse array of polymers decorated with bis-1,5 DST units. In general, monomer and dithiol derivatives with longer alkyl chains had a higher propensity to undergo polymerization, leading to increased molecular weights. On the other hand, shorter alkyl chains were more likely to undergo cyclization. Moreover, all polymers exhibited a distinctive two-step degradation process, demonstrating considerable stability even up to 300 °C. Furthermore, almost complete degradation of all polymers was observed around 470 °C. Other than that, all polymers showed T_d values below ambient temperature. Of significant note, CTE feature was observed in all the polymers because of conjugated aromatic 1,5 DST units. In addition, the adjustability of this fluorescence behaviour by changing the dithiol derivatives during the polymerization process is also exhibited, providing tuneable character for the possible applications.

5.3 Pendant chain 1,5 DS Tetrazole-decorated networks

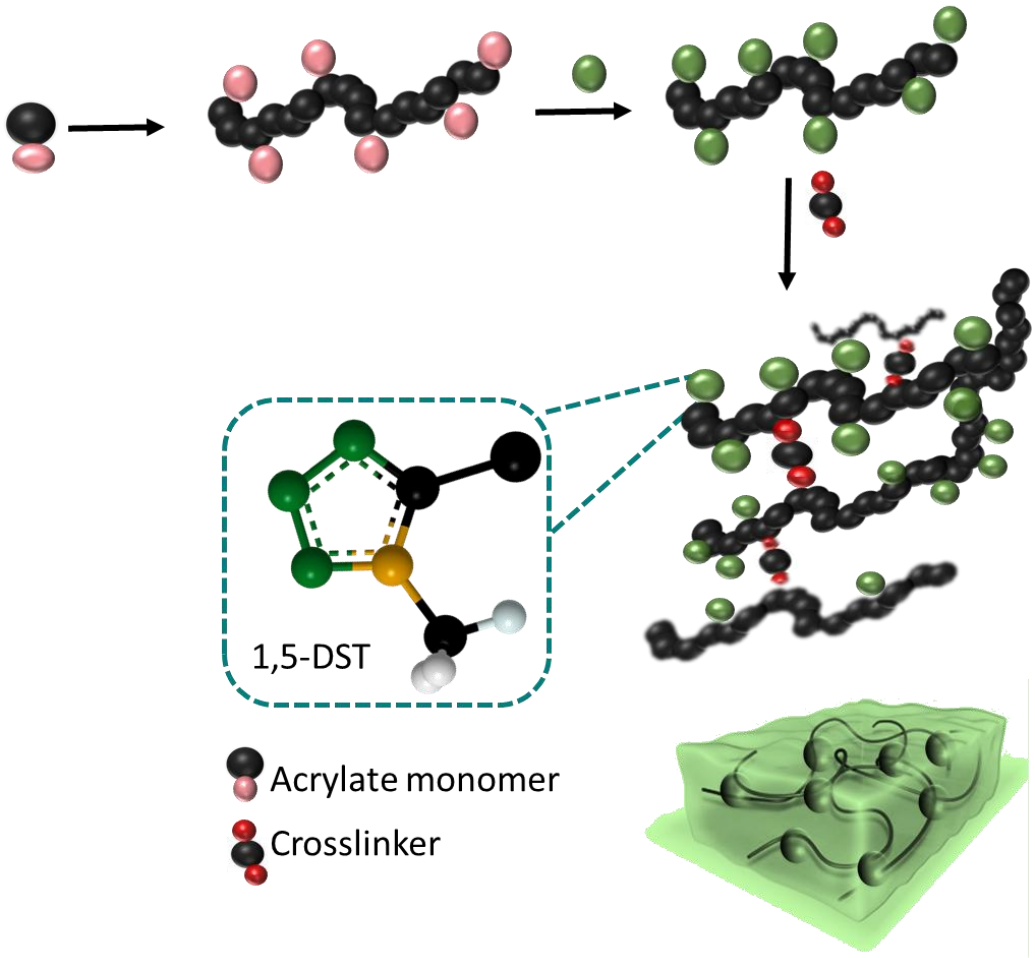

Parts of this chapter are submitted as "Akdemir, M. S., Werner P., Simian, M., Mutlu, H., Theato, P., Synthesis and characterization of 1,5-Disubstituted-1*H*-Tetrazole-containing fluorescence hydrogels. *ACS Macro Letters*, **2023**.Submitted.

5.3.1 Prologue

Indeed, an acknowledged drawback associated with existing tetrazole-containing polymers discussed in the literature is their notably poor solubility in protic solvents, which hinders their practical applicability.[264] As a result, these polymers are commonly utilized as copolymers, frequently in combination with styrene[12, 277]. However, the latter approaches suffer disadvantages such as high costs and comparatively harsh conditions. Moreover, it is also underlined in the literature that the direct polymerization of functionalized monomers can have the disadvantage of limited functional group tolerance under the polymerization conditions.[217] Recently, an improved synthetic strategy has been introduced to the literature in which different degrees of tetrazole integration has been performed using poly(pentafluorophenyl acrylate) p(PFPA) polymers *via* post-polymerization modification to obtain copolymeric structure. Nonetheless, the polymer properties have not been explored in detail.[209] [278] However determining the effect of different degrees of tetrazole modification is a promising avenue for a more comprehensive understanding of tetrazole-containing polymers. In addition, the unique structural and electronic properties of 1,5 DSTs, besides their high physiological activity and low toxicity, enable them to form a wide range of applications from sensing, medicine, and materials science.[279] Moreover, one of the most important properties of 1,5 DSTs is their ability to fluoresce.[121] As is also represented in **Chapter 5.1** and **Chapter 5.2,** the photoluminescent properties of 1,5 DST make them an up-and-coming candidate synthesizing fluorescence materials (i.e., hydrogels, membranes). Nevertheless, a detailed study on the 1,5 DST decorated formability of material, and correspondingly, its thermal and optical property was not found so far, even though 1,5 DST units potential for diverse applications such as sensors[280-281], imaging probes[282], and vehicles for drug delivery.[283-284]

Therefore, a comprehensive investigation of the incorporation of 1,5 DST unit into the p(PFPA)-based polymer chain *via* a post-polymerization modification was performed in this study. Particularly, different degrees of 1,5 DST modification (from 20 to 60%, by weight) was targeted to investigate how the presence of different 1,5 DST content affects the characteristics of polymer. Subsequently, *in-situ* crosslinking of different tetrazole content-containing polymer chains is performed to investigate the feasibility of hydrogel formation. Accordingly, the obtained polymers were subjected to detailed analysis using various techniques, including size SEC, NMR, ATR-IR TGA, DSC, UV-Vis and fluorescence spectroscopy, and confocal fluoresce microscopy (CFM). Additionally, scanning electron microscopy (SEM) was used to reveal the morphological properties of novel tetrazole- containing polymeric networks beside water uptake studies. Subsequently, the following section presents a comprehensive explanation of the experimental part, coupled with the presentation of characterization results and an in-depth discussion thereof.

5.3.2 Synthesis and Characterization

To enable facile access to p(PFPA) polymers, it is of significant interest to commence the synthetic pathway by preparing of the pentafluorophenyl acrylate (p(PFPA)) monomer. This strategic decision is rooted in superior cost-efficiency and straightforward synthesis of p(PFPA) compared to commercially available partners. Thus, p(PFPA) was synthesized accordingly the literature.[285] (see Experimental part, Section 7.3.3) Comprehensive characterization of the molecular structure was carried out through ^{1}H-NMR and ^{19}NMR analyses, as demonstrated in **Figure 8.17** in Appendix. Upon the synthesis of the p(PFPA) monomer, preparation of the p(PFPA) polymer was accomplished through thermal-initiated radical polymerization. Briefly, p(PFPA) was polymerized in the presence of AIBN as the initiator under inert conditions in anhydrous 1,4-dioxane at 80 °C overnight (**Scheme 5.3.1**). The obtained product was isolated through precipitation in cold methanol (see Experimental part, Section 7.3.3).

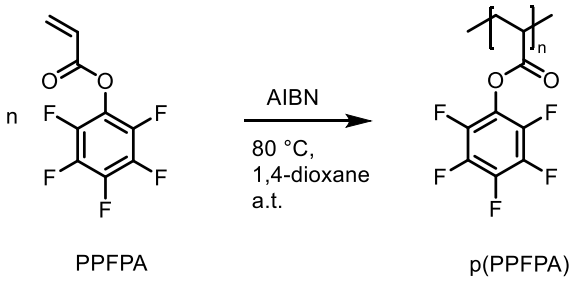

Scheme 5. 3. 1 Synthesis of poly (pentafluorophenyl acrylate) (p(PFPA)) *via* thermal-initiated radical polymerization.

Upon purification, the chemical structure of the polymer was characterized by using ^{1}H NMR, ^{19}NMR spectroscopy and ATR-IR. **Figure 5.3.1** illustrates the results of p(PFPA) analyses including SEC data. Initially, the SEC analysis confirmed the polymer formation with a molecular weight (M_n) of 11.0 kg·mol^{-1} and a typical radical polymerization $Đ$ of 2.2 (**Figure 5.3.1.a**). Moreover, the ^{19}NMR characterization revealed peaks at δ= 153.2, -156.8, and 162.2 ppm, corresponding to *ortho,* para, and meta positions of the fluorine atom within the structure of polymer (**Figure 5.3.1.b**). Additionally, ATR-IR spectroscopy provided further evidence by showing a carbonyl vibrational band at 1782 cm^{-1}, indicating the presence of acrylate functionality in the polymers (**Figure 5.3.1.c**). Furthermore, ^{1}H NMR spectra of polymer exhibited broad peaks in the regions of δ= 3.21-2.95 ppm and δ = 2.34-1.73 ppm, attributed to the polymeric backbone (**Figure 5.3.1.d**). Additionally, the molecular weight of the polymer, as determined by ^{1}H NMR, was found to be approximately 11.1 kg mol^{-1}, which exhibited a good

correlation with M_n obtained by SEC. The latter revealed that the polymer comprised approximately 45 repeating units.

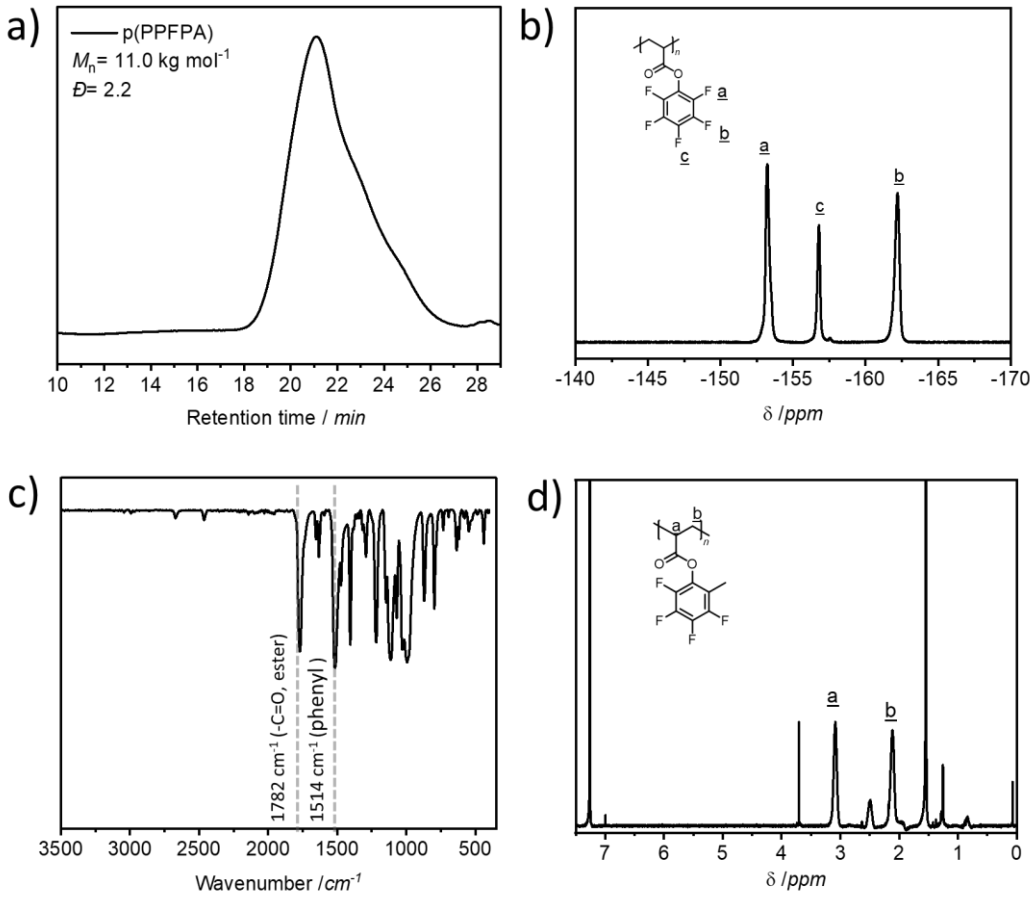

Figure 5. 3. 1 a) SEC_{THF} trace, b) ^{19}F NMR ($CDCl_3$, 377 MHZ) spectrum, c) ATR-IR spectrum; d) ^{1}H NMR ($CDCl_3$, 400 MHz) spectrum of p(PPFPA).

As reported previously documented in the literature, p(PFPA) polymers can be effectively substituted with various amines in the presence of a catalyst (i.e., TEA, DMAP, DBU) at high temperature.[222, 286] Based on that, the p(PFPA) was subjected to nucleophilic substitution with primary amine 1,5 DST derivative by slightly changing the procedure in the literature.[287] However, previous studies have indicated that carboxylic acid formation (-COOH) might occur during amidation[287] because of the following reasons: i) elevated temperatures and extended reaction times can increase the occurrence of side reactions, one of which involves the hydrolysis of esters leading to the formation of carboxylic acids, ii) the presence of trace amounts of water in the reaction mixture can also promote ester hydrolysis and subsequent carboxylic acid formation, iii) ineffectiveness or deactivation of the catalyst can result in incomplete transesterification and a subsequent rise in the production of carboxylic acids.[217, 224, 288] Therefore, it was essential to establish the optimal conditions for the integration of 1,5 DST moiety before attaining different degrees of polymer modification. Hence, the optimization

reactions for the selection of solvent, catalyst, catalyst feeding ratio, and temperature were performed, For this purpose, complete conversion of the active ester group of p(PFPA) by reacting with 1-methyl-5-aminotetrazole in *N*-methyl pyrrolidone (NMP), DMF, and dry-DMF has been conducted by varying the temperature from ambient temperature to 80 °C. DMAP was used as the catalyst, and the reaction was carried out overnight (as indicated in **Scheme 5.3.2**) under an inert (N_2) atmosphere.

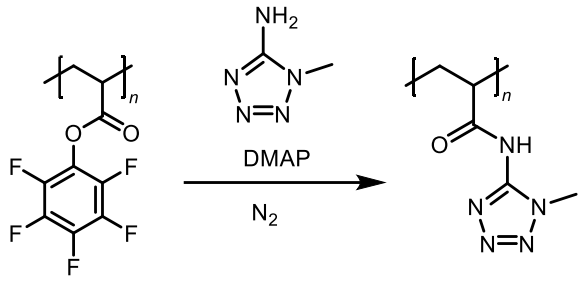

Scheme 5. 3. 2 Synthetic route for the post-polymerization reaction of p(PFPA) polymer with 1-ethyl-5-aminotetrazole to determine the optimal solvent, catalyst, catalyst feeding ratio, and temperature.

Subsequently, the reactions were monitored using ATIR-IR analysis (**Figure 5.3.2.a)** following the purification step. The peaks corresponding to p(PFPA) ester bonds (1782 cm^{-1} for C=O) were partially diminished and transformed into amide bonds, which are characterized by the appearance of the amide band (-C(=O)-N-) at 1650 cm^{-1} in ATIR-IR. Nevertheless, it was found that the modification reaction of p(PFPA) showed a carboxylic peak at around 1720 cm^{-1}, regardless of the solvent when DMAP was used as a catalyst. The hydrolysis can be attributed to the presence of trace amounts of water derived from the standard analytical NMP, DMF used in the reaction, and a high loading of DMAP. Conversely, the most suitable conditions for the amidation reaction have been identified at 80 °C in a dry-DMF.

Indeed, it has been reported that the reaction can be influenced, not only by the selection of solvent and temperature, but also by the type of catalyst and its ratio in the mixture.[287] Therefore, several catalysts (e.g., TEA and DBU, DMAP) with different ratios (e.g., 1.20 and 0.40 eq. to p(PFPA)) have been tested. Thus, the post-polymerization reactions were performed in dry-DMF at 80 °C as following aforementioned procedure. As seen in **Figure 5.3.2.b,** the disappearance of the carboxylic peak around 1720 cm^{-1} indicates the strong inhibition of hydrolysis achieved by employing TEA as a catalyst. Significantly, using an excess amount of TEA (1.20 eq.) led to the full conversion of the p(PFPA) ester bond to amide bonds, as evidenced by the presence of the amide C=O band at 1650 cm^{-1} and the complete disappearance of the C=O band at 1782 cm^{-1}. Based on these findings, TEA (1.20 eq.) was chosen as the optimum catalyst to ensure efficient conversion of the ester bonds to amide bonds during the different degrees of 1,5 DST modification of p(PFPA).

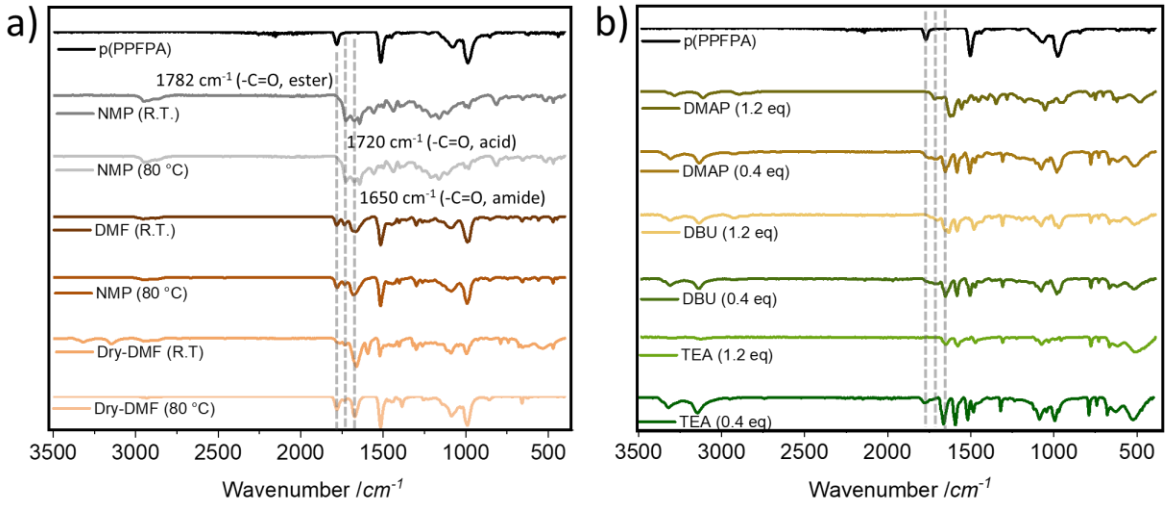

Figure 5. 3. 2 Comparative ATIR-IR spectra of p(PFPA) after the post-polymerization modification reaction with 1,5-DST moiety a) in the presence of DMAP as a catalyst in different solvents by varying temperature b) in the presence of DMAP, DBU and TEA by their varying feeding ratio (0.40 and 1.20 eq. to p(PFPA)) at 80 °C in dry-DMF.

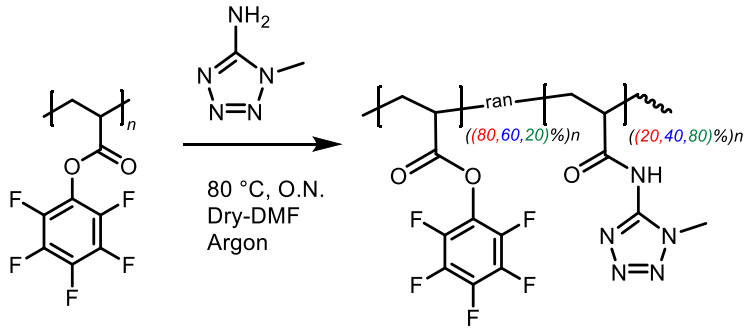

Scheme 5. 3. 3 Synthetic route for different levels of modification of p(PFPA) polymer by using 1,5 DST.

Upon optimizing reaction conditions, different levels of p(PFPA) modification using 1,5 DST were executed to synthesize three different 1,5 DST compositions (20%, 40%, and 60%, by weight). Briefly, p(PFPA) was reacted with different ratios of 1-methyl-5-aminotetrazole (20%, 40%, and 60%) in the presence of the excess amount of TEA at 80 °C in dry-DMF (**Scheme 5.3.3**) (see Experimental part, Section 7.3.3). The reactions were performed under argon (Ar) atmosphere instead of aforementioned conditions (N_2), aiming to exclude any traces of oxygen. The polymers are named p(PFPA)-Tet_x, where x represents the percentage of targeted functionalization of tetrazole (e.g., 20%, 40%, and 60%). These polymers are color-coded as red, blue, and green, corresponding to p(PFPA)-$Tet_{20\%}$, p(PFPA)-$Tet_{40\%}$, and p(PFPA)-$Tet_{60\%}$, respectively (**Scheme 5.3.3).** After the precipitation, it is important to note that the polymers displayed limited solubility in organic solvents. Consequently, it was not feasible to analyse the conversion *via* ^{1}H-NMR due to overlapping signals. (**Figure 8.18** in Appendix). As an alternative, ^{19}F NMR spectroscopy was used to assess the modification efficiency. The results are presented in **Figure 5.3.3**. Upon the modification reaction with 1,5 DST, the ^{19}F-NMR of

crude products showed (**Figure 5.3.3.a**) three characteristic signals at δ=-162.8, -165.2, and -172.0 ppm of pentafluorophenol, along with three other characteristic signals at δ= 153.2, -156.8, and 162.2 ppm of p(PFPA) polymers, consistent with the previously reported ^{19}F NMR chemical shifts for p(PFPA) for all degrees of modification (see **Figure 5.3.3.a**). The pale red line represents p(PFPA)-Tet$_{20\%}$, the light blue line corresponds to p(PFPA)-Tet$_{40\%}$, and the soft green line indicates p(PFPA)-Tet$_{60\%}$. After purification, no detectable signals belonging to pentafluorophenol were observed, indicating the successful removal of pentafluorophenol from the modified polymer, while the chemical shifts for p(PFPA) still remain (**Figure 5.3.3.a**). Furthermore, based on the ^{19}F-NMR data, it was calculated that 15, 35, and 48% modifications were achieved for 1,5 DST compositions of 20, 40, and 60%, respectively. After the post-polymerization reaction, polymers were also examined by ATIR-IR. As shown in **Figure 5.3.3.b**, the appearance of a new amide band at 1650 cm^{-1}, along with the ester band at 1782 cm^{-1}, provided evidence of the successful integration of the 1,5 DST unit into the p(PFPA) polymer structure. In addition, the characteristic peaks at 1386, 1254, and 1081 cm^{-1}, which correspond to the antisymmetric stretching mode of the -N=N- and the vibration bands of the -C=N- and -N-N- bonds within the 1,5 DST unit have been observed, indicating the presence of 1,5 DST. Moreover, the SEC graphs of the modified polymers demonstrate a slight decrease in the original M_n of p(PFPA) from 11.0 kg mol^{-1} ($Đ$=2.2) to 10.7 kg mol^{-1} ($Đ$=1.7), 10.1 kg mol^{-1} ($Đ$=1.7), and 9.4 kg mol^{-1} ($Đ$=1.8) for p(PFPA)-Tet$_{20\%}$, p(PFPA)-Tet$_{40\%}$, and p(PFPA)-Tet$_{60\%}$, respectively (**Figure 5.3.3.c**). This particular behaviour can be solely explained by the incorporation of the 1,5 DST unit with different degree of modification due to the replacement of PFP units (184 g mol^{-1}) by 1,5 DST unit (99 g mol^{-1}). This alteration leads to a decrease in M_n of p(PFPA).

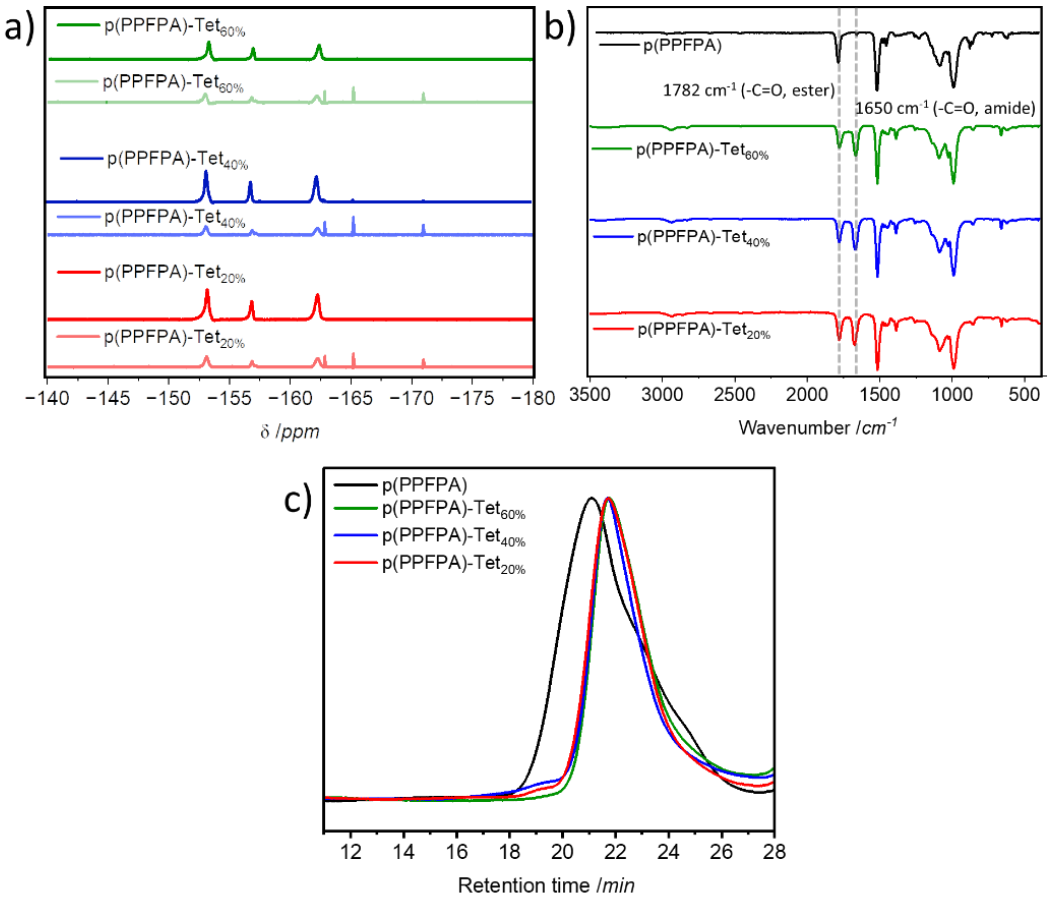

Figure 5. 3. 3 Comparative a) ^{19}F NMR ($CDCl_3$: d_6-DMF, 400 MHz) spectra, b) ATR-IR spectra, c) SEC_{THF} traces of p(PPFPA) polymers with different degree of 1,5 DST modification (p(PPFPA); black line, p(PPFPA)-$Tet_{20\%}$; red line, p(PPFPA)-$Tet_{40\%}$; blue line, and soft p(PPFPA)-$Tet_{60\%}$; green line)

Subsequently, TGA was applied under inert conditions (N_2) at a heating rate of 10 K min^{-1} in order to detect the thermal properties of the p(PFPA)-$Tet_{20\%}$, p(PFPA)-$Tet_{40\%}$, and p(PFPA)-$Tet_{60\%}$. All degradation steps, the corresponding weight loss, and the peak maxima are summarized in **Table 5.3.1**. As depicted in **Figure 5.3.4**, the degradation characteristics of p(PFPA) show a one-step degradation profile with $T_{d,5\%}$ at 368 °C. In contrast, **(**P(PFPA))-$Tet_{20\%}$, p(PFPA)-$Tet_{40\%}$, and p(PFPA)-$Tet_{60\%}$ displayed a two-step degradation pattern, suggesting the occurrence of multiple degradation processes at distinct temperature ranges. In general, this indicates that the 1,5 DST modification introduces additional complexity to the degradation behaviour compared to p(PFPA). The relative thermal stability of modified polymers has been evaluated by comparing the decomposition temperatures at different percentage weight loss **(Table 5.3.1**) The results indicate that the initial decomposition step leads to weight losses of 21, 36, and 47% for (p(PFPA))-$Tet_{20\%}$, p(PFPA)-$Tet_{40\%}$, and p(PFPA)-$Tet_{60\%}$, respectively (**Figure 5.3.4**). Additionally, the first degradation temperatures were around ~192, 202, and 204 °C, followed by the second degradation step at ~420, 408, and 399 °C for (p(PFPA))-$Tet_{20\%}$, p(PFPA)-$Tet_{40\%}$, and p(PFPA)-$Tet_{60\%}$, respectively. In order to determine the source of the initial

degradation step of the modified polymers, TGA analysis of the completely modified p(PFPA) polymer, referred to as (p(PFPA))-Tet$_{100\%}$, was conducted. TGA result showed a one-step degradation profile with $T_{d,5\%}$ at ~200, accompanied by approximately 10% char formation (**Figure 8.19** in Appendix). Accordingly, the weight loss observed in the initial step can be ascribed to the degradation of the polymer's 1,5 DST unit, which is also found to be correlated with the degree of targeted modification (i.e., 21% for (p(PFPA))-Tet$_{20\%}$). Importantly, comparable information, such as $T_{d,5\%}$ of tetrazole-containing systems, has also been documented in the literature within the temperature range of 200-230 °C.[201, 289] Accordingly, the second degradation step can be linked to the degradation of the polymer's backbone. Interestingly, it has been observed that a higher number of 1,5 DST groups attached to the polymer structure leads to an increase in the temperature at which the second degradation step occurs. Indeed, it is a well-established fact that when a polymer chain`s molecular weight decreases, the polymer`s degradation temperature tends to decrease as well. This is because low molecular weight polymers are more susceptible to chain scission, which makes them more prone to thermal degradation. As seen from **Table 5.3.1**, a similar situation has been observed with the decreasement of the molecular weight from (p(PFPA))-Tet$_{20\%}$ to (p(PFPA))-Tet$_{60\%}$ for the second degradation step. However, for the first degradation step of tetrazole-modified polymers, when M_n decreased from (p(PFPA))-Tet$_{20\%}$ to p(PFPA)-Tet$_{60\%}$, compared to p(PFPA), the thermal stability slightly increased. This phenomenon can only be explained by the higher degree of π-π stacking of polymeric chains facilitated by 1,5 DST.[290-292] Last but not least, the transition profile for each modified polymer occurring between 230 and 380 °C can be rationalized by considering the impact of side reactions during the degradation process (**Figure 5.3.4**). In other words, higher temperatures are likely to result in the degradation of 1,5 DST units, leading to their conversion into amino- and imino-tautomeric forms. This cleavage of the tetrazole ring induces the formation of carbodiimide crosslinks between polymer chains or the formation of melamine or polyamine that may trigger side reactions causing a transitional phase.[293] Additionally, due to inherent aromatic structure, (p(PFPA))-Tet$_{20\%}$, p(PFPA)-Tet$_{40\%}$, and p(PFPA)-Tet$_{60\%}$ exhibited a char formation exceeding 20%.

Table 5. 3. 1. Thermal analysis of 1,5 DST-decorated p(PFPA) polymers with different degrees of 1,5 DST modification.

Polymer	T_d (°C)[a]	
	1st step	*2nd step*
p(PFPA)	368	-
p(PFPA)-Tet$_{20\%}$	192	420
p(PFPA)-Tet$_{40\%}$	202	408
p(PFPA)-Tet$_{60\%}$	204	399

[a]The decomposition temperatures were detected by TGA.

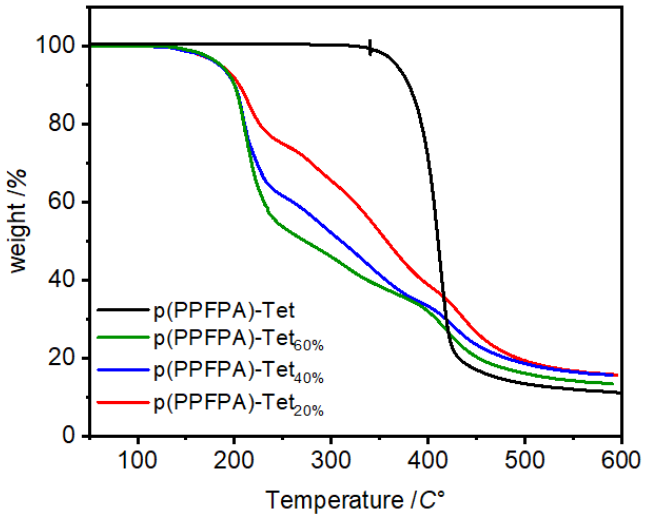

Figure 5. 3. 4 Comparative TGA traces of p(PFPA) polymers with different degree of 1,5 DST modification (p(PFPA); black line, p(PFPA)-$Tet_{20\%}$; red line, p(PFPA)-$Tet_{40\%}$; blue line, and soft p(PFPA)-$Tet_{60\%}$; green line).

Upon implementing different levels of 1,5 DST modification to p(PFPA), the intention was to prompt hydrogel formation through the utilization of the modified polymers. Nevertheless, it was noticed that both ester bond hydrolysis and amide bond degradation take place during purifying and drying process of the resultant polymer. When the polymer subjected to the drying process under vacuum at 100 °C for 4 hours, the peak associated with amide bonds at 1650 cm^{-1} vanished (**Figure 8.20.a** in Appendix). Meanwhile, the investigation to remove the solvent, from the polymer by applying a vacuum at 60 °C for overnight did not adequately eliminate the solvent from the polymer composition. This fact is supported by the TGA analysis, which reveals a weight loss below 100 °C origination from solvent presence, likely DMF or moisture (**Figure 8.20.b** in Appendix). Therefore, an *in-situ* crosslinking approach has opted to form the hydrogel to avoid particular complications as mentioned earlier in the system.

Accordingly, as previously stated, the p(PFPA) was modified with different degree of 1,5 DST content in the beginning. Afterward, in order to evaluate the reactivity of the network formation, *in-situ* crosslinking reactions were performed by adding excess amount of O,O'-bis-(3-aminopropyl)-polyethylene glycol (M_w=1500, to PPFA unit) (**Scheme 5.3.4**). (see Experimental part, Section 7.3.3) Surprisingly, the cross-linking procedure resulted in swift gel formation, establishing a structure in 10 minutes. Nonetheless, the reaction mixture was allowed to remain undisturbed overnight to provide full conversion. Later on, the gels were subjected to a three-day dialysis process using ethanol: water (1:1) mixture to remove DMF. Later, the gels were dried using a freeze-dryer. (see Experimental part, Section 7.3.3) The respective hydrogels are denoted as H-Tet_x (with x abbreviating the number of targeted functionalization of the respective tetrazole).

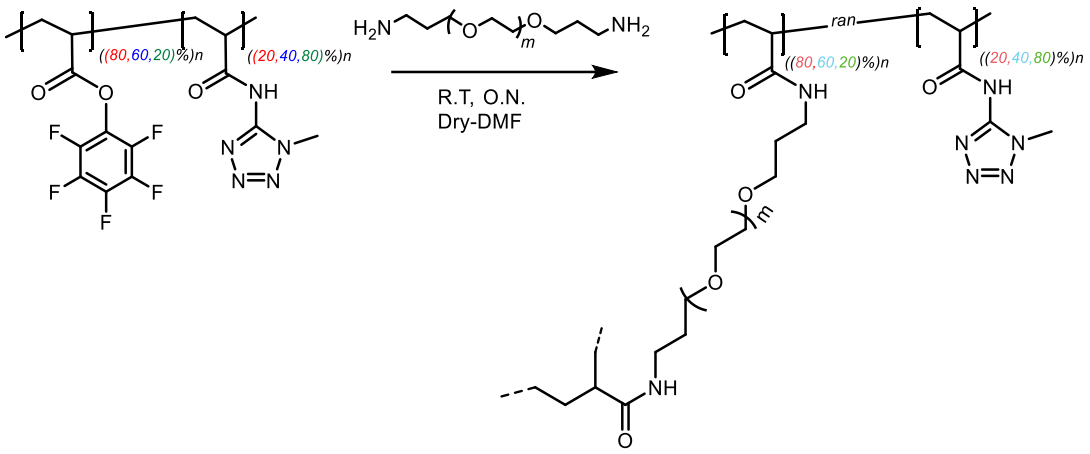

Scheme 5. 3. 4 Synthetic route for the *in-situ* hydrogel formation of 1,5 DST-decorated polymers; p(PFPA)-Tet$_{20\%}$; soft red colour, p(PFPA)-Tet$_{40\%}$; soft blue colour, and p(PFPA)-Tet$_{60\%}$; soft green colour.

Depending on the ATIR-IR findings, all PFP ester bonds (with characteristic peaks at 1782 cm^{-1} for C=O) were fully transformed into amide bonds, indicated by the appearance of the C=O amide band at 1650 cm^{-1} for H-Tet$_{20\%}$, H-Tet$_{40\%}$, and H-Tet$_{60\%}$ (**Figure 5.3.5**). In addition, the presence of PEG was determined based on specific spectral characteristics, with C-H stretching vibrations occurring at 2800-2950 cm^{-1}, -C-O-C- asymmetrical stretching vibrations at 1145-1153 cm^{-1} (**Figure 5.3.5**).

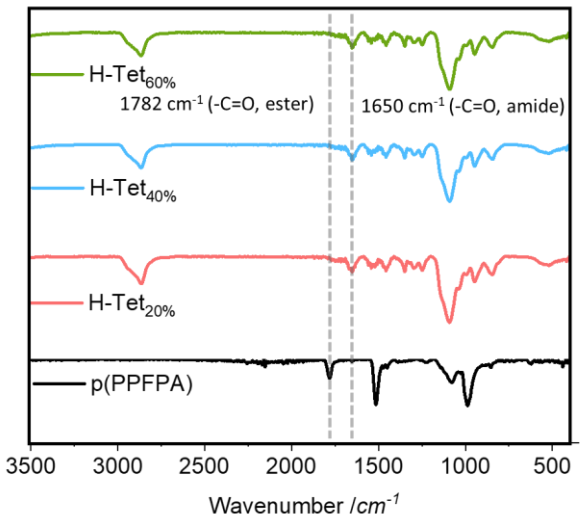

Figure 5. 3. 5 Comparative ATIR-IR spectra of different degrees of 1,5 DST-decorated hydrogels; p(PFPA)-Tet$_{20\%}$; soft red line, p(PFPA)-Tet$_{40\%}$; soft blue line, and p(PFPA)-Tet$_{60\%}$; soft green line.

Furthermore, the decomposition temperature ($T_{d,5\%}$) of H-Tet$_{20\%}$, H-Tet$_{40\%}$, and H-Tet$_{60\%}$ were determined using a heat rate of 10 K min^{-1} by TGA. It is important to mention that samples were subjected to a preheating isothermal step at 120 °C for approximately two hours prior to the measurements to prevent humidity. **Figure 5.3.6.a** shows that each hydrogel exhibited a single-step degradation profile with approximately $T_{d,5\%}$ values of 396, 398, and 401 °C for H-Tet$_{20\%}$,

H-Tet$_{40\%}$, and H-Tet$_{60\%}$, respectively. Surprisingly, the presence of 1,5 DST did not have a considerable effect on the thermal properties of the resulting gel, as evidenced by only a minor increase of $T_{d,5\%}$. However, H-Tet$_{20\%}$, H-Tet$_{40\%}$, and H-Tet$_{60\%}$ hydrogels demonstrated heightened thermal stability in comparison to the research in the literature, wherein $T_{d,5\%}$ was observed at approximately 330 °C [294], or at 380 °C [295] when the same PEG derivative utilized as a crosslinker within the hydrogel structure. The latter has proved that the hydrogel's thermal stability is increased by the presence of 1,5 DST compared to its PEG-based counterparts. Expectedly, DSC analysis of the hydrogels showed multiple glass transition temperatures (T_g) with a heat rate of 5 K min^{-1} between -150 and 100 °C (**Figure 5.3.6.b**). The first T_g occurred at low temperatures, specifically -121, -119, and -119 °C for H-Tet$_{20\%}$, H-Tet$_{40\%}$, and H-Tet$_{60\%}$, respectively, which can be attributed to the presence of the PEG-chain.[296] Subsequently, a second T_g was observed at relatively higher temperatures, specifically -51, -49, and -42 °C for H-Tet$_{20\%}$, H-Tet$_{40\%}$, and H-Tet$_{60\%}$, respectively (**Figure 5.3.6.b**). On the one hand, the melting points (T_m) of H-Tet$_{20\%}$, H-Tet$_{40\%}$, and H-Tet$_{60\%}$ have been found to be about 31, 35, and 34°C, correspondingly (**Figure 5.3.6.b**). On the other hand, crystallization temperatures (T_c) have been measured at 0.7, -3, and -12 °C for the same modification degree in the mentioned order (**Figure 5.3.6.b**). The results indicate that incorporating a 1,5 DST ring into the polymer's structure enhances its capacity to endure ring fatigue and promotes strong intramolecular π-π interaction due to 1,5 DST units within the polymer chains. Accordingly, as the degree of modification of the 1,5 DST unit increases, it gives rise to a more amorphous phase. As a result, incorporating of

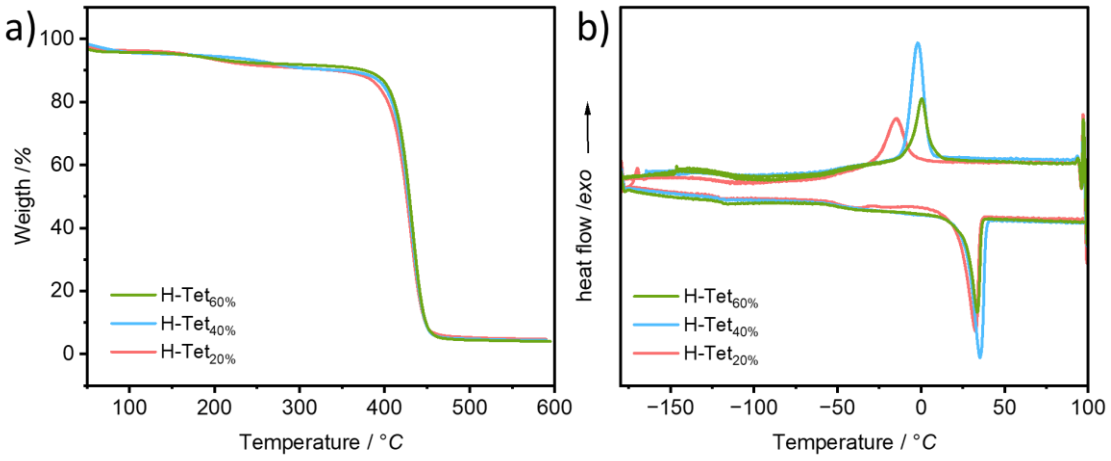

1,5 DST into the structure of polymer makes it more suitable for various processing techniques.

Figure 5. 3. 6 Comparative a) TGA traces, b) DSC traces (during the second heating) of different degrees of 1,5 DST-decorated hydrogels; p(PFPA)-Tet$_{20\%}$; soft red line, p(PFPA)-Tet$_{40\%}$; soft blue line, and p(PFPA)-Tet$_{60\%}$; soft green line.

Afterwards, considering the importance of swelling capacity in hydrogels, as it significantly affects their performance as absorbent materials in applications, the gravimetric swelling ratio of

hydrogels has been analysed. For this purpose, H-Tet$_{20\%}$, H-Tet$_{40\%}$, and H-Tet$_{60\%}$ were thoroughly dehydrated in a vacuum oven at 60 °C for over 24 hours before assessing their swelling capacity. Subsequently, the gravimetric swelling ratio of each hydrogel was calculated using the formula: Gravimetric swelling ratio = $(W_s - W_i) / W_i$, where W_s represents the weight of the hydrogel or hydrogel composite after swelling in ultrapure water at different time points, and W_i is the initial weight of the dried hydrogel. Three measurements were taken, and the swelling profile charts displayed the standard de*via*tions with error bars. The swelling kinetics of hydrogels in distilled water are shown in **Figure 5.3.7.a**. Almost all hydrogels reached their equilibrium state in approximately 10 minutes. Additionally, H-Tet$_{20\%}$ and H-Tet$_{40\%}$ achieved their maximum swelling capacity after 5 hours, whereas H-Tet$_{60\%}$ continued to swell beyond that time. Specifically, it was noticed that H-Tet$_{60\%}$ exhibited the most significant swelling capacity in comparison to other counterparts (**Figure 5.3.7.a**). These observations can be explained in two possible aspects. On the one hand, an increase of 1,5 DST content leads to a decrease in the degree of crosslinking, resulting in a less densely crosslinked structure in H-Tet$_{60\%}$. Consequently, this promotes the formation of more open channels, leading to enhanced water uptake compared to the more crosslinked H-Tet$_{20\%}$ and H-Tet$_{40\%}$. On the other hand, it is well-established that decreased PEG chain length reduces the capacity to form hydrogen bonds with water molecules. Given that, a higher 1,5 DST content can be regarded as only a factor contributing to the increased polarity and swelling capability of the polymeric networks. Moreover, SEM was used to assess the porosity of freeze-dried hydrogel samples. As can be seen in **Figure 5.3.b-d**, the hydrogels exhibit a solid and nonporous structure, regardless of the PEG content. Hence, these outcomes strengthen the notion that the highest swelling capacity is derived from the presence of 1,5 DST.

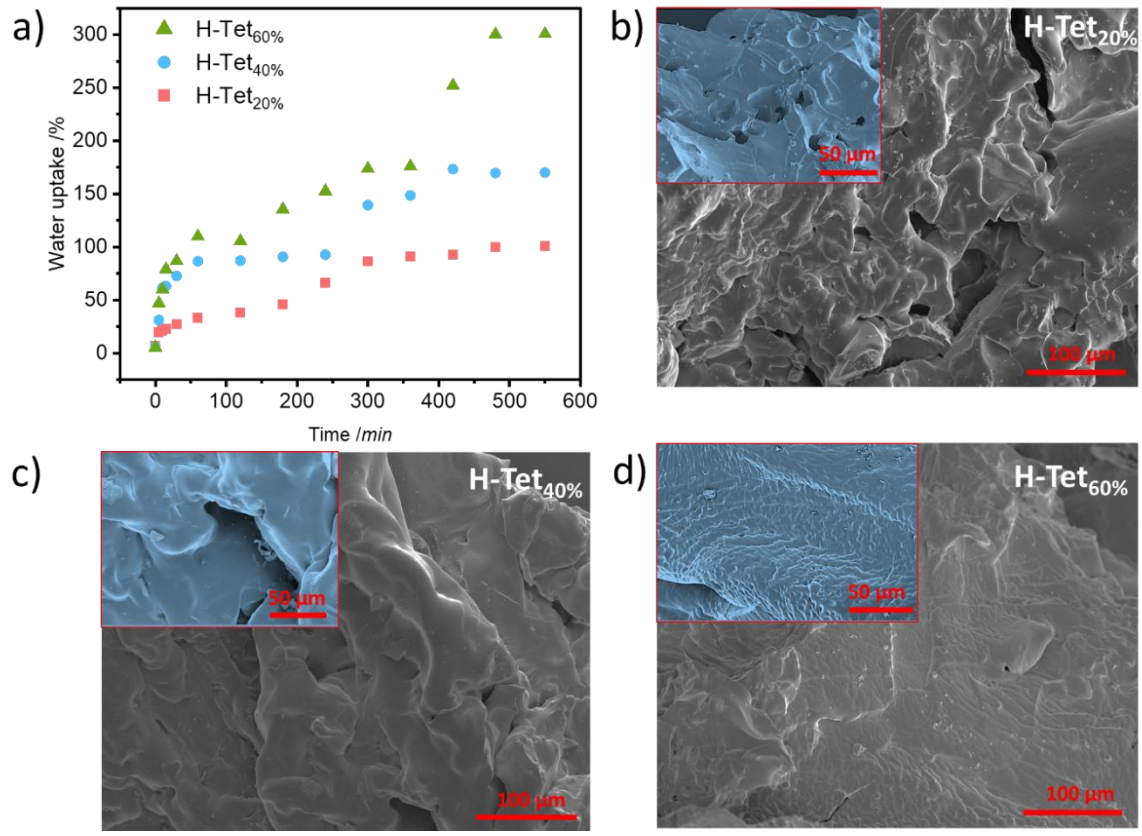

Figure 5. 3. 7 a) Swelling behaviours of different degrees of 1,5 DST-decorated hydrogels; p(PFPA)-$Tet_{20\%}$; soft red dot, p(PFPA)-$Tet_{40\%}$; soft blue dot, and p(PFPA)-$Tet_{60\%}$; soft green dot b, c, d) SEM pictures of different degrees of 1,5 DST-decorated hydrogels and controls at two different magnifications.

Last but not least photophysical properties of obtained hydrogels have been investigated by utilizing UV-Vis analysis while the hydrogels were in a water medium, and by conducting fluorescence microscopic imaging once the hydrogels were dry phase. All hydrogels exhibit absorption between the wavelengths of 320-420 nm (**Figure 5.3.8.a**). However, with the increment of the 1,5 DST content from H-$Tet_{20\%}$, H-$Tet_{40\%}$ to H-$Tet_{60\%}$**,** the maxima at 353 nm for H-$Tet_{20\%}$ has shown redshift of the absorbance maxima to 360 and 368 nm H-$Tet_{40\%}$ to H-$Tet_{60\%}$, respectively (**Figure 5.3.8.a**). Additionally, it is apparent from **Figure 5.3.8.b** that the Em (photoluminescent emission) peaks are centered at 438 nm (λ_{ex}= 300 nm), showing no emission change for all hydrogels. However, there was a slight change in the f the emission spectra intensity when 1,5 DST content increased by 20 to 60% (**Figure 5.3.8.b**). These results can only be attributed to the multiple intra- and intermolecular interactions arising from n–π* or π–π* transitions between electron-rich -C-C-, -N=N- and -N–N-, and the conjugated aromatic 1,5 DST units since PEG itself is not known to exhibit intrinsic fluorescence or luminescence properties. The luminesce effect of 1,5 DST unit is further supported by fluorescence

microscopy, as presented in **Figure 5.3.8.c**. Confocal fluorescence microscopy displayed visible blue emission for all polymers between 410-550 nm (**Figure 5.3.8.c**). In addition, the hydrogels emit a bright bluish fluorescence upon irradiation at 365 nm from a hand-held UV (**Figure 5.3.8.d,** shown in circle). From the displayed images, it can be assumed that hydrogels exhibit different fluorescence intensities with the incensement of the tetrazole content. In addition, it can be seen that the emitted light is more red-shifted when the degree of modification is increased. This result further confirmed that the structure of hydrogels exhibited strong fluorescence, indicating the important application of this material as a fluorescent hydrogel.

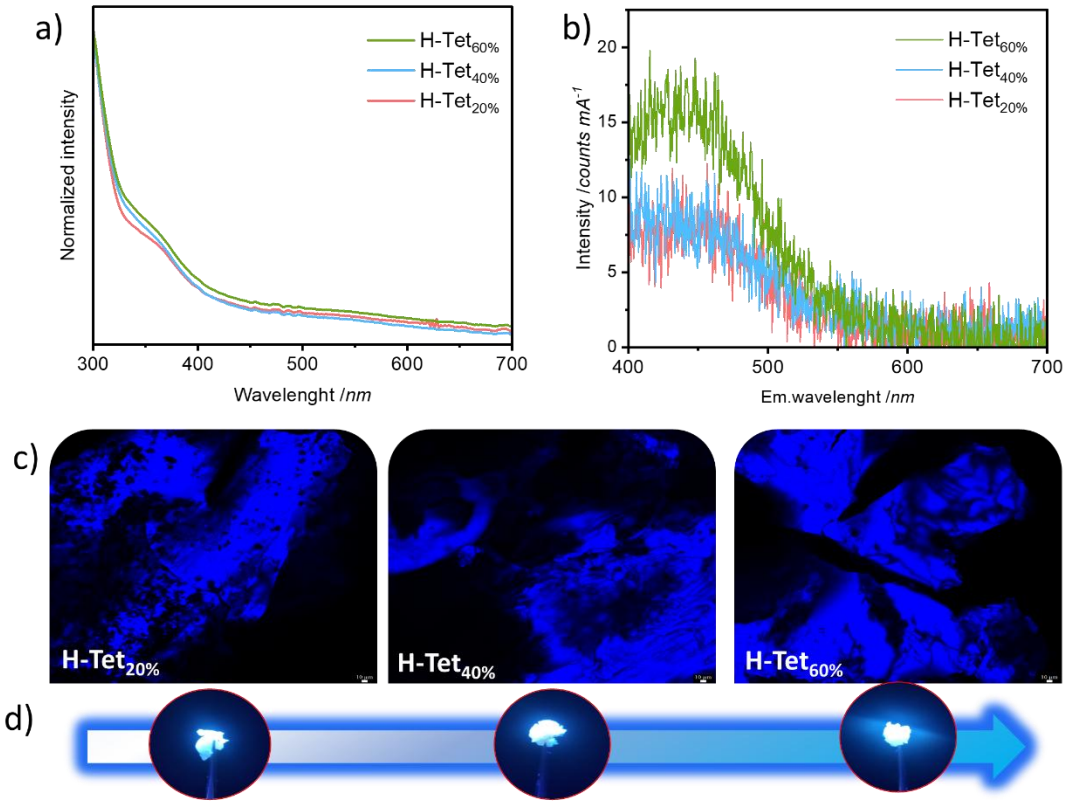

Figure 5. 3. 8 a and b) Comparative absorption and emission spectra (λex=350 nm) of hydrogels in water, c) Fluorescence microscopy images of hydrogels upon UV irradiation (in the range of λ=410-550 nm), and d) Images of hydrogels upon hand-held UV irradiation (λ=365 nm).

5.3.1 Recapitulation

This chapter of the thesis illustrated the process of synthesizing p(PFPA) monomers followed synthesizing of p(PFPA) polymers at the beginning. Afterwards, the first attempt to synthesize pendant chain 1,5 DST-containing p(PFPA) through the post-polymerization modification was investigated. For this purpose, the optimal conditions (e.g., solvent, temperature, catalyst and catalyst feeding ratio) for the integration of 1,5 DST moiety into p(PFPA) without allowing hydrolysis of active ester bond to ensure the reliability and effectiveness of the post-polymerization modification reaction was explored. Upon the successful establishment of the synthetic procedure, different degrees of 1,5 DST modification (20, 40 and 60%, by weight) were conducted strategically in order to explore the effect of 1,5 DST presence on polymer properties. Consequently, the results showed that each polymer displayed a two-step degradation profile, remaining stable up to 200 °C and undergoing complete degradation at around 470 °C. Following the 1,5 DST modification, *in-situ* hydrogel formation was performed to deliver crosslinked networks. While the impact of the 1,5 DST components was not notably apparent, all the hydrogels demonstrated high degradation temperatures of up to 400 °C, indicating thermal stability and suitability for potential applications where thermal endurance is essential. Other than that, hydrogels showed two T_g values below ambient temperature around -120 and -47 °C. Moreover, increased T_g values (from -51 to -42 °C) are detected with the increase of 1,5 DST content. Explicitly, the hydrogels showed compact morphology in the SEM images. Nonetheless, with the incensement of 1,5 DST content, increased swelling ratio was found. Notably, all hydrogels showed CTE behaviour under UV irradiation due to conjugated aromatic 1,5 DST units in the network. Lastly, the fluorescence property of hydrogels was discovered to be associated with 1,5 DST content.

6 Conclusion and Outlook

The present dissertation dealt with the formation of 1,5 DST-containing polymeric structures, employing innovative strategies to address the existing gap in polymer synthesis, and aimed to create a library of diverse polymers.

Firstly, a highly efficient one-pot synthetic strategy for the synthesis main chain 1,5 DST-based polymers was covered *via* the UA-4MCP strategy for the first time, under relatively mild conditions. Herein, suitable conditions for the synthesis of polymers were identified by considering concentration, solvent and reaction time. Later on, the polymers were synthesized by utilizing various aromatic and aliphatic aldehyde derivatives to substitute of different side groups. This approach granted insight into how the presence of various side chains influenced the thermal and optical properties of the main chain 1,5 DST-based polymers. All the polymers showed a two-step degradation, remaining stable up to temperatures of 310 °C and 308 °C initially, and then completely degraded around 450 °C and 434 °C for aliphatic and aromatic substitutions, respectively. Furthermore, aliphatic substituted polymers showed lower T_g (from -30 °C to 0 °C) compared to aromatic counter partners (from -26 to 54 °C). Accordingly, the latter demonstrated the potential to adjust the physical characteristics of main chain 1,5 DST-based polymers considering the need of possible applications. Critically, one of the objectives of this research was to reveal the CTE properties of main chain 1,5 DST-based polymers, potentially paving the way toward nonconventional luminescent polymeric materials.

In the second project, the synthesis of 1,5 DST-decorated monomers by employing the Ugi-azide four-multicomponent reaction (UA-4MCR), featuring different lengths of olefin handles was reported. Subsequently, these monomers underwent polymerization through thiol-ene chemistry, utilizing different lengths of dithiol derivatives. By doing so, the effect of the different lengths of the α,ω-diene monomers olefin handles and dithiol derivatives on polymerization was investigated. The presence of a longer alkyl chain led to an increased tendency for polymerization through thiol-ene reactions. This is attributed to the greater flexibility and conformational freedom exhibited by compounds containing longer alkyl chains, facilitating the polymerization process. Furthermore, irrespective of thiol derivatives, all polymers exhibited a moderate thermal stability at approximately 290 °C. Crucially, the results indicated that pendant chain 1,5 DTS decorated polymers exhibited decreased thermal stability compared to the main chain 1,5 DTS-based polymers that were investigated in the first project. However, all 1,5 DTS-decorated polymers showcased reduced T_g values (ranging from -13 to -42 °C) compared to the main-chain 1,5 DTS-based polymers. Hence, it can be stated that shifting the 1,5 DTS unit position form the main chain to the pendant group allows the changing of polymer properties by decreasing T_g values. Meanwhile, this leads to improved processability, expanding the range of potential uses for 1,5 DTS-decorated polymers for possible applications (e.g., drug delivery, antifouling materials). Lastly, it is important to highlight that all the polymers showcased CTE properties,

despite their slightly less pronounced intensity compared to the main chain counterparts. Overall, both projects also displayed the implementation of thiol-ene click chemistry for the 1,5 DST-containing polymers without causing any thiol-tetrazole reaction.

In a third project, an alternative approach to second project for synthesizing of pendant chain 1,5DST-decorated polymer was introduced by employing the post-polymerization modification method. This approach allowed the control of modification degrees in the p(PFPA) polymer structure and provided the facility for *in-situ* network formation. With a series of three different degree 1,5 DST modification (20, 40 and 60%) of p(PFPA) polymer, a comprehensive view was provided, highlighting the effect of the 1,5 DST unit on the thermal properties of polymers. In this regard, 1,5 DST-decorated p(PFPA) polymers exhibited a degradation mechanism characterized by two-step. In the first step, 1,5 DST-decorated p(PFPA) polymers remained structurally stabile until reaching about 200 °C. Subsequently, the second step of degradation occurred at approximately 410°C on average. Considering the results, 1,5 DST-decorated p(PFPA) polymers showcased the lowest degradation temperature in the first stage, irrespective of the degrees of modification, compared to first and second projects involving 1,5 DST-containing polymeric structures. This behaviour can be attributed to the restricted orientation and alignment of 1,5 DST units due to the copolymeric nature or low molecular weight of the 1,5 DST-decorated p(PFPA) polymers. Nevertheless, with the formation of hydrogels, all polymeric networks showed high thermal stability (up to 400 °C) along with low T_g values ranging from -120 to -42 °C. Moreover, an enhancement in the water absorption capability of hydrogels was noticed when the 1,5 DST content was elevated from 20% to 60% which can be attributed to the contribution of polar nature of the 1,5 DST component. Furthermore, all hydrogels demonstrated fluorescence properties when subjected to UV light, regardless of whether they were in the dry solid state or in solutions. This phenomenon is a result of CTE property of 1,5 DST units. Accordingly, it can be considered that 1,5 DST-decorated polymeric networks represent a promising class of luminescent materials that show great potential in many frontier applications such as sensing, bioimaging, biomimetic soft robotics.

In summary, all the results impressively demonstrated the possibility of easy approaches towards synthesizing 1,5 DST-containing polymers either by using direct polymerization or monomer synthesis and respective polymerization beside the post-polymerization approach. Within this thesis, a comprehensive view, both from a theoretical and practical viewpoint, on the relationships between the position of the 1,5 DST unit, either a main chain or pendant chain and properties were clearly identified. Beyond this, an alternative approach for the synthesis of material with fluorescence feature along with improved thermal properties were elaborated. Overall, all approaches obtaining 1,5 DST-containing polymers exemplify a remarkable milestone in polymer chemistry. The demonstrated versatility, structural robustness, and tunability of physical properties make these polymers promising candidates for various cutting-

edge applications. Especially their fluorescent properties can play a crucial role in advancing scientific research, medical diagnostics, and technological applications.

7 Experimental Part

7.1 Materials

1-Dodecanthiol (Sigma Aldrich, 98%), 1,4-Butandithiol (TCI Deuts. GmbH; 97%), 1,6-Hexanedithiol (TCI Deuts. GmbH; 97%), 1,8-Diazabicyclo[5.4.0]-7-undecene (Sigma Aldrich, 99%), 1,8-Octanedithiol (Across.95%), 1,9-Nonanedithiol (Sigma Aldrich, 95%), 10-Undecenal (Sigma Aldrich, 97%), 1-Octanthiol (Sigma Aldrich, 98,5%), 2,2-Azobis(2-methylpropionitrile) (Sigma Aldrich, 98%), 2,2-Dimethoxy-2-phenylacetophenone (Sigma Aldrich, 99%), 3,6-dioxa-1,8-octanedithiol (Sigma Aldrich, 95%), 4-Pentenal (VWR Int., 97%), Azidotrimethylsilane (VWR Int., 97%), Butyl isocyanide (Across.97%), Chloroform (VWR chemicals, 99.1%), Diethylamine (Sigma Aldrich, 99:5%), Dichloromethane (VWR chemicals, 99.8%), Dithiothreitol (Sigma Aldrich, 97%), *N,N*-Dimethyl-1,6-hexanediamine (Sigma Aldrich, 98%); Methanol (VWR Chemicals), 1-Octanthiol (Sigma Aldrich, 98%), 10-Undecenal (Sigma Aldrich, 97%), 2,2-Dimethoxy-2-phenylacetophenone (Sigma Aldrich, 99%), 4-(Trifluoromethyl)benzaldehyde (Across.98%), 5-Norbornene-2-carboxaldehyde (Sigma Aldrich, 95 %), Benzaldehyde (VWR Int., for Synthesis), Chloroform (VWR chemicals, 99.1%), Citronellal (TCI Deuts. GmbH; >95 %), Decanal (Sigma Aldrich, >98 %), Dichloromethane (VWR chemicals, 99.8%), Hexanal (Sigma Aldrich, 98%), Methanol (VWR Chemicals), Trimethylsilyl azide (Sigma Aldrich, 95 %), 2,3,4,5,6-Pentafluorophenol (99%, Sigma-Aldrich), Acryloyl Chloride (stabilized with phenothiazine)(TCI Deuts. GmbH; >98 %), 1,8-Diazabicyclo[5.4.0]undec-7-ene (Sigma Aldrich, 98 %), O,O`-Bis(3-aminopropyl)polyethylene glycol (1.500, Sigma Aldrich). All other solvents and reagents were of analytical grade or higher and were used without further purification.

7.2 Instrumentation

7.2.1 Nuclear Magnetic Resonance (NMR) Spectroscopy

^{1}H NMR, ^{13}C NMR and ^{19}F NMR measurements were performed on a Bruker Avance III 400 MHz spectrometer with a frequency of 400 MHz, 101 MHz and 377 MHz for proton, carbon and fluorine spectra, respectively. Samples were dissolved in $CDCl_3$ or deuterated DMF-d_6. Chemical shifts are reported relative to the solvent residual peaks (^{1}H NMR: δ 7.26 for $CDCl_3$, ^{13}C NMR: δ 77.16 for $CDCl_3$). Deuterated solvents were purchased from euriso-TOP and used without further purification. Unless otherwise stated, all NMR-measurements were performed at ambient temperature.

7.2.2 Liquid Flash Chromatography Purification

The column chromatography was performed *via* automated flash system Biotage® Selekt (SEL-2EV) equipped with two column channels, a flow rate range between 1-300 mL·min^{-1}, and pressure range between 0-30 bar. The purifications were performed with the Biotage® Sfär Silica 50 g.

7.2.3 Size Exclusion Chromatography (SEC)

Due to changing analytics devices, two THF SEC systems were used in the context of this thesis. For individual projects, measurements were always conducted using the same system, to enable comparison. Samples insoluble in THF or incompatible with the employed THF systems were measured in DMAc.

THF Systems:

System1

The apparent number average molar mass (M_n) and the molar mass distribution ($Đ$ = Mw/Mn) values of the polymers were determined using a Size Exclusion Chromatography (SEC) system equipped with Shimadzu LC20AD pump, Wyatt Optilab rEX refractive index detector and four PLgel 5µ Mixed-C columns. The characterization was performed at 35 °C in THF with a flow rate of 1 mL·min^{-1} with a sample concentration of 2 g L^{-1}. The samples were filtered through polytetrafluorethylene (PTFE) membranes with a pore size of 0.2 µm prior to injection.

System 2

Size-exclusion chromatography was carried out a TOSOH Eco-SEC HLC-8320 GPC System comprising an autosampler, a SDV 5 µm bead size guard column (50 × 8 mm, PSS) followed by three SDV 5 µm columns (300 × 7.5 mm, subsequently 100 Å, 1000 Å, and 105 Å pore size, PSS), and a differential refractive index (DRI) detector, using tetrahydrofuran (THF) as the eluent at 30 °C with a flow rate of 1 mL min^{-1}.

DMAc System:

Agilent Technologies 1260 Infinity II System, comprising an autosampler, a guard column followed by two PSS GRAM Lux 1000A 5µm (300 × 8 mm) and one PSS GRAM Lux 30A 5µm (300 × 8 mm) column, a differential refractive index detector (RID) as well as a UV detector (VWD) using DMAc (HPLC grade + 0,79g/2,5L LiBr) as the eluent at 40 °C with a flow rate of 1 mL·min-1. The SEC system was calibrated using the same ReadyCal Standards as for the THF systems.

Both SEC systems were calibrated using ReadyCal Standards: PS standards S3 ranging from 370 to 2.25·106 Da, PMMA standards S3 ranging from 800 to 2.2·106 Da

7.2.4 Ultraviolet–visible (UV-Vis) and Fluoresce Spectroscopy

UV-VIS spectra were recorded on a Duetta/Horiba Scientific Absorbance Transmission Fluorescence Excitation Emission (A-TEEM) spectrometer. Spectra were recorded in MeOH at 20 °C with different concentrations. Samples were baseline corrected with respect to the pure solvent

7.2.5 Thermogravimetric Analysis (TGA)

TGA was performed on a TA/TGA5500 instrument under nitrogen atmosphere at a heating rate of 10 °C·min^{-1} over a temperature range from 50 to 600 °C. The weights of the samples were in the range of 3-10 mg.

7.2.6 Differential scanning calorimetry (DSC)

Thermal properties were measured on a TA/DSC 2500 with a heat rate of 10 K·min^{-1} between -75 °C and 50 °C in TA Tzero sample holders. The glass transition temperature T_g was determined in the second heat run to eliminate possible interference from the polymer's thermal history.

7.2.7 IR Spectroscopy

All IR measurements were performed on a Bruker Alpha II ATR-IR from 350-3500 cm^{-1} at ambient temperature.

7.2.8 Photoreactor and lamps for irradiation

The photoreactions were conducted in a custom-build photoreactor equipped with a ventilator, rotating support, lamp holder and magnetic stirrer. While the Philips Cleo Compact (PL-L) (5*36W) lamp for the reactions in the UV-range (300-700 nm) can be placed directly into the lamp holder, were placed closely around the reaction vessel in the photoreactor.

7.2.9 Scanning Electron Microscopy (SEM)

Scanning electron microscopy (SEM) measurements were performed with a JSM7800F field emission scanning electron microscope (SEM, JEOL, Japan).

7.2.10 Confocal Fluorescence Microscopy

Confocal microscopy images were obtained on a Leica TCS SP% Confocal Laser Scanning Microscopy, operated in variable gain mode using 10x water immersion objective (Plan-Apo, 1.2 NA). Zen software (Zeiss) was used for the acquisition image processing.

7.2.11 Freeze drier

Lyophilisation was carried out using a Telstar LyoQuest benchtop freeze dryer (0.008 mBar, -70 °C).

7.2.12 Centrifuge

For centrifugation, Sigma 2-7 and Sigma 2-16P centrifuges were used. Usual centrifugation time was four minutes at maximum RPM settings.

7.3 Synthesis Procedures

7.3.1 Experimental Procedures for Chapter 5.1

7.3.1.1 General procedure of synthesis of 1,6-diisocyanide

A solution of hexane-1,6-diamine (1 eq.) and ethyl formate (10.0 eq.) was refluxed at 60 °C for 12h. Then, the solvent was removed by vacuum evaporation. The crude product (*N*-(6-formamidohexyl)formamide) was used in the next step without further purification. In a three-neck-flask, *N*-(6-formamidohexyl)formamide (1.00 eq.) was suspended in 100 mL dry DCM, and then triethylamine (5.00 eq.) was added at 0 °C. Phosphoryl trichloride (2.00 eq.) was added dropwise such that the reaction temperature was maintained below 0 °C. After being stirred for 1 h, the reactant was poured into a 500 mL beaker with 150 mL ice-water mixture containing 30 g of K_2CO_3. During the above operation, the temperature was maintained below 15 °C. The resulting emulsion was stirred for a while. The organic layer was removed, and the aqueous layer was extracted with dichloromethane (DCM) (2x40mL). Then, the combined organic layer was collected and dried with anhydrous K_2CO3. After evaporation of the solvent, the residue was purified by aluminium oxide column chromatography (CH_2Cl_2: Cyclohexane, 1:1) to give a brown liquid. Yield: 75%. ^{1}H-NMR (400 MHz, $CDCl_3$): δ / ppm= 3.40 (m, 4H, CH_2NC), 1.70 (m, 4H, CH_2CH_2NC), 1.48 (m, 4H, $CH_2CH_2CH_2NC$), ^{13}C-NMR (500 MHz, $CDCl_3$): δ / ppm = 157.3 , 41.0, 22.6.

7.3.1.2 General procedure of synthesis of Polymers (MC-Tet$_1$ - MC-Tet$_7$)

According to the specified design criteria, certain chemicals have been intentionally chosen with respect to the intended concept. N, N-Dimethyl-1,6-hexanediamine has been selected as a bio-based derivative to imitate adipic acid, a precursor for nylon synthesis. Additionally, specific aldehydes have been chosen from a wide range of commercially available options for various reasons as following; Hexanal (6 carbons) has been selected due to its sustainable nature, often used in the flavour industry. Decanal, citronellal, and undecanal (10 carbons) have been chosen to explore the impact of different aliphatic alkyl chain lengths on the project. Moreover, 4-(trifluoromethyl) benzaldehyde (8 carbons, 3 fluorine) has been selected for comparison with other benzaldehyde derivatives, providing the ability to mimic fluorinated polyamides and possessing excellent properties such as thermal-oxidative stability and good electrical insulation. Last but not least, 5-norbornene-2-carboxaldehyde has been chosen for its significant properties like high-temperature resistance and improved material stiffness, providing an olefin group for further post-polymerization modification of the designed polymeric structure through the thiol-ene photo-click reaction. Accordingly, 1,6-diisocyanide (1.00 eq.), N,N-dimethyl-1,6-hexanediamine (1.00 eq.), trimethylsilyl azide ($TMSN_3$) (2.00 eq.) and corresponding aldehyde derivatives (10-undecenal, 4-(trifluoromethyl)benzaldehyde,5-norbornene-2-carboxaldehyde, benzaldehyde, citronellal, decanal, hexanal) (2.00 eq.) were reacted in the presence of the catalyst 1,8-diazabicyclo(5.4.0)undec-7-ene (DBU)(0.3 eq.) under inert atmosphere (N_2) at 50 °C in MeOH:DMF(1:1) mixture. The resulting polymers were purified by precipitation into cold MeOH except for MC-Tet$_1$, which was precipitated into diethyl ether, and all the polymers were dialyzed against mixture of DCM: MeOH (1:1) for 2 days. The precipitated polymers were separated *via* centrifugation and dried at 40 °C under.

7.3.2 Experimental Procedures for Chapter 5.2

7.3.2.1 General procedure for the post-polymerization of MC-Tet$_3$ and MC-Tet$_7$

The reactions were conducted by combining 1-dodecanthiol (5.00 eq.), and MC-Tet$_3$ or MC-Tet7 (1.00 eq.) with the addition of 0.3 wt.% of 2,2-dimethoxy-2-phenyl acetophenone (DMAP) as the photo initiator. The reaction took place in a solvent mixture of dichloromethane DCM: MeOH in a 1:1 ratio, followed by exposure to UV irradiation at a wavelength of 365 nm for a duration of 2 hours. The resulting polymers were purified by precipitation into cold MeOH, and the precipitated polymers were separated *via* centrifugation and dried at 40 °C under. (yield: 90% for MC-Tet$_3$ and 70% MC-Tet$_7$).

7.3.2.2 Synthesis of model compound (MC)

All the synthesis of bis-tetrazole containing compound are adopted from the literature which allows preparing bis-1,5 DST derivatives in good yields.[183] Diethylamine (1.00 eq.) was dissolved in MeOH (1 M) and the corresponding butyl isocyanide (1.00 eq.), 10-Undecenal (1.00 eq.), azidotrimethylsilane ($TMSN_3$) (1.00 eq.) and a few drops of diazabicyclo[5.4.0]-7-undecene (DBU) were added, and the solution was stirred for overnight at ambient temperature. Upon the completion of the reaction, methanol was removed under reduced pressure and a mixture of product with the unreacted starting materials was obtained as yellowish oil. Subsequently, the pure product was isolated *via* purification by column chromatography (DCM:MeOH =1:0.05 by v:v) as clear, transparent oil. (yield:75 %). 1H-NMR (400 MHz, CDCl3): δ / ppm= (5.85-5.70 (m, 1H), 5.03-4.85 (m, 2H), 4.47-4.16 (m, 2H), 3.95 (dd, J= 10.4, 3.4 Hz, 1H), 6.33 -0.00 (m, 1H), 2.69-2.04 (m, 5H), 2.05-1.63 (m, 5H), 2.05-1.78 (m, 5H), 2.05-0.88 (m, 29H). ^{13}C NMR (101 MHz, $CDCl_3$): δ/ ppm 155.03 (s), 139.15 (s), 114.11 (s), 55.22 (s), 47.02 (s), 43.85 (s), 33.76 (s), 31.62 (s), 29.67-29.22 (m), 28.95 (d, J= 17.8 Hz), 27.15 (s), 25.67 (s), 19.81 (s), 13.91 (s), 13.54 (s)

7.3.2.3 Procedure for thiol-ene model reaction (MR)

The thiol-ene model reactions were performed by dissolving MC (1.00 eq.) in a *via*l in dry DCM (1M) and mixed on a shaker until a homogenous mixture was obtained. Subsequently, the corresponding thiol derivative 1-dodecanthiol (1.00 eq.) was introduced and mixed again into a homogenous blend. Subsequently, the mixture was degassed with N_2 for 15 min. A solution of dimethoxy-2-phenylaceto-phenone (DMPA) (0.3 wt %) was added as photo initiator and mixed on a shaker. Afterward, the reaction was let to stir magnetically (500 rpm) for 18 h under UV at λ = 365 nm in a photo reactor. Upon the completion of the reaction, the resulting MR was obtained as slightly yellowish viscous oil product with a reasonable total yield of 98 % upon purification by column chromatography (DCM:MeOH =1:0.05 by v:v).

7.3.2.4 Synthesis of M1 and M2

Diethylamine (1.00 eq.) was dissolved in MeOH (1M) and the corresponding butyl isocyanide (2.00 eq.), 10-Undecenal (2.00 eq.) and 4-pentenal (2.00 eq.) for M1 and M2, respectively, azidotrimethylsilane ($TMSN_3$, 2.00 eq.) and a few drops of diazabicyclo[5.4.0]-7-undecene (DBU) were added, and the solution was stirred for overnight at ambient temperature. Upon the completion of the reaction, methanol was removed under reduced pressure and a mixture of product with the unreacted starting materials was obtained as yellowish oil. Subsequently, the pure product was isolated *via* purification by column chromatography (DCM:MeOH =1:0.05 by v:v) as clear, transparent oil, (yield: 95 % and 89 % for M1 and M2, respectively)

M1= ^{1}H NMR (400 MHz, CDCl3) δ 5.79 (ddt, J= 16.9, 10.2, 6.7 Hz, 1H), 5.08-4.77 (m, 2H), 4.47-4.23 (m, 2H), 4.01-3.67 (m, 1H), 2.37 (t, J= 7.2 Hz, 2H), 2.19 (s, 3H), 2.07-1.98 (m, 2H), 1.97-1.83 (m, 3H), 1.46-1.19 (m, 17H), 1.14 (dd, J= 18.4, 3.8 Hz, 3H), 0.96 (t,J=7.4Hz,3H). 13C NMR (101 MHz, CDCl3) δ 154.67 (s), 139.27 (s), 114.25 (s), 59.19 (s), 53.36 (d, J= 4.9 Hz), 47.43 (s), 37.80 (s), 33.89 (s), 29.54 (dd, J= 12.8, 10.6 Hz), 29.31 – 28.70 (m), 28.04 (s), 27.14 (s), 26.29 (d, J= 6.1 Hz), 22.25 (s), 14.31 (s), 13.96 (s).

M2= ^{1}H NMR (400 MHz, CDCl3) δ 5.89-5.63 (m, 1H), 5.07-4.82 (m, 2H), 4.32 (t, J= 7.4 Hz, 2H), 3.94- 3.74 (m, 1H), 2.48-2.29 (m, 2H), 2.23-2.15 (m, 4H), 2.05 – 1.80 (m, 4H), 1.45-1.24 (m, 4H), 1.12 (dt, J= 6.9, 4.3 Hz, 2H), 1.02 -0.89 (m, 3H). 13C NMR (101 MHz, CDCl3) δ 154.66 (s), 139.25 (s), 114.24 (s), 59.16 (s), 53.33 (d, J= 4.2 Hz), 47.16 (s), 37.77 (s), 33.87 (s), 31.72 (s), 29.54 (dd, J= 11.3, 7.2 Hz), 29.09 (dd, J= 18.5, 4.3 Hz), 28.01 (s), 27.12 (s), 26.21 (d, J= 4.8 Hz), 20.27 (s), 19.91 (s), 13.87 (s), 13.64 (s).

7.3.2.5 General procedure of synthesis of Polymers (PC-Tet$_1$ - PC-Tet$_{12}$)

The thiol-ene polymerization reactions for M1 were performed with different kinds of thiols by following the same procedure of the model thiol-ene reaction. In an exemplary way, M1 (1.00 eq.) were added to a small transparent vial and dissolved in DCM (1M), followed by the addition of the corresponding dithiol maintaining a 1:1 functional group stoichiometry. After the degassing with N2, the solution was continuously stirred when dimethoxy-2-phenylacetophenone (DMPA) (0.3 wt%) was added as the initiator. Subsequently, the samples were exposed to 365 nm irradiation for 18 h at ambient temperature in a photo reactor. Similarly, the bulk thiol-ene polymerizations of M2 were prepared with the different kinds of thiols which are as listed in Scheme 2. Although all the reaction conditions have been kept in the same manner as the above-mentioned polymerization of M1, for M2, it was necessary to magnetically stir the reaction mixture above 800 rpm for 24h to provide a homogenous mixture and ensure the synthesis of high molecular weight polymers. Upon the completion of the polymerization reactions, the solutions were diluted with DCM. After that, the polymer solutions of M1 and M2 were precipitated two times into ice cold diethyl ether. The precipitated polymers of M1 and M2 were separated *via* centrifugation and dried at 40 °C under the vacuum to yield a transparent, slightly yellowish viscous products.

Yield of the obtained polymers: PC-Tet$_1$=55.8%, PC-Tet$_2$=82%, PC-Tet$_3$=61%, PC-Tet$_4$=75%. PC-Tet$_5$=73%, PC-Tet$_6$=94%, PC-Tet$_7$=61%, PC-Tet$_8$=73%, PC-Tet$_9$=81%, PC-Tet$_{10}$=89%, PC-Tet$_{11}$=97%, PC-Tet$_{12}$=80%.

7.3.3 Experimental Procedures for Chapter 5.3

7.3.3.1 Synthesis of pentafluorophenyl acrylate (p(PFPA)) monomer

p(PFPA) was synthesized as literature suggested.[297] To a solution of pentafluorophenol (PFP, 9.20 g, 50.00 mmol) in anhydrous DCM (42 mL) at 0 °C was added TEA (5.57 g, 55.00 mmol) dropwise. Acryloyl chloride (4.98 g, 55.00 mmol) was added dropwise to the cooled reaction mixture under vigorous stirring, after 30 min, the mixed solution was allowed to reach room temperature and stirred for an additional 12 hr. Monitoring of the reaction was performed by thin-layer chromatography (TLC), petroleum ether/ethyl acetate = 15/1, v/v) until complete consumption of PFP was observed. The reaction mixture was filtered prior to two-fold extraction with brine and dried over Na2SO4, concentrated by rotary evaporation and suddenly vacuum distilled. The crude product was purified by column chromatography (silica gel, petroleum ether/ethyl acetate = 15/1, v/v). Finally, a colourless liquid was obtained (9.43 g,79%). The analytical data of pentafluorophenyl acrylate matches published data. ^{1}H NMR (400 MHz, $CDCl_3$): δ 6.72 (dd, J = 17.3, 0.8 Hz, 1H), 6.37 (dd, J = 17.3, 10.6 Hz, 1H), 6.18 (dd, J= 10.6, 0.8 Hz, 1H).

7.3.3.2 Synthesis of poly(pentafluorophenyl acrylate) (p(PFPA) polymer

p(PFPA) was synthesized in accordance with previous reports of the research group.[224] A solution of PFPA (1.00 eq.) and azobisisobutyronitrile (AIBN) (0.01 eq.) in dry 1,4-dioxane (5 mL) were placed in a Schlenk tube. Three freeze-pump-thaw cycles were performed to degas the solution. The flask was transferred to a preheated oil bath at 70 °C and stirred overnight. The reaction was exposed to air to quench the polymerization. The solution was diluted with chloroform and precipitated from methanol to afford a white solid. It was redissolved in chloroform and reprecipitated from MeOH. The process was repeated thrice and received as a white solid. After drying under vacuum at 40 °C, the polymer was given in 94% yield. ^{1}H NMR (400 MHz, $CDCl_3$): δ 3.27-2.70 (m, 1H), 2.55-1.69 (m, 2H). ^{19}F NMR (377 MHz, $CDCl_3$): δ 153.19 (s), 157.14 (d, J = 279.3 Hz), 162.20 (s). FTIR (ATR mode): 17820cm^{-1} (C=O stretching of PFP-ester), 1516 cm^{-1} (aromatic ring stretching).

7.3.3.3 Post-polymerization modification reactions of p(PFPA) polymer

Optimization studies:

p(PFPA) (1 eq. of PFP groups) was dissolved in 1 mL solvent (e.g., NMP, DMF or dry-DMF). Afterwards, corresponding catalyst (e.g., DMAP, TEA or DBU) with varying equivalents (e.g., 0.40 eq., 1.20 eq.) was dissolved in respective solvent and subsequently was added to the p(PFPA) solution. The reaction solution was stirred for 30 min under N_2. Then, 5-aminotetrazole (1.10 eq.) PFP groups of p(PFPA) in 2 mL respective solvent was added to the p(PFPA) solution.

The solution was stirred either at ambient temperature or 80 °C for 24 h and then precipitated in methanol or diethyl ether/n-hexane (v/v = 1/1). The products were dried at 60 °C in a vacuum oven until dry.

Different degrees of 1,5 DST modifications:

p(PFPA) (1 eq. of PFP groups) and TEA (1.2 eq.) were dissolved in dry-DMF in closed vial. Then, 5-aminotetrazole of varied equivalents to PFP groups of p(PFPA) (0.20, 0.40, and 0.60 eq.) in dry-DMF was added to the p(PFPA) solution under argon. The reaction solution was stirred at 60 °C for 30 min. Later on, the mixture was stirred at room temperature at 80 °C for 24 h and then precipitated in diethyl ether/n-hexane (v/v = 1/1) twice. The products were dried at 50 °C in a vacuum oven until dry.

7.3.3.4 Hydrogel formation

In initial stage different degrees of 1,5 DST modifications were performed by following the procedure abovementioned. Upon synthesizing modified polymers, the solutions were cooled down until they reached 60 °C. Amino-terminated PEG derivative O,O`-Bis(3-aminopropyl)polyethylene glycol, with varying equivalents (e.g.,0.85, 0.45 and 0.65 eq.) to PFP groups of p(PFPA), dissolved in dry-DMF and was s added into the suspensions of 1,5 DST-modified p(PFPA). The mixtures were stirred at 60 °C for 5 min. Later, the solution was allowed to complete the crosslinking and remove bubbles after standing at ambient temperature for overnight. Obtained hydrogels were dialysed against EtOH: water mixture for three days, subsequently dried using a freeze dryer.

Bibliography

[1] F. R. Benson, *Chemical Reviews* **1947**, *41*, 1-61.

[2] M. V. Gorn, N. P. Gritsan, C. F. Goldsmith, V. G. Kiselev, *The Journal of Physical Chemistry A* **2020**, *124*, 7665-7677.

[3] V. Ostrovskii, E. Popova, R. Trifonov, *Advances in heterocyclic chemistry* **2017**, *123*, 1-62.

[4] V. A. Ostrovskii, G. I. Koldobskii, R. E. Trifonov, in *Comprehensive Heterocyclic Chemistry III*, Elsevier, Oxford, **2008**, 257-423.

[5] M. Nasrollahzadeh, Z. Nezafat, N. S. S. Bidgoli, N. Shafiei, *Molecular Catalysis* **2021**, *513*, 111788.

[6] D. Srinivas, V. D. Ghule, K. Muralidharan, H. D. B. Jenkins, *Chemistry-An Asian Journal* **2013**, *8*, 1023-1028.

[7] C. Y. Cao, S. Lu, D. Zhang, L. L. Gong, H. P. Zhang, *RSC Advances* **2017**, *7*, 13808-13816.

[8] M. Benz, T. M. Klapötke, J. Stierstorfer, *Zeitschrift für anorganische und allgemeine Chemie* **2020**, *646*, 1380-1388.

[9] C. X. Wei, M. Bian, G. H. Gong, *Molecules* **2015**, *20*, 5528-5553.

[10] T. M. Klapötke, S. M. Sproll, *European Journal of Organic Chemistry* **2010**, 1169-1175.

[11] E. Bakangura, Y. He, X. Ge, Y. Zhu, L. Wu, J. Ran, C. Cheng, K. Emmanuel, Z. Yang, T. Xu, *Frontiers of Chemical Science and Engineering* **2018**, *12*, 306-310.

[12] L. da Silva, M. M. Salas, A. de León Santillán, A. A. Siller-Ceniceros, D. M. Acosta, R. F. Magnago, R. Benavides, *Reactive and Functional Polymers* **2021**, *167*, 105007.

[13] P. N. Gaponik, O. A. Ivashkevich, V. P. Karavai, A. I. Lesnikovich, N. I. Chernavina, G. T. Sukhanov, G. A. Gareev, *Die Angewandte Makromolekulare Chemie: Applied Macromolecular Chemistry and Physics* **1994**, *219*, 77-88.

[14] C. G. Neochoritis, T. Zhao, A. Domling, *Chemical Reviews* **2019**, *119*, 1970-2042.

[15] W. K. Su, Z. Hong, W. G. Shan, X. X. Zhang, Wiley Online Library, **2006**.

[16] R. Vishwakarma, C. Gadipelly, L. K. Mannepalli, *Chemistry Select* **2022**, *7*.

[17] N. J. Leonard, B. Zwanenburg, *Journal of the American Chemical Society* **1967**, *89*, 4456-4465.

[18] M. J. S. Dewar, G. J. Gleicher, *The Journal of Chemical Physics* **1966**, *44*, 759-773.

[19] L. S. Crawley, S. R. Safir, *Journal of Heterocyclic Chemistry* **1975**, *12*, 1075-1076.

[20] G. B. Barlin, T. J. Batterham, *Journal of the Chemical Society B: Physical Organic* **1967**, 516-518.

[21] M. Sainsbury, *Rodd's Chemistry of Carbon Compounds, Vol. 4, Part D, 211*, Elsevier, **1986**.

[22] J. S. R. Huisgen, H. J. Sturm, J. Mafckgraf, *Chemische Berichte* **1960**, *93*, 2106-2124.

[23] J. H. Markgraf ; W. T. Bachmann; D. P. Hollis, *Journal of Organic Chemistry Research* **1965**, *30,* 3472.

[24] J. Rein, J. M. Meinhardt, J. L. Hofstra Wahlman, M. S. Sigman, S. Lin, *Angewandte Chemie International Edition* **2023**, *62*, e202218213.

[25] P. Scheiner, J. F. Dinda, *Tetrahedron* **1970**, *26*, 2619-2629.

[26] P. Scheiner, *Tetrahedron Letters* **1971**, *12*, 4489-4492.

[27] L. M. Frija, A. Ismael, M. L. Cristiano, *Molecules* **2010**, *15*, 3757-3774.

[28] J. A. Bladin, *Berichte der deutschen chemischen Gesellschaft* **1885**, *18*, 1544-1551.

[29] R. M. Acheson, Edition, 2; Publisher, Interscience Publishers **1960**.

[30] R. E. Ford, P. Knowles, E. Lunt, S. M. Marshall, A. J. Penrose, C. A. Ramsden, A. J. H. Summers, J. L. Walker, D.E. Wright, *Journal of Medicinal Chemistry* **1986**, *29*, 538-549

[31] A. Rajasekaran, P.P. Thampi, *European Journal of Medicinal Chemistry* **2004**, *39*, 273-279.

[32] M. Uchida, M. Komatsu, S. Morita, T. Kanbe, K. Yamasaki, K. Nakagawa, *Chemical & Pharmaceutical Bulletin* **1989**, *37*, 958-961.

[33] R. A. S. Powers, B. K., *J. Med. Chem.* **2002**, *45*, 3222-3234.

[34] G. Karabanovich, J. Roh, O. Soukup, I. Pávková, M. Pasdiorová, V. Tambor, J. Stolaříková, M. Vejsová, K. Vávrová, V. Klimešová , A. Hrabáleka, *Medicinal Chemistry Communications* **2015**, *6*, 174-181.

[35] S. G. Vedpathak, G. K. Kakade, V. S. Ingale, *IRA-International Journal of Applied Scienc*es, **2016**, *3*, 2455-4499

[36] P. An, Q. Lin, *Organic and Biomolecular Chemistry* **2018**, *16*, 5241-5244.

[37] P. J. Wright, J. L. Kolanowski, W. K. Filipek, Z. Lim, E. G. Moore, S. Stagni, E. J. New, M. Massi, *European Journal of Inorganic Chemistry* **2017**, 5260-5270.

[38] A. K. West, L. J. Kaylor, M. Subir, S. Rayat, *RSC Advances* **2022**, *12*, 22331-22341.

[39] Y. Xiao, S. H. Wang, Y.-P. Zhao, F.-K. Zheng, G. C. Guo, *CrystEngComm* **2016**, *18*, 2524-2531.

[40] X. Dou, Q. Zhou, X. Chen, Y. Tan, X. He, P. Lu, K. Sui, B. Z. Tang, Y. Zhang, W. Z. Yuan, *Biomacromolecules* **2018**, *19*, 2014-2022.

[41] G. I. Koldobskii, V. A. Ostrovskii, V. S. Popavskii, *Chemistry of Heterocyclic Compounds* **1981**, *17*, 965-988.

[42] S. N. Dighe, K. S. Jain, K. V. Srinivasan, *Tetrahedron Letters* **2009**, *50*, 6139-6142.

[43] A. Sarvary, A. Maleki, *Molecular diversity* **2015**, *19*, 189-212.

[44] T. Jin, S. Kamijo, Y. Yamamoto, *Tetrahedron letters* **2004**, *45*, 9435-9437.

[45] T. Amanpour, P. Mirzaei, A. Bazgir, *Tetrahedron Letters* **2012**, *53*, 1421-1423.

[46] P. Mohite, R. Pandhare, S. Khanage, V. Bhaskar, *Digest Journal of Nanomaterials and Biostructures* **2009**, *4*, 803-807.

[47] Y. Li, L. X. Gao, F. S. Han, *Chemical Communications* **2012**, *48*, 2719-2721.

[48] T. Aoyama, T. Shioiri, *Chemical and Pharmaceutical Bulletin* **1982**, *30*, 3450-3452.

[49] J. V. Duncia, M. E. Pierce, J. B. Santella III, *The Journal of Organic Chemistry* **1991**, *56*, 2395-2400.

[50] M. Mojzych, Z. Karczmarzyk, W. Wysocki, Z. Urbańczyk-Lipkowska, N. Żaczek, *Journal of Molecular Structure* **2014**, *1067*, 147-153.

[51] M. Mojzych, Z. Karczmarzyk, A. Rykowski, *Journal of Chemical Crystallography* **2005**, *35*, 151-155.

[52] J. Hill, J. Ehrlich, *The Journal of Organic Chemistry* **1971**, *36*, 3248-3251.

[53] H. Naeimi, F. Kiani, *Ultrasonics sonochemistry* **2015**, *27*, 408-415.

[54] F. Abrishami, M. Ebrahimikia, F. Rafiee, *Applied Organometallic Chemistry* **2015**, *29*, 730-735.

[55] Y. Yıldız, İ. Esirden, E. Erken, E. Demir, M. Kaya, F. Şen, *ChemistrySelect* **2016**, *1*, 1695-1701.

[56] İ. Esirden, E. Erken, M. Kaya, F. Sen, *Catalysis Science & Technology* **2015**, *5*, 4452-4457.

[57] G. Qiu, M. Mamboury, Q. Wang, J. Zhu, *Angewandte Chemie* **2016**, *128*, 15603-15607.

[58] S. B. Bhagat, V. N. Telvekar, *Synlett* **2018**, *29*, 874-879.

[59] M. Ramanathan, Y. H. Wang, S. T. Liu, *Organic Letters* **2015**, *17*, 5886-5889.

[60] D. Habibi, M. Nasrollahzadeh, A. R. Faraji, Y. Bayat, *Tetrahedron* **2010**, *66*, 3866-3870.

[61] D. Habibi, M. Nasrollahzadeh, *Synthetic Communications* **2010**, *40*, 3159-3167.

[62] V. Khorramabadi, D. Habibi, S. Heydari, *Green Chemistry Letters and Reviews* **2020**, *13*, 50-59.

[63] M. Atarod, J. Safari, H. Tebyanian, *Synthetic Communications* **2020**, *50*, 1993-2006.

[64] J. J. Shie, J. M. Fang, *The Journal of Organic Chemistry* **2007**, *72*, 3141-3144.

[65] S. Voitekhovich, *Polish Journal of Chemistry* **2001**, *75*, 253-264.

[66] H. Xia, W. Zhang, Y. Jin, S. Song, K. Wang, Q. Zhang, *ACS applied materials & interfaces* **2019**, *11*, 45914-45921.

[67] *Physics Bulletin* **1968**, *19*, 93.

[68] M. L. Gettings, M. T. Thoenen, E. F. Byrd, J. J. Sabatini, M. Zeller, D. G. Piercey, *Chemistry-A European Journal* **2020**, *26*, 14530-14535.

[69] P. K. Swain, H. Singh, S. P. Tewari, *Journal of Molecular Liquids* **2010**, *151*, 87-96.

[70] G. K. Lund, R. J. Blau, Google Patents, **1996**.

[71] C. Wentrup, *Chemical Reviews* **2017**, *117*, 4562-4623.

[72] S. Manzoor, X. Yin, J. G. Zhang, *Defence Technology* **2021**, *17*, 1995-2010.

[73] Q. X. Jia, H. Tian, L. Yan, Y. Ma, E. Q. Gao, *Inorganica Chimica Acta* **2010**, *363*, 3750-3756.

[74] M. Uemura, Y. Yoshikawa, K. Yoshikawa, T. Sato, Y. Mino, M. Chikuma, S. Komeda, *Journal of Inorganic Biochemistry* **2013**, *127*, 169-174.

[75] S. Komeda, H. Takayama, T. Suzuki, A. Odani, T. Yamori, M. Chikuma, *Metallomics* **2013**, *5*, 461-468.

[76] J. C. Flores-Reyes, P. Islas-Jácome, A. Gutiérrez-Carrillo, M. A. Rincón-Guevara, G. V. Suárez-Moreno, Ó. Vázquez-Vera, L. Lomas-Romero, E. González-Zamora, A. Islas-Jácome, *Chemistry Proceedings* **2022**, *8*, 25.

[77] L.-B. Enache, V. Anăstăsoaie, L. Birzan, E.-M. Ungureanu, P. Diao, M. Enachescu, *Coatings* **2020**, *10*, 869.

[78] X. Wang, X. Bai, H. Lin, J. Sun, G. Liu, X. Wang, *CrystEngComm* **2018**, *20*, 6438-6448.

[79] A. Q. Wu, Q.-Y. Chen, M. F. Wu, F. K. Zheng, F. Chen, G. C. Guo, J. S. Huang, *Australian Journal of Chemistry* **2009**, *62*, 1622-1630.

[80] Y. Allab, S. Chikhi, S. Zaater, M. Brahimi, S. Djebbar, *Inorganica Chimica Acta* **2020**, *504*, 119436.

[81] Y. Qiu, Y. Li, G. Peng, J. Cai, L. Jin, L. Ma, H. Deng, M. Zeller, S. R. Batten, *Crystal Growth & Design* **2010**, *10*, 1332-1340.

[82] M. Massi, S. Stagni, M. I. Ogden, *Coordination Chemistry Reviews* **2018**, *375*, 164-172.

[83] N. A. Meanwell, in *Burger's Medicinal Chemistry and Drug Discovery*, 1-81.

[84] N. Brown, in *Bioisosteres in Medicinal Chemistry*, **2012**, 1-14.

[85] N. R. Council, *First Symposium on Chemical-Biological Correlation,* The National Academies Press, Washington, DC, **1951**.

[86] A. S. Kalgutkar, J. S. Daniels, *Metabolism, Pharmacokinetics and Toxicity of Functional Groups: Impact of Chemical Building Blocks on ADMET* **2010**, 99-167.

[87] H. L. Friedman, *NAS-NRS Publication* **1951**, *206*, 295-358.

[88] L. Myznikov, A. Hrabalek, G. Koldobskii, *Chemistry of Heterocyclic Compounds* **2007**, *43*.

[89] G. A. Patani, E. J. LaVoie, *Chemical Reviews* **1996**, *96*, 3147-3176.

[90] C. Ballatore, D. M. Huryn, A. B. Smith, 3rd, *ChemMedChem* **2013**, *8*, 385-395.

[91] K. Bredael, S. Geurs, D. Clarisse, K. De Bosscher, M. D'hooghe, *Journal of Chemistry* **2022**, 2164558.

[92] V. R. Pattabiraman, J. W. Bode, *Nature* **2011**, *480*, 471-479.

[93] R. M. De Figueiredo, J. S. Suppo, J. M. Campagne, *Chemical reviews* **2016**, *116*, 12029-12122.

[94] S. Sun, Q. Jia, Z. Zhang, *Bioorganic & medicinal chemistry letters* **2019**, *29*, 2535-2550.

[95] N. A. Meanwell, *Journal of medicinal chemistry* **2011**, *54*, 2529-2591.

[96] V. Subramanian, J. S. Knight, S. Parelkar, L. Anguish, S. A. Coonrod, M. J. Kaplan, P. R. Thompson, *Journal of medicinal chemistry* **2015**, *58*, 1337-1344.

[97] J. Zabrocki, G. D. Smith, J. B. Dunbar, H. Iijima, G. R. Marshall, *Journal of the American Chemical Society* **1988**, *110*, 5875-5880.

[98] E. A. Popova, R. E. Trifonov, V. A. Ostrovskii, *Russian Chemical Reviews* **2019**, *88*, 644.

[99] N. Dhiman, K. Kaur, V. Jaitak, *Bioorganic and Medicinal Chemistry* **2020**, *28*, 115599.

[100] S. Q. Wang, Y. F. Wang, Z. Xu, *uropean Journal of Medicinal Chemistry* **2019**, *170*, 225-234.

[101] A. Warrilow, C. Hull, J. Parker, E. Garvey, W. Hoekstra, W. Moore, R. Schotzinger, D. Kelly, S. Kelly, *Antimicrobial agents and chemotherapy* **2014**, *58*, 7121-7127.

[102] M. Bialer, S. I. Johannessen, R. H. Levy, E. Perucca, T. Tomson, H. S. White, *Epilepsia* **2017**, *58*, 181-221.

[103] L. V. Myznikov, S. V. Vorona, Y. E. Zevatskii, *Chemistry of Heterocyclic Compounds* **2021**, *57*, 224-233.

[104] S. Rajamanickam, C. Sah, B. A. Mir, S. Ghosh, G. Sethi, V. Yadav, S. Venkataramani, B. K. Patel, *The Journal of Organic Chemistry* **2020**, *85*, 2118-2141.

[105] P. Matzneller, M. Kussmann, S. Eberl, A. Maier-Salamon, W. Jäger, M. Bauer, O. Langer, M. Zeitlinger, W. Poeppl, *European Journal of Drug Metabolism and Pharmacokinetics* **2018**, *43*, 599-606.

[106] G. Reynard, H. Lebel, *The Journal of Organic Chemistry* **2021**, *86*, 12452-12459.

[107] D. P. G. Norman, A. E. Bunnell, S. R. Stabler, L. A. Flippin, *The Journal of Organic Chemistry* **1999**, *64*, 9301-9306.

[108] T. Luxford, J. Fedor, J. Kočišek, *The Journal of Chemical Physics* **2021**, *154*.

[109] J. Rein, J. M. Meinhardt, J. L. H. Wahlman, M. S. Sigman, S. Lin, *ChemRxiv* **2021**.

[110] O. Y. Shyyka, N. T. Pokhodylo, Y. I. Slyvka, E. A. Goreshnik, M. D. Obushak, *Tetrahedron Letters* **2018**, *59*, 1112-1115.

[111] J. Hénin, J. Gardent, *Journal of heterocyclic chemistry* **1986**, *23*, 975-979.

[112] E. Duchamp, B. D. n. Simard, S. Hanessian, *Organic Letters* **2019**, *21*, 6593-6596.

[113] R R. A. Laforge, C. E. Cosgrove, A. D'adamo, *The Journal of Organic Chemistry* **1956**, *21*, 988-992.

[114] P. He, J. G. Zhang, X. Yin, J. T. Wu, L. Wu, Z. N. Zhou, T. L. Zhang, *Chemistry-A European Journal* **2016**, *22*, 7670-7685.

[115] Y. Wang, W. J. Hu, W. Song, R. K. V. Lim, Q. Lin, *Organic Letters* **2008**, *10*, 3725-3728.

[116] Y. Wang, C. I. Rivera Vera, Q. Lin, *Organic Letters* **2007**, *9*, 4155-4158.

[117] A. Burke, S. Spiccio, M. Di Filippo, M. Baumann, *SynOpen* **2023**, *7*, 69-75.

[118] W. Feng, L. Li, C. Yang, A. Welle, O. Trapp, P. A. Levkin, *Angewandte Chemie International Edition* **2015**, *54*, 8732-8735.

[119] M. Abdessalam, M. A. Sidhoum, F. Z. Zradni, H. Ilikti, *Molbank* **2021**.

[120] S. Paudel, S. Wang, E. Kim, D. Kundu, X. Min, C. Y. Shin, K. M. Kim, *iomolecules and Therapeutics* **2022**, *30*, 191-202.

[121] I. Niño-Pantoja, A. Gallardo-Alfonzo, M. Solis-Santos, M. Ordoñez, C. Contreras-Celedón, A. Islas-Jácome, L. Chacón-García, C. J. Cortés-García, *European Journal of Organic Chemistry* **2022**, e202200230.

[122] C. N. S. S. P. Kumar, D. K. Parida, A. Santhoshi, A. K. Kota, B. Sridhar, V. J. Rao, *Medicinal Chemistry Communications* **2011**, *2*.

[123] B. Umamahesh, N. S. Karthikeyan, K. I. Sathiyanarayanan, J. M. Malicka, M. Cocchi, *Journal of Materials Chemistry C* **2016**, *4*, 10053-10060.

[124] G. Arthur, Wiley-Interscience New York, **2000**.

[125] M. C. Bryan, P. J. Dunn, D. Entwistle, F. Gallou, S. G. Koenig, J. D. Hayler, M. R. Hickey, S. Hughes, M. E. Kopach, G. Moine, *Green Chemistry* **2018**, *20*, 5082-5103.

[126] M. T. Sabatini, L. T. Boulton, H. F. Sneddon, T. D. Sheppard, *Nature Catalysis* **2019**, *2*, 10-17.

[127] R. J. Herr, *Bioorganic & medicinal chemistry* **2002**, *10*, 3379-3393.

[128] B. J. Al-Hourani, B. F. Ali, Z. Judeh, M. I. El-Barghouthi, W. Al-Awaida, Y. Snobar, F. El Soubani, K. Matalka, F. Wuest, *Journal of Molecular Structure* **2018**, *1164*, 317-327.

[129] A. R. Katritzky, C. Cai, N. K. Meher, *Synthesis* **2007**, 1204-1208.

[130] J. R. Hanson, *Natural product reports* **2010**, *27*, 887-899.

[131] E. A. Popova, A. V. Protas, R. E. Trifonov, *Anti-Cancer Agents in Medicinal Chemistry (Formerly Current Medicinal Chemistry-Anti-Cancer Agents)* **2017**, *17*, 1856-1868.

[132] E. Saltiel, R. N. Brogden, *Drugs* **1986**, *32*, 222-259.

[133] L. W. Tremblay, H. Xu, J. S. Blanchard, *Biochemistry* **2010**, *49*, 9685-9687.

[134] Z. P. Demko, K. B. Sharpless, *Angewandte Chemie International Edition* **2002**, *41*, 2110-2113.

[135] T. M. Klapötke, B. Krumm, R. Moll, *European Journal of Inorganic Chemistry* **2011**, *2011*, 422-428.

[136] A. Sarvary, A. Maleki, *Mol Divers* **2015**, *19*, 189-212.

[137] W. R. Carpenter, *The Journal of Organic Chemistry* **1962**, *27*, 2085-2088.

[138] M. Aldhoun, A. Massi, A. Dondoni, *The Journal of Organic Chemistry* **2008**, *73*, 9565-9575.

[139] Z. P. Demko, K. B. Sharpless, *Angewandte Chemie* **2002**, *114*, 2217-2220.

[140] F. Couty, F. Durrat, D. Prim, *Tetrahedron Letters* **2004**, *45*, 3725-3728.

[141] T. Kereszty, *Chemical Abstracts, 89*, **1935**, 59949.

[142] L. J. Kennedy, *Tetrahedron Letters* **2010**, *51*, 2010-2013.

[143] N. T. Pokhodylo, Y. O. Teslenko, V. S. Matiychuk, M. D. Obushak, *Synthesis* **2009**, 2741-2748.

[144] B. J. Al-Hourani, S. K. Sharma, J. Y. Mane, J. Tuszynski, V. Baracos, T. Kniess, M. Suresh, J. Pietzsch, F. Wuest, *Bioorganic & Medicinal Chemistry Letters* **2011**, *21*, 1823-1826.

[145] Y. H. Joo, J. n. M. Shreeve, *Angewandte Chemie International Edition* **2009**, *48*, 564-567.

[146] G. I. Georg, X. Guan, J. Kant, *Tetrahedron Letters* **1988**, *29*, 403-406.

[147] A. A. S. El-Ahl, S. S. Elmorsy, H. Soliman, F. A. Amer, *Tetrahedron Letters* **1995**, *36*, 7337-7340.

[148] A. Hassner, R. Fibiger, A. S. Amarasekara, *The Journal of Organic Chemistry* **1988**, *53*, 22-27.

[149] H. J. Cristau, X. Marat, J. P. Vors, J. L. Pirat, *Tetrahedron Letters* **2003**, *44*, 3179-3181.

[150] Y. A. Efimova, T. V. Artamonova, G. I. Koldobskii, *Russian Journal of Organic Chemistry* **2009**, *45*, 725-727.

[151] P. Moutevelis-Minakakis, M. Filippakou, C. Sinanoglou, G. Kokotos, *Journal of Peptide Science* **2006**, *12*, 377-382.

[152] L. E. Cardenas-Galindo, A. Islas-Jacome, K. M. Colmenero-Martinez, A. Martinez-Richa, R. Gamez-Montano, *Molecules* **2015**, *20*, 1519-1526.

[153] B. H. Rotstein, S. Zaretsky, V. Rai, A. K. Yudin, *Chemical reviews* **2014**, *114*, 8323-8359.

[154] J. Zhu, H. Bienaymé, *Multicomponent reactions*, John Wiley & Sons, **2006**.

[155] P. Patil, K. Khoury, E. Herdtweck, A. Domling, *Bioorganic and Medicinal Chemistry* **2015**, *23*, 2699-2715.

[156] A. Dömling, W. Wang, K. Wang, *Chemical Reviews* **2012**, *112*, 3083-3135.

[157] E. Ruijter, R. Scheffelaar, R. V. Orru, *Angewandte Chemie International Edition* **2011**, *50*, 6234-6246.

[158] L. F. Tietze, *Chemical reviews* **1996**, *96*, 115-136.

[159] A. Strecker, *Justus Liebigs Annalen der Chemie* **1850**, *75*, 27-45.

[160] A. Dömling, I. Ugi, *Angewandte Chemie International Edition* **2000**, *39*, 3168-3210.

[161] S. Sadjadi, M. M. Heravi, N. Nazari, *RSC Advances* **2016**, *6*, 53203-53272.

[162] X. Zhang, L. Evanno, E. Poupon, *European Journal of Organic Chemistry* **2020**, 1919-1929.

[163] T. Zarganes-Tzitzikas, A. L. Chandgude, A. Domling, *Chem Rec* **2015**, *15*, 981-996.

[164] B. Jiang, T. Rajale, W. Wever, S. J. Tu, G. Li, *Chemistry-An Asian Journal* **2010**, *5*, 2318-2335.

[165] Q. Xiong, S. Dong, Y. Chen, X. Liu, X. Feng, *Nature Communications* **2019**, *10*, 2116.

[166] L. Banfi, A. Basso, C. Lambruschini, L. Moni, R. Riva, *Chemical Science* **2021**, *12*, 15445-15472.

[167] R. O. Rocha, M. O. Rodrigues, B. A. D. Neto, *ACS Omega* **2020**, *5*, 972-979.

[168] G. Koopmanschap, E. Ruijter, R. V. Orru, *Beilstein Journal of Organic Chemistry* **2014**, *10*, 544-598.

[169] I. Ugi, R. Meyr, *Chemische Berichte* **1961**, *94*, 2229-2233.

[170] A. Singh, R. Kumar, *Chemical Communications* **2021**, *57*, 9708-9711.

[171] A. L. Chandgude, A. Dömling, *Green Chem* **2016**, *18*, 3718-3721.

[172] T. Sela, A. Vigalok, *Advanced Synthesis & Catalysis* **2012**, *354*, 2407-2411.

[173] E. S. Schremmer, K. T. Wanner, *Heterocycles* **2007**, *74*, 661-671.

[174] M. J. Thompson, B. Chen, *The Journal of Organic Chemistry* **2009**, *74*, 7084-7093.

[175] S. Ramezanpour, S. Balalaie, F. Rominger, N. S. Alavijeh, H. R. Bijanzadeh, *Tetrahedron* **2013**, *69*, 10718-10723.

[176] A. Nikbakht, S. Ramezanpour, S. Balalaie, F. Rominger, *Tetrahedron* **2015**, *71*, 6790-6795.

[177] R. O. Rocha, M. O. Rodrigues, B. A. Neto, *ACS omega* **2020**, *5*, 972-979.

[178] S. Gunawan, J. Petit, C. Hulme, *ACS Combinatorial Science* **2012**, *14*, 160-163.

[179] A. L. Chandgude, A. Dömling, *European Journal of Organic Chemistry* **2016**, 2383-2387.

[180] T. Nixey, C. Hulme, *Tetrahedron letters* **2002**, *43*, 6833-6835.

[181] P. Capurro, L. Moni, A. Galatini, C. Mang, A. Basso, *Molecules* **2018**, *23*, 2758.

[182] I. V. Kutovaya, D. P. Zarezin, O. I. Shmatova, V. G. Nenajdenko, *European Journal of Organic Chemistry* **2019**, 2675-2681.

[183] I. V. Kutovaya, D. P. Zarezin, O. I. Shmatova, V. G. Nenajdenko, *European Journal of Organic Chemistry* **2019**, 3908-3915.

[184] F. Medda, C. Hulme, *Tetrahedron Letters* **2012**, *53*, 5593-5596.

[185] L. Mohammadkhani, M. M. Heravi, *Molecular Diversity* **2020**, *24*, 841-853.

[186] L. E. Cárdenas-Galindo, A. Islas-Jácome, C. J. Cortes-García, L. El Kaim, R. Gámez-Montaño, *Journal of the Mexican Chemical Society* **2013**, *57*, 283-289.

[187] Q. Wang, K. C. Mgimpatsang, M. Konstantinidou, S. V. Shishkina, A. Domling, *Organic Letters* **2019**, *21*, 7320-7323.

[188] S. Pathan, G. P. Singh, *Journal of Saudi Chemical Society* **2021**, *25*, 101295.

[189] P. Patil, J. Zhang, K. Kurpiewska, J. Kalinowska-Tłuścik, A. Dömling, *Synthesis* **2016**, *48*, 1122-1130.

[190] A. Boltjes, A. Shrinidhi, K. van de Kolk, E. Herdtweck, A. Dömling, *Chemistry-A European Journal* **2016**, *22*, 7352-7356.

[191] S. C. Ramírez-López, À. Rentería-Gómez, L. E. Cárdenas Galindo, R. Gámez-Montaño, *Chemistry Proceedings* **2021**, *3*, 44.

[192] Y. S. Vygodskii, O. Mel'nik, E. Kazakova, A. Shaplov, L. Komarova, V. Kizhnyaev, *Polymer Science Series B* **2008**, *50*, 193-197.

[193] P. Aleshunin, U. Dmitrieva, V. Ostrovskii, *Russian Journal of Organic Chemistry* **2011**, *47*, 1882-1888.

[194] P. Eric, in *New Polymers for Special Applications*, IntechOpen, Rijeka, **2012**, 10.

[195] A. Taden, A. H. Tait, A. Kraft, *Journal of Polymer Science Part A: Polymer Chemistry* **2002**, *40*, 4333-4343.

[196] F. M. Betzler, R. Boller, A. Grossmann, T. M. Klapötke, *Zeitschrift für Naturforschung B* **2013**, *68*, 714-718.

[197] C. G. Miller, G. K. Williams, Google Patents, **2010**.

[198] Y. Wang, H. Chen, Y. Xu, J. Sun, L. Bai, R. Qu, D. Wang, L. Yu, *Journal of Macromolecular Science, Part A* **2015**, *52*, 707-712.

[199] D. Henkensmeier, N. M. H. Duong, M. Brela, K. Dyduch, A. Michalak, K. Jankova, H. Cho, J. H. Jang, H.-J. Kim, L. N. Cleemann, Q. Li, J. O. Jensen, *Journal of Materials Chemistry A* **2015**, *3*, 14389-14400.

[200] N. Du, M. D. Guiver, Google Patents, **2014**.

[201] D. Henkensmeier, N. M. H. Duong, M. Brela, K. Dyduch, A. Michalak, K. Jankova, H. Cho, J. H. Jang, H.-J. Kim, L. N. Cleemann, *Journal of Materials Chemistry A* **2015**, *3*, 14389-14400.

[202] V. Kizhnyaev, F. Pokatilov, L. Vereshchagin, *Polymer Science Series C* **2008**, *50*, 1-21.

[203] V. N. Kizhnyaev, F. A. Pokatilov, L. I. Vereshchagin, *Polymer Science Series A* **2007**, *49*, 28-34.

[204] V. Kizhnyaev, F. Pokatilov, L. Vereshchagin, E. Krakhotkina, R. Zhitov, T. Golobokova, O. Verkhozina, *Polymer Science Series B* **2011**, *53*, 317-323.

[205] T. V. Golobokova, F. A. Pokatilov, A. G. Proidakov, L. I. Vereshchagin, V. N. Kizhnyaev, *Russian Journal of Organic Chemistry* **2013**, *49*, 130-137.

[206] F. A. Pokatilov, V. N. Kizhnyaev, R. G. Zhitov, E. A. Krakhotkina, *Russian Journal of Applied Chemistry* **2016**, *89*, 2102-2108.

[207] F. A. Pokatilov, H. V. Akamova, V. N. Kizhnyaev, *e-Polymers* **2022**, *22*, 203-213.

[208] X. Xue, J. Yang, W. Huang, H. Yang, B. Jiang, *Reactive and Functional Polymers* **2015**, *96*, 61-70.

[209] E. Dallerba, M. Massi, A. B. Lowe, *European Polymer Journal* **2020**, *126*, 109559.

[210] E. Dallerba, D. Hartnell, M. J. Hackett, M. Massi, A. B. Lowe, *Macromolecular Chemistry and Physics* **2022**, *223*, 2200021.

[211] E. Grignon, S. Y. An, A. M. Battaglia, D. S. Seferos, *Macromolecules* **2022**, *55*, 10167-10175.

[212] J. Roh, K. Vávrová, A. Hrabálek, *European Journal of Organic Chemistry* **2012**, *2012*, 6101-6118.

[213] S. M. Sproll, PhD Thesis, **2010**.

[214] T. M. Klapötke, S. M. Sproll, *Journal of Polymer Science Part A: Polymer Chemistry* **2010**, *48*, 122-127.

[215] M. K. Song, H. Li, J. Li, D. Zhao, J. Wang, M. Liu, *Advanced Materials* **2014**, *26*, 1277-1282.

[216] M. A. Gauthier, M. I. Gibson, H.-A. Klok, *Angewandte Chemie International Edition* **2009**, *48*, 48-58.

[217] A. Das, P. Theato, *Chemical Reviews* **2016**, *116*, 1434-1495.

[218] H. Gaballa, S. Lin, J. Shang, S. Meier, P. Theato, *Polymer Chemistry* **2018**, *9*, 3355-3358.

[219] P. Ferruti, A. Bettelli, A. Feré, *Polymer* **1972**, *13*, 462-464.

[220] H. G. Batz, G. Franzmann, H. Ringsdorf, *Angewandte Chemie International Edition in English* **1972**, *11*, 1103-1104.

[221] S. R. Devenish, J. B. Hill, J. W. Blunt, J. C. Morris, M. H. Munro, *Tetrahedron letters* **2006**, *47*, 2875-2878.

[222] W. Xue, H. Mutlu, H. Li, W. Wenzel, P. Theato, *Polymer Chemistry* **2021**, *12*, 2643-2650.

[223] C. Battistella, Y. Yang, J. Chen, H. A. Klok, *ACS Omega* **2018**, *3*, 9710-9721.

[224] A. Das, P. Theato, *Macromolecules* **2015**, *48*, 8695-8707.

[225] H. Zhao, W. Gu, M. W. Thielke, E. Sterner, T. Tsai, T. P. Russell, E. B. Coughlin, P. Theato, *Macromolecules* **2013**, *46*, 5195-5201.

[226] H. Son, Y. Jang, J. Koo, J.-S. Lee, P. Theato, K. Char, *Polymer Journal* **2016**, *48*, 487-495.

[227] C. E. Hoyle, C. N. Bowman, *Angewandte Chemie International Edition* **2010**, *49*, 1540-1573.

[228] H. C. Kolb, M. Finn, K. B. Sharpless, *Angewandte Chemie International Edition* **2001**, *40*, 2004-2021.

[229] A. B. Lowe, *Polymer Chemistry* **2010**, *1*, 17-36.

[230] N. B. Cramer, S. K. Reddy, A. K. O'Brien, C. N. Bowman, *Macromolecules* **2003**, *36*, 7964-7969.

[231] B. H. Northrop, R. N. Coffey, *Journal of the American Chemical Society* **2012**, *134*, 13804-13817.

[232] A. B. Lowe, *Polymer Chemistry* **2014**, *5*, 4820-4870.

[233] Y. Zhang, C. W. Chu, W. Ma, A. Takahara, *ACS Omega* **2020**, *5*, 7488-7496.

[234] C. Resetco, B. Hendriks, N. Badi, F. Du Prez, *Materials Horizons* **2017**, *4*, 1041-1053.

[235] H. Choi, M. Kim, J. Jang, S. Hong, *Angewandte Chemie International Edition* **2020**, *59*, 22514-22522.

[236] R. Zandi Shafagh, KTH Royal Institute of Technology **2019**.

[237] M. Ahangarpour, I. Kavianinia, P. W. Harris, M. A. Brimble, *Chemical Society Reviews* **2021**, *50*, 898-944.

[238] Z. Gao, Y. You, Q. Chen, M. North, H. Xie, *Green Chemistry* **2023**, *25*, 172-182.

[239] D. Sticker, R. Geczy, U. O. Hafeli, J. P. Kutter, *ACS applied materials & interfaces* **2020**, *12*, 10080-10095.

[240] V. Mishra, J. Desai, K. I. Patel, *Journal of Coatings Technology and Research* **2017**, *14*, 1069-1081.

[241] L. Infante Teixeira, K. Landfester, H. Thérien-Aubin, *Macromolecules* **2021**, *54*, 3659-3667.

[242] J. M. Sarapas, G. N. Tew, *Macromolecules* **2016**, *49*, 1154-1162.

[243] O. Okay, S. K. Reddy, C. N. Bowman, *Macromolecules* **2005**, *38*, 4501-4511.

[244] B. Tieke, *Makromolekulare Chemie: Eine Einführung*, John Wiley & Sons, **2014**.

[245] J. K. Stille, *Journal of Chemical Education* **1981**, *58*, 862.

[246] S. K. Gupta, A. Kumar, *Reaction engineering of step growth polymerization*, Springer Science & Business Media, **2012**.

[247] S. Wang, N. Zhang, X. Ge, Y. Wan, X. Li, L. Yan, Y. Xia, B. Song, *Soft Matter* **2014**, *10*, 4833-4839.

[248] B.-B. Sun, K. Liu, Q. Gao, W. Fang, S. Lu, C. R. Wang, C. Z. Yao, H. Q. Cao, J. Yu, *Nature Communications* **2022**, *13*, 7065.

[249] K. Król-Morkisz, K. Pielichowska, in *Polymer composites with functionalized nanoparticles*, Elsevier, **2019**, 405-435.

[250] S. Rahmatkhah, S. Mehdipour-Ataei, *International Journal of Polymer Analysis and Characterization* **2022**, *27*, 87-98.

[251] C. Berti, A. Celli, P. Marchese, E. Marianucci, G. Barbiroli, F. D. Credico, *e-Polymers* **2007**, *7*, 057.

[252] D. T. Tran, A. Gumyusenge, X. Luo, M. Roders, Z. Yi, A. L. Ayzner, J. Mei, *ACS Applied Polymer Materials* **2019**, *2*, 91-97.

[253] E. K. Riga, J. S. Saar, R. Erath, M. Hechenbichler, K. Lienkamp, *Polymers* **2017**, *9*, 686.

[254] G. T. Sukhanov, K. K. Bosov, Y. V. Filippova, A. G. Sukhanova, I. A. Krupnova, E. V. Pivovarova, *Materials* **2022**, *15*, 6936.

[255] Y. Jin, M. Joshi, T. Araki, N. Kamimura, E. Masai, M. Nakamura, T. Michinobu, *Polymers* **2023**, *15*, 1349.

[256] K. Sykam, S. Donempudi, P. Basak, *Journal of Applied Polymer Science* **2022**, *139*, e52771.

[257] Z. Qian, S. Luo, T. Qu, L. A. Galuska, S. Zhang, Z. Cao, S. Dhakal, Y. He, K. Hong, D. Zhou, *Journal of Materials Research* **2021**, *36*, 191-202.

[258] G. N. Kangovi, S. Lee, *Macromolecules* **2017**, *50*, 8678-8687.

[259] H. Jacobson, C. O. Beckmann, W. H. Stockmayer, *The Journal of chemical physics* **1950**, *18*, 1607-1612.

[260] C. Shang, Y. Zhao, J. Long, Y. Ji, H. Wang, *Journal of Materials Chemistry C* **2020**, *8*, 1017-1024.

[261] L. Yang, L. Wang, C. Cui, J. Lei, J. Zhang, *Chemical Communications* **2016**, *52*, 6154-6157.

[262] X. Zhou, W. Luo, H. Nie, L. Xu, R. Hu, Z. Zhao, A. Qin, B. Z. Tang, *Journal of Materials Chemistry C* **2017**, *5*, 4775-4779.

[263] E. Zakerzadeh, R. Salehi, M. Mahkam, *Drug Development and Industrial Pharmacy* **2017**, *43*, 1963-1977.

[264] N. V. Tsarevsky, K. V. Bernaerts, B. Dufour, F. E. Du Prez, K. Matyjaszewski, *Macromolecules* **2004**, *37*, 9308-9313.

[265] T. M. Klapötke, S. M. Sproll, *Journal of Polymer Science Part A: Polymer Chemistry* **2010**, *48*, 122-127.

[266] M.-R. Huang, X. G. Li, S. X. Li, W. Zhang, *Reactive and Functional Polymers* **2004**, *59*, 53-61.

[267] A. Maleki, A. Sarvary, **2015**.

[268] W. Feng, L. Li, C. Yang, A. Welle, O. Trapp, P. A. Levkin, *Angewandte Chemie* **2015**, *127*, 8856-8859.

[269] T. Saegusa, S. Kobayashi, Y. Ito, *The Journal of Organic Chemistry* **1970**, *35*, 2118-2121.

[270] K. Singh, S. Sharma, *Tetrahedron letters* **2017**, *58*, 197-201.

[271] A. Barthelon, L. El Kaïm, M. Gizolme, L. Grimaud, Wiley Online Library, **2008**.

[272] H. R. Kricheldorf, *Macromolecular Rapid Communications* **2008**, *29*, 1695-1704.

[273] T. Endo, T. Higashihara, *ACS omega* **2022**, *7*, 8753-8758.

[274] S. M. Weidner, H. R. Kricheldorf, F. Scheliga, *Journal of Polymer Science Part A: Polymer Chemistry* **2016**, *54*, 197-208.

[275] H. R. Kricheldorf, S. M. Weidner, F. Scheliga, in *Macromolecular Symposia, 375*, Wiley Online Library, **2017**, 1600169.

[276] S. Levchik, O. Ivashkevich, L. Costa, P. Gaponik, T. Andreeva, *Polymer Degradation and Stability* **1994**, *46*, 225-234.

[277] V. N. Kizhnyaev, F. A. Pokatilov, A. I. Shabalin, R. G. Zhitov, *e-Polymers* **2019**, *19*, 421-429.

[278] E. Dallerba, Curtin University **2021**.

[279] E. A. Popova, R. E. Trifonov, V. A. Ostrovskii, *Online Journal of Organic Chemistry* **2012**.

[280] X. Guo, D. Xu, H. Yuan, Q. Luo, S. Tang, L. Liu, Y. Wu, *Journal of Materials Chemistry A* **2019**, *7*, 27081-27088.

[281] H. Ehtesabi, S. Roshani, Z. Bagheri, M. Yaghoubi-Avini, *Journal of Environmental Chemical Engineering* **2019**, *7*, 103419.

[282] N. Mehwish, X. Dou, Y. Zhao, C.-L. Feng, *Materials Horizons* **2019**, *6*, 14-44.

[283] W. Zhou, Z. Hu, J. Wei, H. Dai, Y. Chen, S. Liu, Z. Duan, F. Xie, W. Zhang, R. Guo, *Chinese Chemical Letters* **2022**, *33*, 1245-1253.

[284] Y. Xu, M. Yang, Q. Ma, X. Di, G. Wu, *New Journal of Chemistry* **2021**, *45*, 3079-3087.

[285] W. Xue, Karlsruher Institut für Technologie (KIT) (10.5445/IR/1000127436), **2020**.

[286] P. Theato, *Journal of Polymer Science Part A: Polymer Chemistry* **2008**, *46*, 6677-6687.

[287] W. Xue, H. Mutlu, P. Theato, *European Polymer Journal* **2020**, *130*, 109660.

[288] K. Nilles, P. Theato, *Polymer Chemistry* **2011**, *2*, 376-384.

[289] C. Guhrenz, A. Wolf, M. Adam, L. Sonntag, S. V. Voitekhovich, S. Kaskel, N. Gaponik, A. Eychmüller, *Zeitschrift für Physikalische Chemie* **2017**, *231*, 51-62.

[290] J. Zhang, B. Jin, Y. Song, W. Hao, J. Huang, J. Guo, T. Huang, Z. Guo, R. Peng, *Langmuir* **2021**, *37*, 7118-7126.

[291] H. Huang, J. Zhang, T. Zhang, S. Zhang, *Journal of Wuhan University of Technology-Mater. Sci. Ed.* **2014**, *29*, 488-491.

[292] M. Dharmarwardana, B. M. Otten, M. M. Ghimire, B. S. Arimilli, C. M. Williams, S. Boateng, Z. Lu, G. T. McCandless, J. J. Gassensmith, M. A. Omary, *Proceedings of the National Academy of Sciences* **2021**, *118*, e2106572118.

[293] S. Levchik, A. Balabanovich, O. Ivashkevich, P. Gaponik, L. Costa, *Polymer degradation and stability* **1995**, *47*, 333-338.

[294] M. Suhail, I. H. Chiu, I. L. Lin, M. J. Tsai, P. C. Wu, *Micro, 3*, **2023**, 578-590.

[295] H. Kiuchi, W. Kai, Y. Inoue, *Journal of Applied Polymer Science* **2008**, *107*, 3823-3830.

[296] F. Carrasco, O. Santana Pérez, N. León Albiter, M. L. Maspoch, *Polymers* **2022**, *15*, 105.

[297] R. De Coen, N. Vanparijs, M. D. P. Risseeuw, L. Lybaert, B. Louage, S. De Koker, V. Kumar, J. Grooten, L. Taylor, N. Ayres, S. Van Calenbergh, L. Nuhn, B. G. De Geest, *Biomacromolecules* **2016**, *17*, 2479-2488.

8 Appendix

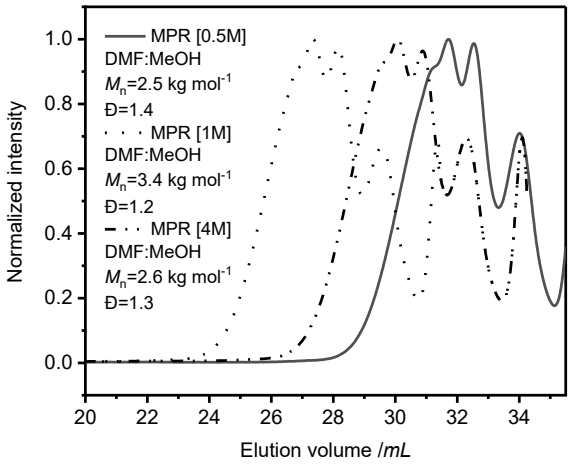

Figure 8. 1 Comparative SEC diagram of concentration optimization studies of model polymerization reaction (MPR) *via* UA-4MCR.

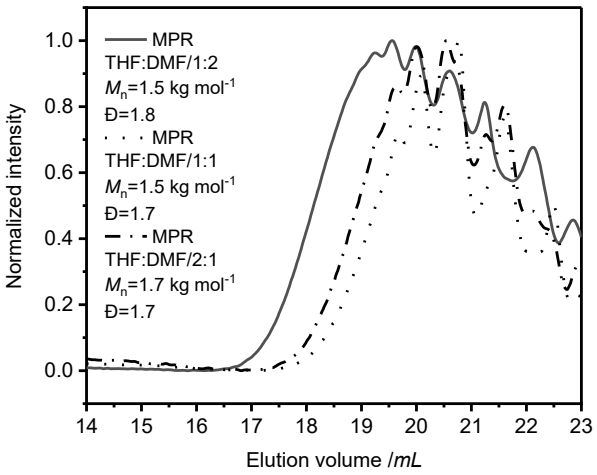

Figure 8. 2 Comparative SEC diagram of solvent optimization studies of model polymerization reaction (MPR) *via* UA-4MCR in THF: DMF mixture.

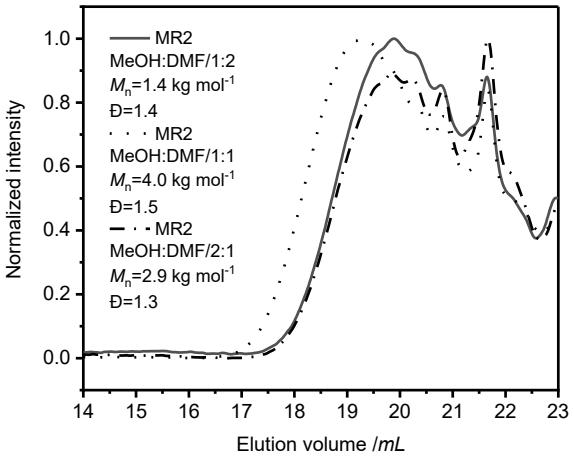

Figure 8. 3 Comparative SEC diagram of concentration optimization studies of model reaction (MPR) *via* UA-4MCR in MeOH: DMF mixture.

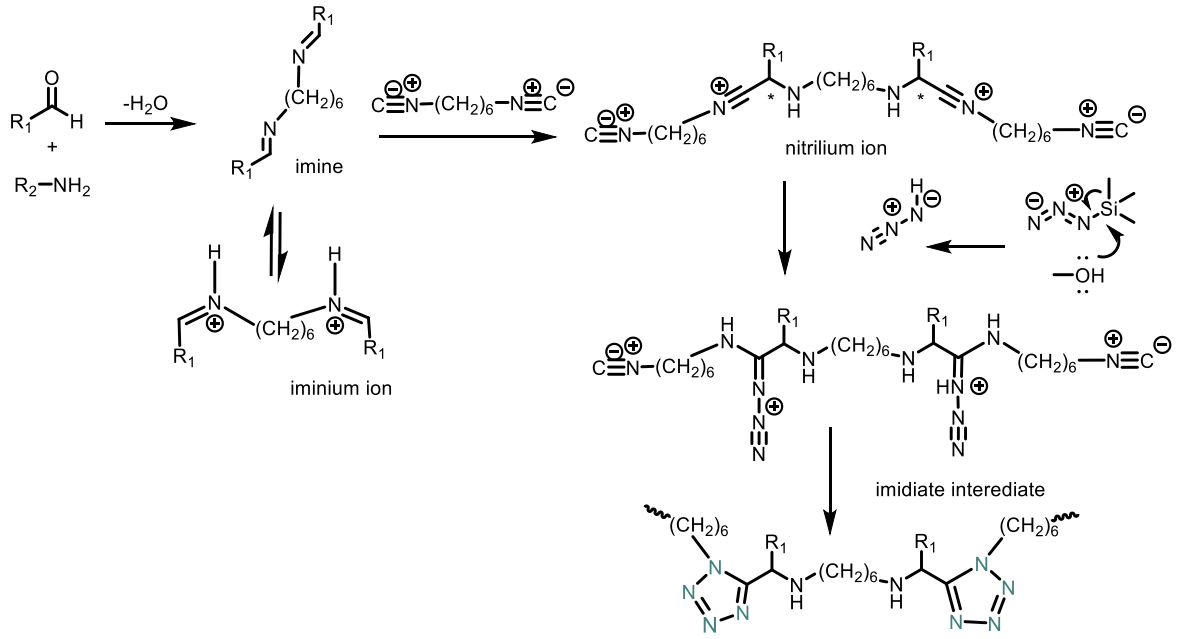

Figure 8. 4 Estimated mechanism of the reaction of Ugi-azide four-multicomponent reaction (UA-4MCR); In the initially step, the iminium-ion is formed by a reaction between an aldehyde with a secondary amine. Upon the formation of an iminium-ion, the isocyanide reacts as a nucleophilic reaction partner and undergoes an addition reaction on the charged side of the iminium ion. Thereby a further charged intermediate is generated, which undergoes an addition with the formed hydrazoic acid. The last step of the reaction is the ring-forming step which delivers 1,5 DSTs**.**

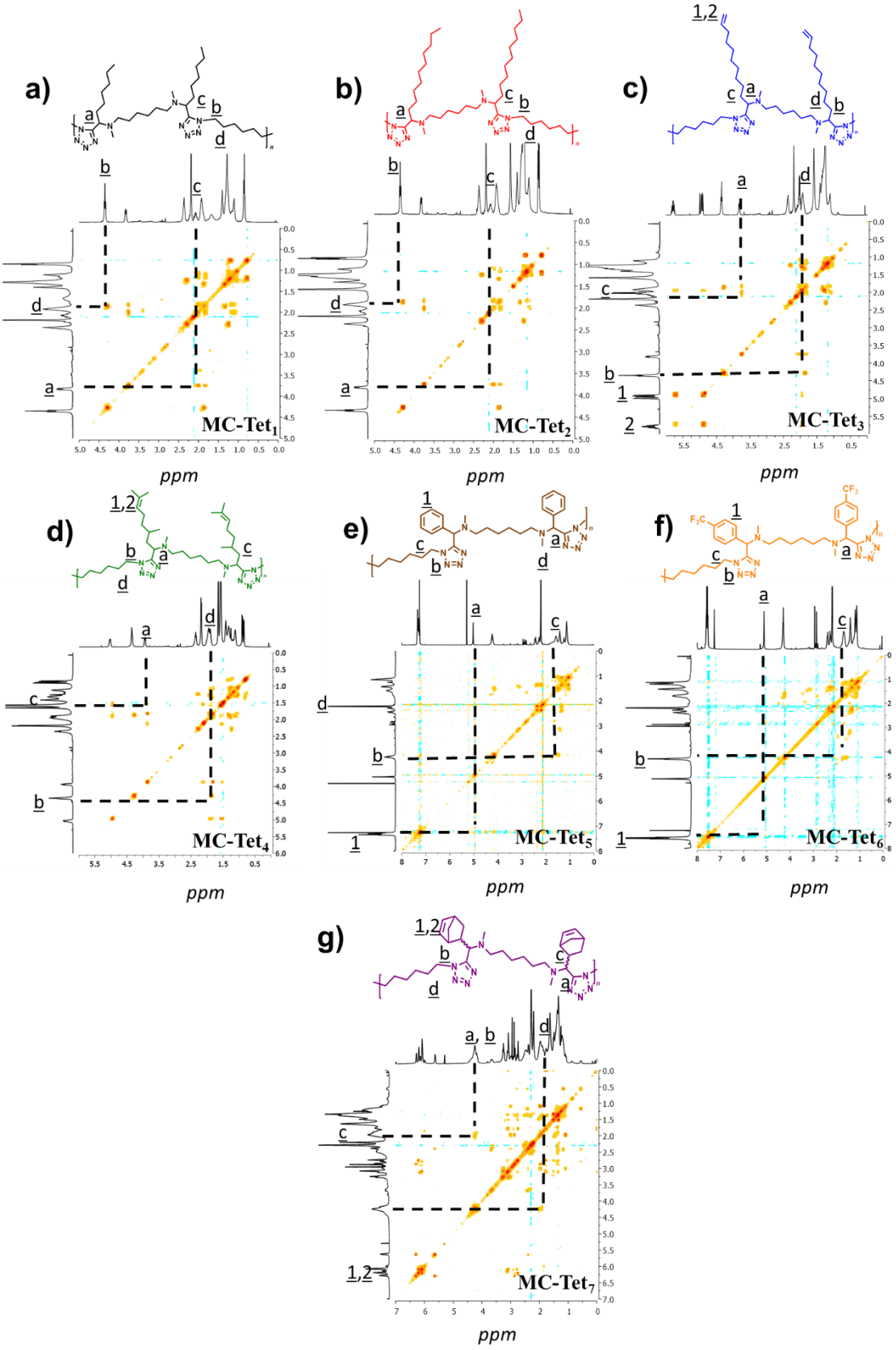

Figure 8. 5 COSY-NMR ($CDCl_3$, 400 MHz) spectrum of a) MC-Tet_1 (black), b) MC-Tet_2 (red), c) MC-Tet_3 (blue), c) MC-Tet_4 (green), c) MC-Tet_5 (brown), c) MC-Tet_6 (orange), c) MC-Tet_7 (purple

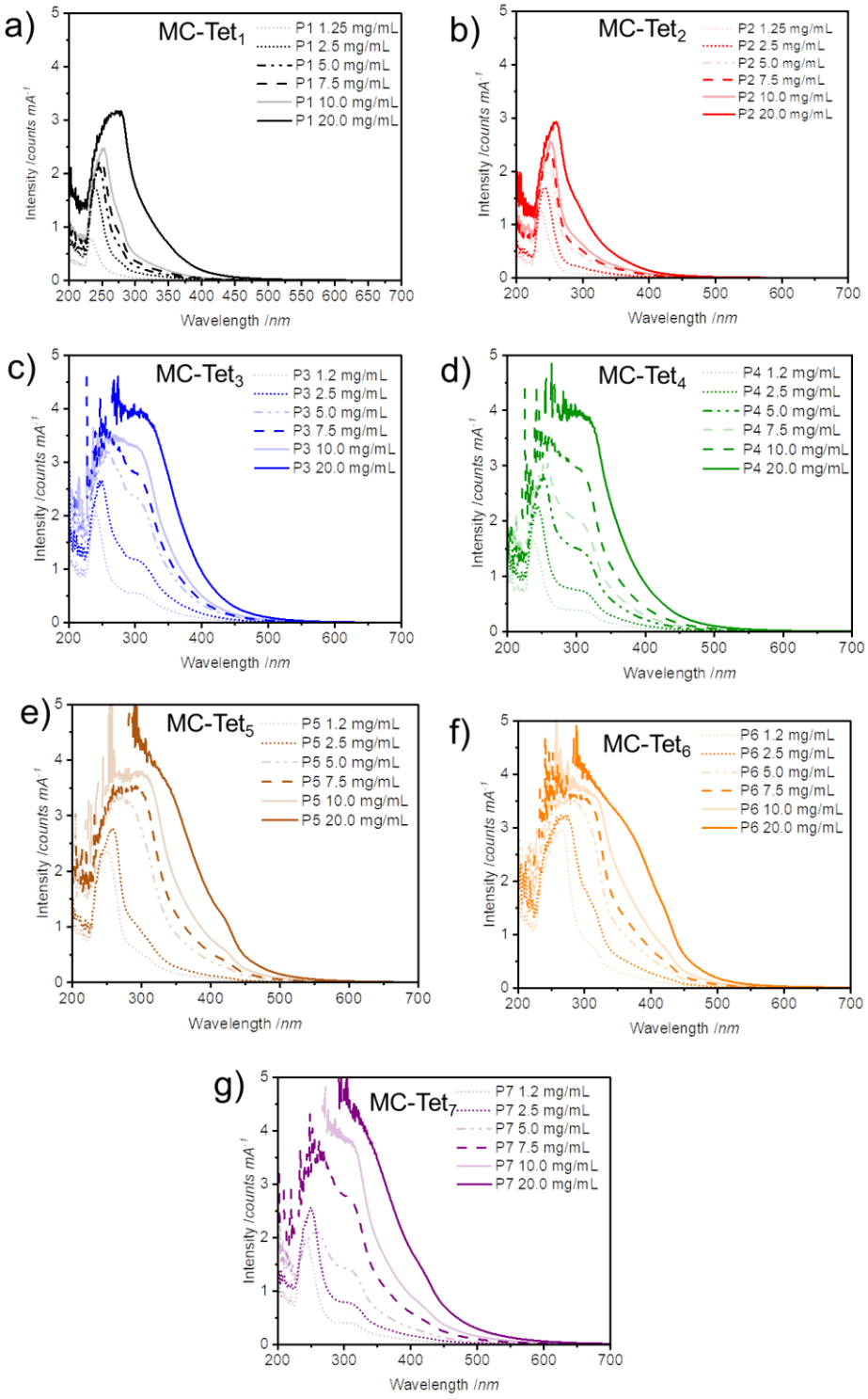

Figure 8. 6 Absorption spectra of a) MC-Tet$_1$ (black), b) MC-Tet$_2$ (red), c) MC-Tet$_3$ (blue), c) MC-Tet$_4$ (green), c) MC-Tet$_5$ (brown), c) MC-Tet$_6$ (orange), c) MC-Tet$_7$ (purple).

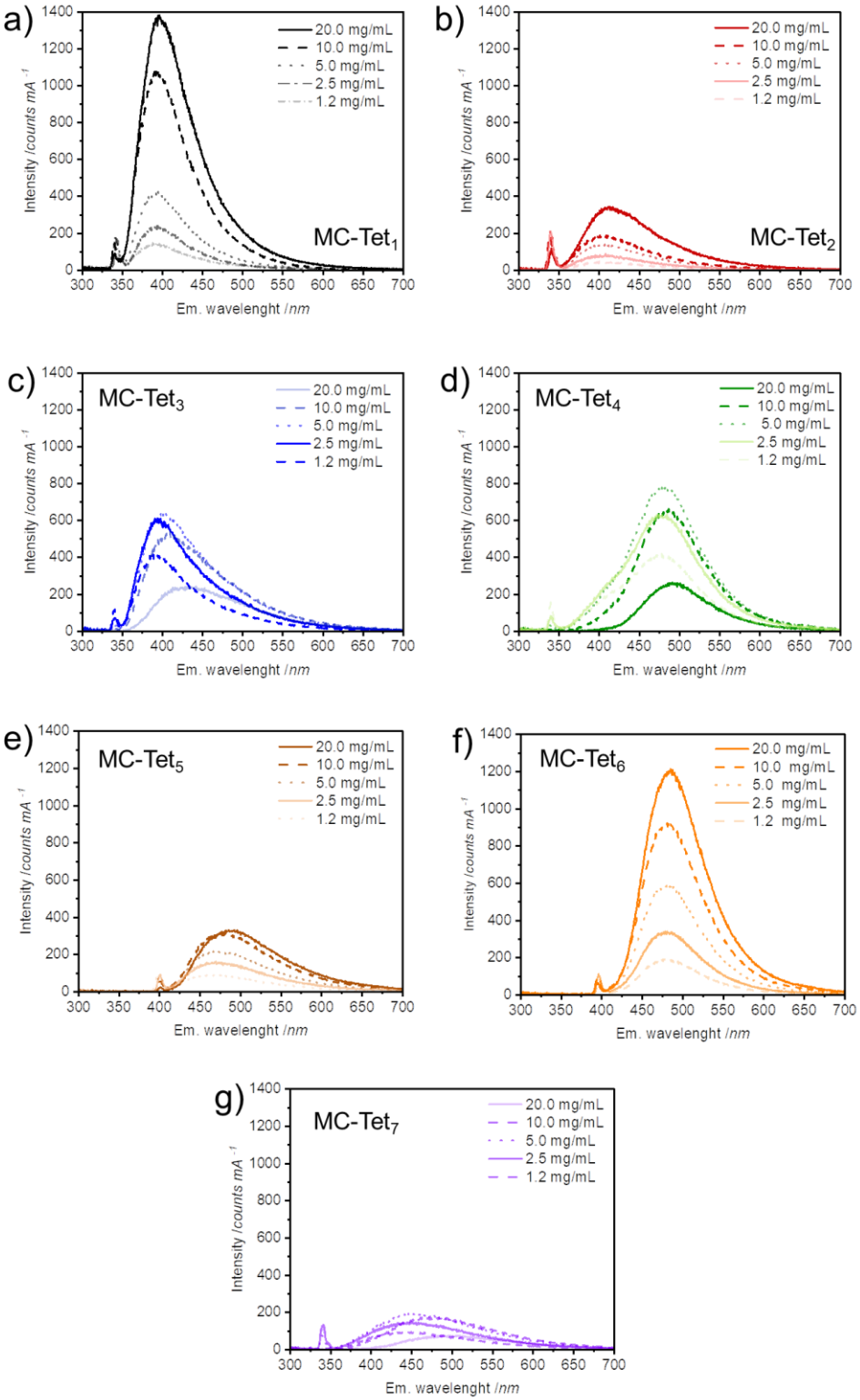

Figure 8. 7 Emission spectra of a) MC-Tet$_1$ (black), b) MC-Tet$_2$ (red), c) MC-Tet$_3$ (blue), c) MC-Tet$_4$ (green), c) MC-Tet$_5$ (brown), c) MC-Tet$_6$ (orange), c) MC-Tet$_7$ (purple).

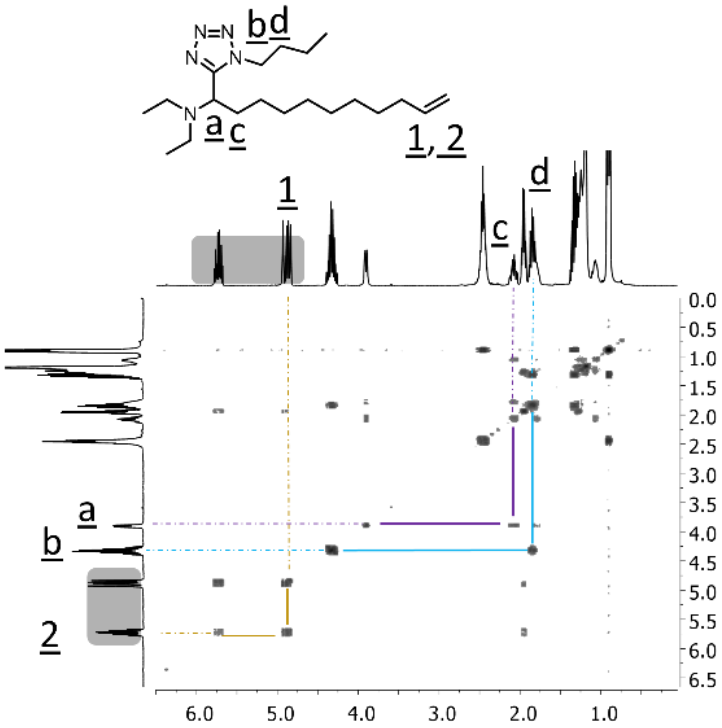

Figure 10. 8 COSY-NMR ($CDCl_3$, 400 MHz) spectra of model compound (MC) synthesized *via* UA-4MCR**.**

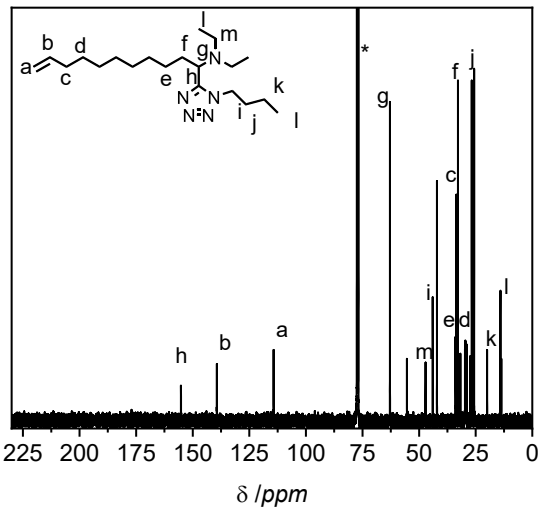

Figure 8. 9 ^{13}C NMR ($CDCl_3$, 400 MHz) spectra of model compound (MC) synthesized *via* UA-4MCR**.**

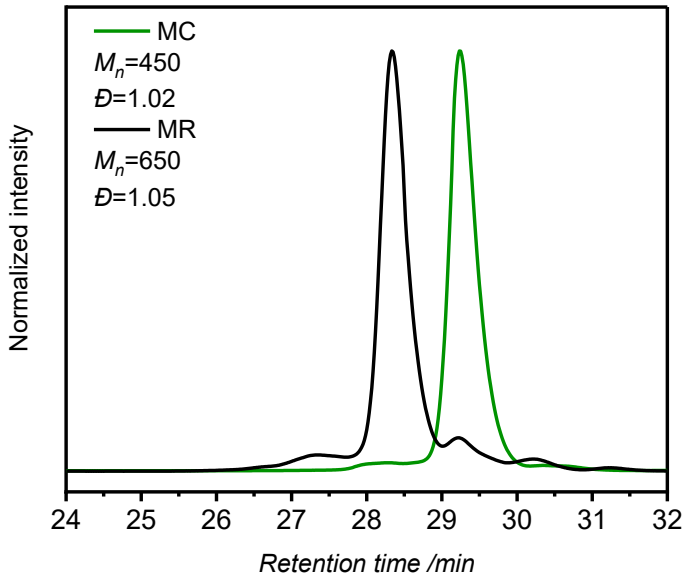

Figure 8. 10 Comparative SEC traces of model compound (MC) and model reaction (MR).

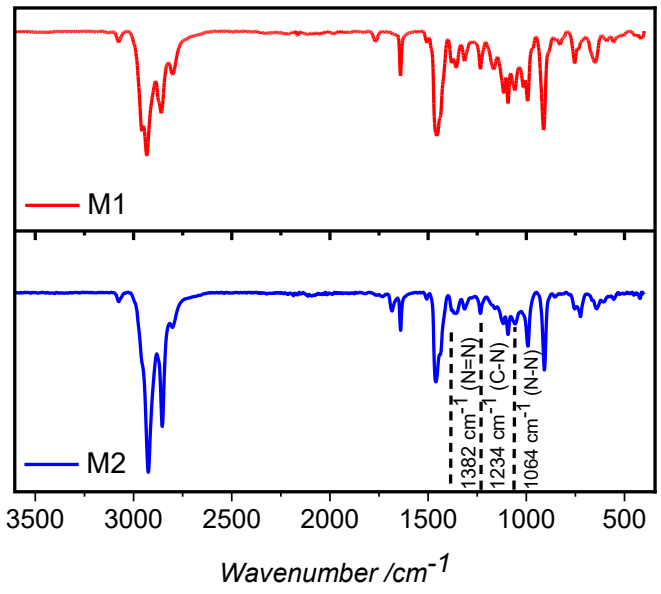

Figure 8. 11 ATR-IR spectra of ω-diene monomers M1 and M2.

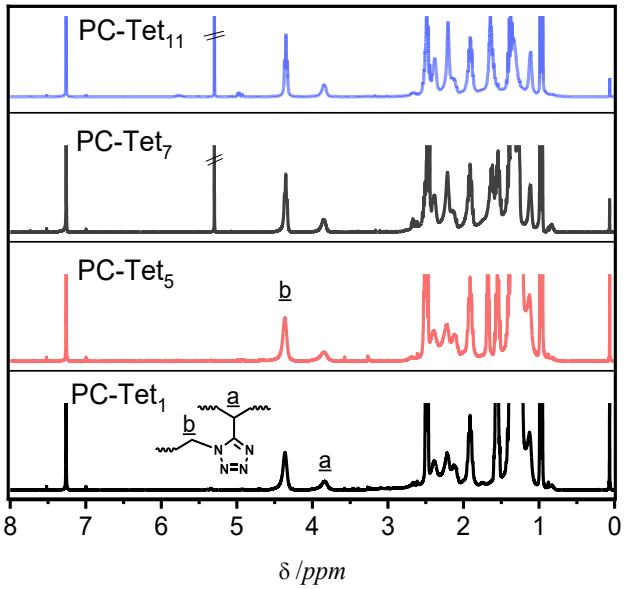

Figure 8. 12 Comparative ^{1}H NMR ($CDCl_3$, 400 MHz) spectra of PC-Tet_1, PC-Tet_5, PC-Tet_7 and PC-Tet_{11}.

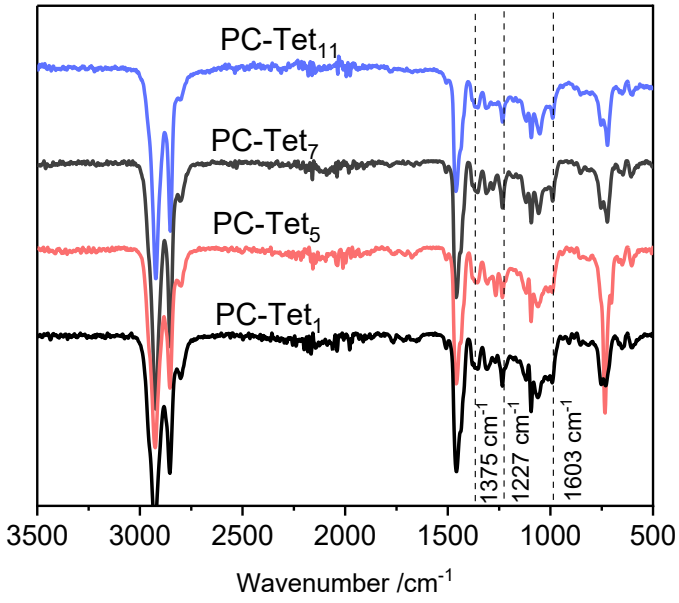

Figure 8. 13 ATR-IR spectra of PC-Tet_1, PC-Tet_5, PC-Tet_7 and PC-Tet_{11}.

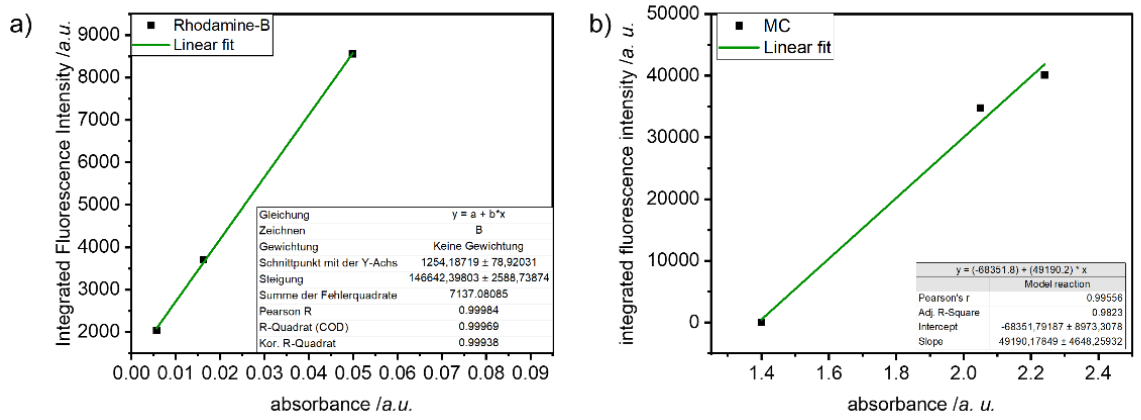

Figure 10. 14 a) Linear plot of Rhodamine-B as reference for quantum yield (QY) determination, b) Linear plot of model reaction (MR) for quantum yield (QY) determination.

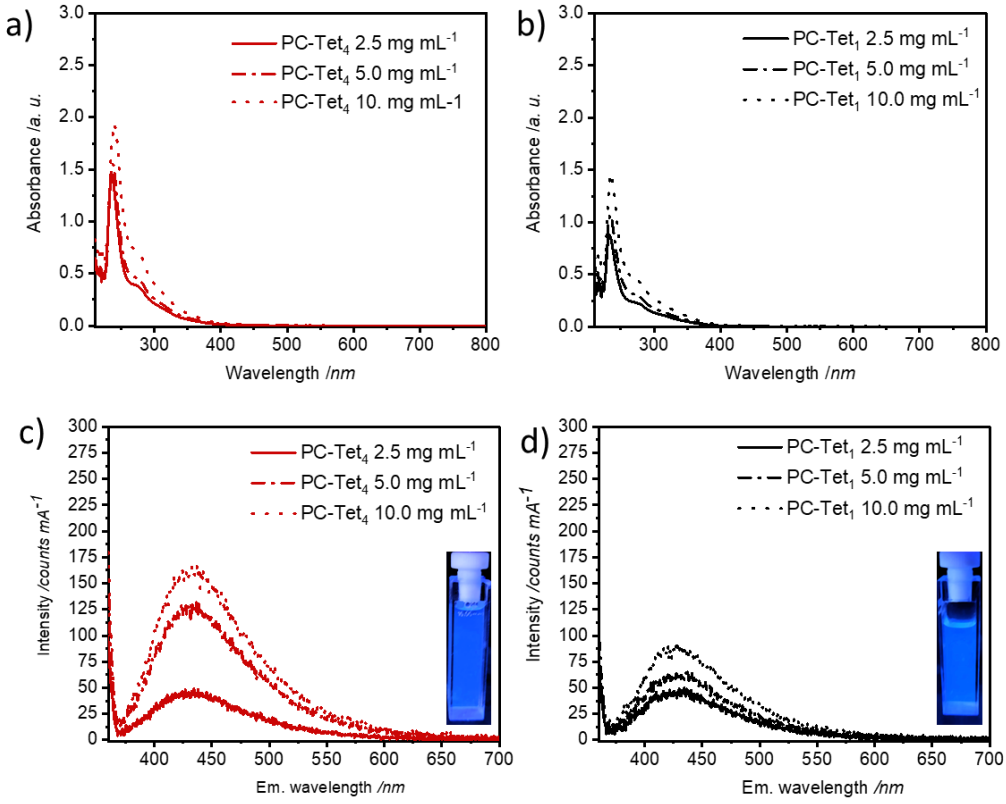

Figure 8. 15 a, b) Absorption, c, d) emission (λ_{ex}=355 nm) traces of PC-Tet$_1$ and PC-Tet$_4$, respectively, at different concentrations in DCM**.**

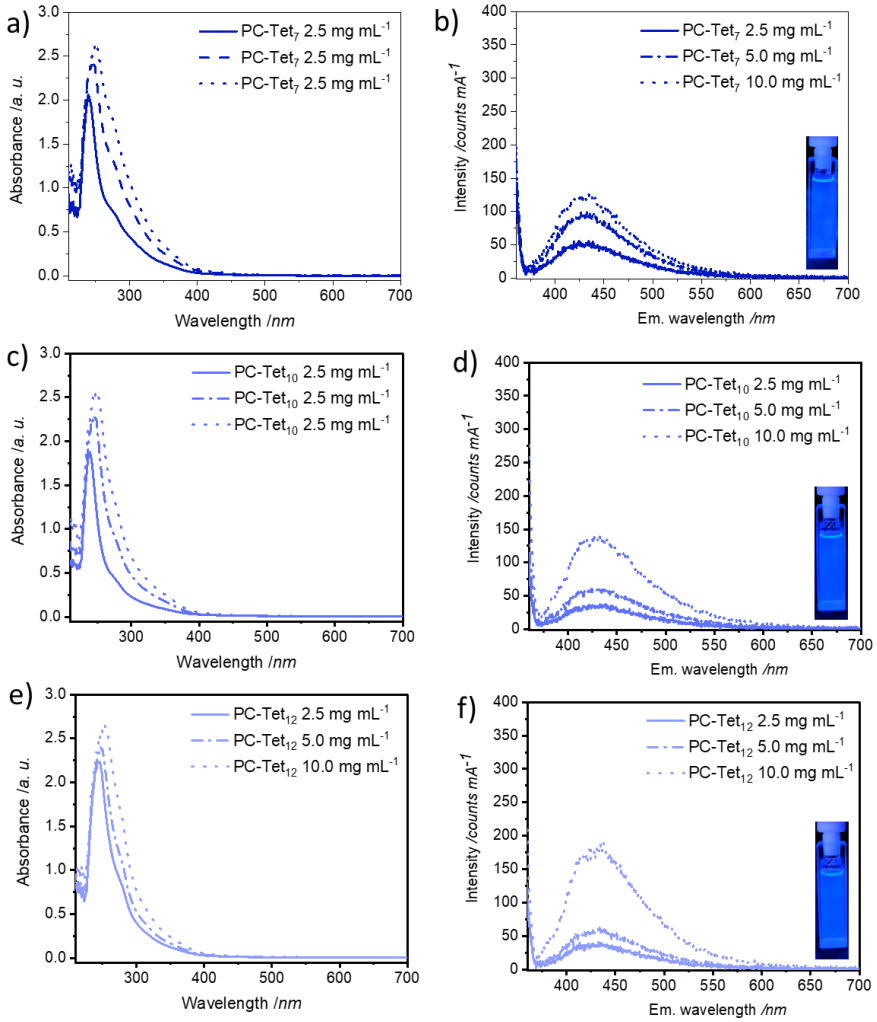

Figure 8. 16 a, c, e) Absorption, b, d, f) emission (λ_{ex}=355 nm) traces of PC-Tet$_7$, PC-Tet$_{10}$ and PC-Tet$_{12}$, respectively, at different concentrations in DCM.

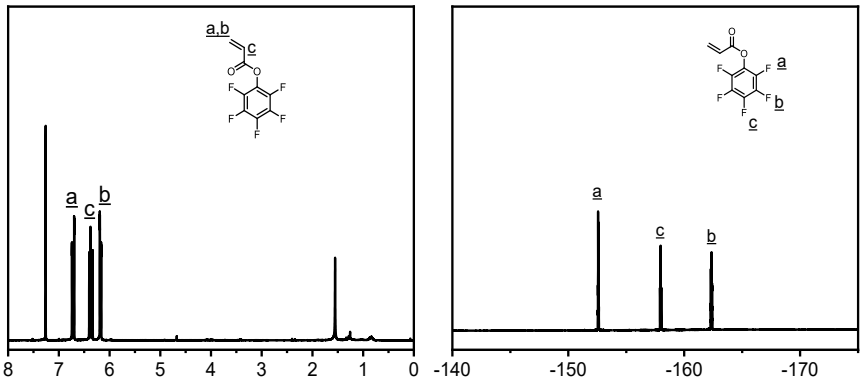

Figure 8. 17 ^{13}C-NMR ($CDCl_3$, 400 MHz (left) and ^{19}F-NMR (right) of pentafluorophenyl acrylate (PPFPA) monomer**.**

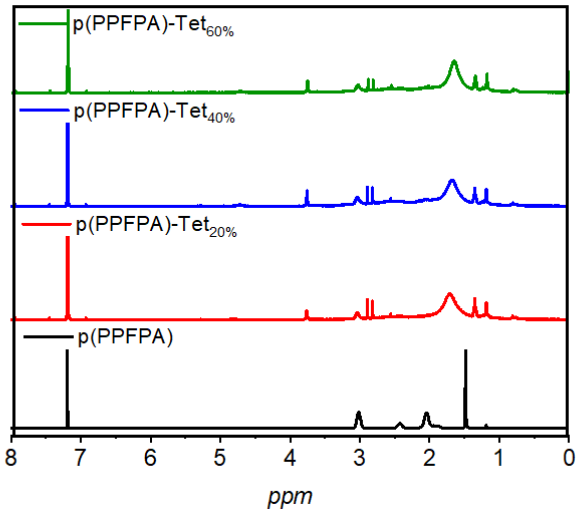

Figure 8. 18 ^{1}H-NMR ($CDCl_3$: d_6-DMF, 400 MHz) of p(PFPA) polymers with different degrees of 1,5 DST-decorated.

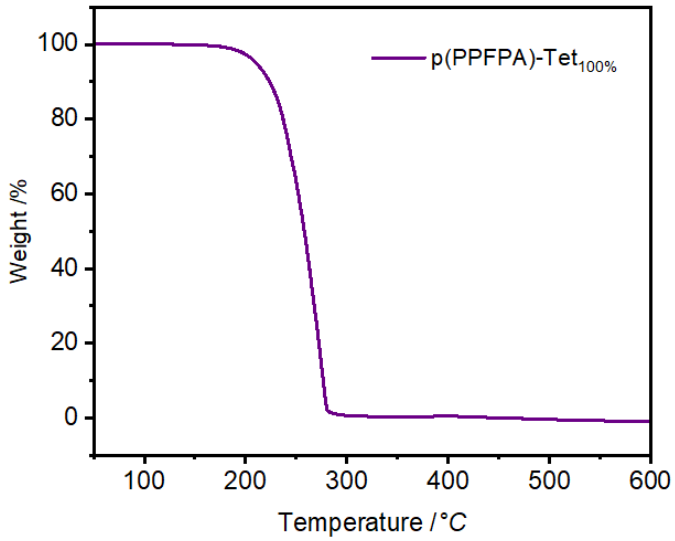

Figure 8. 19 TGA trace of p(PFPA) polymer with 100% modification with 1,5 DST moiety.

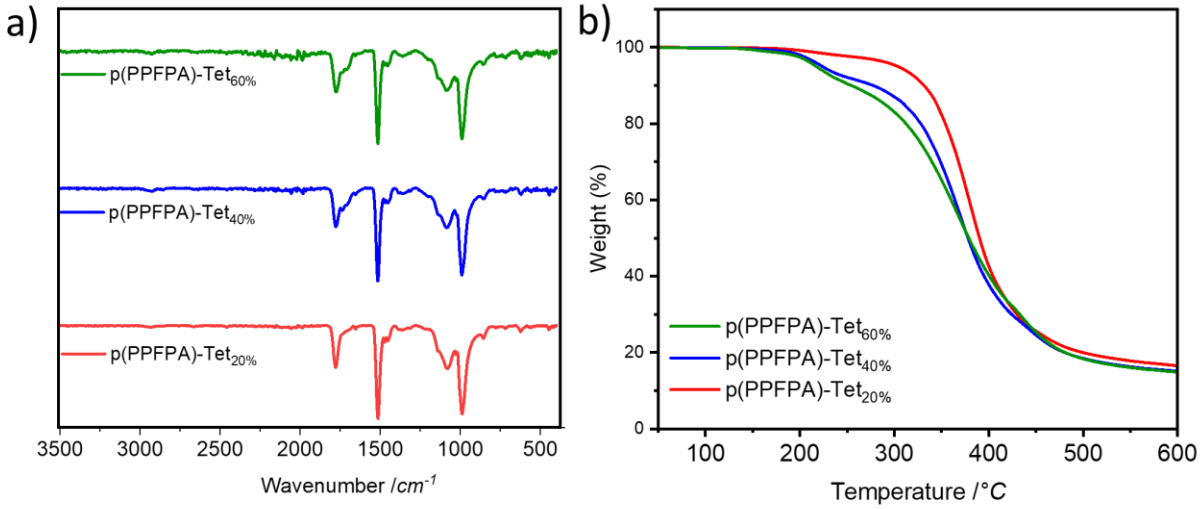

Figure 8. 20 Comparative: a) ATIR-IR spectra, and b) TGA traces of p(PFPA) polymers with different degree of 1,5 DST modification after drying 100 °C for four hour and 60 °C for overnight, respectively.

Table 8. 1. Absorbance and emission wavelength shifts of MC-Tet$_1$- MC-Tet$_7$ at different concentrations

Polymer	Absorbance shifts (nm)						Emission shifts (nm)				
	*Concentration (mg/mL)						Concentration (mg/mL)				
	1.2*	2.5*	5.0*	7.5*	10.0*	20.0*	1.2*	2.5*	5.0*	10.0*	20.0*
MC-Tet$_1$	233	242	250	252	253	272	388	389	391	395	398
MC-Tet$_2$	235	241	247	250	251	260	384	387	392	406	410
MC-Tet$_3$	242/309	247/313	257/334	259/-	289/-	309/-	386	393	404	408	419
MC-Tet$_4$	236/309	243/311	253/316	258/-	268/-	312/-	470	474	481	488	490
MC-Tet$_5$	251/297	257/304	272/-	292/-	303/-	313/-	460	464	468	475	480
MC-Tet$_6$	265/312	273/322	282/-	295/-	305/-	315/-	472	476	477	481	483
MC-Tet$_7$	242/307	250/315	261/318	266/318	311/-	317/-	428	431	443	455	498

Abbreviations

1,5 DST	1,5 disubstituted tetrazole
2,5 DST	2,5 disubstituted tetrazole
AIBN	Azobisisobutyronitrile
ATR-IR	Attenuated total reflectance infrared spectroscopy
BFE	Bond forming efficiency
CFM	Confocal fluoresce microscopy
CTE	Cluster-triggered emission
DBU	1,8-diazabicyclo(5.4.0)undec-7-ene
DCM	Dichloromethane
DMAP	4-Dimethylaminopyridine
DMF	Dimethylformamide
DMSO	Dimethyl sulfoxide
DSC	Differential scanning calorimetry
DT1	1,4-butanedithiol
DT2	1,6-hexanedithiol
DT3	1,8-octanedithiol
DT4	1,9-nonanedithiol
DT5	Dithiothreitol
DT6	3,6-dioxa-1,8-octanedithiol
GABA	Gamma-aminobutyric acid
HCl	Hydrochloric acid
HIV	Human immunodeficiency virus
HOMO	Highest occupied molecular orbital
IMCR	Isocyanide-based multi component reaction

LUMO	Lowest unoccupied molecular orbital
MC	Model compound
MCR	Multi-component reaction
MeCN	Acetonitrile
MeOH	Methanol
M_n	Molecular weight
MPR	Model polymerization reaction
MR	Model reaction
N_2	Nitrogen
NAD(P)H	Nicotinamide adenine dinucleotide phosphate
NHS	*N*-hydroxysuccinimide
NMP	*N*-methyl pyrrolidone
NMR	Nuclear magnetic resonance
OLEDs	Organic light-emitting diodes
p(PFPMA)	Poly(pentafluorophenyl methylacrylate
p(PFPA)	Poly(pentafluorophenyl acrylate)
P-3CR	Passerini three-component reaction
PFP	Pentafluorophenyl
PFSR	Para-fluoro substitution reaction
PFTR	Para-fluoro-thiol reaction
PMI	Process mass intensification
PNAS	Poly(*N*-hydroxysuccinimide acrylate)
PNMAS	Poly(*N*-hydroxysuccinimide methacrylate)
PPM	Post-polymerization modification
PVC	Polyvinylchloride

PVT	Polyvinyl tetrazole
QA	Quaternary ammonium
RAFT	Reversible addition fragmentation chain transfer
SEC	Size-exclusion chromatography
SEM	Scanning electron microscopy
T_c	Crystallization temperatures
T_d	Thermal degradation temperature
TEA	Triethylamine
TGA	Thermogravimetric analysis
THF	Tetrahydrofuran
T_m	Melting points
$TMSN_3$	Azidotrimethylsilane
TsCN	p-toluenesulfonyl cyanide
U-4CR	Ugi four-component reaction
UA-3MCR	Ugi-Azide three-component reaction
UA-4MCP	Ugi- azide four- multicomponent polymerization
UA-4MCR	Ugi- azide four- multicomponent reaction
UA-5MCR	Ugi-azide five-component reaction
UA-6MCR	Ugi-azide six-component reaction
UA-7MCR	Ugi-azide seven-component reaction
Ugi-MCR	Ugi-multicomponent reaction
UV-Vis	Ultraviolet-visibl

List of Schemes, Figures and Tables

List of Schemes

List of Figures

List of Tables

Acknowledgement

It's almost unbelievable that I've reached the end of an endless journey towards becoming a “Dr.”. I remember the day I took a daring step from bioengineering into the world of polymer chemistry. Against all odds, I adapted to polymer chemistry and came to genuinely appreciate and somehow love it. Of course, I can't forget those who have supported me on this journey.

Foremost, I want to express my appreciation to Prof. Dr. Patrick Theato for allowing me to join his research group. You have supported and assisted me during my research journey, offering guidance and understanding throughout my PhD experience. I am immensely thankful for the motivation, respect and flexibility that propelled me to successfully complete my Ph.D. In various aspects, I have gained a wealth of knowledge from your teachings, Prof. Theato. Thank you very much for all.

Of course, my biggest thanks go to Jun. Prof. Dr. Hatice Mutlu. When I think back to the journey we started together, I am unable to fully talk about the impact you've had on me. Your meaningful contributions have left a lasting mark on my academic growth and personal development, greatly influencing the course of my future. I want to express my deep gratitude for your constant support during times of need, for presenting and teaching projects that continuously expand my horizons, for your dedication in helping me complete my doctoral studies, and for the unwavering commitment you've shown in offering valuable opportunities. Without your encouragement and supervision, this work would not have succeeded. I am deeply grateful for all your contributions to my life.

Furthermore, Dear Dr. Marina Simian, I'm thankful for the opportunities you've provided by supporting my thesis financially. Your consistent presence and assurance of support throughout this journey have been a great source of confidence for me. I also sincerely appreciate the positive impressions you've left on me. I look forward to reconnecting in the future. Additionally, I express my infinite gratitude to Prof. Dr. Guillaume Delaittre for trusting me and initiating my doctoral adventure in Karlsruhe. Lastly, I express my appreciation to Dr. Ljijana Fruk, someone I greatly admire, for allowing me to join her working group. This opportunity has allowed me to gain diverse insights. Thank you very much for all.

Besides my advisors, Dear Birgit Huber, I was fortunate to have you along my journey. You've consistently been by my side whenever I faced “little problems” (hahahha:). Your presence was a constant whenever I required guidance from an “adultier adult” :). Through our deep conversations, shared laughter, and the rollercoaster of emotions, your endless support was a cornerstone. I sincerely appreciate your presence. I'm thankful to you for contributing enjoyment

to my workspace and your humorous encouragement during tough times. In truth, this thesis would never have reached its conclusion without your indispensable contributions. You are my hero!

My special thanks go to Dr. Dominik Voll and Dr. Christian Schmitt. Even though we may not engage frequently, you have consistently been there for me whenever I required assistance, whether related to my studies or personal matters. I want to express my appreciation for your support. Furthermore, I want to thank Katharina Kuppinger and Bärbel Seufert-Dausmann. They have consistently been exceptionally generous in assisting me with chemical management and navigating bureaucratic hurdles. I am genuinely thankful for their invaluable support.

I want to express my deep appreciation to the funding providers for my PhD with the UNSAM-KIT (SPUK) (43.32.01, PoF) project. Additionally, I am grateful for the continuous support I received from the Karlsruhe House of Young Scientists (KHYS) (KIT), which included emergency funding scholarships and research travel grants during the concluding stage of my Ph.D.

Yunji…Thanks for being a perfect human being and my friend, as you are always there beside me no matter what goes wrong. I enjoy every single day working with you. We cooked, ate, appreciated, and enlightened each other a lot…thanks for everything. As we work on our thesis together daily and sing with you, “Seasons, they will change, Life will make you grow, Dreams will make you cry, cry, cry, Everything is temporary, Everything will slide, Love will never die, die, die, I know that, ooh, birds fly in different directions, Ooh, I hope to see you again” …

Oh, Daniel…My big boss:). I somehow appreciated everything you did for me:). Thanks once again for your “kind” :) support during my journey in KIT. Ja ja, we know “you are perfect:),” but let me say again how much I enjoyed meeting someone like you, who has a brilliant mind and a kind heart. Please, Dani, do not continue learning Turkish to avoid potential future problems. :) And, Martina, my second boss:), it was significant collaborating with you. I want to express my heartfelt gratitude for all your valuable contributions to shaping my thesis. Hence, I extend an exceptional thank to you. Thanks for being very kind to me; thank you very much for being in my life!

Members of the Soft Matter Lab team, my fantastic support network! Jan, Timo, Philipp...You all have my deepest gratitude for coming into my life. Each of you is truly remarkable. We sometimes experienced days where work slipped our minds due to "scientific challenges." ;) I don't really miss those days, but I truly miss all of you. Jan and Timo, your support in all aspects means the world to me. Philipp, we share a common destiny when it comes to working on tetrazoles. I apologize for getting your hands dirty:), but I have full faith in your ability to handle anything. Thank you for your assistance and everything you've done for me! Furthermore, I'd

like to convey my appreciation to Dr. Patrick Hodapp for consistently offering his assistance whenever I require it.

Vaishali, Isabella, Victoria and Johannes…It was my pleasure to meet you guys. I want you to know how much I value your support. Isabella, it was an absolute honour being a colleague with you, and I am sure we will never stop our meaningful linkage. Victoria, your support for everyone, including me, is deeply appreciated. Vaishali, even though we connected later on, your help during my thesis was indispensable. I'm sure you'll achieve remarkable success as well, and I'll be there to hug you and be proud of your accomplishments when that day arrives. Thanks for being very kind to me. Thank you very much for being in my life!

I also extend my appreciation to my friends Alex, Cornelius. Although I enjoy disturbing each of you individually:), I thank you for your response to my sense of humour. You are truly wonderful people. Yibo, my "sweet but psycho" friend. You have a big, big big heart besides a sharp mind. I appreciate your support in every aspect of life. And Yifan, I am glad to meet with you. Thank you very much for all the good times we had together. Of course, Azra… I am pleased that I know you. I thank you very much for your unconditional support in every sense. You are one of the rarest strong women I have seen who can balance between her mind and heart. We have had unforgettable moments together, and I am sure there will be more in the future. I'm so glad you're here, Azra.

Moreover, Nico, Sven, Klara, and Yosuke deserve my thanks for always being there whenever I need them. Thank you, guys. Additionally, all the alumni of the Theato group, such as Wenyuan, Wenwen, Zengwen, Xiaohui, Xia, Marvin, Xiang, Martin, Sergej, Edgar, Stefan, Andreas, David, Miriam, and numerous others, have created unforgettable memories in my life. I want to express my appreciation to all of you for being a part of my life and contributing to the positive changes it has undergone.

Heyy…Karlsruhe Genclik…Hatice, Eren and Ahmet…My friends, my masters who always listen to my troubles:). We have created unforgettable memories with you. I thank you for not leaving me alone on this journey from the beginning, for helping me unconditionally whenever I needed it, and for being my friend. Thank you again and again!

Fatma, Seda, my unique friends, I want to express my heartfelt gratitude to each of you for your constant presence in my life. We've shared countless beautiful moments together and having you in my life brings me immense joy. I know you always believed me more than I did. I also want to sincerely thank the Isik family for their support in my journey. I am truly grateful for all of you being a part of my life! And unworldly sibling Zeynep, we've been acquainted for a long time. You never released my hand, not even for a day. You were constantly there for me. Your

faith and trust in me exceeded that of anyone else. This achievement belongs to you as well, my beloved sister. I'm incredibly thankful for your presence.

I extend my heartfelt appreciation to Fatih. In my journey, thank you for always being the safest place to lean my head and supporting me mentally, no matter the circumstances. The countless beautiful days, smiles, joys, travels, and fun in my doctoral adventure together have made unforgettable memories. Thank you for always being there.

My sister Sudenur... You are the greatest blessing in my life. This success belongs to you as much as it belongs to me. I thank you very much for never leaving me alone in any matter. My nieces Eren and Beren, years from now, know that your aunt's success is thanks to you, children. Hearing you shout over the phone that you love me motivated me to start a new day. And Gökhan…I'm so glad you're in my life, my dears.

Most importantly, I want to express my heartfelt appreciation to my parents. Mum and Dad, I am immensely grateful for your constant support, deep understanding, and enduring patience, which have been invaluable during my doctoral journey and throughout my entire life. My love for you both is boundless.

Lastly, during my PhD journey in Germany, I had the pleasure of meeting numerous people who have not been mentioned earlier. However, I extend my heartfelt thanks to all of you for adding significance to my time here.